



**Metal free α -Oxygenation of Carbonyl
Compounds**

Paul H. Taylor

**A Thesis Submitted for the Degree of
Doctor of Philosophy**

at

Cardiff University

2010

UMI Number: U580178

All rights reserved

INFORMATION TO ALL USERS

The quality of this reproduction is dependent upon the quality of the copy submitted.

In the unlikely event that the author did not send a complete manuscript and there are missing pages, these will be noted. Also, if material had to be removed, a note will indicate the deletion.



UMI U580178

Published by ProQuest LLC 2013. Copyright in the Dissertation held by the Author.
Microform Edition © ProQuest LLC.

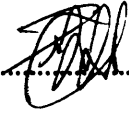
All rights reserved. This work is protected against
unauthorized copying under Title 17, United States Code.



ProQuest LLC
789 East Eisenhower Parkway
P.O. Box 1346
Ann Arbor, MI 48106-1346


DECLARATION

This work has not previously been accepted in substance for any degree and is not concurrently submitted in candidature for any degree.

Signed  (candidate) Paul H. Taylor Date 5/8/11

STATEMENT 1

This thesis is being submitted in partial fulfillment of the requirements for the degree of PhD

Signed  (candidate) Paul H. Taylor Date 5/8/11

STATEMENT 2


This thesis is the result of my own independent work/investigation, except where otherwise stated.

Other sources are acknowledged by explicit references.

Signed  (candidate) Paul H. Taylor Date 5/8/11

STATEMENT 3

I hereby give consent for my thesis, if accepted, to be available for photocopying and for inter-library loan, and for the title and summary to be made available to outside organisations.

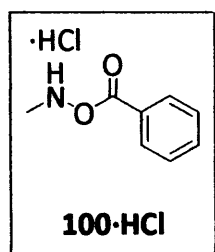
Signed  (candidate) Paul H. Taylor Date 5/8/11

"Organic chemistry just now is enough to drive one mad. It gives me the impression of a primeval tropical forest full of the most remarkable things, a monstrous and boundless thicket, with no way of escape, into which one may well dread to enter."

Friedrich Wöhler, 1835

Abstract

This thesis describes a metal-free approach to the formation of C–O bonds α - to a carbonyl group to give α -oxygenated carbonyl compounds. This moiety is a significant building block in organic synthesis, demonstrated by the extensive synthetic efforts directed towards introduction of this group in a chemo- regio-, stereo-, and enantioselective manner. Traditional methods for the α -oxygenation of carbonyl compounds involve the formation and reaction of air-sensitive intermediates.



Chapter 1 provides an overview of the literature methods for the α -oxygenation of carbonyl compounds, incorporating recent advances in this field achieved previously within the group, following discovery of **100·HCl** to affect a one-pot α -oxygenation transformation. Chapter 2 outlines our project goals and discusses a proposed strategy for a catalytic process. Chapter 3 describes our initial efforts towards constructing a catalytic cycle, particularly with reference to varying the structure of the *N*-substituent of the α -oxygenating species. In Chapter 4, a re-assessment of the project goals is discussed in light of the unsuccessful findings to date. Chapter 5 describes the development of an analytical methodology which would enable us to initiate a mechanistic study. Chapter 6 continues this theme, and relates how information from a range of analytical techniques was used to unravel the mechanism of the α -oxygenation reaction and identify key intermediate species. In Chapter 7, improvements were made to the protocol which enabled reaction times to be significantly shortened.

Acknowledgements

I would like to first of all express my gratitude to my supervisor, Dr. Nick Tomkinson; for not only providing me with the opportunity to study for a PhD. under his supervision, but also for the continuing mentorship and guidance over the course of 3 years of research. It can be a rare phenomenon to be truly valued and respected in a work environment – I am very happy to say that these attributes are the norm within the Tomkinson group.

This thesis relies heavily on results gained via several analytical techniques; the design and execution of many experiments depended to a large extent on the considerable knowledge of the technical support staff along the way. For his expertise and willingness to go the extra mile, I wish to particularly thank Dr. Rob Jenkins of Cardiff University. Due credit must also be given to my CASE supervisor, Dr. Euan Arnott of AstraZeneca, Macclesfield.

I have been fortunate to work with a lively and warm group of people and wish to thank all group members past and present for helping to make my time so enjoyable and rewarding: Dr. Teyrnon Jones, Dr. Jacky Yau, Dr. Rob Strevens, Dr. Niall Killeen, Dr. Tim Gibbs, Dr. Antonio Ruda, Dr. Huw Davies, Dr. Ellie Merritt, Dr. Caz Widdowson, Dr. Krishna Chapaneri and Kerri Jones. A special thank you goes to my bench neighbor, Dr. Deb Knowles.

Among the academic staff who contributed their knowledge and expertise, I would like to highlight Prof. Thomas Wirth and Dr. David Kelly for their positive and spirited examination of this work during Interim Examinations. Sadly, Dr. Kelly has since passed away; he not only taught me the value of ‘dotting the ‘is’ but also the importance of having the correctly shaped dot.

Finally, my love and heartfelt appreciation goes to my wife Deborah for her part in this. Actually, she started it all, and has never stopped supporting and believing in me. Last month, Deb gave birth to our beautiful daughter, Sophie – the finest example of a ‘natural product synthesis’ I will ever be involved in...

TABLE OF CONTENTS

DECLARATION	I
FORWARD.....	II
ABSTRACT	III
ACKNOWLEDGEMENTS	IV
TABLE OF CONTENTS	V
DETAILED TABLE OF CONTENTS	VI
ABBREVIATIONS.....	IX
CHAPTER 1: INTRODUCTION.....	1
CHAPTER 2: PROJECT DESIGN AND PLANNING	35
CHAPTER 3: THE FIRST SIX MONTHS	45
CHAPTER 4: PROJECT RE-EVALUATION.....	58
CHAPTER 5: REACTION MONITORING – EARLY EXPERIMENTS	72
CHAPTER 6: REACTION MONITORING – REFINEMENTS AND FURTHER TECHNIQUES	118
CHAPTER 7: CONCLUDING NMR EXPERIMENTS AND REACTION OPTIMISATION	186
CHAPTER 8: CONCLUSION.....	203
CHAPTER 9: EXPERIMENTAL	210
APPENDICES.....	244
REFERENCES.....	249

DETAILED TABLE OF CONTENTS

DECLARATION	I
FORWARD.....	II
ABSTRACT	III
ACKNOWLEDGEMENTS	IV
TABLE OF CONTENTS.....	V
DETAILED TABLE OF CONTENTS	VI
ABBREVIATIONS.....	IX
 CHAPTER 1: INTRODUCTION.....	 1
1 Metal-free methods in Organic Chemistry.....	2
1.1 Literature precedent	4
1.1.1 <i>N</i> -sulfonyloxaziridines	5
1.1.2 Organocatalytic α -oxygenation	7
1.1.3 House.....	8
1.1.4 Coates.....	10
1.2 [3,3]-Sigmatropic rearrangements.....	11
1.2.1 Claisen rearrangements	11
1.2.2 Hetero-Claisen rearrangements.....	13
1.2.3 Cope rearrangements.....	15
1.2.4 Oxy-Cope rearrangement.....	15
1.2.5 Aza-Cope rearrangements.....	16
1.3 Applications of [3,3]-sigmatropic rearrangements	19
1.3.1 The Fischer Indole Synthesis	19
1.3.2 Total synthesis of (-)-Malynolidide	21
1.3.3 Industrial synthesis of citral	22
1.3.4 A [3,3]-sigmatropic rearrangement in nature	23
1.4 Previous group work	23

1.4.1 A novel oxygenation of aldehydes	25
1.4.2 A general method for the α -acyloxylation of carbonyl compounds	28
1.4.3 The methodology extended	32
1.4.4 Testing the mechanism	33
CHAPTER 2: PROJECT DESIGN AND PLANNING	35
2.1 Development of a novel catalytic procedure	38
CHAPTER 3: THE FIRST SIX MONTHS	45
3.1 Activation by Lewis acids	46
3.2 Structure of reagent	48
3.3 Testing reactivity	53
CHAPTER 4: PROJECT RE-EVALUATION	58
4.1 Thiourea work	59
4.2 Attempted hydroxylamine syntheses	64
4.3 Work with nitrones	66
4.4 New directions	69
CHAPTER 5: REACTION MONITORING - EARLY EXPERIMENTS	72
5.1 Groundwork to kinetic studies	75
5.1.1 Initial observations by ^1H NMR	75
5.1.2 Choice of substrates and reaction conditions	79
5.2 Initial ^1H NMR monitoring experiments	85
5.2.1 A flawed experiment	85
5.2.2 Evolving the method	87
5.2.3 Relationship between temperature and rate of reaction	93
5.2.3 Examination of the intermediates	96
5.3 Further variables in ^1H NMR work	103
5.3.1 Aromatic substituents	103
5.3.2 Stoichiometry	109
5.3.3 Solvent water content	111
5.3.4 A further ketone substrate	114

CHAPTER 6: REACTION MONITORING – REFINEMENTS AND FURTHER TECHNIQUES	118
6.1 Reaction monitoring by ^1H NMR	120
6.1.1 The effect of temperature.....	121
6.1.2 Identification of intermediates	131
6.1.3 Explaining the <i>cis:trans</i> ratio	139
6.1.4 The effect of water	140
6.1.5 Reaction stoichiometry	150
6.2 Fate of reagent	157
6.3 Reaction monitoring by ReactIR™	164
6.4 Kinetic modelling.....	176
CHAPTER 7: CONCLUDING NMR EXPERIMENTS AND REACTION OPTIMISATION	186
7.1 Final ^1H NMR reaction monitoring experiments	187
7.2 Reaction optimisation	190
7.2.1 Additional water.....	190
7.2.2 Concentration.....	195
7.2.3 Structure of reagent	196
CHAPTER 8: CONCLUSION.....	203
CHAPTER 9: EXPERIMENTAL	210
9.1 General	211
9.2 Preparation of α -oxygenating reagents	213
9.3 α -Oxygenated Carbonyl Compounds	226
9.4 Miscellaneous Compounds	236
9.5 Analytical experiments.....	242
APPENDICES.....	244
REFERENCES.....	249

Abbreviations

Ac	acetyl
APCI	atmospheric pressure chemical ionisation
Ar	aromatic
atm.	atmosphere(s)
Bn	benzyl
Bz	benzoyl
Boc	<i>tert</i> -butoxycarbonyl
br	broad
Bu	butyl
cat.	catalyst
Cbz	benzyloxycarbonyl
column chromatography	flash column chromatography
CDI	1,1'-carbonyldiimidazole
CSO	(camphorsulfonyl) oxaziridine
d	day(s)
d	doublet
DCCSO	(8,8-dichlorocamphoryl)sulfonyl oxaziridine
DEPT	distortionless enhancement by polarization transfer
DMCSO	(8,8-dimethoxycamphoryl)sulfonyl oxaziridine
DMF	dimethylformamide
DMPU	<i>N,N'</i> -dimethylpropyleneurea
DMSO	dimethyl sulfoxide
DNPH	2,4-dinitrophenylhydrazine
ee	enantiomeric excess
Et	ethyl
EI	electron impact
ES	electrospray
ether	diethyl ether

EWG	electron withdrawing group
equiv. (eq.)	equivalent(s)
GC	gas chromatography
GLC	gas-liquid chromatography
h	hour(s)
HMBC	heteronuclear multiple bond coherence
HMPA	hexamethylphosphoramide
HOMO	highest occupied molecular orbital
HPLC	high performance liquid chromatography
HRMS	high resolution mass spectrometry
HSQC	heteronuclear single quantum coherence
<i>i</i>	<i>iso</i>
IR	infra red
k	kilo
LA	Lewis acid
LCMS	liquid chromatography–mass spectrometry
LDA	lithium diisopropylamide
light petrol	petroleum ether 40–60 °C
Lit.	Literature
LITMP	lithium 2,2,6,6-tetramethylpiperidide
LUMO	lowest unoccupied molecular orbital
M	molar
<i>m</i>	mass
m	multiplet
mCPBA	<i>meta</i>-chloroperoxybenzoic acid
Me	methyl
min	minute(s)
mmol	millimole(s)
MoOPD	oxodiperoxymolybdenum (pyridine) 1,3-dimethyl-3,4,5,6-tetrahydro-2(1<i>H</i>)-pyrimidinone

MoOPH	oxodiperoxymolybdenum (pyridine) hexamethylphosphoric triamide
NMR	nuclear magnetic resonance
MO	molecular orbital
mol	mole(s)
Mp	melting point
MHz	megahertz
MS	mass spectrometry
NMR	nuclear magnetic resonance
NOESY	nuclear Overhauser enhancement spectroscopy
Nu	nucleophile
<i>p</i>	<i>para</i>
p	pentet
Ph	phenyl
Pr	propyl
PSPO	<i>trans</i>-2-(phenylsulfonyl)-3-phenyloxaziridine
q	quartet
quant.	Quantitative
RAMP	(<i>R</i>)-1-Amino-2-methoxymethylpyrrolidine
RDS	rate determining step
R_f	retention factor
r.t.	room temperature
s	singlet
sept.	septet
soln.	solution
<i>t</i>	tertiary
t	triplet
<i>tert</i>	tertiary
TFA	trifluoroacetic acid
THF	tetrahydrofuran

TLC	thin layer chromatography
TMSI	trimethylsilyl iodide
Ts	tosyl
<i>p</i>TSA	<i>para</i>-toluene sulfonic acid
<i>z</i>	charge
Å	Angstroms
Δ	heat
π	pi
σ	sigma

Chapter 1: Introduction

1 Metal-free methods in synthetic organic chemistry

For a synthetic organic methodology to find wide applicability within the chemical community in the modern era requires that due attention be given to the selectivity of the process, its general practicability, amenability for industrial scale and economy. Environmental considerations have become a priority in recent decades, and hence there is a need to cease or minimise the use of hazardous and inefficient processes and materials, reduce the amounts of chemicals and energy being used, and to recycle wherever possible. The Chemical Industry also seeks *atomically efficient* processes, i.e. transformations where the so-called E-factor (ratio of waste to product) is kept to a minimum. Waste materials should then be disposed of with a minimal environmental impact.

It is particularly apt that there has been a recent upsurge in the use of metal-free methods to accomplish organic reactions.¹ These systems utilise organic molecules as catalysts, and enjoy several advantages over their metal-based counterparts. These so-called organocatalysts have benefits from an economic, social and political viewpoint since they are generally cheaper, less toxic and more environmentally benign than their metal-based counterparts.

Also there are a number of synthetic benefits which accrue from the use of organic molecules. For instance, the catalysts are generally stable and can be stored under ambient conditions rather than needing to be generated *in situ* as is the case with many metal-based reagents. In many cases the reactions can be performed at room temperature and are tolerant of the presence of moisture and air, sometimes even using water as the reaction medium. In particular, the use of iminium ion catalysts has proved an extremely versatile area of contemporary organic synthesis. The groups of MacMillan and List have been at the forefront of this area of research; having reported asymmetric Diels-Alder,² conjugate addition,³ [3 + 2] cycloaddition,⁴ Mannich,⁵ aldol,⁶ α -oxyamination⁷ and α -amination⁸ reactions within the last ten years.

The methodology has been successfully applied to the asymmetric syntheses of the marine metabolite solanapyrone D **1** via an enantioselective organocatalytic intramolecular Diels-Alder reaction,⁹ and to the preparation of (-)-littoralisone **2** and (-)-brasoside **3**, with a proline-catalysed intramolecular Michael addition as the key step in the synthetic pathway.¹⁰ These two molecules are found naturally in *Verbena littoralis*, a plant used widely in traditional folk remedies, and whose extracts have been shown to possess interesting biological activity (Figure 1).

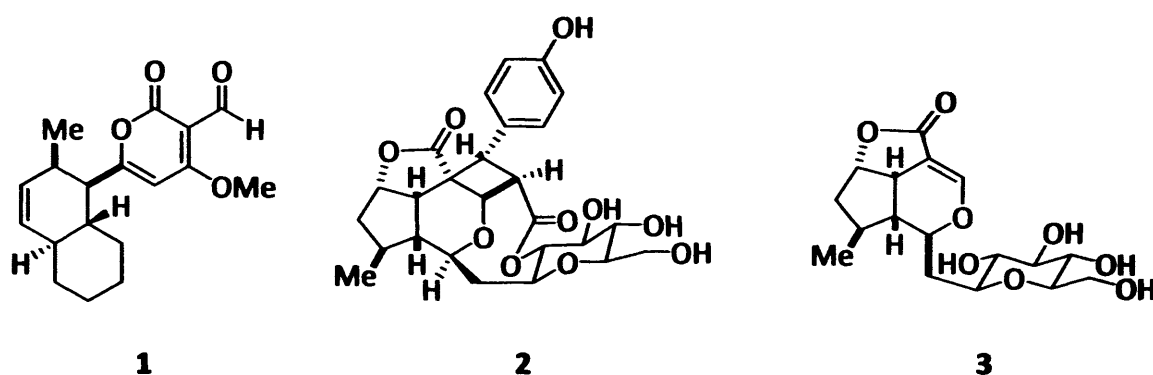


Figure 1

Brasoside and littoralisone are typical of many natural products in that these molecules are often highly oxygenated – it follows then that C-O bond forming reactions comprise a valuable part of the synthetic toolkit in Organic Chemistry. Classical reactions of this type include the oxidation of alkenes to give epoxides (forming two new C-O bonds),¹¹ and the Baeyer-Villiger oxidation,¹² where an oxygen atom is effectively inserted next to the carbonyl group (Figure 2). In both cases a peroxy-acid is used as the oxidising agent.

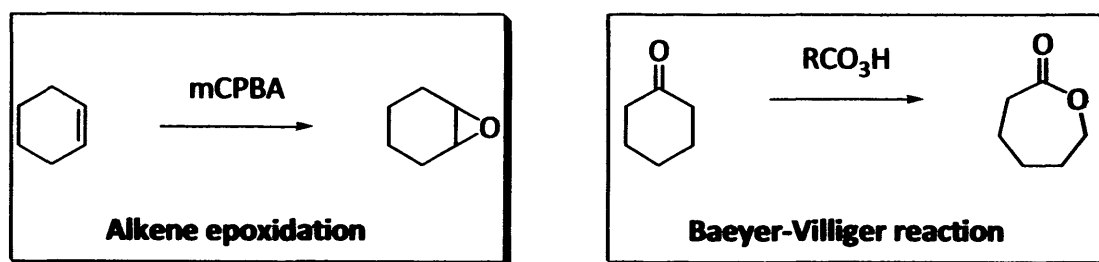


Figure 2

1.1 Literature precedent

An important motif in organic chemistry is the α -hydroxycarbonyl functionality. This is not only a versatile building block in synthesis which can be further homologated and functionalised, but it is also a common theme to many naturally occurring biologically active molecules, as well as other synthetic compounds of interest. Two famous examples are taxol 4 and camptothecin 5 (Figure 3), both of which were discovered in the mid-1960's and found to inhibit cancer cell growth, with profound implications for medical research in the ensuing decades.¹³

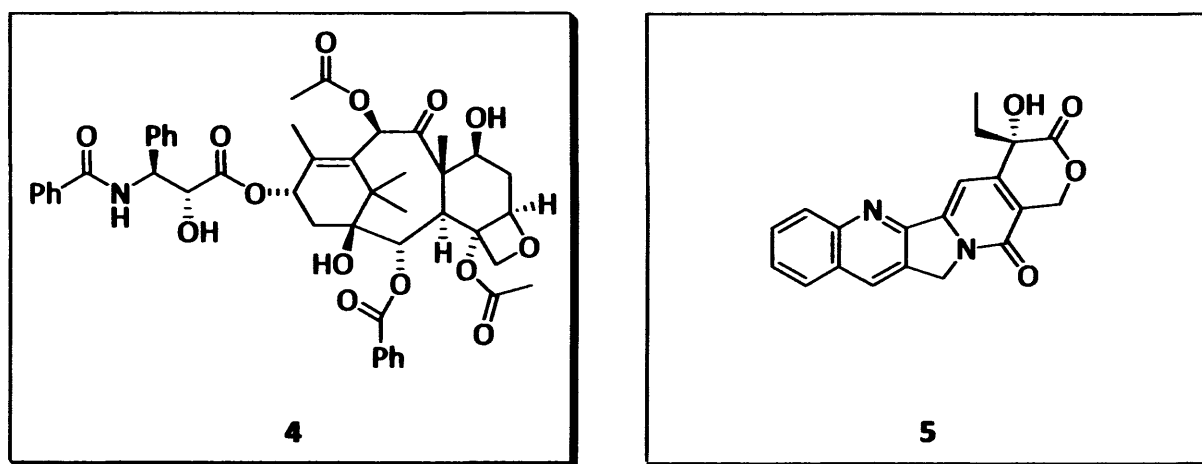


Figure 3

There are a great many methods in the primary chemical literature for the preparation of this useful and biologically relevant functional group; a significant number of which use metal enolates or preformed enol ethers as substrates. These can be α -hydroxylated by a variety of reagents which include molecular oxygen, peroxy reagents, osmium tetroxide, hypervalent iodine reagents, metal oxides, and *N*-sulfonyloxaziridines.¹⁴

For example, lithium enolates can be oxidised to the corresponding α -hydroxy carbonyl compounds by treatment with either oxodiperoxymolybdenum (pyridine) hexamethylphosphoric triamide (MoOPH)¹⁵ or oxodiperoxymolybdenum (pyridine) 1,3-dimethyl-3,4,5,6-tetrahydro-2(1*H*)-pyrimidinone (MoOPD),¹⁶ the latter being preferable as it employs the DMPU (*N,N'*-dimethylpropyleneurea) ligand, which is less toxic than HMPA.

1.1.1 *N*-sulfonyloxaziridines

A commonly used group of reagents, comprising a source of electrophilic oxygen for direct enolate oxidation are the *N*-sulfonyloxaziridines.¹⁷ These are characterised by the bulky and electronegative sulfonyl group; prominent examples include racemic *trans*-2-(phenylsulfonyl)-3-phenyloxaziridine **6** (PSPO, also commonly known as the Davis reagent) and the chiral, non-racemic camphorylsulfonyl oxaziridines (+)-**7** and (-)-**7** (Figure 4).

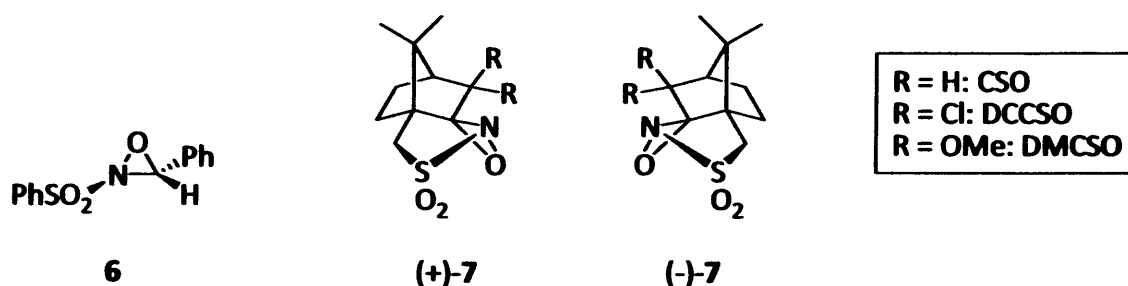
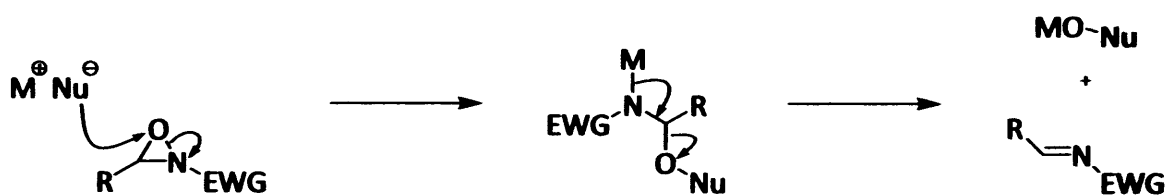


Figure 4

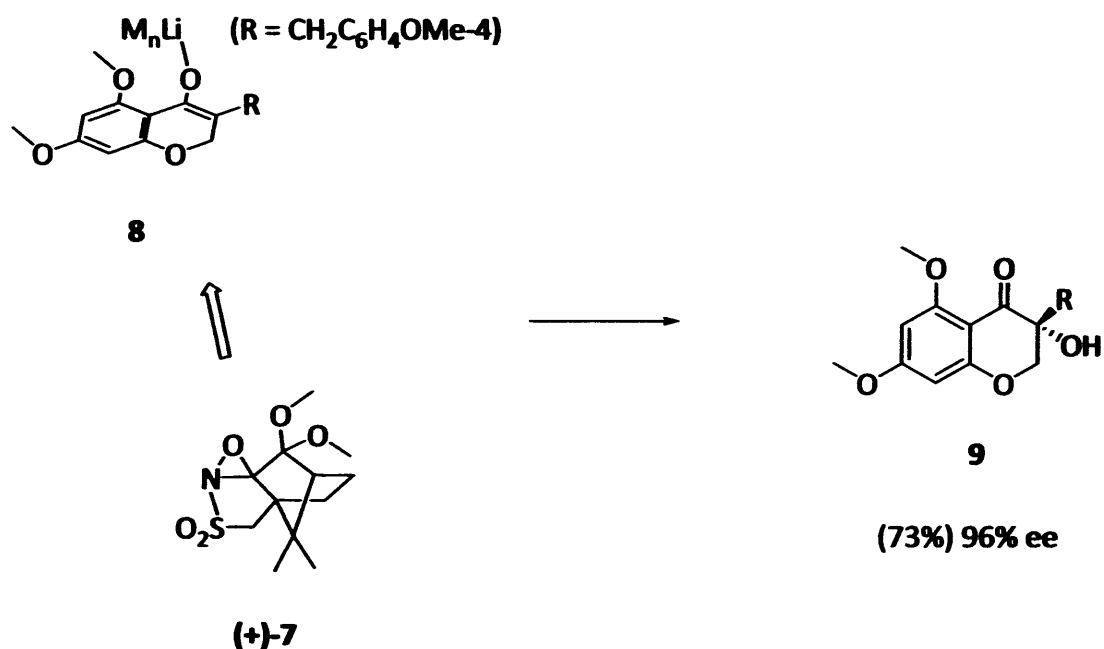
Generally, oxaziridines can be used as both oxygenating and aminating agents in their reactions with a wide variety of nucleophiles. Whether the oxygen or the nitrogen atom is transferred is determined by the nature of the nitrogen substituent. Usually, oxaziridines with small groups on nitrogen act as aminating agents, whereas those with bulky or electron-withdrawing *N*-substituents transfer the oxygen atom preferentially.¹⁸



Scheme 1

Scheme 1 depicts a generalised oxaziridine as an oxygen-transfer reagent and the mechanism is thought to involve S_N2 nucleophilic attack on oxaziridine oxygen with simultaneous N-O bond cleavage.¹⁹ The intermediate then breaks down to furnish the oxygenated adduct and a sulfonyl imine by-product.²⁰

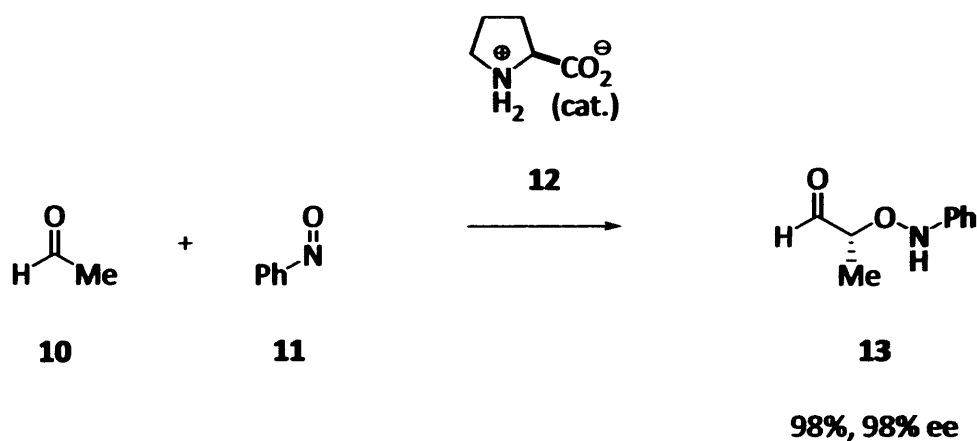
The chiral (camphorylsulfonyl) oxaziridines can be applied effectively to the enantioselective α -hydroxylation of prochiral enolates such as the benzopyranone derivative **8**. The absolute configuration of the three-membered oxaziridine ring in (+)-**7** controls the configuration of the product **9**; in this manner the desired enantiomer of an α -hydroxy carbonyl can be obtained by using the appropriate oxaziridine. Scheme 2 shows that the oxaziridine oxygen can approach only from below the plane of the substrate, primarily because of the steric demand associated with the oxygen-lithium aggregate. Chelation of the metal with one of the methoxy groups may also assist by stabilising the transition state in the example shown.²¹



Scheme 2

1.1.2 Organocatalytic α -oxygenation

Still more recent advances in the α -hydroxylation of carbonyl compounds have been made using organocatalysts. Using nitrosobenzene **11** as an oxidant, and L-proline **12** as catalyst, it has been shown that aldehydes²² (such as acetaldehyde **10**, see Scheme 3) and ketones²³ can be α -aminoxylation directly and enantioselectively.



Scheme 3

It was proposed that the transition state model (Figure 5) accounted for the absolute stereochemistry of the α -hydroxylated aldehyde **13**, which was formed in excellent yield and enantioselectivity when the reaction was conducted at low temperatures ($-20\text{ }^\circ\text{C}$). However, this procedure – although novel and attractive – remained somewhat limited by the requirement for up to 10 equivalents of carbonyl compound, and the need for syringe pump techniques.

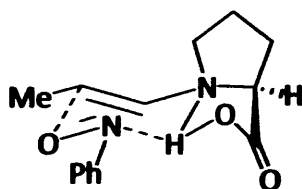
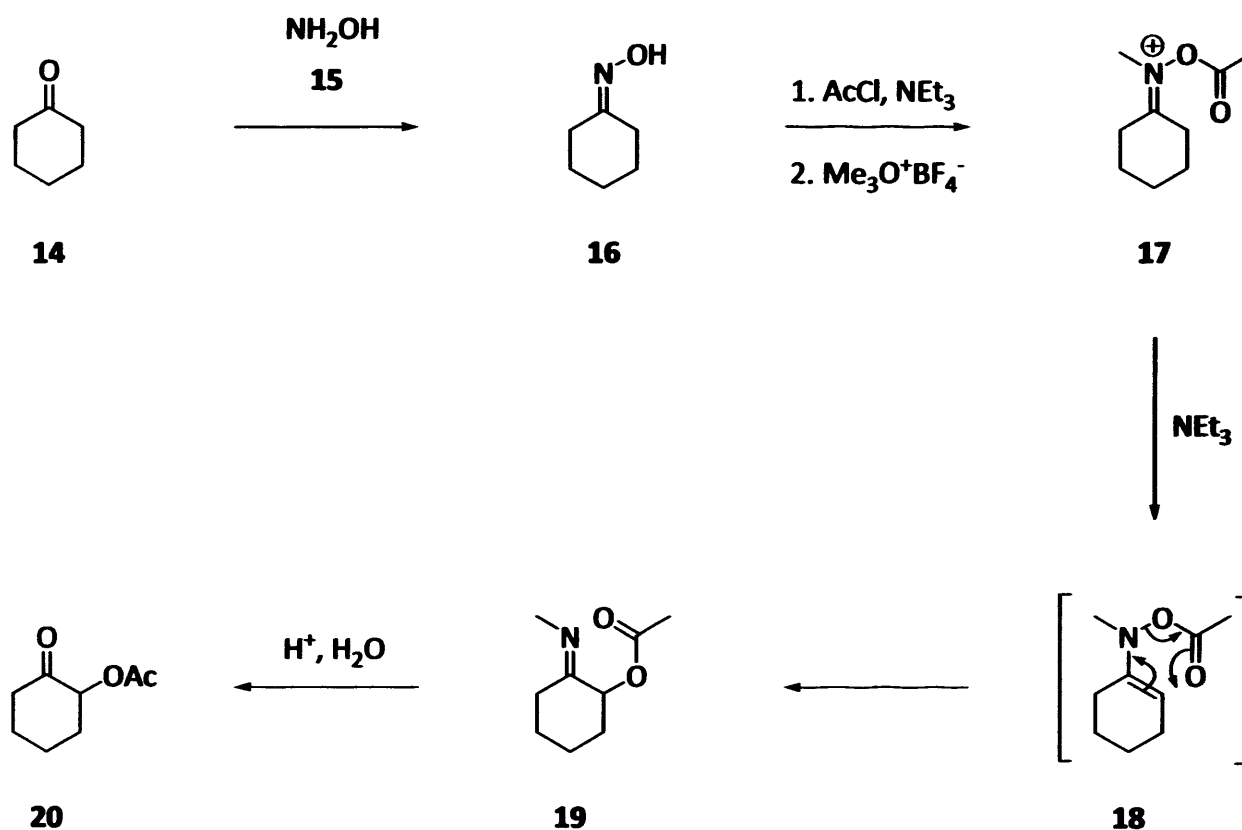


Figure 5

1.1.3 House method

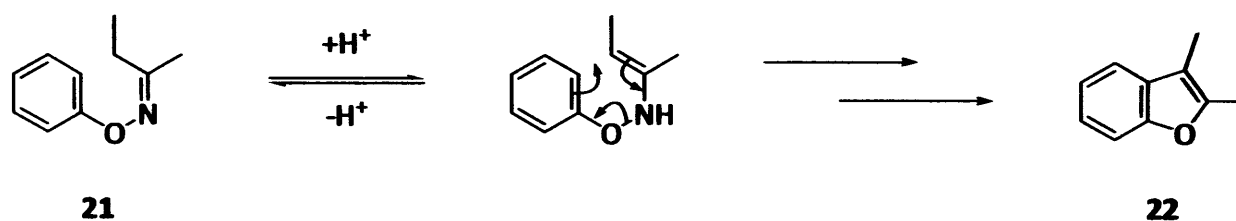
A relatively obscure method for the α -oxygenation of carbonyl compounds was reported in 1969 by House, who described a novel reaction sequence commencing with cyclohexanone **14** and proceeding over 5 steps to give the corresponding α -acetoxy carbonyl compound (Scheme 4)²⁴.



Scheme 4

Treatment of cyclohexanone **14** with hydroxylamine **15** gave the corresponding oxime **16**, which was converted to the iminium salt **17** by *O*-acetylation followed by *N*-methylation. Addition of anhydrous triethylamine to the salt **17** produced the enamine species **18**, which it was to undergo a rapid, [3,3] sigmatropic pericyclic rearrangement to give the α -acetoximine **19**. Finally, hydrolysis of the imine under aqueous acidic conditions gave the α -functionalised ketone **20** in 45% isolated yield after 5 steps.

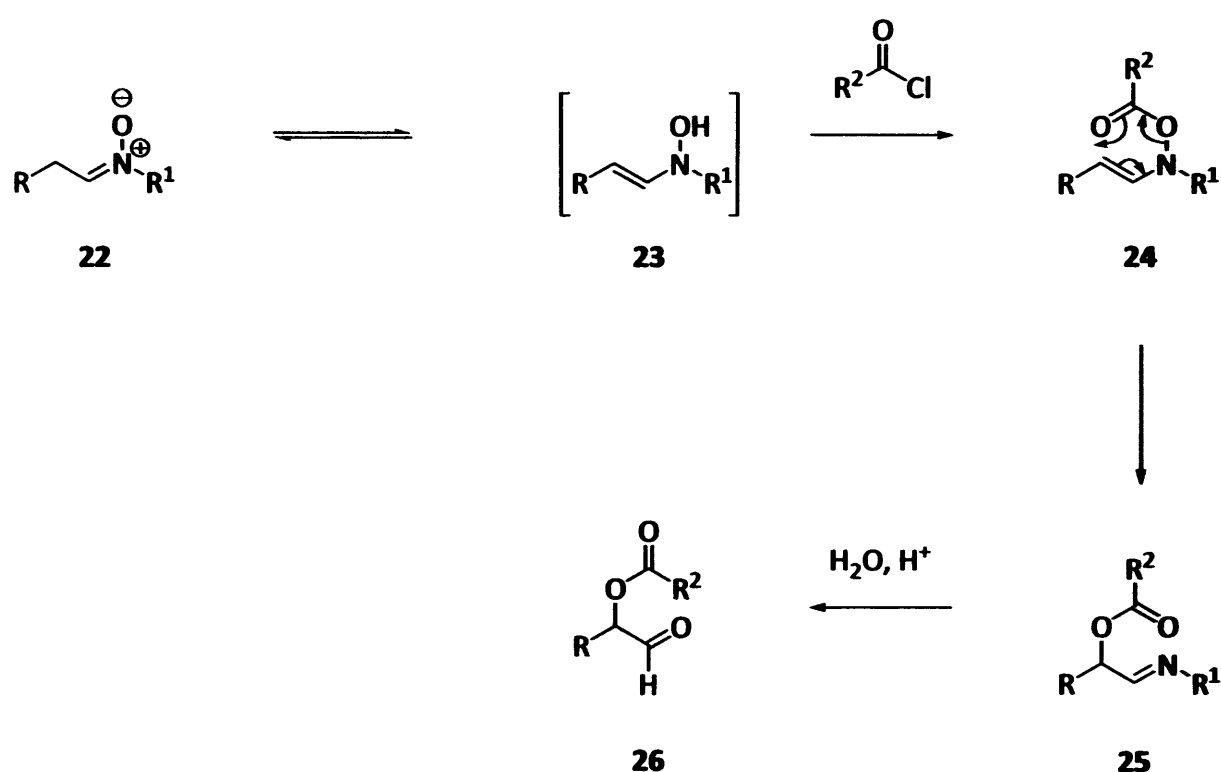
Whilst House undoubtedly reported a very elegant synthesis, his methodology has not found its way into general usage owing to the number of steps involved. Although not necessarily of immediate synthetic utility, the process is of chemical interest, particularly because of the proposed concerted pericyclic rearrangement step. House asserted that the breaking of the relatively weak N-O bond (200 kJ mol^{-1}) and the concurrent formation of the much stronger C-O single bond (350 kJ mol^{-1}) provided a thermodynamic driving force and thereby facilitated the rearrangement. Whilst concrete evidence for the rearrangement step was not described at this time, a similar rearrangement (that of an oxime aryl ether **21** to form benzofuran **22**, Scheme 5) involving N-O bond cleavage was reported some years previously.²⁵



Scheme 5

1.1.4 Coates

Since the time of House, a number of similar approaches have been described in the literature.²⁶ In 1983 Coates showed that α -oxygenated aldehydes **26** (and cyclic ketones) could be successfully prepared by successive acylation of the nitrones **22** (as the alkylhydroxylamine tautomer **23**) with acid chloride, [3,3]-sigmatropic rearrangement of the *N*-vinyl-*O*-acylhydroxylamine intermediates **24** and hydrolysis of the resulting α -acyloxy imines **25** (Scheme 7).²⁷



Scheme 7

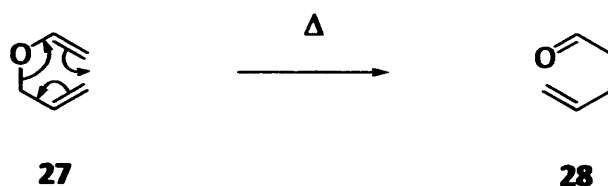
This offered a new method of obtaining the α -oxygenation adducts in good yield, under fairly mild reaction conditions and without the need for harsh electrophilic oxidising agents. However, the reaction still comprised a three-step sequence starting from the commercially available carbonyl compounds.

1.2 [3,3]-Sigmatropic rearrangements

The rearrangement type suggested by House and Coates is by no means an uncommon feature in organic synthesis. A sigmatropic rearrangement is defined by the migration of a sigma bond from one position in a conjugated system to another position in the system, accompanied by reorganization of the connecting π -bonds.

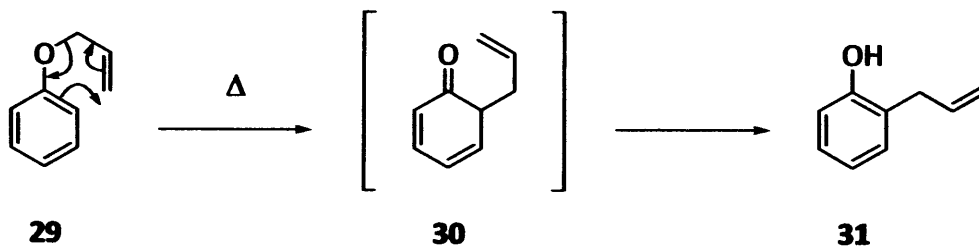
1.2.1 Claisen rearrangements

The classic, and first recorded example of a [3,3]-sigmatropic rearrangement was discovered in 1912 by Rainer Claisen (the transformation which bears his name), in which an allyl vinyl ether **27**, on heating gives rise to a γ,δ -unsaturated carbonyl compound **28** (Scheme 8).²⁸



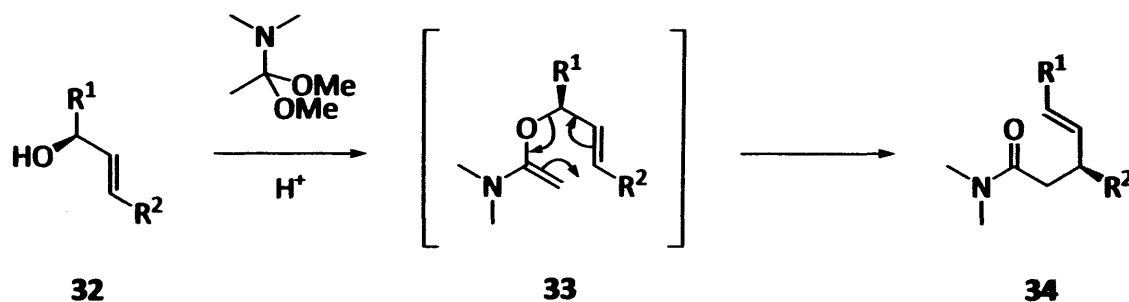
Scheme 8

There are several variants of the Claisen rearrangement. In the aromatic Claisen rearrangement, an allyl phenyl ether **29** undergoes the same rearrangement followed by rearomatisation of the intermediate species **30** to form an ortho-substituted phenol **31** (Scheme 9).²⁹



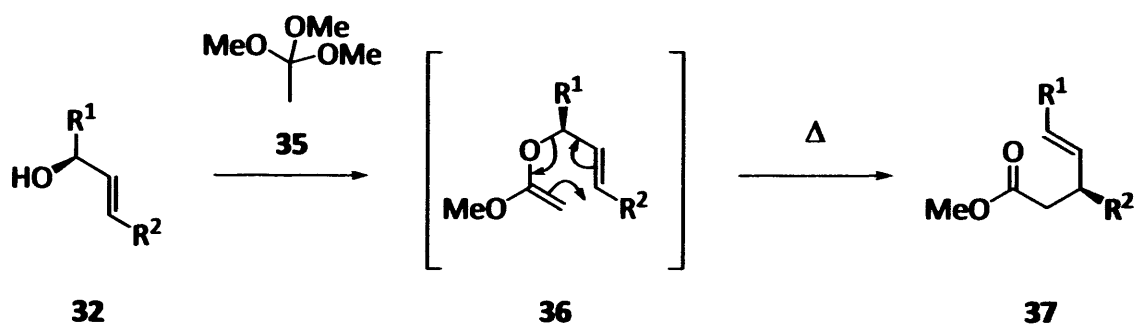
Scheme 9

Starting with an allylic alcohol **32**, the Eschenmoser-Claisen rearrangement proceeds to give a γ,δ -unsaturated amide **34** (Scheme 10).³⁰



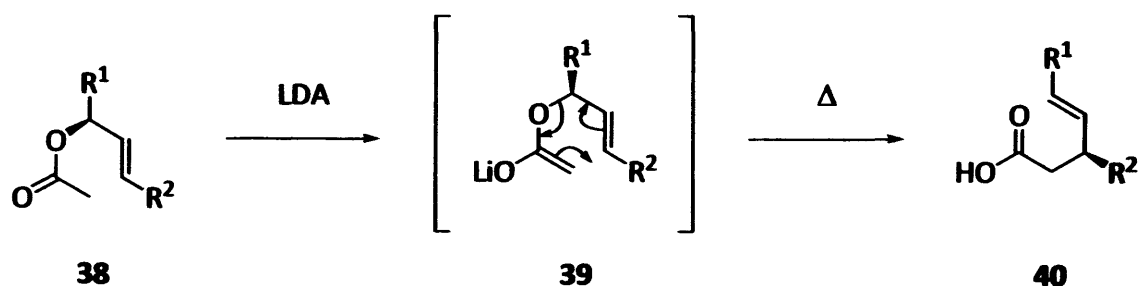
Scheme 10

In an analogous fashion, the reaction of an allylic alcohol **32** with trimethyl orthoacetate **35** gives a γ,δ -unsaturated ester **37**; this is the Johnson-Claisen rearrangement (Scheme 11).³¹



Scheme 11

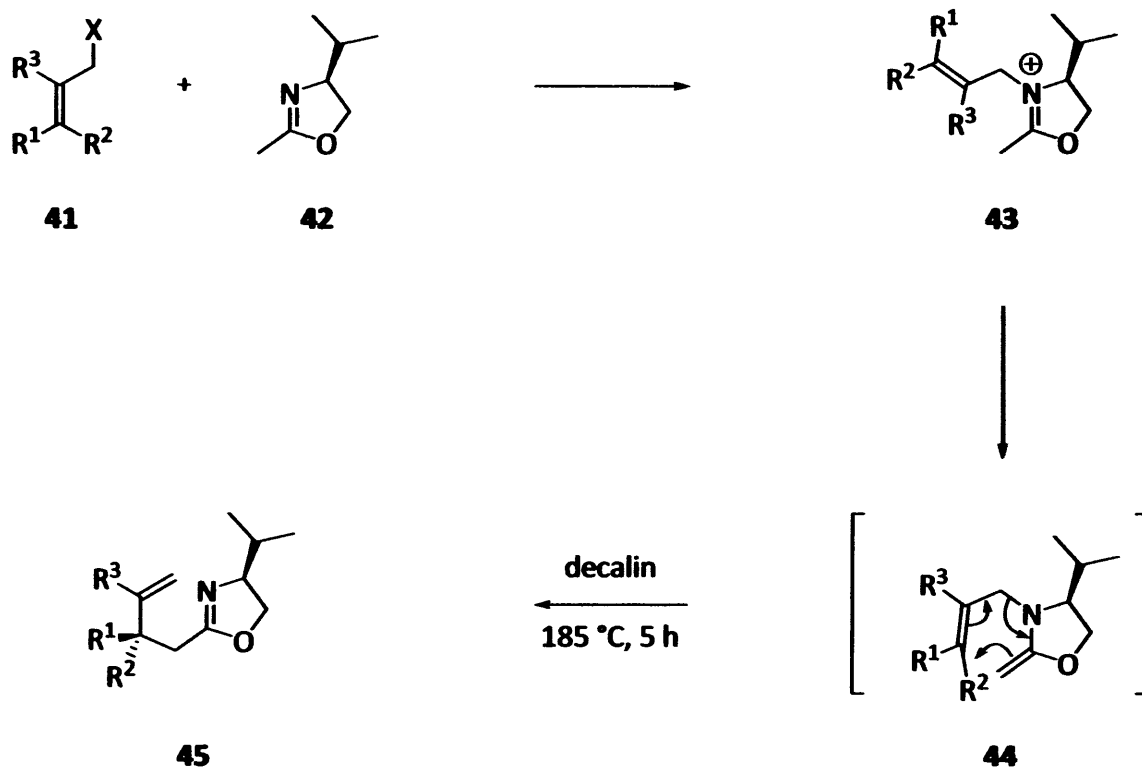
During the Ireland-Claisen rearrangement, treatment of an allylic ester **38** with strong base yields a γ,δ -unsaturated carboxylic acid **40** (Scheme 12).³²



Scheme 12

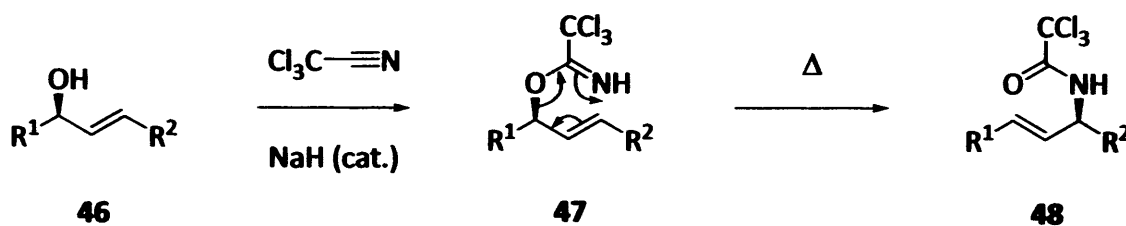
1.2.2 Hetero-Claisen rearrangements

As the Aza-Claisen shows, an iminium ion **43** can serve as one of the components of the rearrangement (Scheme 13).³³



Scheme 13

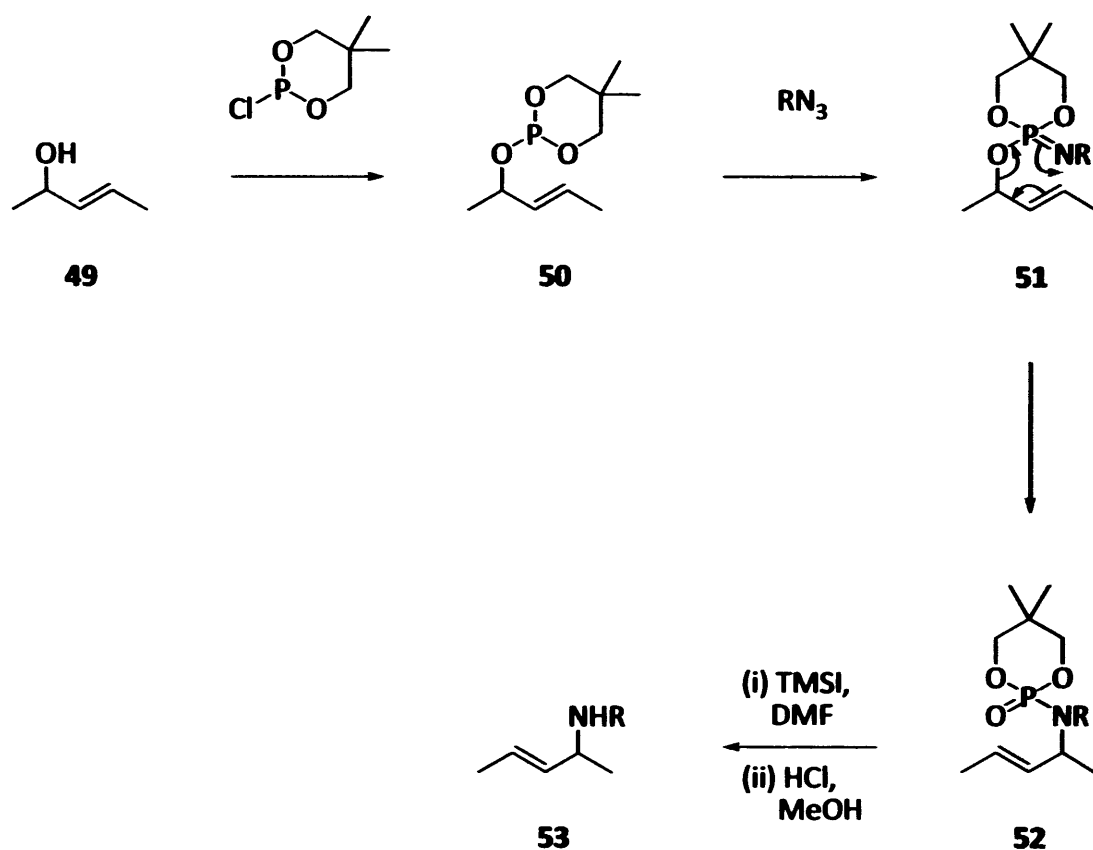
The Overman rearrangement is a Claisen rearrangement of allylic trichloroacetimidates **46** to allylic trichloroacetamides **48** via an imidate intermediate **47** (Scheme 14).³⁴



Scheme 14

The rearrangement is diastereoselective and may be promoted by either heat, Pd(II) or Hg(II).³⁵ The reaction provides access to allylamines which can be homologated to natural and unnatural amino acids.³⁶ An asymmetric variant has also been reported.³⁷

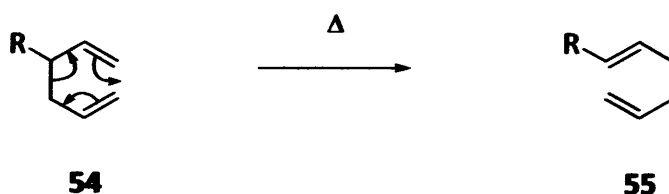
The Chen-Mapp reaction (also known as the Staudinger-Claisen reaction) is a transformation in which a hydroxyl species **49** is converted to a phosphite **50**. Subsequent treatment with an azide gives an iminophosphorane **51** (Staudinger reaction) which is set up to undergo [3,3]-sigmatropic rearrangement; this is thermodynamically driven by the formation of the strong P=O double bond. Hydrolysis of the rearrangement product **52** leads to synthetically useful allylic amines **53** (Scheme 15).³⁸



Scheme 15

1.2.3 Cope rearrangements

The Cope rearrangement is the conversion of a 1,5-hexadiene derivative **54** to an isomeric 1,5-hexadiene **55** by the [3,3] sigmatropic mechanism, differing from the Claisen rearrangement (in the classical version) in that only carbon atoms are in the ring (Scheme 16).³⁹

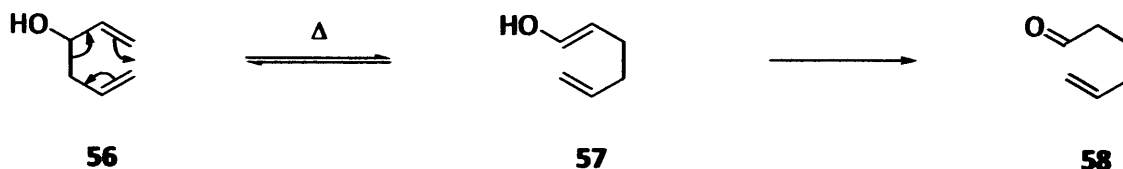


Scheme 16

The Cope rearrangement is a reversible reaction, with the preference being the thermodynamically more stable isomer as the dominant product.

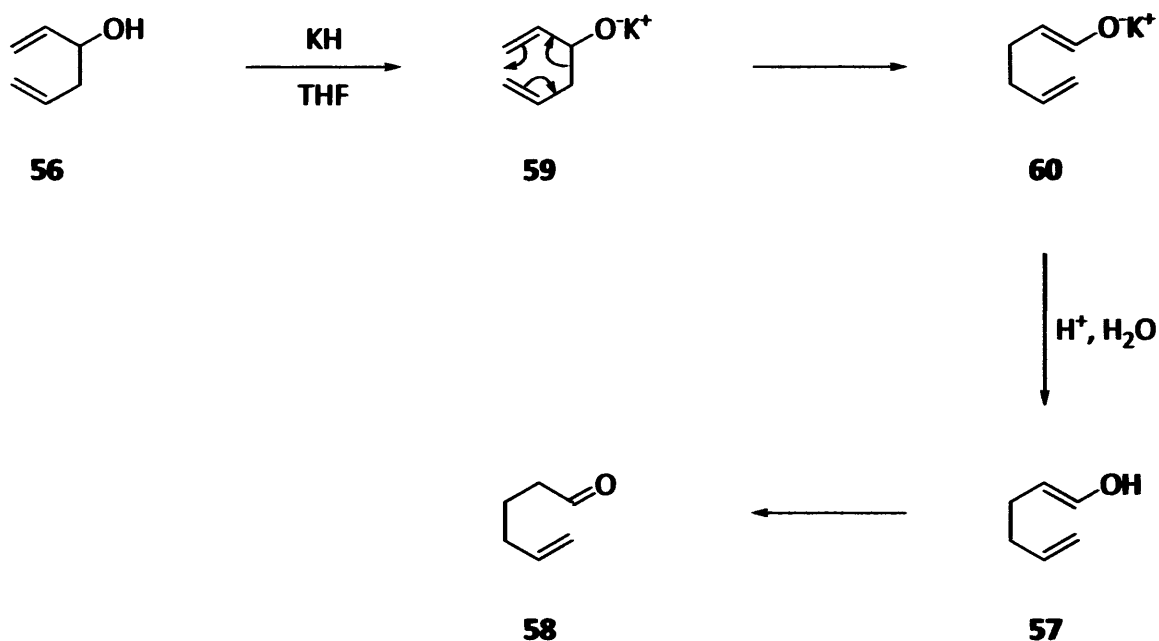
1.2.4 Oxy-Cope rearrangement

In this variant, a hydroxyl group is introduced at C-3.⁴⁰ Starting from a 3-hydroxy-1,5-diene **56**, the rearrangement is not reversible, because the initial Cope product **57** tautomerizes to an aldehyde or ketone **58**, and is therefore removed from the equilibrium (Scheme 17). The net result is that the equilibrium is shifted to the right.



Scheme 17

The rate of the Cope rearrangement is strongly accelerated if the starting alcohol **56** is treated with base (typically potassium hydride) to give an oxy-anion substituent at C-3 in the intermediate **59**. Known as the anionic oxy-Cope rearrangement, this tweak can result in reaction rate enhancement by factors of between 10^{10} and 10^{17} (Scheme 18).⁴¹

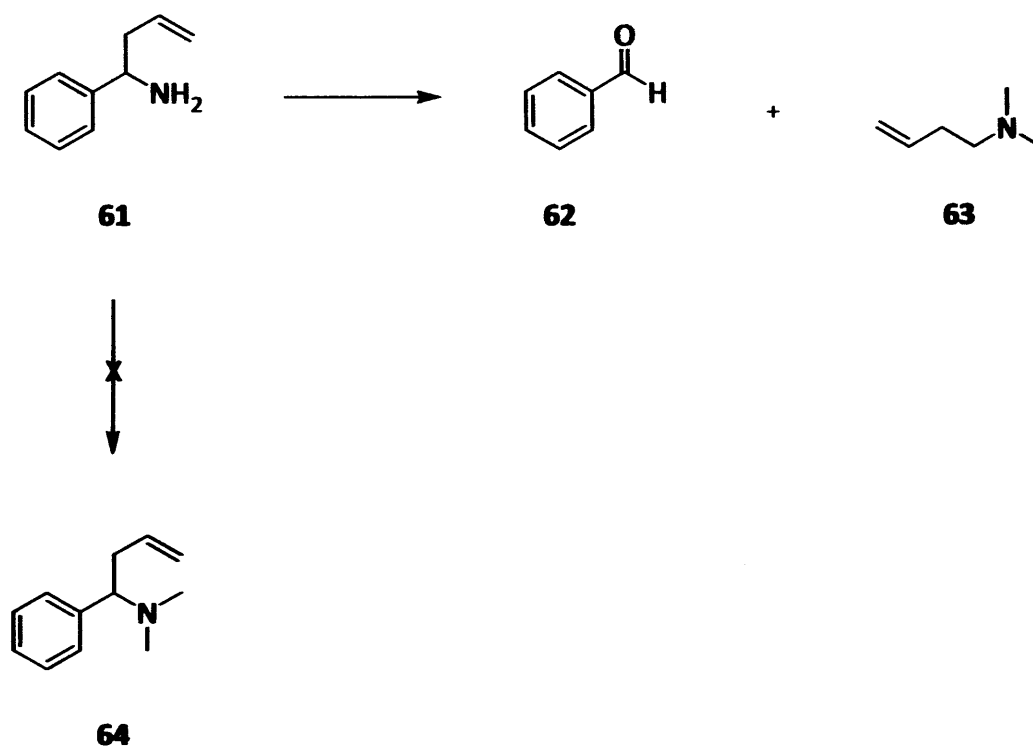


Scheme 18

This is advantageous in that there is now no need of the elevated temperatures at which side reactions may occur.

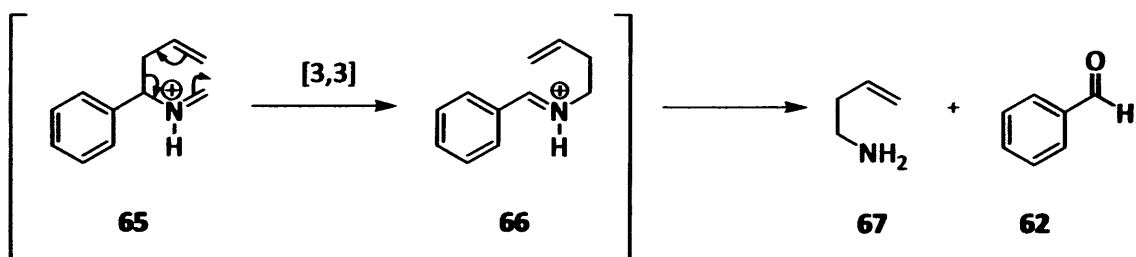
1.2.5 Aza-Cope rearrangements

Discovered in 1950, the so-called Aza-Cope rearrangement occurred when α -allylbenzylamine **61** was treated with formic acid and formaldehyde.⁴² Instead of the expected Eschweiler-Clarke adduct **64**, the reaction took a different course, leading to the cleavage of starting material **61**, and formation of benzaldehyde **62** and 1-(dimethylamino)but-3-ene **63** (Scheme 19).



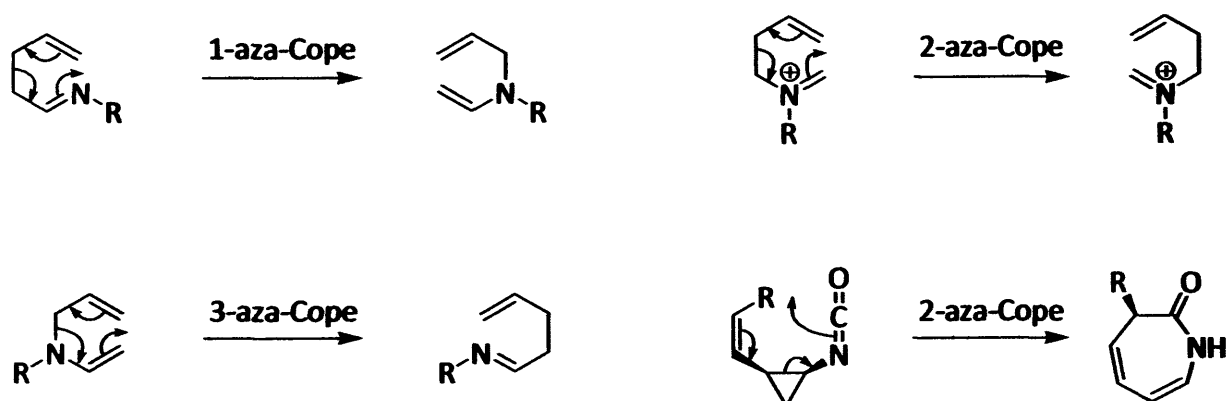
Scheme 19

It was postulated that the cleavage proceeded in an analogous manner to the Cope rearrangement, such that the iminium ion 65 underwent [3,3]-sigmatropic shift to a second iminium ion 66, and that this species furnished benzaldehyde 62 and the allylamine 67 after hydrolysis (Scheme 20). Subsequent *N*-alkylation under the reaction conditions then provided the observed product 63.



Scheme 20

Since then, many variants of the Aza-Cope have been reported; Scheme 21 displays a few examples for various *N*-substituted dienes.⁴³



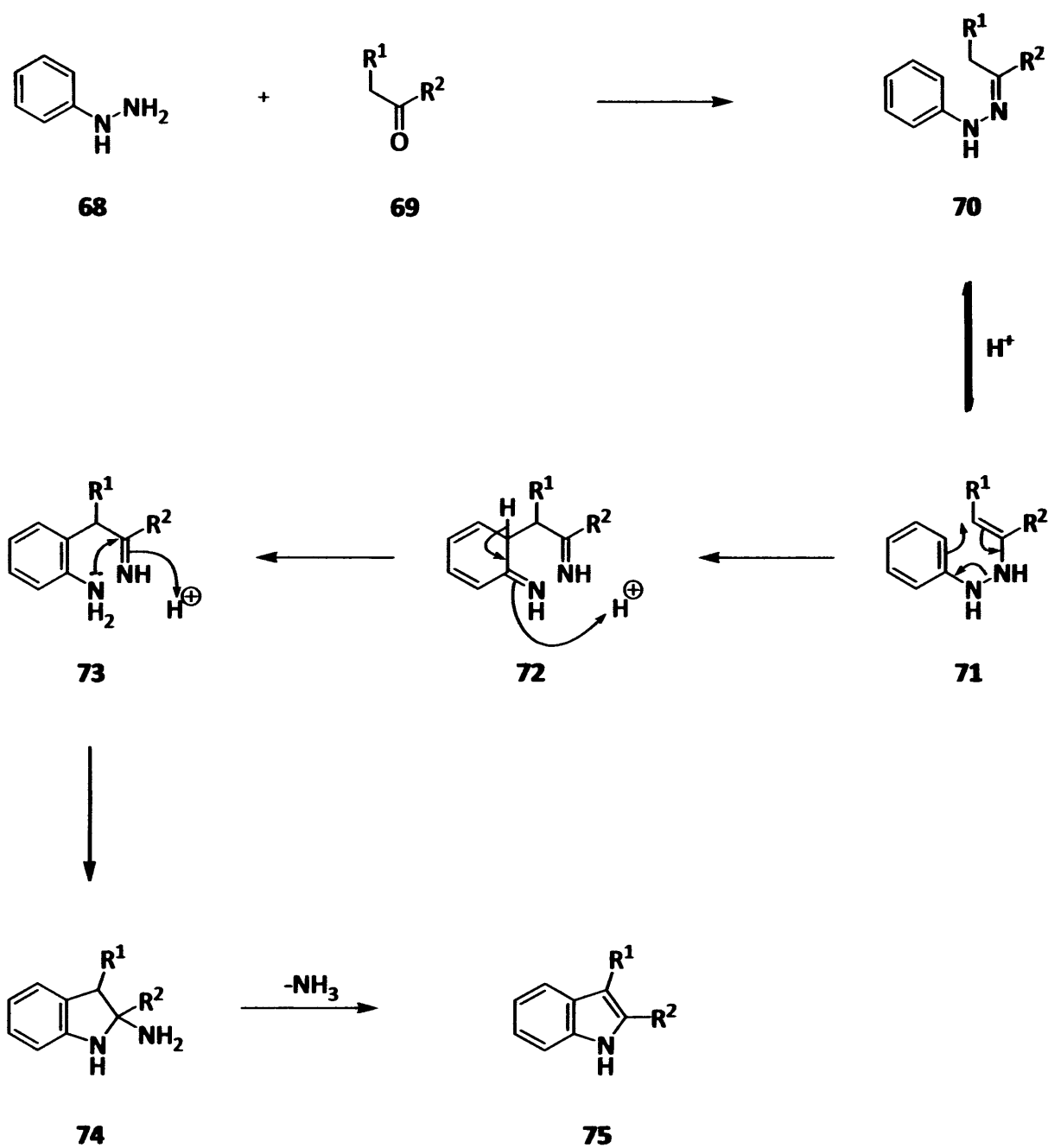
Scheme 21

1.3 Applications of [3,3]-sigmatropic rearrangements

The preceding schemes highlight the 'textbook' prevalence of these kinds of shifts; the following examples provide examples of [3,3]-sigmatropic rearrangements in synthetic, industrial and naturally occurring contexts.

1.3.1 The Fischer Indole Synthesis

Under acidic conditions, a phenylhydrazine **68** and an aldehyde or ketone **69**, react to give a phenylhydrazone **70**.⁴⁴ Protonation of this hydrazone **70** gives the enamine **71** (or ene-hydrazine); this species is set up for a [3,3]-sigmatropic rearrangement, which is driven by the cleavage of the weak N-N σ -bond and the formation of a stronger C-C bond. Rearomatisation of the double imine **72** furnishes a species **73**, which can undergo cyclisation to the aminoacetal intermediate **74**. Elimination of NH_3 and a proton shift then gives the indole **75** (Scheme 22).

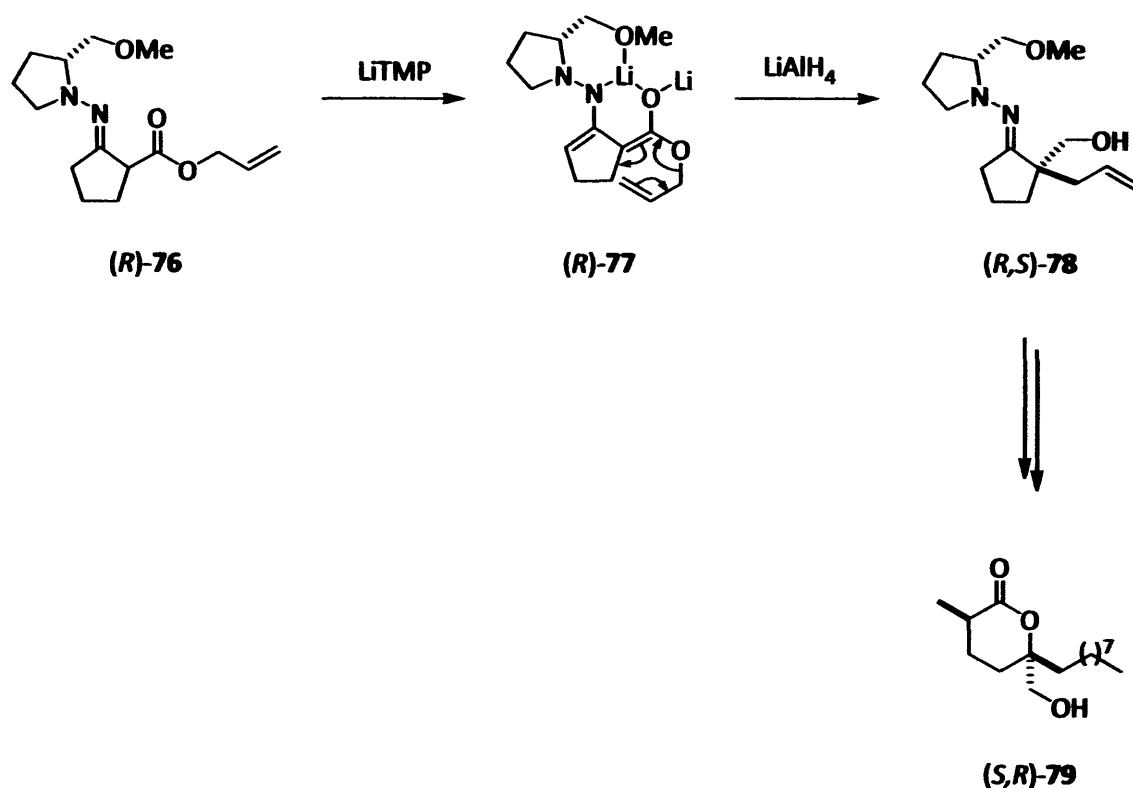


Scheme 22

First discovered in 1883 by Emil Fischer, this synthesis still has wide applicability in the chemical community, particularly the pharmaceutical industry, where the reaction is used in the preparation of tryptamine derivatives for the treatment of migraine. More recently, the synthesis has been accomplished in one pot under microwave conditions.⁴⁵

1.3.2 Total synthesis of (-)-Malyngolide

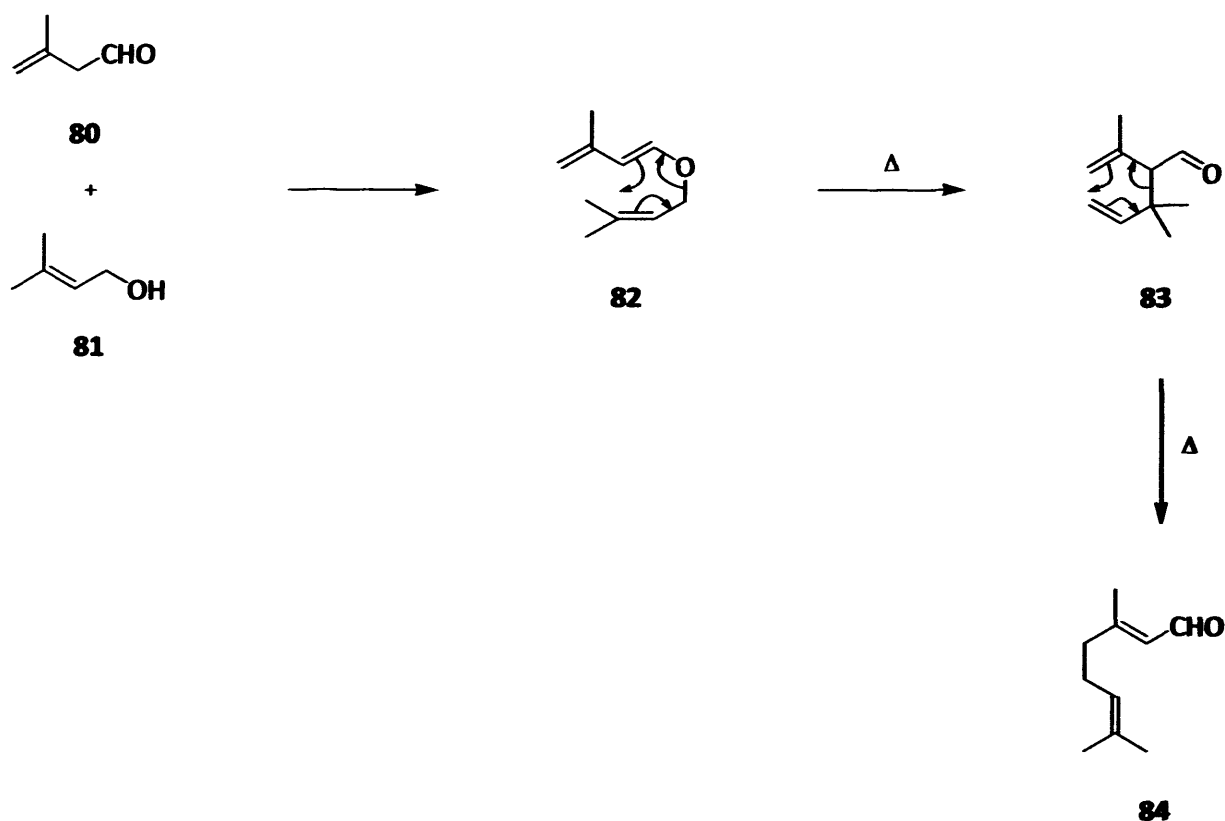
In 1996, Enders reported the synthesis of (-)-malyngolide (*S,R*)-**79**, an antibiotic isolated from the blue-green marine algae *Lyngbya majuscula*.⁴⁶ The key step is an asymmetric Carroll rearrangement (the transformation of a β -keto allyl ester into an α -allyl- β -ketocarboxylic acid) of the RAMP hydrazone (*R*)-**76**. Upon double deprotonation with 2.4 equivalents lithium 2,2,6,6-tetramethylpiperidide (LiTMP) in toluene the intermediate dianion (*R*)-**77** underwent rearrangement and was then immediately reduced with LiAlH_4 in diethyl ether to provide the quarternary hydrazone (*R,S*)-**78**. Further synthetic steps, including a Baeyer-Villiger oxidation, furnished the title compound (*S,R*)-**79** (Scheme 23).



Scheme 23

1.3.3 Industrial synthesis of citral

A key intermediate in the synthesis of vitamin A, citral **84** is manufactured on an industrial scale by BASF in a synthesis (from 3-methylbut-3-enal **80** and 3-methylbut-2-en-1-ol **81**) that involves two successive [3,3]-sigmatropic rearrangements: a Claisen followed by a Cope (Scheme 24).⁴⁷

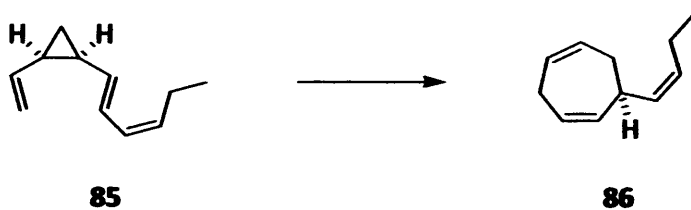


Scheme 24

The Claisen rearrangement of the allyl vinyl ether **82** is driven (as always) by the formation of a carbonyl group; the rearrangement product **83** is set up for a further (Cope) rearrangement, this being favoured by the formation of two trisubstituted double bonds and conjugation. On an industrial scale, this gave citral **84** in a 96.6% yield after purification by distillation.

1.3.4 A [3,3]-sigmatropic rearrangement in nature

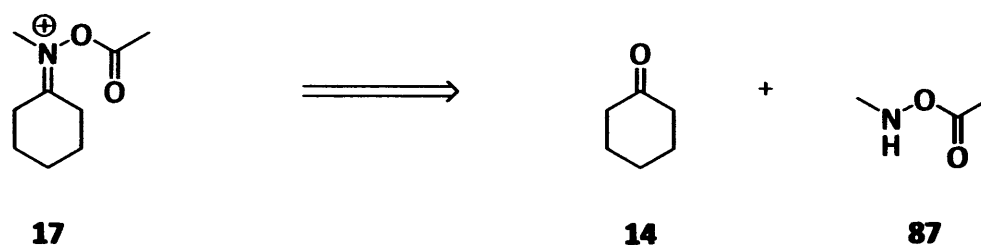
An example is found in the reproductive activity of the marine brown algae *Ectocarpus siliculosus*; whereby female gametes release a pheromone **85** to attract mobile male gametes. This species is deactivated, with a half-life of only several minutes, by a [3,3]-sigmatropic rearrangement to the inactive species **86** (Scheme 25).⁴⁸



Scheme 25

1.4 Previous group work

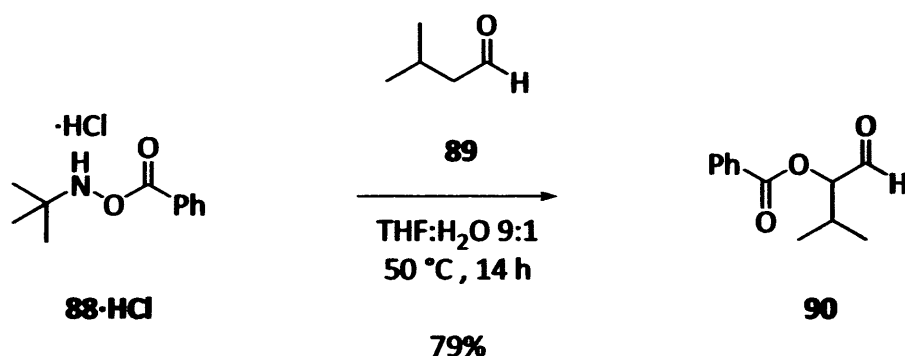
One of the projects carried out by the Tomkinson group was a natural progression from the work of House and Coates, and comprised a novel one-pot α -hydroxylation of carbonyl compounds. It was realised early on that the intermediate iminium salt **17**; which in the original synthesis was deprotonated and rearranged under basic conditions, could be disconnected across the C=N double bond to give an *N*-methyl hydroxylamine species **87** and the parent carbonyl compound **14** (Scheme 26); and this pointed the way towards a new class of reagent with which to affect the transformation.



Scheme 26

1.4.1 A novel oxygenation of aldehydes

N-*tert*-butyl-*O*-benzoyl hydroxylamine **88** was prepared by the reaction of *tert*-butylamine with benzoylperoxide (more details of this transformation are given in Chapter 2), and the reactivity of the new reagent **88·HCl** as the hydrochloride salt was probed with isovaleraldehyde **89**. In a solvent system comprising a 9:1 mixture of THF and water, the benzoate product **90** was isolated in 79% yield (Scheme 27).⁴⁹



Scheme 27

The transformation was found to be applicable to a range of aliphatic aldehydes, was tolerant of a variety of functional groups and also worked with cyclohexane carboxaldehyde to give the expected product with a quaternary carbon centre in excellent yield (Table 1).

It was believed that this represented a novel and innovative means of performing the analogous transformation to that reported by House in one-pot and in good yields over a general range of aldehyde substrates. Crucially for the group, this was a metal-free process, which proceeded under aqueous and aerobic reaction conditions. As such, this process enjoyed several advantages over the traditional methods for this transformation.

One limitation at that time was that the reaction was not applicable to ketone substrates; however it was reasoned that the current reagent allowed for complete chemoselective control for aldehydes over ketones.

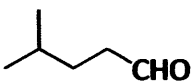
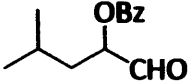
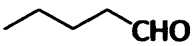
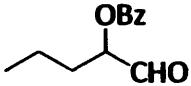
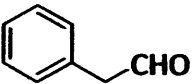
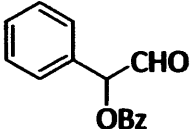
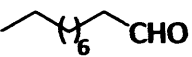
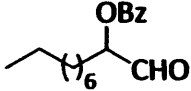
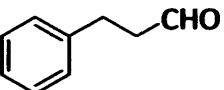
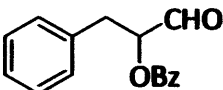

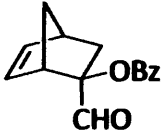
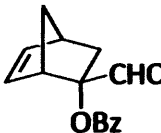
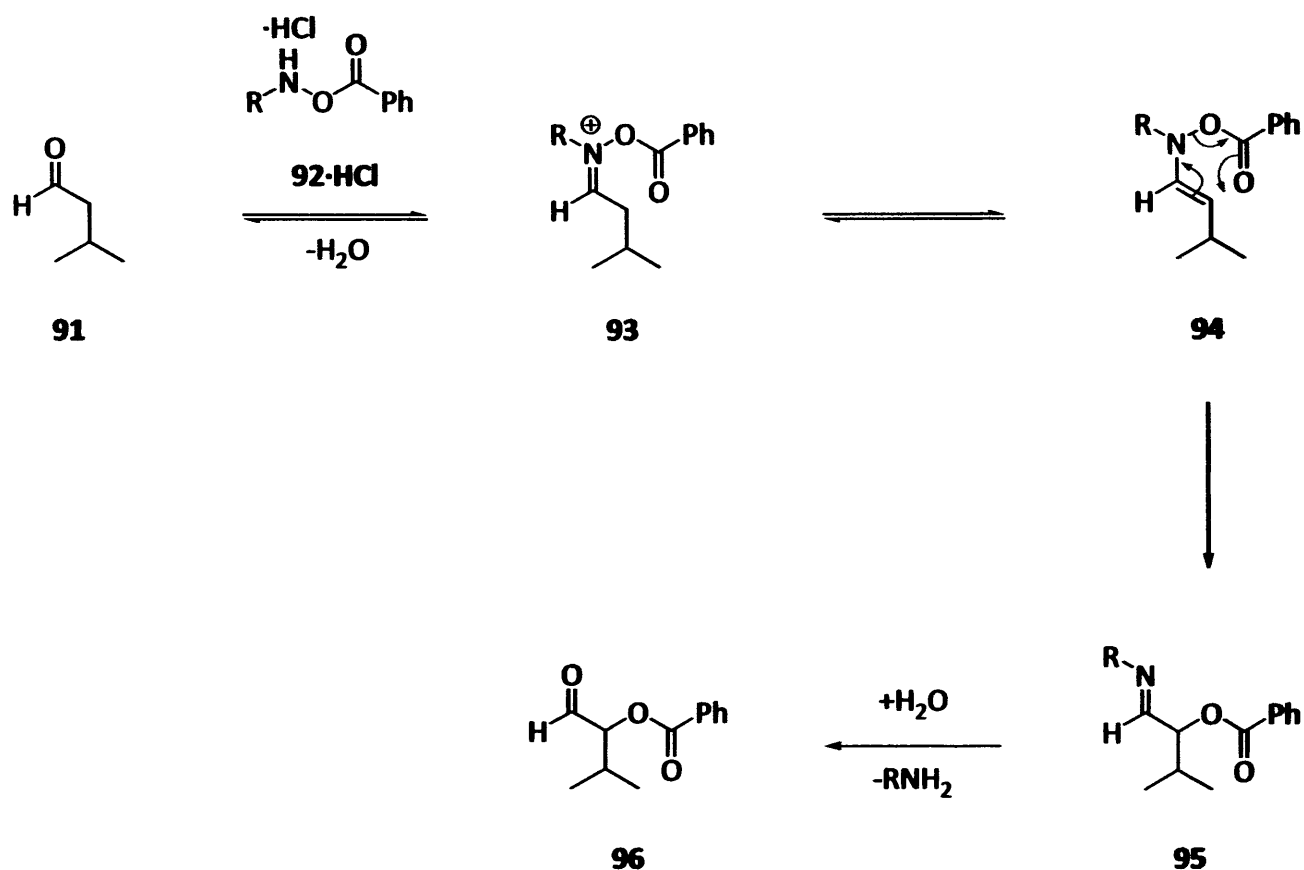
Entry	Substrate	Product	Yield (%)
1			72
2			76
3			67
4			74
5			69
6		 	62

Table 1: The α -oxygenation of aldehydes by *N*-*tert*-butyl-*O*-benzoyl hydroxylamine 88-HCl

Mechanistically, it was proposed that the process proceeded *via* condensation of the aldehyde **91** with the reagent **92-HCl** to give an iminium ion **93**, followed by loss of an α -hydrogen to give the enamine **94**. This underwent a concerted, pericyclic rearrangement to give an α -benzoyloxy imine **95**, which was subsequently hydrolysed under the aqueous acidic reaction conditions to give the observed product **96** (Scheme 28).

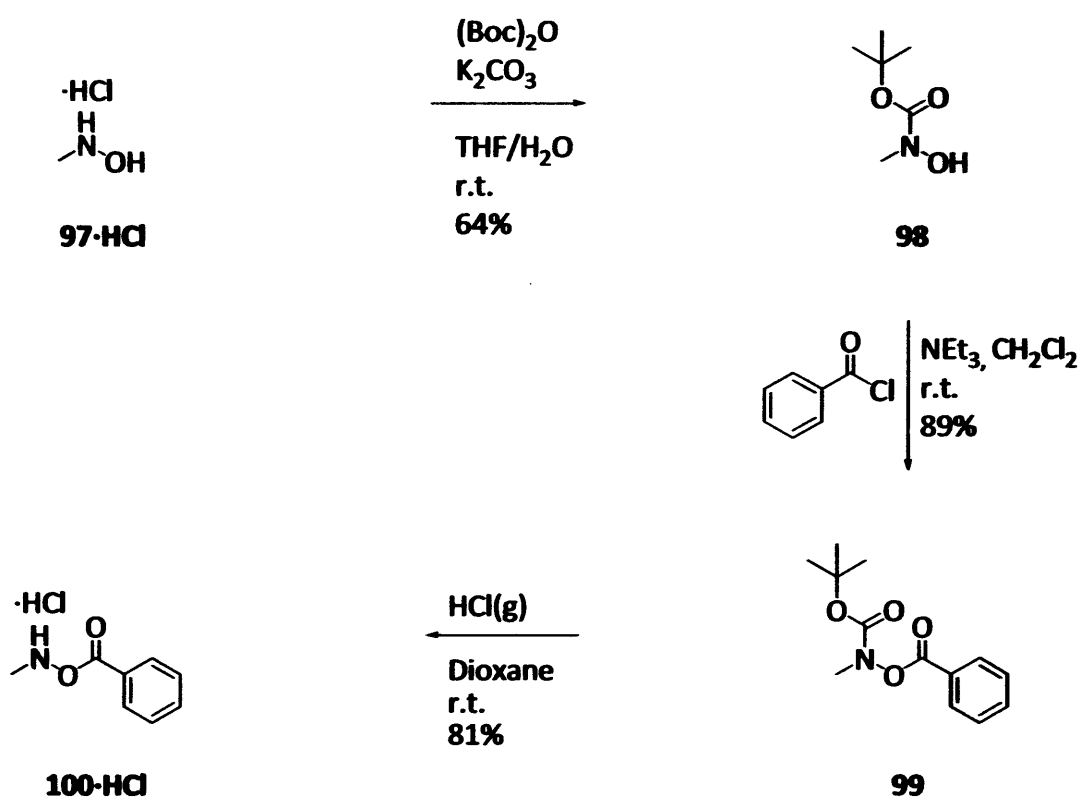


Scheme 28

The lack of reactivity of the hydroxylamine species **92·HCl** with ketone substrates was rationalised by considering the steric hindrance about the nitrogen lone pair as a consequence of the bulky *tert*-butyl group. This was thought to prevent formation of the initial iminium ion with the more hindered ketones, whilst permitting reaction with the less encumbered aldehyde group. In spite of this drawback, the group were encouraged that the process had potential to be developed as a chemoselective process by careful choice of reagent.

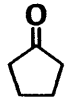
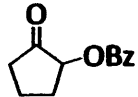

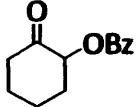
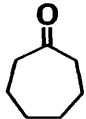
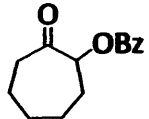
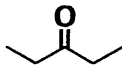
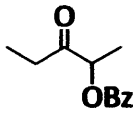
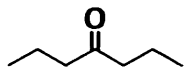
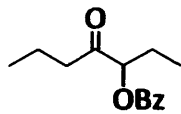
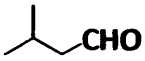
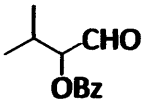
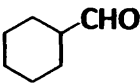
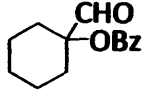
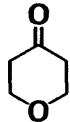
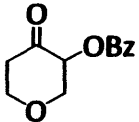
1.4.2 A general method for the α -acyloxylation of carbonyl compounds

Preparation of *N*-methyl-*O*-benzoyl hydroxylamine hydrochloride **100-HCl** furnished a reagent which affected the transformation with ketones as well as aldehydes, thus adding to the applicability of the procedure.⁵⁰ This compound was prepared via a 3-step synthesis involving initial protection of the nucleophilic nitrogen of commercially available *N*-methyl hydroxylamine hydrochloride **97-HCl** with di-*tert*-butyl dicarbonate, *O*-acylation with benzoyl chloride and subsequent Boc-deprotection of the adduct **99** with hydrochloric acid in dioxane to give the target compound as the hydrochloride salt **100-HCl**, with all steps proceeding in good to excellent yields (Scheme 29).



Scheme 29

With the new reagent in hand, the optimum reaction conditions were found to be stirring with a carbonyl substrate at ambient temperature using dimethylsulfoxide as solvent, which affected consistently higher yields and cleaner transformations. Selected results are outlined in Table 2.

Entry	Substrate	Product	Yield (%)
1			73
2			80
3			69
4			74
5			90
6			92
7			74
8			79

Entry	Substrate	Product	Yield (%)
9			75
10			75
11			70
12			72
13			76
14			69
15			92
16			82

Table 2: α -Oxygenation of ketones by *N*-methyl-*O*-benzoyl hydroxylamine hydrochloride 100-HCl

The reaction worked well for a variety of ring systems (entries 1–3), as well as acyclic ketones (entries 4 and 5), although this class of substrates required that the reaction mixtures be warmed to 50 °C in order to achieve maximum conversion to product after 24 h. Aldehydes underwent functionalisation into both secondary (entry 6) and tertiary centres (entry 7), and this suggested that *N*-methyl hydroxylamine hydrochloride **100-HCl** was indeed a general reagent for the α -functionalisation of carbonyl compounds.

Different functional groups elsewhere in the molecule were well tolerated – the presence of ethers (entry 8) and hydrolytically sensitive groups such as esters (entry 10) and ketals (entry 11) not proving detrimental to the outcome of the reaction.

As a rule of thumb, the thermodynamically more stable product was given. For example, the *cis*-substituted isomer was the sole product of the reaction between 4-*tert*-butyl cyclohexanone with 1 equivalent of the reagent **100-HCl** (entry 13), with no trace of the *trans* diastereoisomer being detected by ^1H NMR. However, the less sterically demanding 4-methyl cyclohexanone led to a 1:1 mixture of diastereoisomers being isolated (entry 12).

A variety of aromatic systems were employed to good effect. Although the reaction times were somewhat slower in comparison with other acyclic ketones, good yields were observed for the reactions with propiophenone (entry 14), electron rich (entry 15) and electron deficient aromatics (entry 16).

1.4.3 The methodology extended

In addition to the family of hydroxylamine reagents which were effective for the oxyacylation of aldehydes and ketones, further work within the group resulted in the development of reagents **101-103**, capable of direct introduction of carbonates,⁵¹ carbamates⁵² and oxytosylates (Figure 6).⁵³

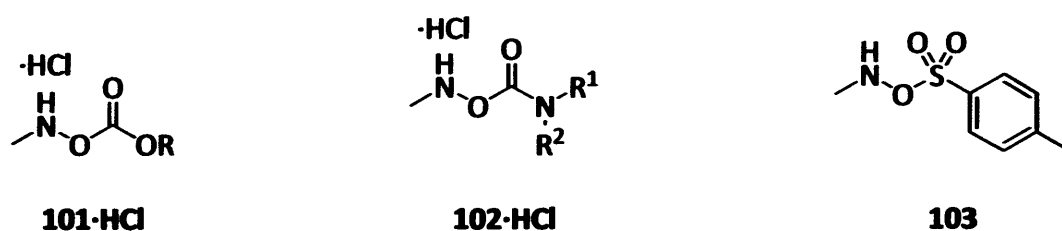
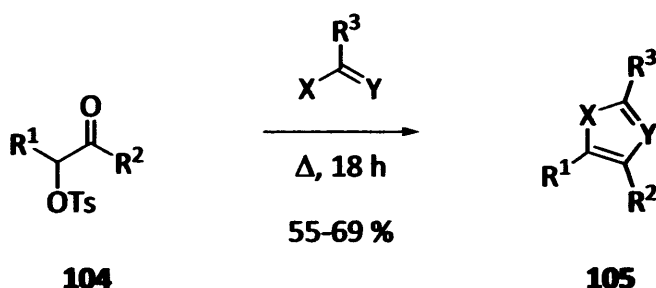


Figure 6

Extending the family of reagents gave reactions that proceeded smoothly at room temperature in the presence of both moisture and air and with good functional group tolerance in the substrate. With nonsymmetrical carbonyl compounds, the preference for the functionalisation of secondary over primary centres was observed with each substrate.

With the oxytosylating family of reagents **103**, it was found that addition of a bis-heteronucleophile directly to the crude reaction mixture in a one-pot process led to the corresponding heterocyclic product **105** (Scheme 30).

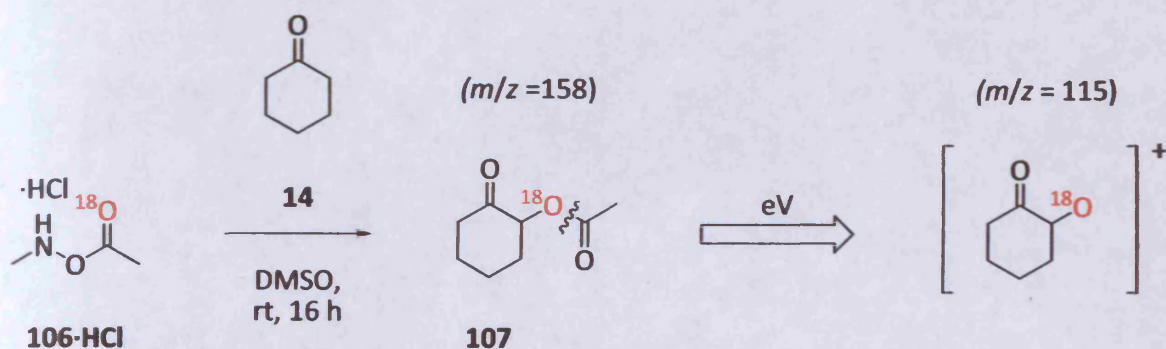


Scheme 30

1.4.4 Testing the mechanism

From the inception of this work, the group were mindful that definitive proof for the proposed mechanism would be impossible. However, we strove to understand the transformation, and understood that probing the transformation ought to allow us to uncover at least some evidence in favour of (or disproving) the supposed mechanistic pathway.

Accordingly, the O-labelled reagent **106** (prepared from commercially available acetic acid- $^{18}\text{O}_2$) was used in the α -oxyacylation of cyclohexanone **14** to give the ^{18}O -labelled adduct **107** (Scheme 31).

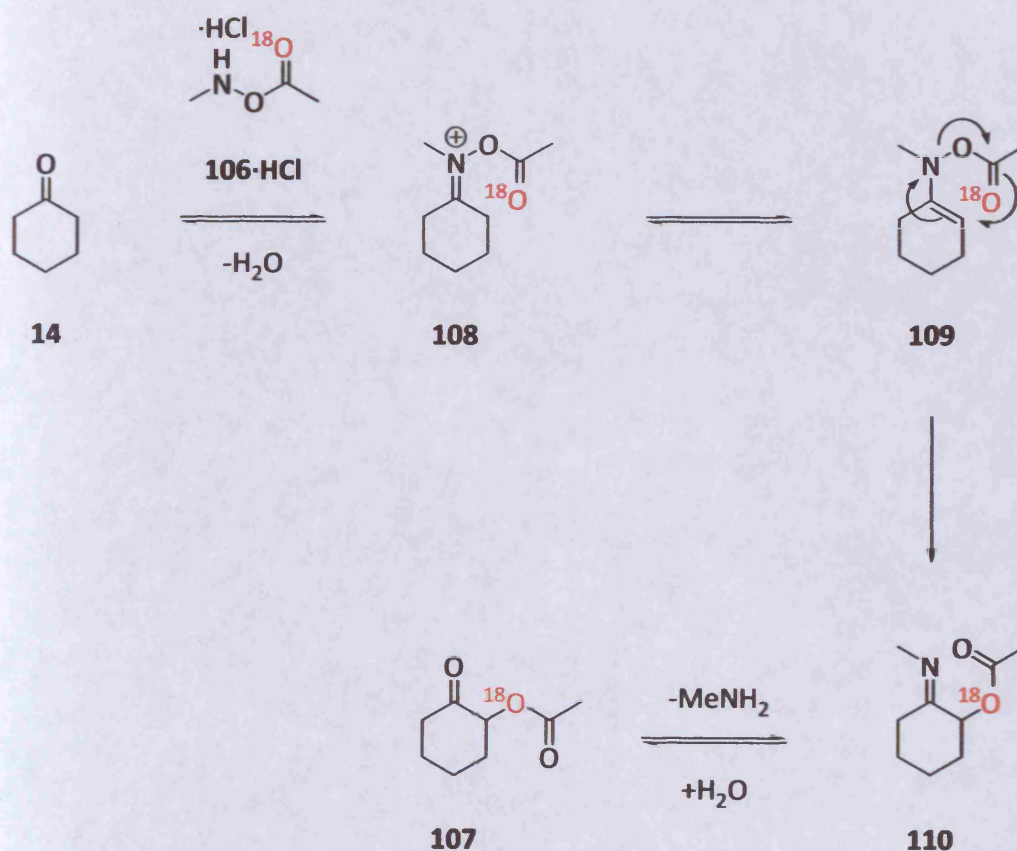


Scheme 31

Mass spectroscopy of the reaction product after silica gel chromatography showed that this consisted exclusively of ^{18}O -labelled 2-oxocyclohexyl acetate **107**, with no unlabelled product being observed.

As Scheme 32 shows, this result lent some credence to our mechanistic hypothesis, particularly with respect to the [3,3]-sigmatropic rearrangement step. Condensation of cyclohexanone **14** with the O-labelled hydroxylamine hydrochloride **106-HCl** gave the expected iminium **108**. This species, after deprotonation, gave an enamine **109** where the labelled oxygen was in the correct position to form the rearrangement product **110**.

The subsequent hydrolytic step furnished the labelled α -oxy ketone **107**, and the proposed mechanism rationalised the observed result, in which 100% incorporation of the ^{18}O was seen.



Scheme 32

[3,3]-Sigmatropic rearrangements are well-documented in the literature as a commonly occurring feature in organic synthesis and in nature. In the course of our research, we wished to define the mechanistic course of the α -oxygenation procedure with respect to the preceding and subsequent steps within this intriguing and useful transformation.

Chapter 2: Project Design and Planning

From the standpoint of the group, a methodology had been developed which enabled an α -oxygenation reaction of carbonyl compounds to be performed smoothly and efficiently. It was strongly believed that the transformation in its then current form constituted a powerful piece of methodology; the most advantageous features of which were as follows:

- Clean reaction mixtures and generally good product yields
- A procedure which was general to aldehyde and ketone functionalities
- Tolerated a wide variety of functional groups elsewhere in the substrate (which may also be either cyclic or acyclic)
- Toleration of the presence of moisture and air in the reaction mixture
- Proceeded without the need for potentially toxic metal-based catalysts

Looking to the future, the key question was how best to proceed with this work – namely to establish sufficiently realistic yet still ambitious goals for the three-year project we were about to undertake.

Within the Tomkinson group, a central ethos was to create new methodologies, under metal-free conditions with which to carry out familiar functional group manipulations and transformations. Clearly, it was felt that this goal had been already realised to a large extent; yet we drew some inspiration from recent developments reported in the field of organocatalysis.

In common with the groups at the forefront of this research, our aim was to develop simple, practical transformations, using environmentally benign reagents and reaction media; affording easily reproducible methodologies which could be applied to entire classes of compounds – as opposed to isolated examples of purely academic interest. Clearly, such a procedure would have broad applicability within organic synthesis as a whole, including the preparation of natural products and other complex and highly functionalised biologically active compounds.

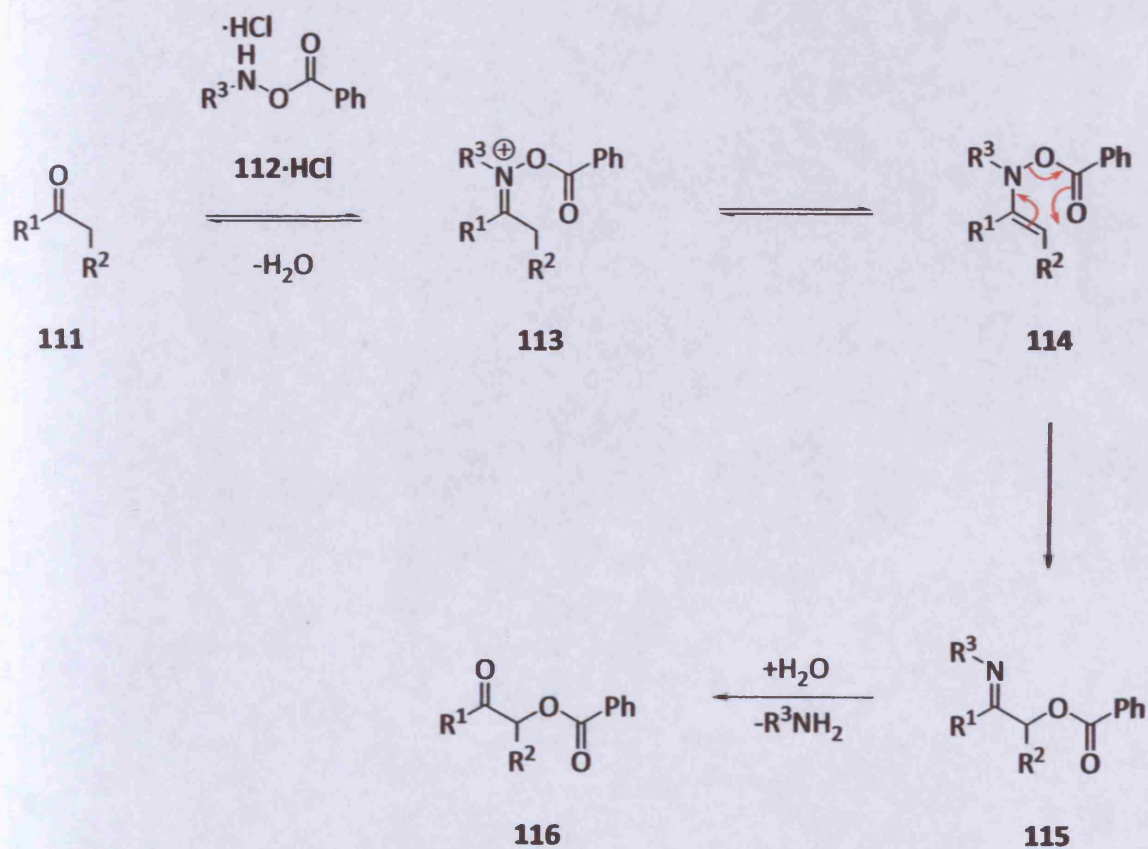
This did not necessarily mean that we were considering a total synthesis of a natural product as the best way of developing our transformation; rather, that a worthy goal would be to report a methodology which would stand alongside the existing methods in metal-free organic synthesis.

Considering this, along with the fact that the pioneering work described in the literature^{22, 23} used cyclic secondary amines in sub-stoichiometric quantities to catalyse asymmetric organic transformations, pointed the way forward in terms of the direction the project should take. It was therefore decided that at the outset we should attempt to develop a catalytic variant of the α -oxygenation procedure. This research, if successful would therefore extend the utility of the procedure and thus facilitate its uptake by the wider chemical community.

Since there were a large number of variations we would need to consider and address in order to fully optimise any proposed catalytic cycle, it was thought that initially focusing on a sub-stoichiometric variant of the transformation would prove to be a more efficient means of conducting this research.

2.1 Development of a novel catalytic procedure

Scheme 33 portrays the reaction sequence as we had become accustomed to visualising it in a mechanistic sense. For us to be successful with any catalytic cycle, it was necessary to have a fundamental understanding of the transformation taking place. As it stood, we knew that addition of a stoichiometric amount of the general reagent **112·HCl** (≥ 1 equivalent) to a carbonyl compound **111**, generated one equivalent of the α -oxygenated adduct **116**, together with one equivalent of primary amine, and that this amine was removed from the reaction mixture by acidic aqueous work-up.

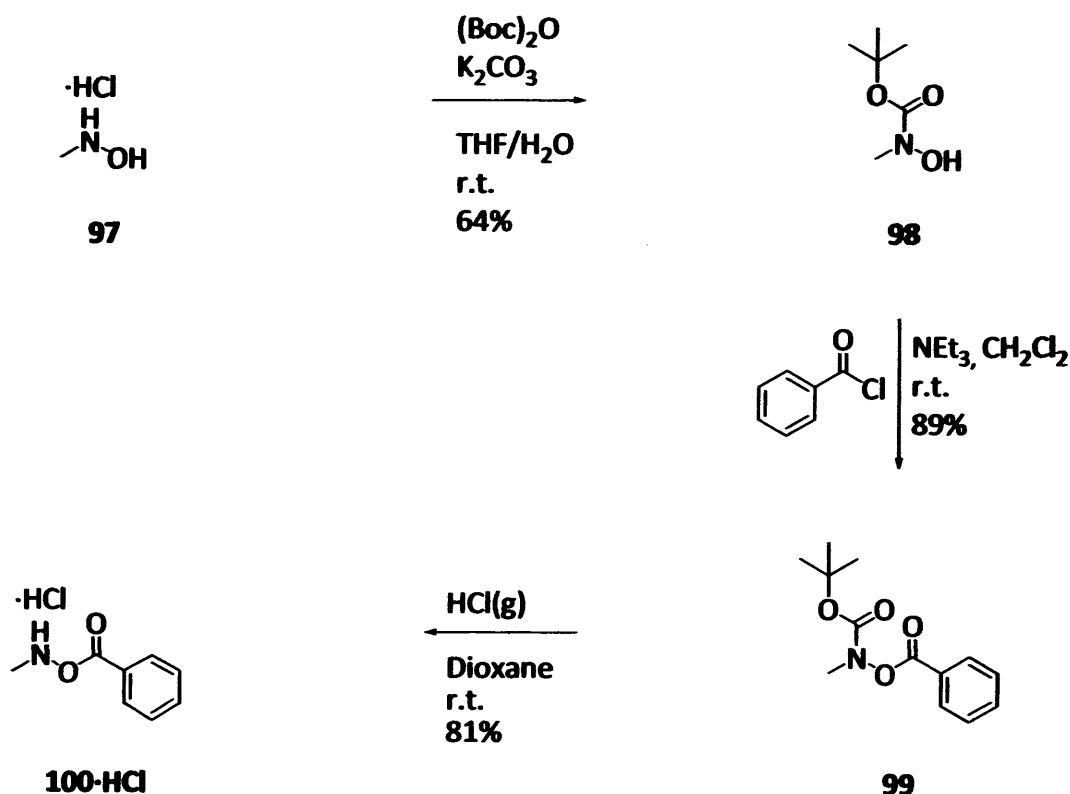


Scheme 33

The reaction was thought to occur by initial nucleophilic attack of the nitrogen lone pair on the carbonyl compound **111**, followed by the elimination of a molecule of water to form an iminium ion **113**. Loss of an α -proton yielded an enamine **114**, which then underwent a concerted, pericyclic, [3,3]-sigmatropic rearrangement to produce an α -benzoyloxyimine **115**. Hydrolysis of the imine generated the α -functionalised species **116** together with a molecule of primary amine.

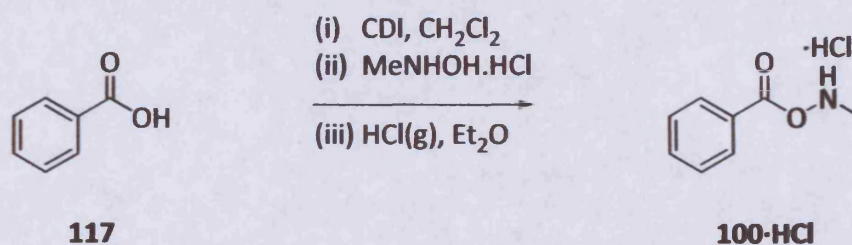
A clear protocol for the reaction to become catalytic would be to develop a method of regenerating the hydroxylamine species **112** *in situ*. At this stage, there were 2 working methods for the synthesis of hydroxylamine reagents bearing relatively simple *N*-alkyl groups:

- Starting from the parent hydroxylamine, successive Boc-protection, *N*-acylation and Boc-deprotection under acidic conditions to give the desired reagent as the hydrochloride salt (Scheme 29).



Scheme 29

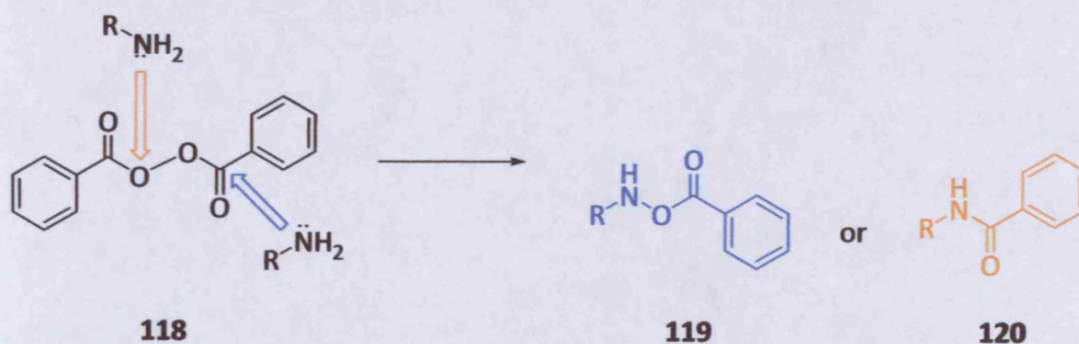
- The CDI-promoted coupling of benzoic acid with hydroxylamine (Scheme 34).



Scheme 34

Whilst the latter was a more direct route to the target reagent, the preparation comprised two steps in a practical sense owing to the necessity of bubbling hydrogen chloride gas through the mixture to generate the salt **100-HCl**. Therefore, this was considered to be an impractical means of regenerating material during a catalytic process.

It was noted from the literature that the conversion of primary amines to hydroxylamines could be accomplished using dibenzoyl peroxide **118** as oxidant.⁵⁴ Early studies by Milewska identified two competing pathways for the reaction; namely *N*-oxidation to form the desired hydroxylamine **119**, or *N*-acylation to give an undesired amide by-product **120** (Scheme 35).⁵⁵

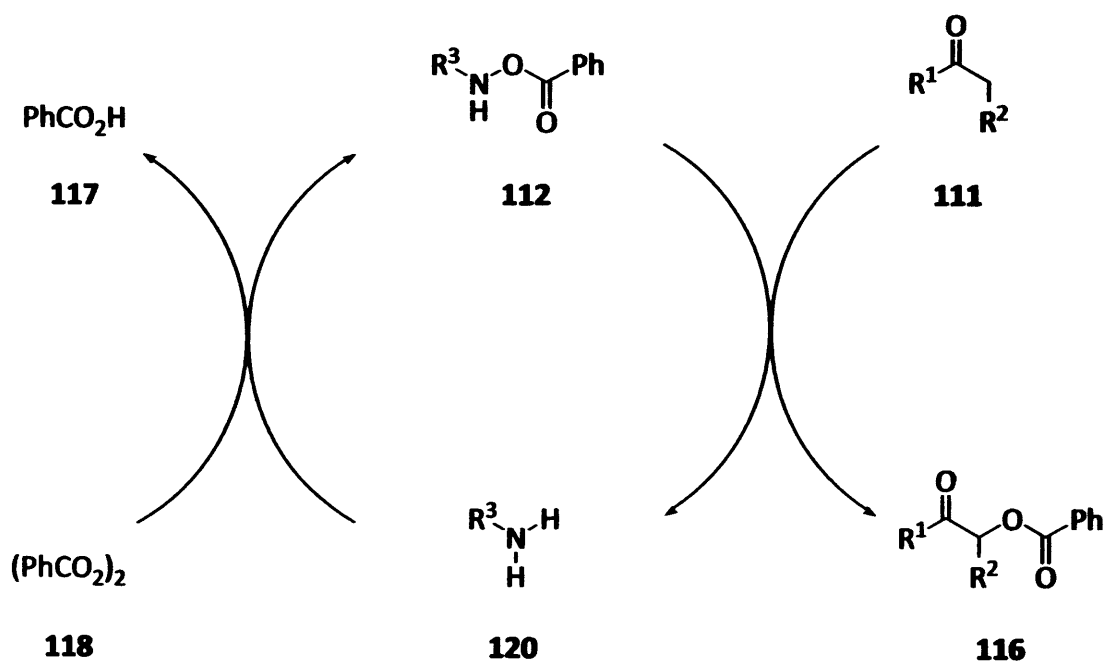


Scheme 35

An optimisation of this procedure by Phanstiel developed conditions for the reaction in a biphasic mixture of CH_2Cl_2 and an aqueous phosphate buffer, which was necessary to neutralise benzoic acid **117** as it was formed and to maintain the optimal pH for *N*-oxidation throughout the duration of the reaction.⁵⁶

It was shown that the highest yields of the desired *N*-oxidation product **112** were obtained when equal volumes of pH 10.5 phosphate buffer solution and a 0.1 M solution of amine in dichloromethane were stirred together at room temperature with 2 equivalents of benzoyl peroxide **118**.

For the α -oxygenation reaction, a catalytic variant (Scheme 36) was therefore proposed, in which the reagent was formed by the condensation reaction between a primary amine **120** and dibenzoyl peroxide **118** to yield the target reagent **112** with the formation of benzoic acid **117**. The *O*-benzoyl hydroxylamine hydrochloride **112·HCl** had been shown to readily undergo reaction with carbonyl compound **111** as previously described (Scheme 33), to give the α -oxygenated adduct **116** after hydrolysis of the imine product **115** of the proposed [3,3]-sigmatropic rearrangement, and regenerating the starting amine **120**.



Scheme 36

When we initially began to evaluate our proposed catalytic process, it was immediately apparent that there were many variables which could be explored in order to establish and optimise the catalytic cycle; for example, the structure and reactivity of the amine **120** (nature of R³), the solvent, the carbonyl substrate **111** and the reaction conditions including concentration, temperature, catalyst loading and pH.

From the outset there were several synthetic challenges to be overcome if the proposed catalytic cycle was to become viable. The Phanstiel method, although instrumental in optimising the reaction with respect to the formation of hydroxylamines, was not able to entirely eliminate the formation of unwanted amide **119**, a factor which could have limiting ramifications in terms of shutting down our catalytic reaction sequence before completion.

In the course of previous studies, the reactions between the general carbonyl compound **111** and the hydroxylamine **112-HCl** were carried out under acidic conditions, using the hydrochloride salt as the proton source. However, the Phanstiel process achieved optimal yields of the desired hydroxylamine adduct under basic conditions. Therefore, within the proposed catalytic cycle (Scheme 36) there were two major transformations, whose optimal pH conditions were mutually opposed.

The real synthetic challenge was therefore to find some variant of the proposed catalytic cycle which combined all the components successfully within a single pot so that each step was tolerant and compatible with the reaction conditions.

Importantly however, the work of Coates (see Scheme 7, Chapter 1) indicated that the key rearrangement step could occur under basic conditions;²⁷ hence there was potentially some scope for altering the pH profile of the transformation.

It was thought that resolving the pH dichotomy would enable the two principal bond-forming components of the catalytic cycle to be linked together successfully, thereby fulfilling the initial aim of the project. From that point it would hopefully be possible to develop and optimise a catalytic process.

From Scheme 33, we reasoned that a proton source was necessary to activate the carbonyl group to nucleophilic attack from the hydroxylamine nitrogen. To this end, one of the first avenues of investigation would be the use of Lewis acids to catalyse the formation of the enamine intermediate **114** in the α -oxygenation reaction, instead of the established Brønsted acid approach. If successful, this would potentially enable the reaction to be carried out under non-protic conditions.

A further goal from the outset of the project was the preparation of novel reagents, which could potentially promote catalysis. The theory was that fundamental changes in reactivity may be accomplished by changing the nature of the nitrogen substituent, and we were intrigued by the possibilities that this line of investigation offered – particularly as we had so far only examined hydroxylamine reagents bearing simple *N*-alkyl groups.

A common theme in many of the reported organocatalysts was the presence of a heteroatom several atoms away from the reactive amine nitrogen (i.e. which was directly involved in iminium ion formation) capable of hydrogen-bonding and thereby potentially stabilising a transition state.

Examples include the abundance of organocatalytic reactions using L-proline **12**, as well as specifically: the Mannich reaction catalysed by (*S*)-1-(2-pyrrolidinylmethyl)pyrrolidine **121**,⁵⁷ the amino alcohol catalysed direct asymmetric aldol with L-prolinol **122**⁵⁸ and enantio- and diastereoselective Michael addition reactions using (*S*)-2-(morpholinomethyl)-pyrrolidine **123**⁵⁹ (Figure 7) all involved a heteroatom β - to the reactive nitrogen in the formation of an intermediate iminium ion. Our speculation was that the presence of the heteroatom may assist formation of the iminium ion by acting as either a hydrogen bond donor and/or acceptor.

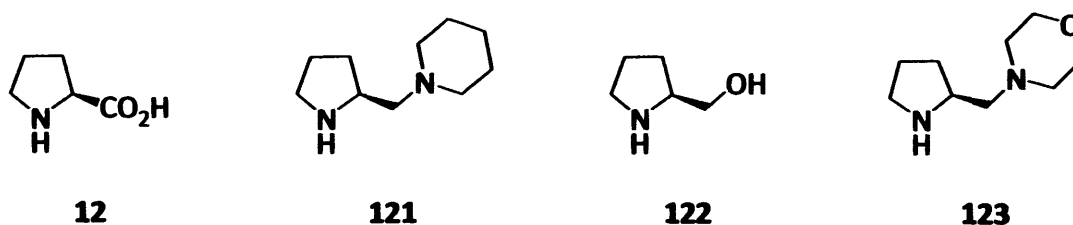
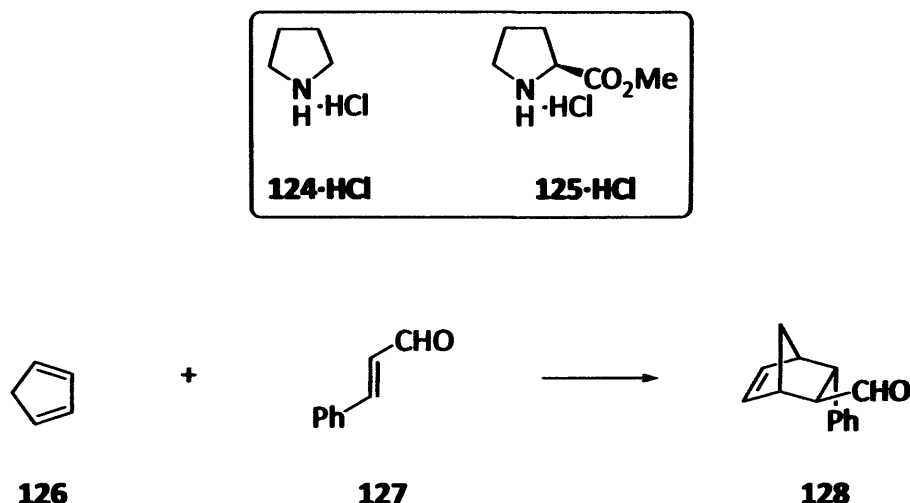


Figure 7

Closer to home, another member of the Tomkinson group working on the α -effect in iminium ion catalysis, had found that pyrrolidine hydrochloride **124·HCl** was ineffective in catalysing the Diels-Alder reaction between cyclopentadiene **126** and cinnamaldehyde **127** in comparison to proline methyl ester hydrochloride **125·HCl** (Scheme 37).⁶⁰



Scheme 37

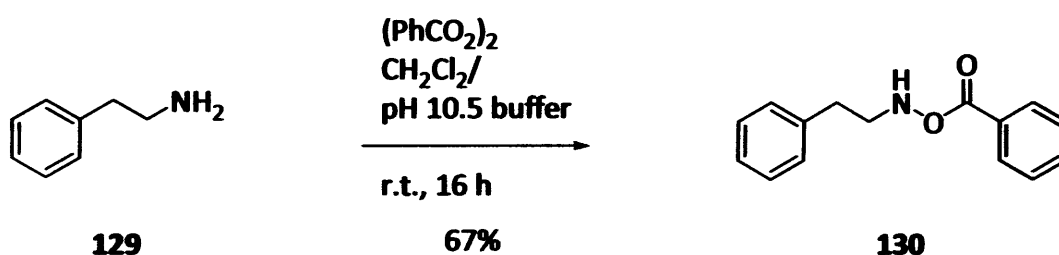
In terms of the structure of our oxygenating reagent, we decided to ascertain whether any changes in the steric and/or electronic properties of the α -oxygenating reagent might have a positive effect on the outcome of the reaction, where the reagent is used as its free-base rather than the hydrochloride salt (previous experiments with the free-base of the existing reagents **88·HCl** and **100·HCl** had been unsuccessful). In tandem with this, we anticipated carefully choosing experimental conditions with which we could explore the effect of the solvent, the carbonyl substrate and the reaction conditions including concentration, temperature, catalyst loading and pH.

Chapter 3: The First 6 Months

3.1 Activation by Lewis acids

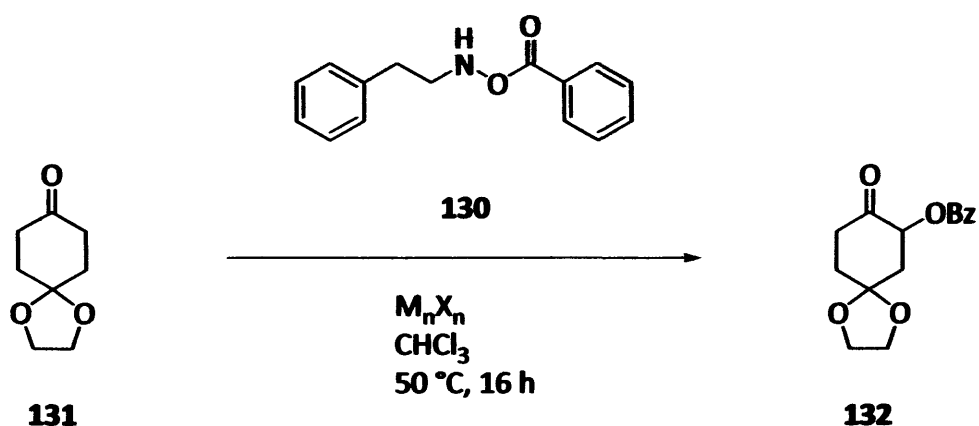
In the early stages, Lewis acid catalysis of the α -oxygenation reaction was briefly investigated as a potential means for working around the pH problem inherent within the proposed catalytic cycle. The use of a Lewis acid in order to activate carbonyl compounds had long been known in the literature,⁶¹ and we sought to utilise this phenomenon in order to promote the formation of the initial iminium ion **113** within the α -oxygenation reaction.

N-Phenethyl-*O*-benzoyl hydroxylamine **130** was prepared as the free base in good yield under Phanstiel conditions (Scheme 38). Reaction of 2-phenylethylamine **129** with benzoyl peroxide **118** at room temperature gave the desired hydroxylamine **130** in 67% isolated yield after purification by column chromatography. Analysis of the crude reaction mixture by ^1H and ^{13}C NMR indicated that the majority of the remaining material comprised the amide by-product.



Scheme 38

Reagent **130** was taken into the α -oxygenation procedure with cyclohexanedione-*mono*-ethylene ketal **131** in the presence of several Lewis acidic species using chloroform as the reaction medium (Scheme 39).



Scheme 39

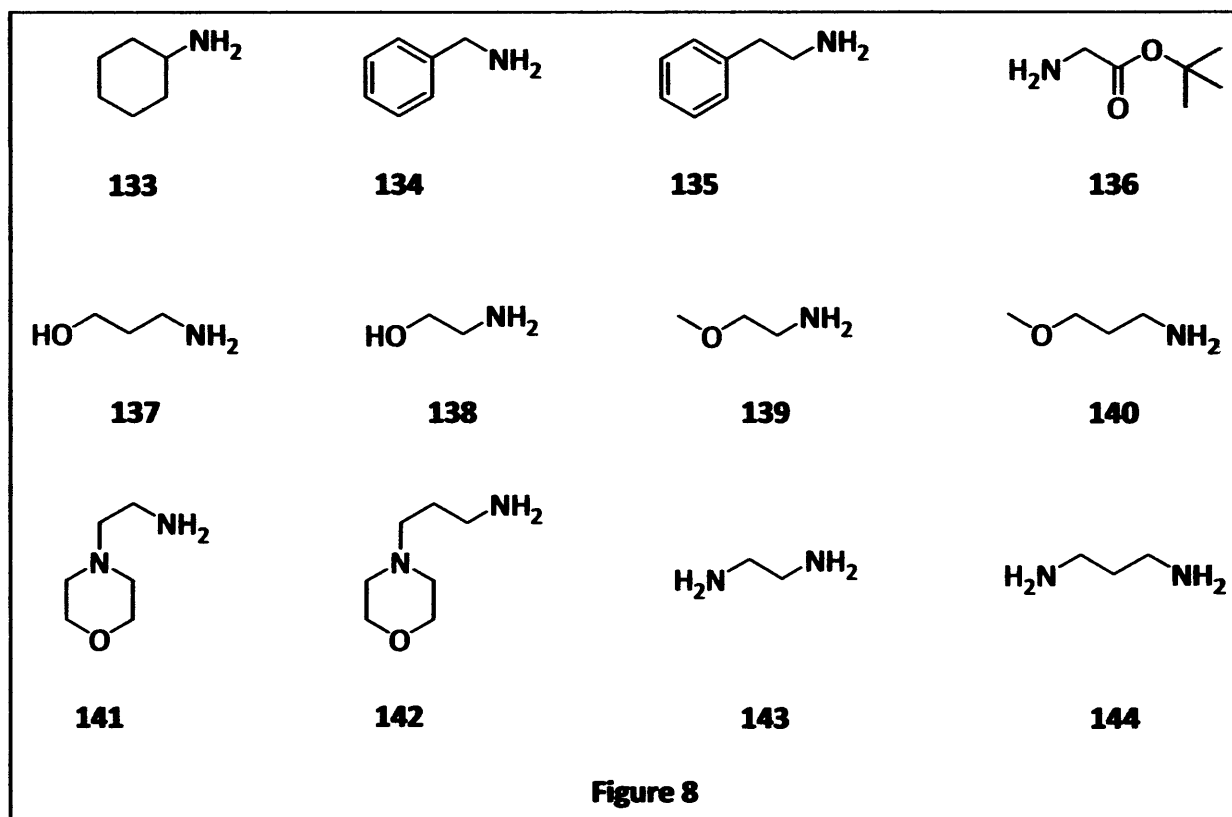
Metallic species from across the Periodic Table – i.e. from the alkali and alkali earths, several transition metals, the p-block and the lanthanides – were chosen in order to attempt a brief, but representative scan of various metallic species within the α -oxygenation reaction. The reaction was conducted in the presence of ZnBr_2 , LiCl_2 , InCl_3 , MnBr_2 , KI and $\text{Yb}(\text{OTf})_3$.

In all but two cases, no reaction was detected by ^1H NMR. However, a small trace of product (not exceeding 10 % conversion) was detected in the crude reaction mixtures when indium trichloride and ytterbium triflate were used as Lewis acids. While the indications were that reaction yields under these conditions would be very poor, and this in turn meant that further involved study of these systems was not necessarily warranted, the fact that a positive result was obtained at all suggested that the α -oxygenation reaction need not be confined to conditions of Brønsted acidity. We therefore drew some encouragement from this.

3.2 Structure of reagent

Thoughts turned to the structure of the hydroxylamine reagent, in order to ascertain whether any changes in the steric and/or electronic properties of the α -oxygenating species might have a positive effect on the outcome of the reaction. In general terms, we believed that the transformation had been optimised to some extent during the development of the methodology, and that further work in terms of varying solvents, concentration, and reaction stoichiometry would be futile. We therefore elected to examine the effect of altering the structure of the nitrogen substituent.

A series of hydroxylamines were targeted from the reaction of the corresponding primary amines **133-144** with dibenzoyl peroxide **118** under standard Phanstiel conditions (Figure 8).



Unfortunately, the Phanstiel method did not work universally for the amines **136**, **137**, **138**, **141**, **142**, **143** and **144**; such that preparation of the corresponding *O*-benzoyl hydroxylamines failed to give any appreciable yield of target compound.

In general, the Phanstiel method was found to be at its least applicable where the starting amine incorporated a heteroatom. This correlated somewhat with the findings in the original paper, whereby the procedure was limited to benzylic and aliphatic amines.⁵⁶

It was proposed that many of these unsuccessful substrates were more soluble in the aqueous buffer phase than in dichloromethane, and therefore that reaction of these amines with benzoyl peroxide in a biphasic system was more difficult than for the more hydrophobic molecules. However, a brief study indicated that all of the amines were partitioned preferentially in the aqueous phase to some extent; it was therefore concluded the lack of reactivity on the part of certain amines towards benzoyloxylation was not a result of their solubility.

This was somewhat frustrating, given our interest in preparing reagents containing a heteroatom – both from a literature standpoint and based on previous results within the group (see Chapter 2). The hydroxylamine product **145** derived from ethanolamine **138** represented a particularly attractive target for study, most notably because of the shared architecture with L-proline **12**, with respect to the presence of an oxygen atom two carbon atoms away from the reactive nitrogen (Figure 9). Several attempts at forming this reagent using the standard Phanstiel protocol failed.

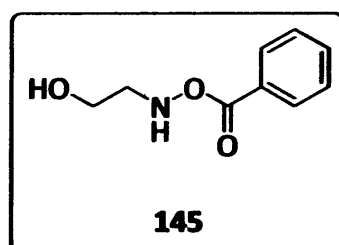
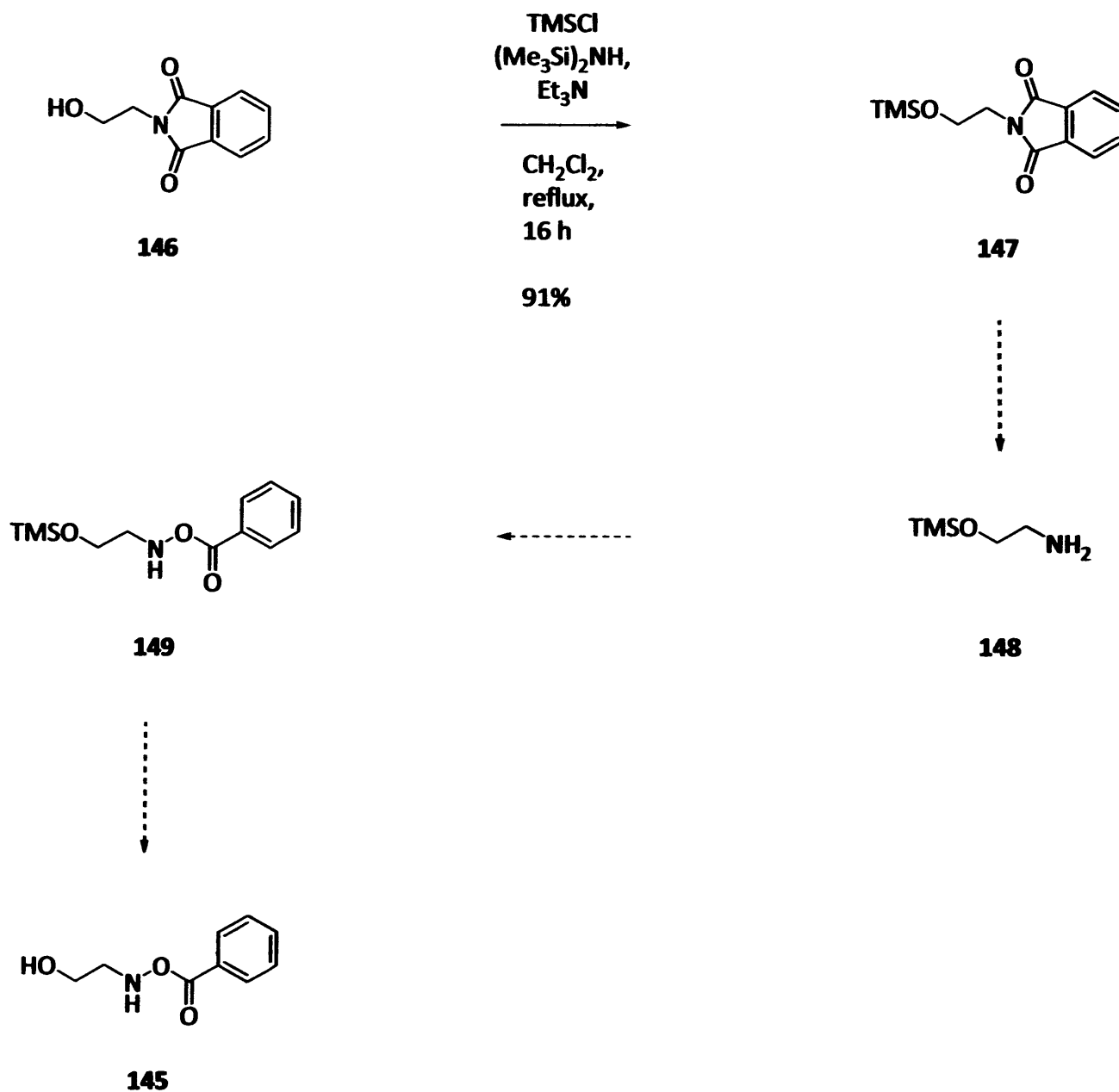


Figure 9

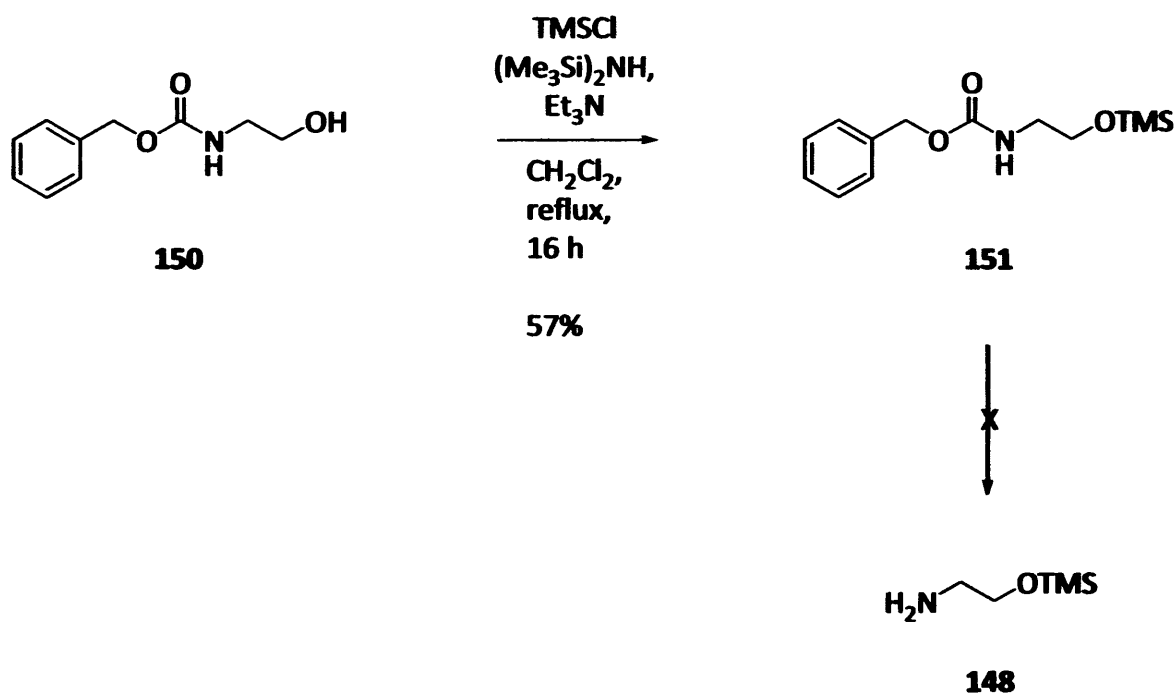
We therefore attempted to synthesize the compound *via* an alternative route starting from commercially available *N*-(2-hydroxyethyl)phthalimide **146** (Scheme 40).



Scheme 40

The phthalimide **146** was *O*-silylated in excellent yield to give the TMS-protected adduct **147**. It was foreseen that phthalimide deprotection should furnish *O*-TMS-protected ethanolamine **148**, which could then be benzoylated selectively at the nitrogen to provide *O*-trimethylsilylethanolamine **149**. α -Oxygenation reactions could then be carried out using both the TMS-deprotected adduct **145** and **149**.

Several attempts to cleave the phthalimide group of **147** were unsuccessful in terms of producing the target *O*-TMS protected ethanolamine **148**. Aqueous methylamine, hydrazine monohydrate and sodium borohydride were all used as potential deprotection reagents but failed on each occasion to selectively deprotect at the nitrogen without also cleaving the TMS group under the reaction conditions. An alternative starting material was identified in the form of benzyl *N*-(2-hydroxyethyl) carbamate **150**. A similar strategy was envisioned involving *O*-silylation followed by deprotection at nitrogen. The initial silylation step was carried out successfully by heating a solution of the reagents in dichloromethane at reflux for 16 hours. After purification by column chromatography, the expected benzoyloxyamine **151** was provided as a colourless oil in 57% isolated yield (Scheme 41). However, removal of the benzyl carbamate group from **151** under standard hydrogenation conditions (H_2 , Pd-C, MeOH, rt), also succeeded in cleaving the TMS group to reform ethanolamine **138**, instead of the desired product **148**.



Scheme 41

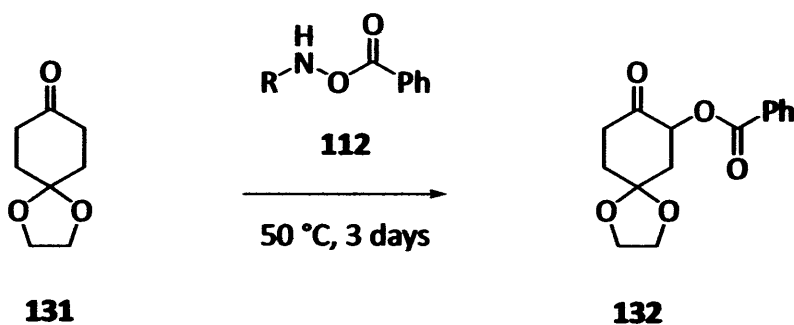
The challenge was therefore to find two orthogonal protecting groups for the ethanolamine substrate **138**. We remained hopeful that milder reaction conditions could be developed to cleave the *N*-protecting group whilst leaving the O-Si bond intact. Another proposed strategy was to silylate ethanolamine **138** directly, albeit with a potentially tricky purification, in order to develop a working route to the desired reagent **145**.

For the time being however, it was decided to suspend this side-project in favour of some more easily accessible compounds. After all, our methodology was developed with the dictum that not only should the α -oxygenation procedure itself be a practically simple transformation to perform, but also that any reagents used in the procedure should themselves be derived from straightforward and reproducible reactions.

3.3 Testing reactivity

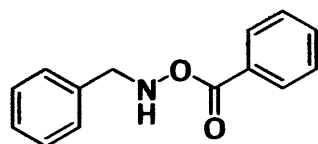
Figure 10 shows the hydroxylamines **152-161**, which were successfully prepared by the reaction of the relevant amine with one equivalent of dibenzoyl peroxide in a vigorously stirred biphasic mixture of dichloromethane and carbonate-based pH 10.5 buffer for 16–24 hours.

With the pH dichotomy of the proposed catalytic cycle uppermost in mind, we decided to examine the disposition of each hydroxylamine substrate *as the free base* towards the α -oxygenation of 1,4-cyclohexandione *mono*-ethylene ketal **131** under a variety of reaction conditions (Scheme 42).



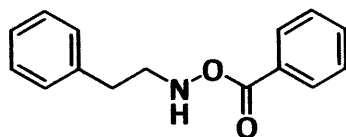
Scheme 42

This was not only to test the existing α -oxygenation reaction under non-acidic reaction conditions for the first time, but also to answer the question as to whether the structure of the parent amine had any bearing on the reactivity of the corresponding *O*-benzoyloxy-hydroxylamine.



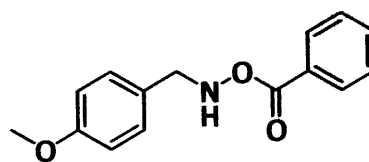
80%

152



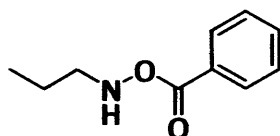
62%

153



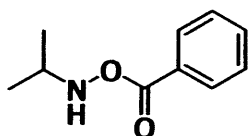
58%

154



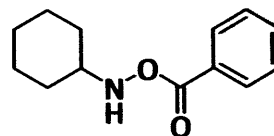
58%

155



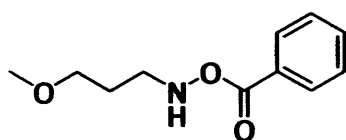
41%

156



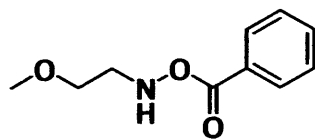
80%

157



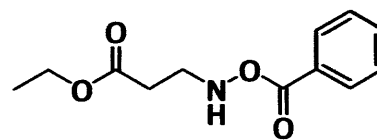
51%

158



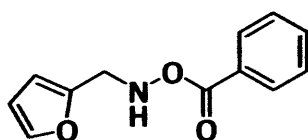
51%

159



42%

160

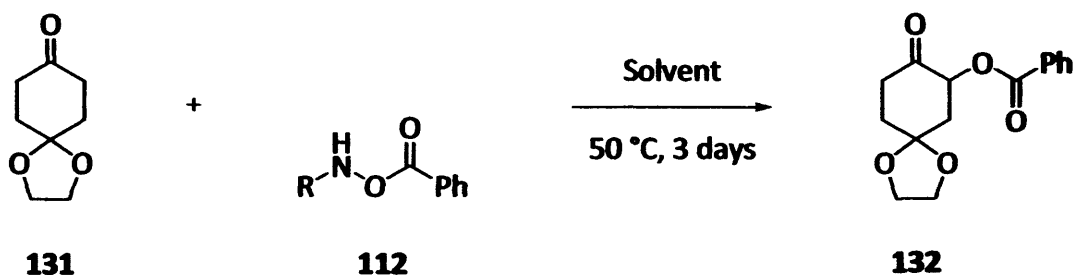


61%

161

Figure 10

Table 3 displays the results of the reaction between the carbonyl compound **131** and each hydroxylamine species in various solvents, conducted at 50 °C for 3 days (Scheme 43) – this rather long reaction time having been shown earlier to be sufficient time for reaction to proceed to a maximum without decomposition of starting materials or products having begun to any detectable extent. The yields quoted are calculated based on addition of a ^1H NMR internal standard.



Scheme 43

Entry	Reagent	CHCl_3	THF	EtOAc	PhMe	H_2O	DMSO
1		29%	30%	20%	14%	11%	32%
2		3%	9%	4%	8%	3%	14%
3		3%	0	0	1%	2%	0
4		11%	0	0	0	0	0
5		18%	21%	3%	10%	0	10%
6		13%	0	0	5%	11%	9%
7		3%	0	5%	10%	17%	0

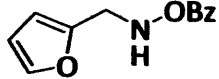

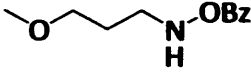
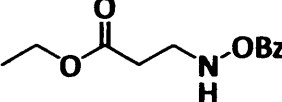
8		19%	23%	0	0	0	0
9		18%	11%	15%	15%	3%	9%
10		38%	19%	25%	12%	5%	2%
11		< 1%	0	0	0	0	< 1%

Table 3: Calculated conversions (from ^1H NMR) to product 132 under non-acidic conditions

There was a substantial degree of variation in the conversions to α -oxygenated adduct **132** as the *N*-substituent was altered. Within the family of four aliphatic *N*-substituents **100**, **155-157** (entries 1-4), the order of reactivity followed that expected solely by considering the steric properties of each reagent. Hence we observed that *N*-methyl(benzoyloxy)amine **100** was the most effective reagent within the aliphatic *N*-substituent group, followed by *N*-(propyl)benzoyloxyamine **155**, with the two reagents bearing tertiary centres adjacent to the nitrogen atom, **156** and **157**, performing least well. These four substrates varied from each other only in terms of the steric bulk α - to the nitrogen atom; it was therefore surmised that the variation in the results from these reagents was a direct consequence of the degree of steric crowding in the vicinity of the lone pair of the nucleophilic nitrogen atom.

Four reagents with an aromatic *N*-substituent, **152-154** and **161**, were prepared and screened (entries 5-8). We noted that *N*-(benzyl)benzoyloxyamine **152** was a significantly better reagent towards α -oxygenation than *N*-(phenethyl)benzoyloxyamine **153**, which differed from the *N*-benzyl reagent **152** only by the inclusion of a single carbon spacer. This seemed to contradict the results with the aliphatic amines, since the *N*-benzyl species **152** was marginally more hindered at the nitrogen atom. However, it may be more correct to conclude that some factor(s) other than simple steric considerations were important, such that the presence of a phenyl ring one carbon atom further out had a detrimental effect on the reaction yield.

Moreover, a comparison between the *N*-benzyl and *N*-propyl substituted reagents **152** and **155** (entries 2 and 5) led us to conjecture that the presence of a phenyl ring β - to the nucleophilic nitrogen was somehow of benefit within the transformation, certainly when the reaction was conducted in either chloroform or THF. This effect was perhaps due to the electron-withdrawing nature of the ring, or by some other more subtle electronic interplay – as was indicated when the performance of *N*-(4-methoxybenzyl)benzoyloxyamine **154** (entry 7) and the *N*-benzyl reagent **152** (entry 5) were compared. In the majority of solvents examined, reagent **152** outperformed reagent **154**, except for when the reaction was conducted in water.

Incorporation of the electron-donating *p*-methoxy group into the molecule therefore resulted in quite dramatic changes to the outcome of the reaction. *N*-((Furan-2-yl)-methyl)benzoyloxyamine **161** (entry 8) worked on a par with *N*-(benzyl)benzoyloxyamine **152** in chloroform and THF, yet this substrate failed entirely in all other solvents we tested.

N-(3-Methoxypropyl)benzoyloxyamine **158** (entry 9) generally worked better than *N*-(2-methoxyethyl)benzoyloxyamine **159** (entry 10), and provided our best conversion (38%) in this series of experiments, when the reaction was carried out in chloroform. *N*-(Ethyl-3-propanoate)benzoyloxyamine **160** (entry 11) was essentially unreactive in all solvents examined.

Overall, the better solvents for the reaction were chloroform and THF, with some isolated but reasonable results occurring with ethyl acetate and DMSO.

Unfortunately, the results generated by this set of experiments fell far short of the conversions and rates demanded by an efficient catalytic process which was our target. However, for the first time we observed that the transformation could take place under conditions other than those of Brønsted or Lewis acidity – albeit to a significantly lesser extent than in the standard conditions adopted for the reaction of *N*-methyl-*O*-benzoyl hydroxylamine hydrochloride **100-HCl** with carbonyl substrates.

Chapter 4: Project Re-evaluation

4.1 Thiourea work

In the field of metal-free catalysis, there has been a recent drive towards the use of double hydrogen bonding interactions to activate carbonyl compounds.⁶²

In 1988, Etter and co-workers reported that diaryl ureas of the form **162**, with electron-withdrawing substituents readily form co-crystals with a variety of proton acceptors including carbonyl compounds.⁶³ This prompted the development of diaryl urea catalysts which found utility in allylations of cyclic sulfinyl radicals⁶⁴, Claisen rearrangements⁶⁵ and Michael additions.⁶⁶

Schreiner later applied the methodology to carbonyl chemistry using thiourea catalysts such as **163** to accelerate the Diels-Alder reaction.⁶⁷ Perhaps most significantly, Jacobsen and co-workers have identified and optimised a series of urea- and thiourea-containing Schiff-base catalysts (e.g. **164**) for the activation of alkyl- or acyl-substituted imines in asymmetric Strecker,⁶⁸ Mannich⁶⁹ and Pictet-Spengler reactions.⁷⁰

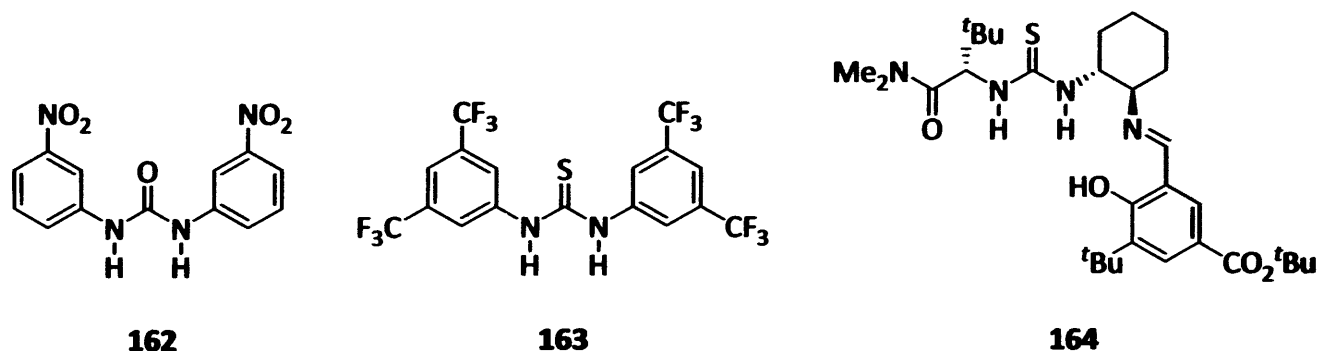
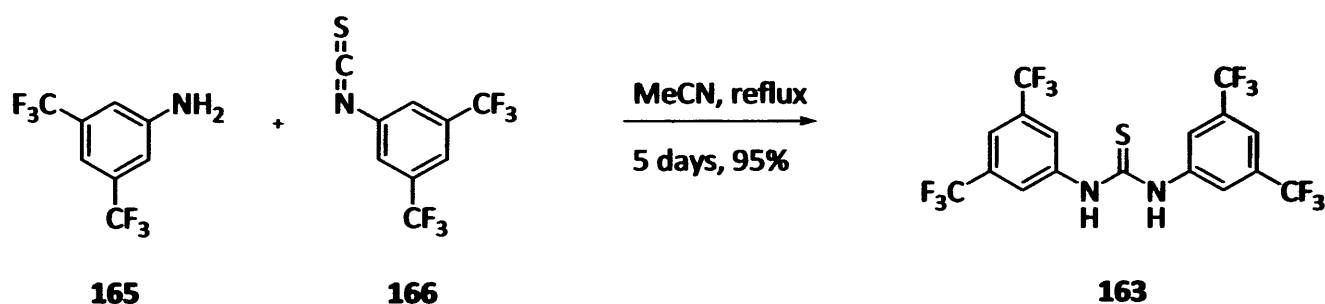


Figure 11

Taken as a whole, this body of work has shown that carbonyl activation by double hydrogen bonding to be a viable and versatile strategy for metal-free catalysis. The Lewis basic lone pairs of the carbonyl oxygen atom can coordinate via explicit hydrogen bonding interactions to the thiourea catalyst, lowering the electron density at the oxygen atom, thus decreasing the energy of the C=O π^* LUMO and activating the group towards nucleophilic attack.

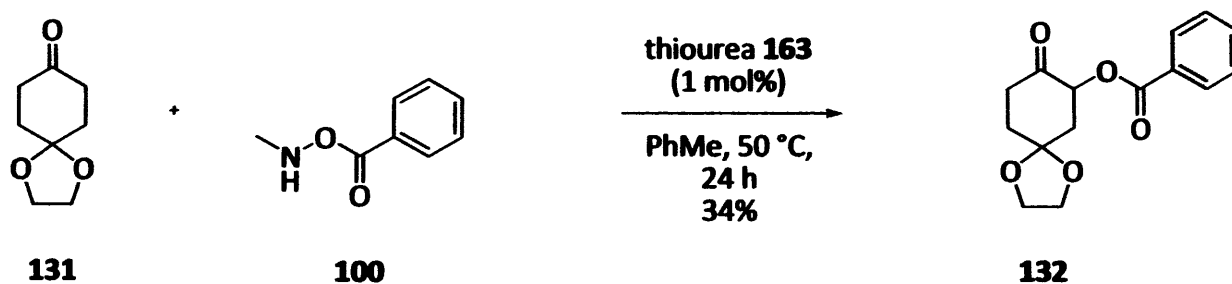
We therefore reasoned that such an approach may be of use within our own work. Considering the plethora of carbonyl chemistry which is performed simply by adding a catalytic amount of protic acid to a mixture of a carbonyl compound and a nucleophile, it is perhaps not surprising that our reaction yields dropped dramatically when the proton source was effectively removed by using our reagent as the free base rather than the HCl salt. Without a detailed understanding of the reasons behind the relative failure of the Lewis acids examined to effectively catalyse our transformation, it nevertheless seemed that a slightly different approach could be adopted via the use of Schreiner's thiourea.

In a highly successful, albeit slow reaction, 1,3-bis-(3,5-bistrifluoromethylphenyl) thiourea **163** was prepared in excellent yield by the reaction of 3,5-bis(trifluoromethyl) aniline **165** with a molar equivalent of 3,5-bis(trifluoromethyl) phenyl isothiocyanate **166** in refluxing acetonitrile (Scheme 44).

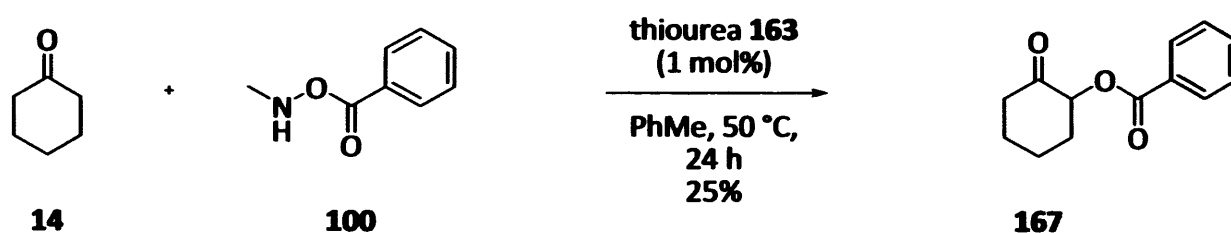


Scheme 44

A sub-stoichiometric amount of the thiourea catalyst was found immediately to accelerate the reaction between carbonyl compounds cyclohexanone **14** and 1,4-cyclohexandione *mono*-ethylene ketal **131** and *N*-(methyl)benzoyloxyamine **100** in toluene at 50 °C, as shown in Schemes 45 and 46. Maximum conversions to product of 34% and 25% of the α -oxygenated adducts **132** and **167** respectively were reached after 1 day, where previously a time of 3 days was necessary before maximum product formation (Schemes 45 and 46).



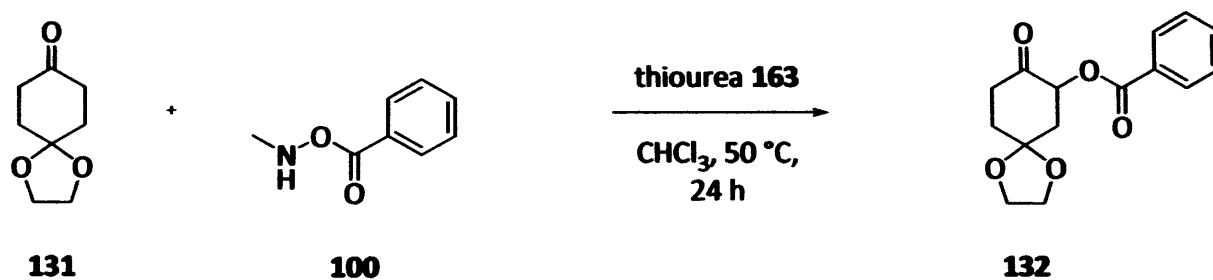
Scheme 45



Scheme 46

Curiously, a decrease in yield was observed upon prolonging the reaction time substantially beyond 24 hours. For example, the reaction of *N*-methyl-*O*-benzoylhydroxylamine **100** with 1,4-cyclohexandione *mono*-ethylene ketal **131** gave 28% product after 48 hours and 18% if left to stir at 50 °C for a further 24 hours. This was possibly suggestive of a pathway involving product decomposition. As before, conversion to product was measured by the use of an internal standard within the NMR sample.

With respect to catalyst loading, we were able to show that a very small sub-stoichiometric amount of the thiourea **163** was necessary in order to promote the reaction (Table 4).



Scheme 45

Loading (mol%)	Conversion
1	30%
0.5	26%
0.3	28%
0.1	23%
0.05	18%
0.01	16%
0	13%

Table 4: Reaction performance at various catalyst loadings

A loading of 1 mol% appeared to be optimal. Higher loadings seemed to have an adverse effect on yield; in fact the reaction has been conducted with one equivalent of thiourea **163** and in this instance *no product* was observed in the crude reaction mixture. Below 1 mol%, the product yield decreased with catalyst loading. We further noted that with no thiourea catalysis, the reaction did proceed, but to a much lesser extent than in the presence of the catalyst – a control experiment which was performed, even though the behaviour of the substrates where no catalyst was present had arguably been thoroughly explored in the work using the free-base substrates.

Figure 12 shows the results of a comparative study, performed by stirring together the substrates **100** and **131** in various solvents at 25 °C for 24 hours, both in the presence, and absence, of the thiourea catalyst **163**.

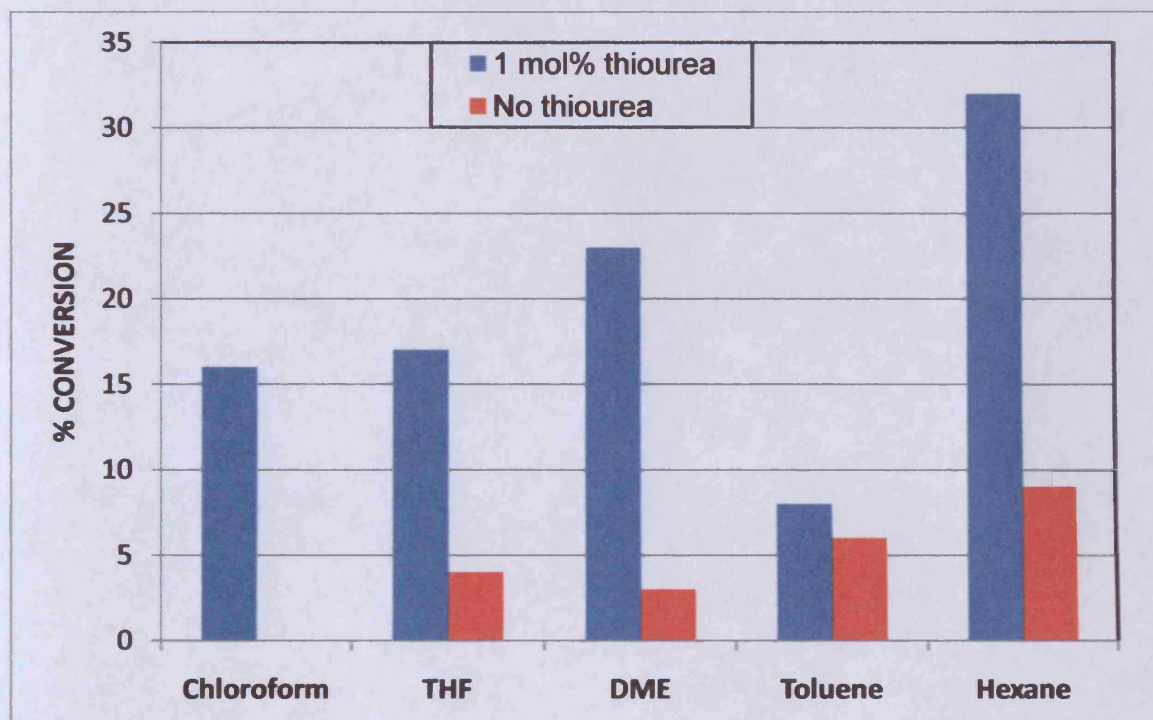
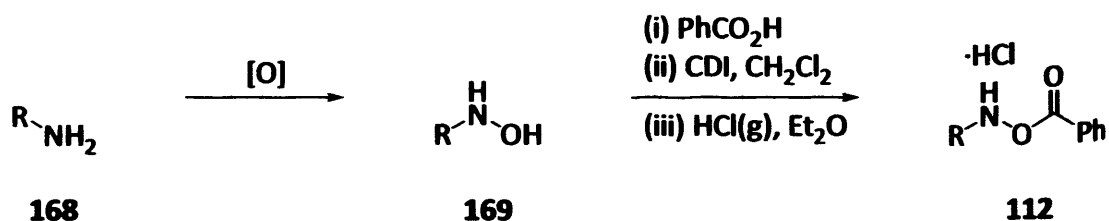


Figure 12: Effect of thiourea **163**

There was a clear advantageous effect when the catalyst was added; however the overall conversion to product in the reaction did not rise far beyond 30%. This represented very little improvement in terms of reaction yield, although both the reaction temperature and time taken to reach maximum conversion under these conditions had been decreased. The thiourea catalyst **163** was therefore concluded to be a useful tool, whilst not representing the ultimate solution to the problems we experienced in trying to establish a catalytic cycle.

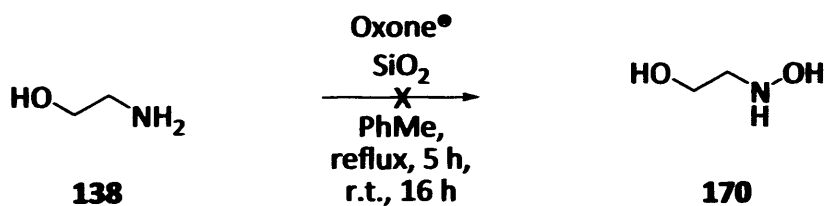
4.2 Attempted hydroxylamine syntheses

With a view to accessing α -oxygenating species which had proved elusive via the Phanstiel protocol, we attempted to oxidise several primary amines **168** to the corresponding hydroxylamines **169** by adapting literature methods to our needs. The plan was then to take the hydroxylamines into the previously described CDI-promoted coupling with benzoic acid in order to furnish the requisite reagents **112**·HCl (Scheme 47).

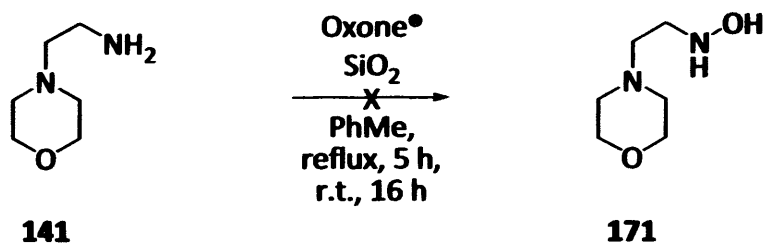


Scheme 47

In 2000, Kropp reported that Oxone[®] over silica gel or, in some cases, alumina could oxidize primary and secondary amines selectively to the corresponding hydroxylamines, in either the presence or absence of a solvent.⁷¹



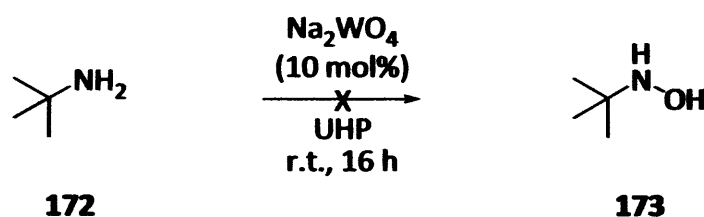
Scheme 48



Scheme 49

In our hands, this reaction was unsuccessful for either ethanolamine **138** or 4-(2-aminoethyl)morpholine **141** (Schemes 48 and 49).

We next attempted the sodium tungstate-catalyzed (10 mol%) oxidation of primary amine **172** with a urea-hydrogen peroxide complex (UHP). The methodology was described in 2005 by Heydari, who reported that the corresponding *N*-monoalkylhydroxylamines were obtained in good to excellent yields.⁷²



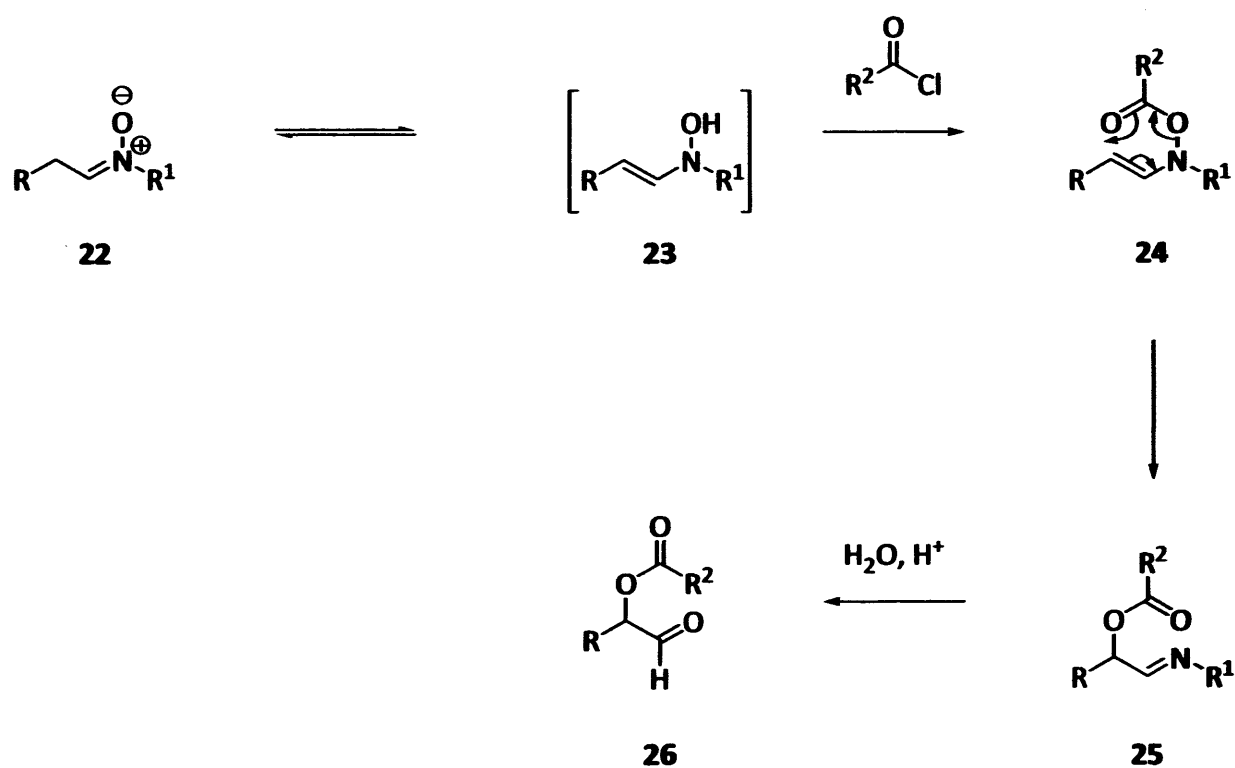
Scheme 50

In our hands, reactions were carried out by stirring the substrates in diethyl ether at ambient temperature. After 2 hours, a remarkable colour change occurred to give a deep blue solution; however it did not prove possible to isolate the desired product from the reaction mixture, either by column chromatography, or precipitation of the hydrochloride salt.

Regrettably, we were unable to reproduce the literature results in the time we had allotted to this part of the investigation (Scheme 50). Rather than become consumed in this synthetic strategy at the expense of the principal project aims, it was decided to abandon this approach.

4.3 Work with nitrones

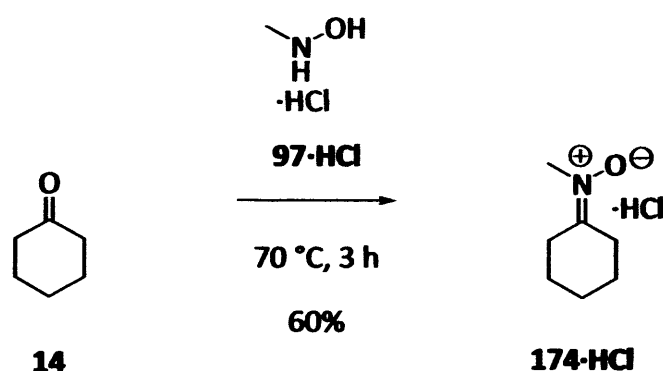
As previously described (see Chapter 1), one of the precedents for the α -oxygenation methodology dated back to 1983 and a report published by Coates²⁷, who showed that α -oxygenated aldehydes **26** (and cyclic ketones) could be successfully prepared by successive acylation of nitrones **22** (as the alkylhydroxylamine tautomer **23**) with acid chloride, followed by [3,3]-sigmatropic rearrangement of the *N*-vinyl-*O*-acylhydroxylamine intermediates **24** and hydrolysis of the resulting α -acyloxy imines **25** (Scheme 7).



Scheme 7

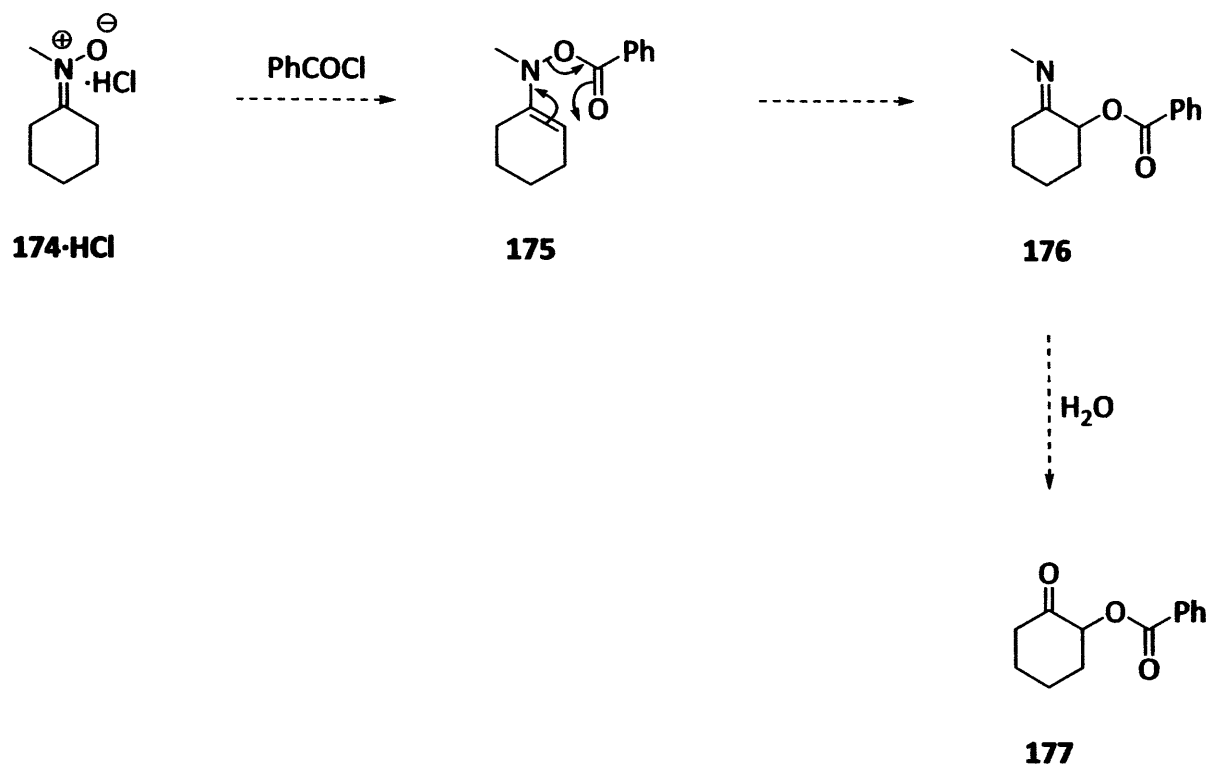
At the time, this offered a new method for affording the α -oxygenation adducts in good yield, under fairly mild reaction conditions and without the need for harsh electrophilic oxidising agents.

Coates reported that in general, no intermediates were detected in the acylation step, although in one instance an enamine species was isolated from the reaction mixture. It therefore appeared that the work of Coates could prove useful with respect to our own efforts to identify reaction intermediates. Consequently, *N*-cyclohexylidene methanamine *N*-oxide **174·HCl** was prepared by the condensation reaction of cyclohexanone **14** (which also serves as the solvent) with *N*-methyl hydroxylamine hydrochloride **97·HCl**, and the resulting pale brown solid recrystallised from cyclohexanone to give the product **174·HCl** as its hydrochloride salt in 60% yield (Scheme 51).



Scheme 51

Attempting to adapt Coates' protocol to the needs of our project, samples of nitron **174·HCl** were each combined with an equivalent of benzoyl chloride (Scheme 52). Various deuterated solvents and reaction temperatures were attempted in order to try and track any intermediate species in the ^1H NMR. It was hoped this would enable us to identify for the first time one or more of the intermediates from within the proposed reaction pathway. Detection of any of these species could provide evidence in support of the proposed reaction mechanism for the one-pot α -oxygenation.



Scheme 52

For this series of experiments, running the reaction in DMSO- d_6 at 30 °C gave the most encouraging result; however we were disappointed that the α -oxygenated adduct **177** was not seen any of the ^1H NMR spectra after up to 2 days intermittent monitoring. However, up to three new signals were observed between 5.0 and 6.0 ppm, and we believed these corresponded to α -protons of intermediate species occurring post-rearrangement in the proposed mechanistic scheme. Unfortunately, the relative integrations indicated that none of these species accounted for more than 5% of the total material observed by ^1H NMR. This meant that not even tentative assignments could be made.

The fact that only minor amounts of the supposed products of rearrangement were observed bore out Coates' observation that such nitrones were particularly unstable, and indicated that a more prudent course of action may have been to prepare such compounds and then perform the benzoylation reaction immediately. Although this sub-project did provide some tantalising mechanistic clues, it was felt that pursuing this avenue further might be a time-consuming digression from the project as a whole.

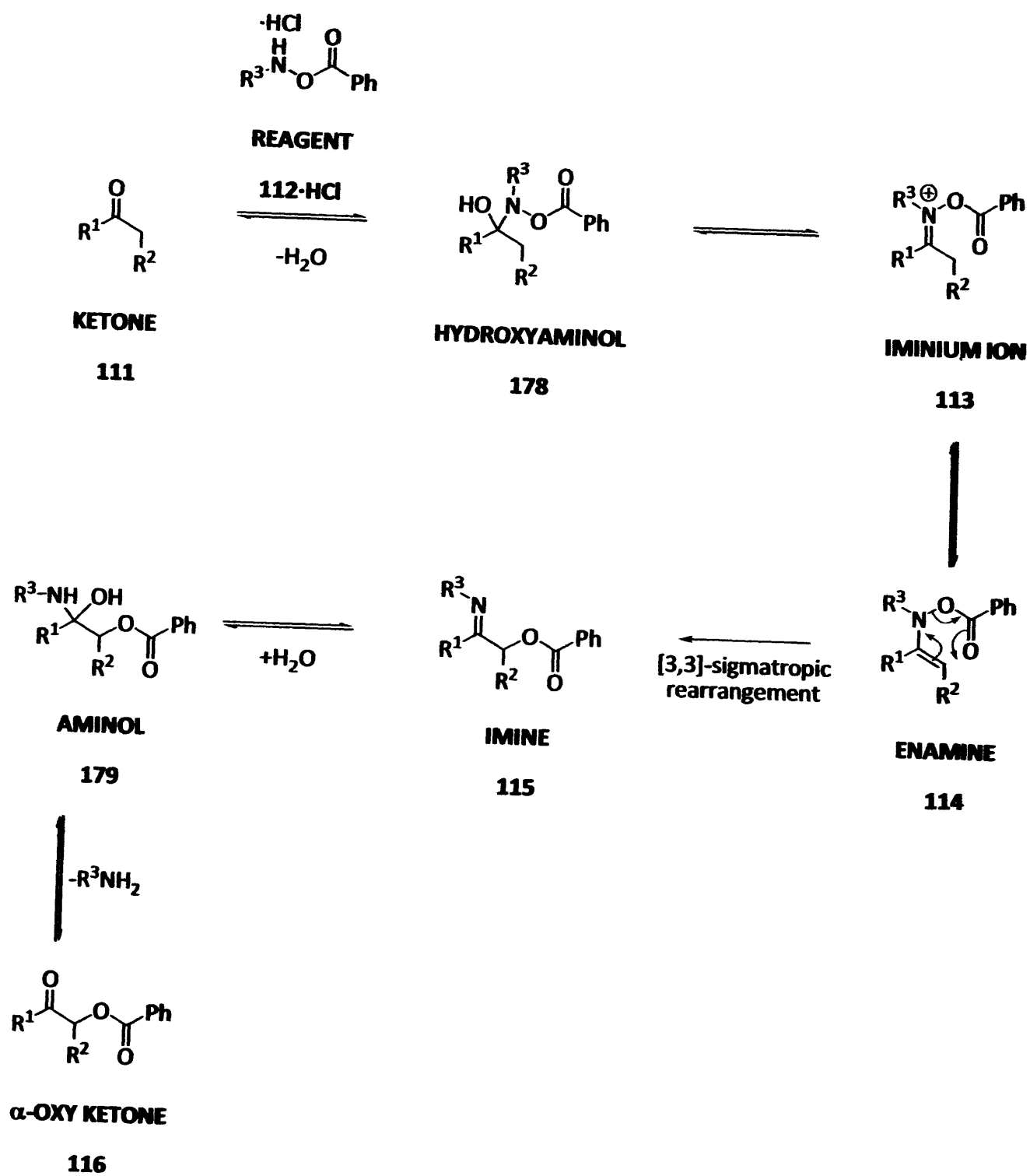
4.4 New directions

Having applied several strategies to our initial project goals with very little tangible success, it became gradually apparent that the α -oxygenation protocol as a catalytic process was not viable in its present proposed form. Consequently, it was deemed that the goals of the project would be best served by striking out in other directions.

We acknowledged that a full understanding of the fundamental processes and equilibria within the overall transformation was lacking. However, the consensus at this time was that the reaction pathway was as set out in Scheme 53.

The proposed mechanism involved initial nucleophilic attack of the nitrogen lone pair on a carbonyl compound **111** to form an iminium ion **113** *via* the hydroxyaminol **178**, with the elimination of a molecule of water. In keeping with the literature precedent discussed previously (Chapter 1), we believed that loss of an α -hydrogen from the iminium species **113** would be a realistic and likely means of forming an enamine **114**. This enamine, according to our hypothesis, would then be set up to undergo a concerted, pericyclic, [3,3]-sigmatropic rearrangement to form an α -benzoyloxyimine **115**. In our scheme, hydrolysis of the imine generated the aminol **179** followed by the final product **166** together with a molecule of primary amine, which was removed by acidic aqueous work-up.

The difficulty with this was that none of the proposed intermediates in the reaction sequence had been isolated; thus, the reaction mechanism was unproven in spite of the literature precedent in support of this pathway (see Chapter 1).²⁴⁻²⁷



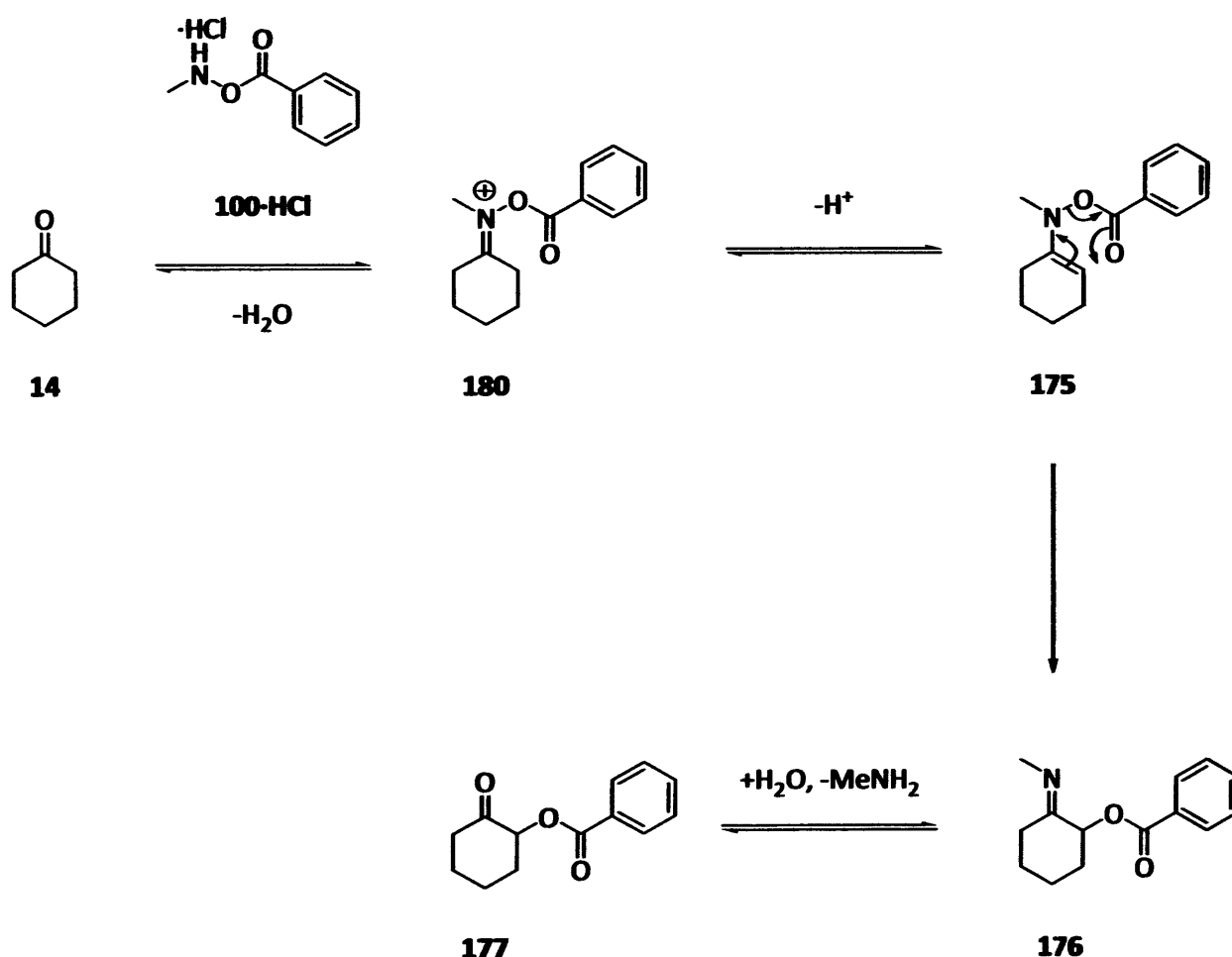
Scheme 53

This prompted an investigation into the kinetics and mechanism of the reaction – initially by means of timed NMR experiments, but later to incorporate other useful analytical techniques – with the aim of not only determining the reaction mechanism, but also to obtain detailed information regarding the individual steps within the transformation. Intuitively, we reasoned that this information could be used to substantially improve on our existing protocol.

Chapter 5: Reaction Monitoring – Early Experiments

The idea of monitoring the reaction had evolved partly as a result of the lack of success at establishing a catalytic variant of our transformation. So far, the approach had been to thoroughly screen the reagents within various reaction media, whilst tweaking the reagent structure and the reaction conditions in the direction which appeared to be most successful based on the data obtained. While this strategy had brought about some positive results, albeit over a period of months, we were forced to acknowledge that this 'trial and error' approach to the project could produce an almost infinite number of possible experiments.

We further acknowledged that a full understanding of the fundamental processes and equilibria within the overall transformation was lacking, although the mechanism made sense based upon literature precedent (Scheme 54).



Scheme 54

We believed the formation of the initial iminium ion **180** to be a slow step within the reaction, if not rate-determining. This assertion was based on the dramatic reduction in yield observed when the reagent was used as the free-base **100** as opposed to its hydrochloride salt **100-HCl**, and it was reasoned that the absence of protic acid meant that the carbonyl compound was no longer activated towards initial nucleophilic attack by the nitrogen atom of the reagent. However, this was conjecture without direct experimental evidence.

It was therefore decided to undertake a detailed investigation of the kinetics and mechanism of the reaction, starting with a series of timed NMR experiments. The aim was not only to uncover new information regarding the reaction mechanism, but also to obtain rate constants and thermodynamic parameters – potentially elucidating the individual steps within the transformation, as well as furnishing valuable information about the reaction process as a whole. Armed with this information, we hoped to readdress the current limitations of the methodology with a greater possibility of success.

5.1 Groundwork to kinetic studies

5.1.1 Initial observations by ^1H NMR

It was already known that *in situ* ^1H NMR experiments showed the presence of the α -oxygenated adduct together with various, as yet mostly unassigned intermediate species within the reaction sequence. Figure 13 is a typical ^1H NMR spectrum obtained 1 hour after thorough mixing of cyclohexanone **14** with a solution of *N*-methyl-*O*-benzoyl hydroxylamine hydrochloride **100-HCl** in DMSO-d_6 .

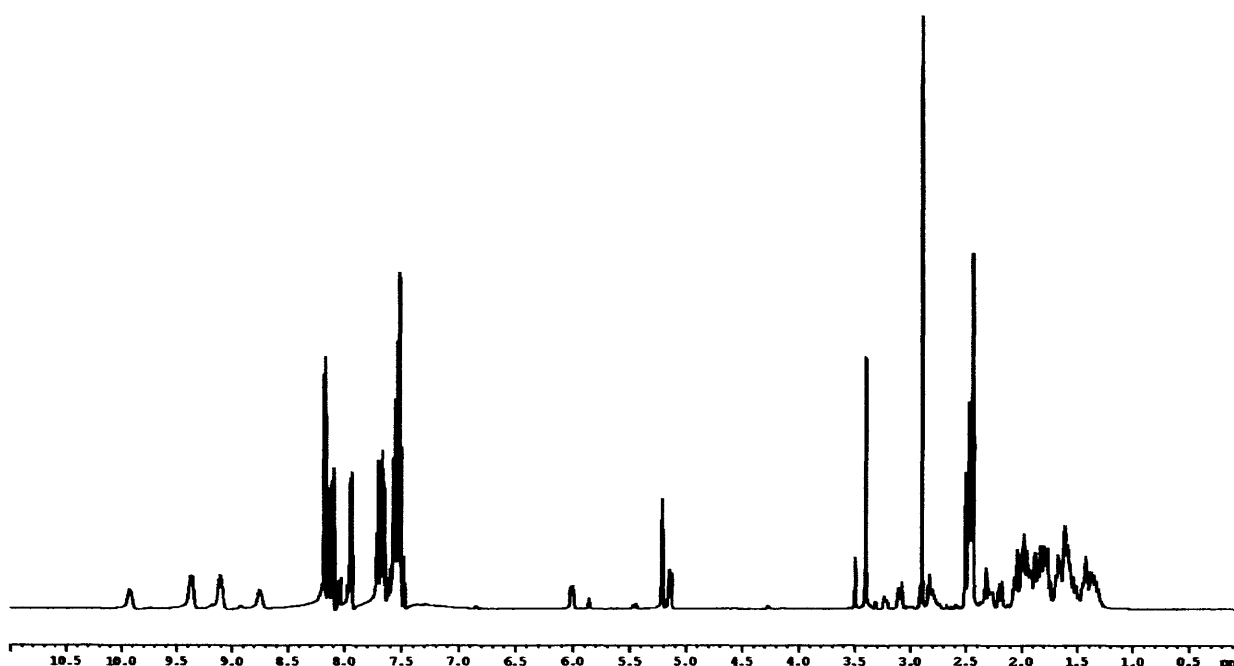


Figure 13: ^1H NMR spectrum of reaction mixture

Even at this early juncture, it was apparent that there were several species present in the reaction mixture; the desymmetrisation of the cyclohexyl ring being an indicator that the reaction was well underway. The region between 4.5 and 6.0 ppm offered the clearest view of the reaction as it took place (Figure 14 shows an expanded view of this region), with all the signals in this region thought to arise due to the resonances of hydrogens α - to the carbonyl carbon.

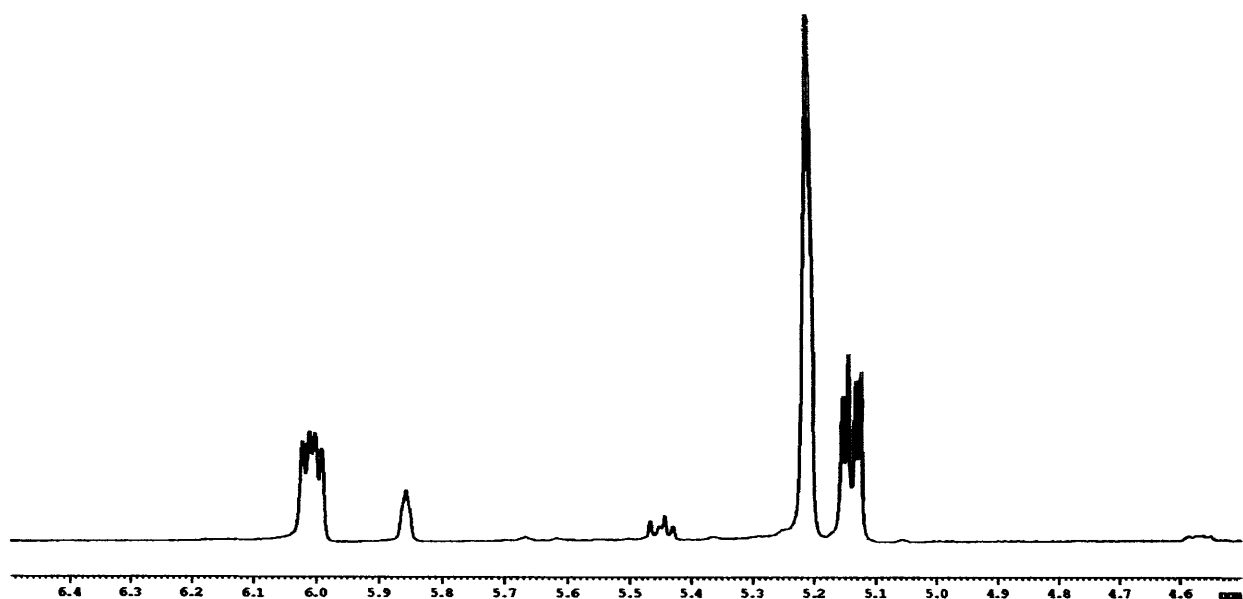


Figure 14: Expansion of Figure 13 – diagnostic region

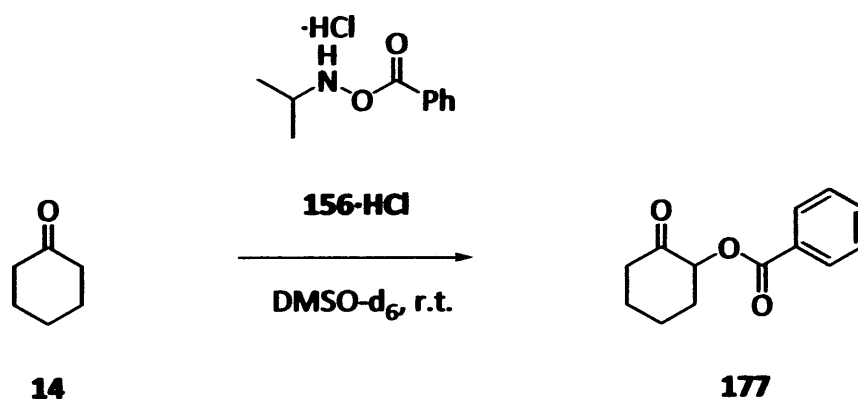
Since the α -oxygenated adduct **177** was known and had been fully characterised within the group, the doubled doublet at 5.45 ppm was readily identified as the proton on the carbon atom which had formed the new C-O bond.

We realised that if any quantitative conclusions were to be drawn, then this would necessitate the measurement of the integrals associated with the formation of product, consumption of starting materials and the formation and conversion of the intermediate species within the reaction mixture. In turn, this would require the correct assignment of each peak corresponding to the intermediate species within the reaction; if the proposed mechanism was correct these would correspond to formation of an iminium ion **180**, its enamine tautomer **175** and the α -(acyl) hydroxylamine **176** which led to the product ketone **177** after hydrolysis under the aqueous acidic reaction conditions.

A degree of caution was also required, in view of the fact that some of the intermediate species may well be very short-lived and therefore not observed in the ^1H NMR spectra. Furthermore, the intermediacy of several other as yet unknown species may have been significant enough to be observed on the NMR timescale.

It was clear that dismantling the one-pot α -oxygenation of cyclohexanone **14**, in terms of isolating – or at least observing – all of the species within the reaction pathway was a significant challenge, and one which almost certainly would not be possible to fully achieve by standard synthetic means. Hence we envisaged the use of a variety of experimental and spectroscopic methods in order to separate and identify the signals belonging to the various intermediate species.

In much the same manner as the previous experiment with the *N*-methyl analogue **100-HCl**, the α -functionalisation of cyclohexanone **14** with *N*-isopropyl-*O*-benzoyl hydroxylamine hydrochloride **156-HCl** (Scheme 55) was carried out and the reaction mixture examined *in situ* by ^1H NMR.



Scheme 55

The resulting spectrum gave an interesting result relating to the signals at 5.2 and 6.0 ppm. The reaction took place more slowly than with the analogous *N*-methyl reagent **100-HCl**, probably due to the increased steric encumbrance around the nitrogen atom. However, on this slightly slower timeframe, virtually the same peaks of interest were seen, with the curious phenomenon of a reversal in intensity of the two peaks at 5.2 and 6.0 ppm (Figure 15).

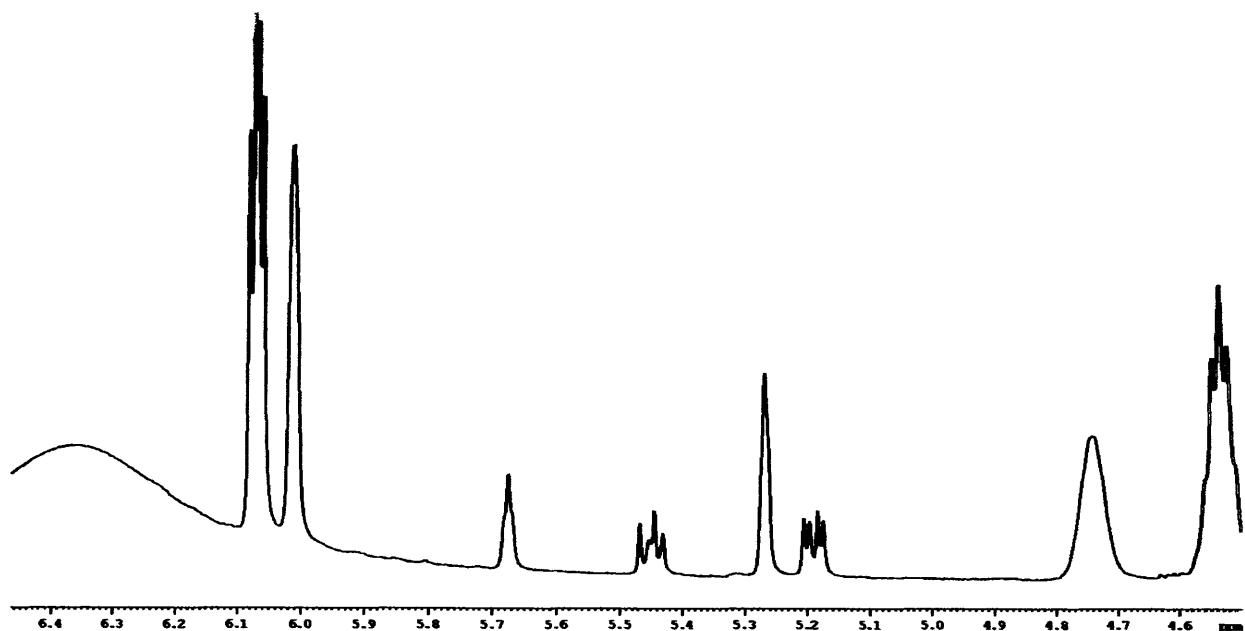


Figure 15: ^1H NMR spectrum (expanded), reaction with *N*-isopropyl analogue

An explanation was suggested, in which the kinetics of the formation of the two possible enamine rotamers were altered by the presence of the more crowded isopropyl group, such that formation of the nonreactive enamine **182** was favoured when compared to its rotamer **181** (Figure 16).

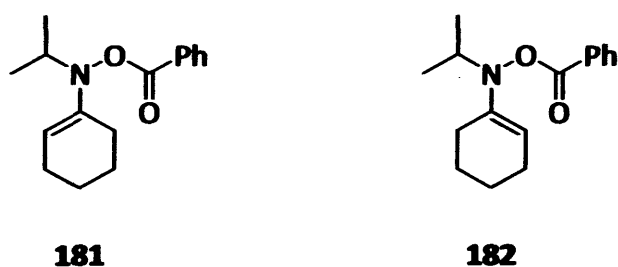


Figure 16

However, it was considered unsound reasoning to make a definite assignment on this basis alone, particularly as one peak was apparently a singlet. Although DEPT experiments showed these resonances to be due to protons of a CH carbon, one would have expected to observe a degree of splitting in the ^1H NMR spectrum due to 3J coupling to the diastereotopic protons on the adjacent carbon atom.

5.1.2 Choice of substrates and reaction conditions

The above experiments hammered home the point that, among many other considerations, a judicious choice of carbonyl compound was required for the kinetic work. It was noted that monitoring the disappearance of starting materials would be a demanding task where cyclohexanone was concerned, owing to the overwhelming array of complicated resonances in the aliphatic region of the ^1H NMR spectrum as the cyclohexane ring was desymmetrised. Furthermore, any chance of obtaining satisfactory data for the reaction intermediates – in addition to drawing concrete conclusions as to the identity of those intermediates – was severely reduced by the sheer complexity of the resulting ^1H NMR spectra.

For reaction-monitoring by NMR to be successful, the following criteria were deemed essential:

- A carbonyl compound and an α -oxygenating reagent of sufficient reactivity was required, such that the reaction could be performed and the data collected within a practical timeframe.
- A suitable internal standard with which to quantitatively measure the components of the reaction in real-time, including any intermediates.
- Suitable reaction conditions, including solvent, reaction time, temperature and concentration; economically viable and compatible with the available NMR hardware.
- A choice of substrates which would provide ^1H NMR spectra in which the product and key intermediates were clearly observed; i.e. their diagnostic peaks could be easily and accurately integrated – hence we required small, simple molecules in terms of proton NMR.

In terms of the carbonyl substrate, more specifically:

- A ketone – aldehydes were perfectly amenable to the α -oxygenation; however clean reactions were at this time only observed in a 9:1 mixture of THF and water. A simple aldehyde was initially thought to be a desirable substrate, but was eventually ruled out because this limited the choice of reaction medium unnecessarily, without furnishing any significant experimental benefits as a trade-off against this limitation.
- A cyclic, symmetrical substrate - providing a starting material which could not interconvert between *cis* and *trans* enamine intermediates, and 'clutter' the spectra with superfluous intermediates. For example, attempting to simplify proceedings by using the acyclic ketone 3-pentanone **183** could have resulted in the resulting NMR spectra becoming further complicated as a result of isomerisation (Figure 17).

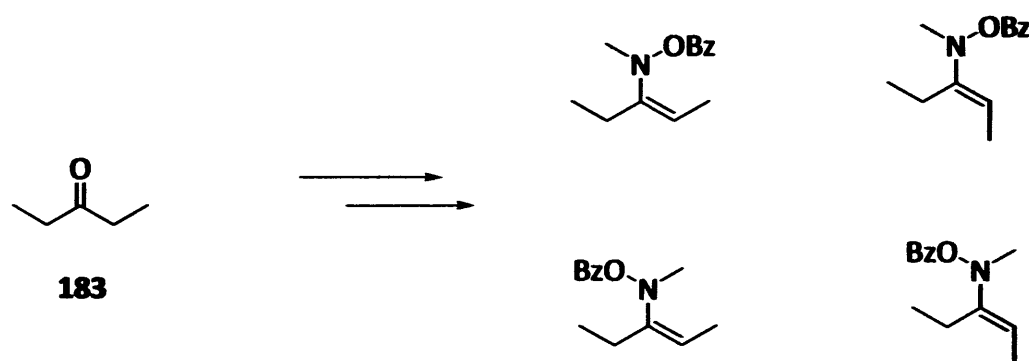
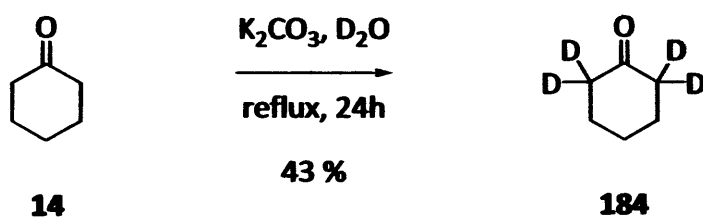


Figure 17

- A compound giving as few signals from hydrogen atoms directly bonded to the carbocycle as possible – diastereotopicity complicated the spectrum to the point where it was virtually unreadable (as with cyclohexanone **14**).

It was proposed that 2,2,6,6-d-cyclohexanone **184** may offer a suitable variant to circumvent the aforementioned issues; and this substrate was therefore prepared by several successive iterations of the reaction shown in Scheme 56, in which cyclohexanone **14** was refluxed for 24 hours in D₂O in the presence of K₂CO₃; with the reaction components present in molar quantities of 1:20:2 respectively.⁷³ After separation of the aqueous and organic layers and vacuum distillation, a clear colourless oil was obtained, comprising greater than 97% of deuterated adduct **184**.

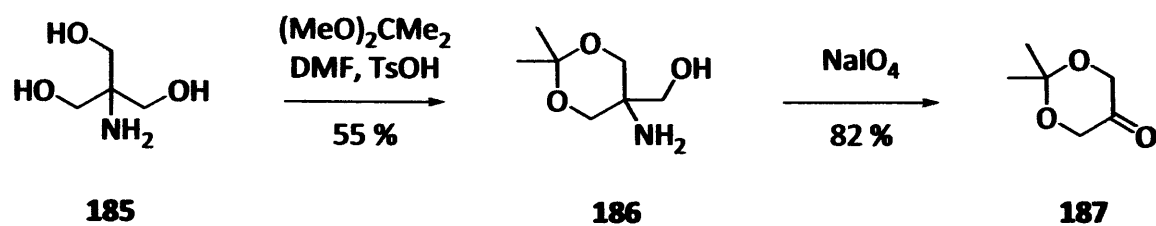


Scheme 56

On subjecting this compound to the α -oxygenation procedure with *N*-methyl-*O*-benzoyl hydroxylamine hydrochloride **100-HCl**, it was found that the ¹H NMR spectrum became greatly simplified; to the extent that the possibility of monitoring consumption of starting material was possible for the first time.

Although this substrate was initially thought to have great potential, it was subsequently decided that this was not an appropriate starting material for the experimental protocol we wished to pursue, due to the kinetic isotope effect which could skew any data which we obtained. However, the possibility still existed that the deuterated adduct **184** could be exploited at a later stage in order to assist in identifying any unknown intermediates which were observed.

Alternative ketone substrates were found to be within relatively easy reach. Firstly, in a two-step synthesis, tris(hydroxymethyl) aminomethane **185** was protected with 2,2-dimethoxypropane to give the acetonide **186**, which underwent oxidative cleavage with NaIO₄ to give 2,2-dimethyl-1,3-dioxan-5-one **187** in 45% overall yield (Scheme 57).⁷⁴



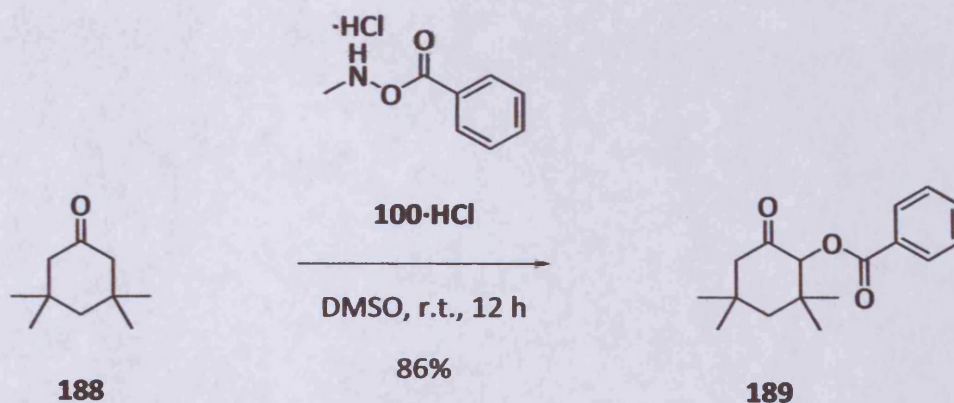
Scheme 57

The synthesis did provide a simple cyclic ketone substrate with which to perform timed ^1H NMR experiments; however for a number of reasons this proved an unsuitable substrate for reaction monitoring.

Firstly, when paired with the α -oxygenating reagent **100-HCl**, the transformation was found to be non-straightforward, giving rise to a more complex ^1H NMR spectrum owing to side reactions and/or decomposition of the starting material. A number of conditions were tested for this reaction in the course of screening this potential substrate; however it was also discovered that the presence of the two additional electronegative oxygen atoms altered the chemical shifts of the crucial and diagnostic α -hydrogen signals by approximately 2 ppm downfield, and into the aromatic region of the spectrum.

With the current generation of hydroxylamine reagents bearing aromatic moieties, particularly *N*-methyl-*O*-benzoyl hydroxylamine hydrochloride **100-HCl** possessing an unsubstituted phenyl ring, it became swiftly apparent that the dioxanone **187** was not a suitable carbonyl compound as far as the NMR work was concerned.

Eventually, commercially available 3,3,5,5-tetramethylcyclohexanone **188** was found to be a useful starting material for our kinetic studies, undergoing the α -oxygenation reaction in excellent yield (86%) using hydroxylamine salt **100-HCl** (Scheme 58).



Scheme 58

This substrate was a quite fortuitous discovery, not least because it was commercially available and was of >99% purity by ^1H NMR. Also, the timeframe of the reaction was optimal to our needs, with the reaction showing an appropriate kinetic profile.

Compared with cyclohexanone **14**, the ^1H NMR spectra became greatly simplified. Figure 18 is a typical ^1H NMR spectrum taken during the functionalisation of gem-dimethyl cyclohexanone **188** by *N*-methyl-*O*-benzoyl hydroxylamine hydrochloride **100-HCl**.

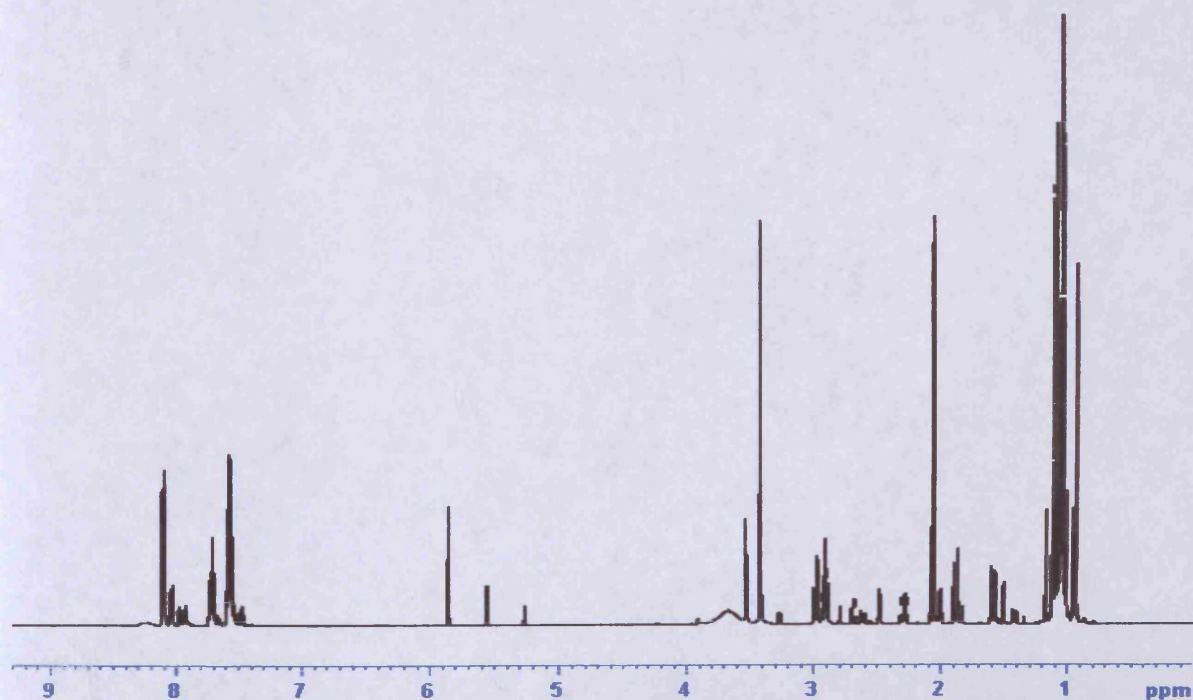


Figure 18: ^1H NMR spectrum with 3,3,5,5-tetramethylcyclohexanone **188 carbonyl substrate**

This showed a vastly simplified picture of the reaction pathway, with the α -hydrogens of the key intermediates observed as easily integrated singlets. For the first time, we were able to accurately quantify the formation of the α -oxygenated adduct **189**, the diagnostic peak of which was observed at 5.3 ppm, as well as at least two intermediates within the reaction sequence (Figure 18). The signal at 5.9 ppm was arbitrarily termed 'Intermediate A', and the signal at 5.6 ppm 'Intermediate B'.

Of further use was the fact that both starting materials are visible when the reaction was in progress and the rate of their disappearance could be monitored. At this point we believed we were within reach of thermodynamic parameters for the transformation, which we hoped would lead to an enhanced understanding of the reaction process.

5.2 Initial ^1H NMR monitoring experiments

5.2.1 A flawed experiment

By this stage, we had become convinced that water content was a potentially important variable in terms of the reaction rate and perhaps outcome in terms of product yield. As an entry to the kinetic study therefore, a 1:1 mixture of 3,3,5,5-tetramethylcyclohexanone **188** and *N*-methyl-*O*-benzoyl hydroxylamine hydrochloride **100-HCl** was stirred at room temperature in three separate reactions, containing DMSO- d_6 with varying water content. The experiment was conducted over a period of 12 hours; 25 μL aliquots were withdrawn from the reaction mixture at known time intervals and diluted with CDCl_3 laced with a known amount of 1,4-dimethoxybenzene as an internal standard. Analysis by ^1H NMR produced a set of data which could be plotted to show the formation of α -functionalised product **189** as a function of time (Figure 19).

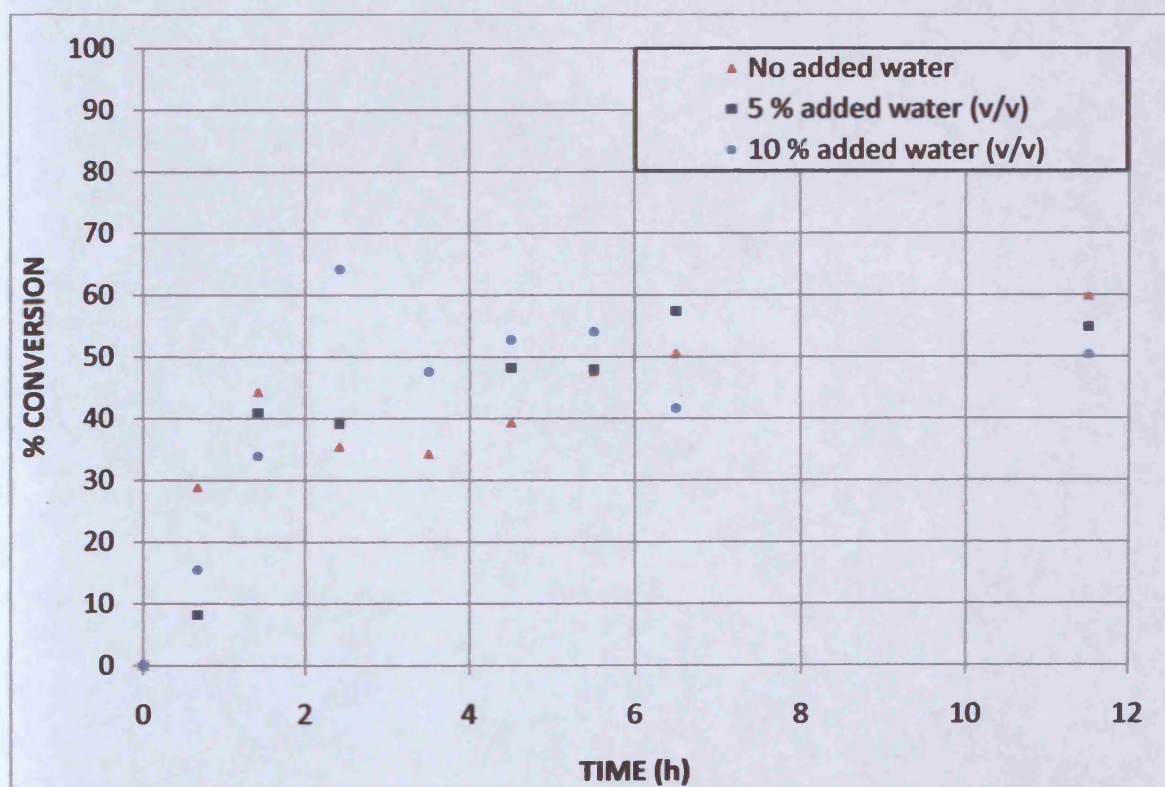


Figure 19: Conversion to product in DMSO- d_6 (varying water content)

This series of experiments showed that it was possible to extract numerical values for concentration of a given species from a reaction mixture, by using the integral data in the ^1H NMR together with a known quantity of an internal standard. However, at this early juncture, it was seen that there were problems with the data that needed to be overcome if this work was to generate accurate data from which reliable conclusions could be drawn.

From the data gathered, it was seen that formation of product appeared to take place almost linearly during the early stages of the reaction in all three cases. However, we were at first puzzled to note that after about 2 hours the reactions seemed to take a very erratic course, with a significant number of data points lying well outside that expected. We had arbitrarily assigned a deviation of $\pm 10\%$ as arising from the various acknowledged sources of experimental error.

In preparing the samples for NMR analysis, we had made the naïve assumption that diluting the aliquots approximately 40-fold would quench the reaction, and we could therefore use the times of these dilutions as the x-axis portion of the data. This was felt to be a necessary step as unrestricted access to the NMR spectrometer had not been arranged for this experiment; hence there was in many instances a sizeable delay between the preparation of the sample and the acquisition of its ^1H NMR spectrum. This in itself was a significant problem which rendered the data virtually meaningless – in that we had introduced a significant error in terms of the time at which each spectrum was taken (for clarity, these deviations are not acknowledged as error bars in Figure 19).

We concluded that formation of product was in fact still occurring after preparation of the NMR samples, and that this was an unforeseen source of error within the experiment. Rerunning a sample after a further time delay confirmed this suspicion in that an increased quantity of product was seen in the ^1H NMR spectrum.

Reflecting on this result not only forced us to re-examine our practical procedure, but also provided an insight into the proposed reaction mechanism.

If our thinking was correct, initial addition of the hydroxylamine species **100-HCl** into the carbonyl compound gave an iminium ion intermediate (analogous to the cyclohexanone-derived species **180**) which underwent deprotonation and rearrangement to form the α -benzoyloxyimine (similar to **176**). From the initial addition product through to the latter imine **176**, the reaction would therefore be unimolecular; it should therefore have come as no surprise that the reaction continued at vastly decreased concentration.

Although the data gathered from this series of experiments was clearly flawed, we learned the value of continually analysing and refining the way experiments were carried out; and this was the self-critical approach we endeavoured to adopt within the future science.

5.2.2 Evolving the method

Turning to a more rigorous, real-time method, the same starting materials were thoroughly mixed in DMSO- d_6 (this having now become firmly established as our solvent of choice) in an NMR tube and monitoring of the formation of product and consumption of intermediates was carried out directly.

Several pieces of data were clearly spurious, and these were removed from the series. Looking at the spectra, the presence of a broad peak with varying chemical shift was noted (in all probability water) – and this peak was particularly prevalent within the spectra from the earlier part of the reaction. Hence, integration of the three peaks of interest from this early stage of the reaction generated some data which was unquestionably incorrect. However, the remaining data represented a vast improvement on the initial experiments (Figure 20).

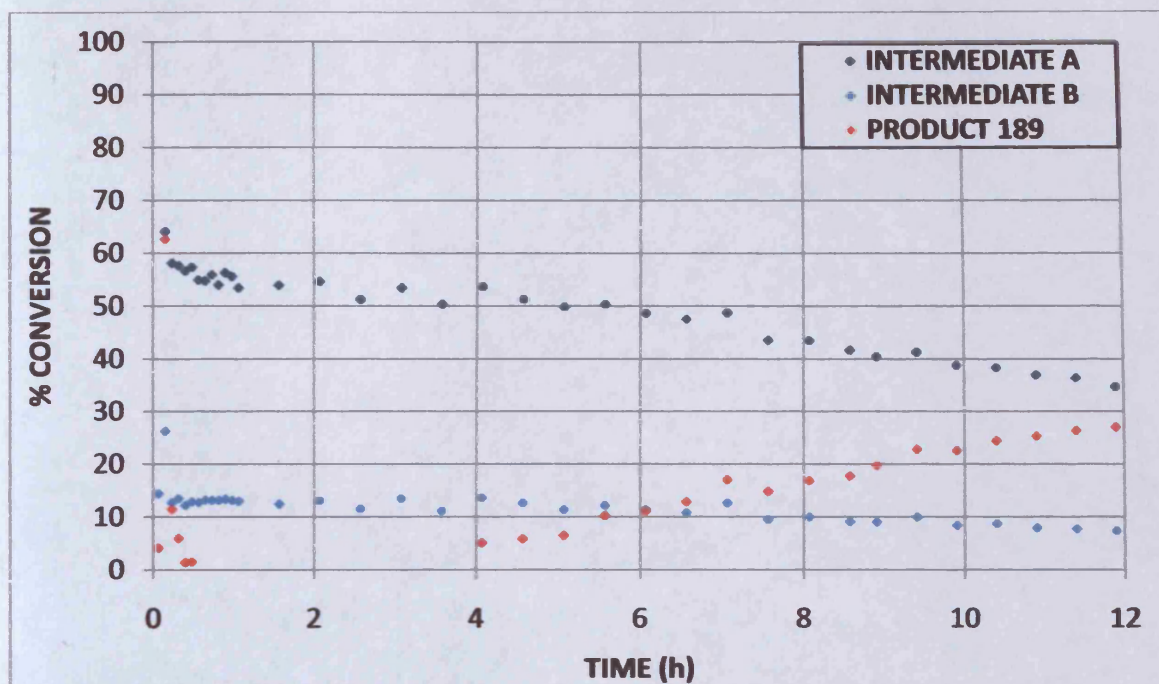


Figure 20: ^1H NMR reaction monitoring (293 K)

A further consequence of this experiment was the fact that it was apparently not possible to measure consumption of starting materials. For this reaction, both starting materials seemed to have been completely consumed by the time the first spectrum was acquired, 5 minutes after mixing. We therefore concluded that the first step to form the initial iminium ion was rapid; after which certain subsequent step(s) in the reaction sequence were rather slower. The identity of the two intermediate species was unknown at this time, although the earlier speculation regarding the possibility of the existence of enamine rotomers, as in the case of cyclohexanone **14**, was applied to this system.

A curious anomaly was that the conversion to product in the ^1H NMR monitoring experiment was far lower than the isolated yield achieved when the reaction was performed in the laboratory. Stirring these same reagents at ambient temperature in DMSO at the same concentration for 12 hours, followed by aqueous work-up and column chromatography had delivered the product in 86% isolated yield. However, it was acknowledged that product formation had not ceased after the end of the 12 hour ^1H NMR monitoring period.

This was confirmed when the reaction mixture was subjected to a single further ^1H NMR analysis the following day and product concentration was found to have increased.

We speculated that the differing behaviour may have arisen from the fact that the reaction components in the NMR tube were not being stirred as efficiently as in the round-bottomed flask. However, we had previously asserted that the reaction was unimolecular except for the initial addition to the carbonyl compound and the hydrolysis of the α -benzoyloxyimine analogous to 176. It was therefore thought likely that the hydrolysis could have been accelerated by aqueous work-up.

With this set of data, it was thought we had the potential for a reproducible practical procedure that could be employed to learn something of the temperature dependence on the overall reaction rate.

We discussed the feasibility of making the reaction 'pseudo first order' by using an excess of one of the substrates, but reasoned that there was not much to be gained by this approach at this time, since both starting materials appeared to be completely consumed within the first 5 minutes of the reaction.

This crucial early stage was one from which it was difficult to obtain data, since there was an inevitable delay (about 20 minutes) between the mixing of the starting materials and the acquisition of the first spectrum. Figures 21 and 22 depict the progress of the reaction at 298 and 303 K respectively.

Beyond the fact that the reaction had progressed further at higher temperature, the two sets of curves possessed a remarkably similar topology, and we derived encouragement from this in terms of the validity of our experimental set-up.

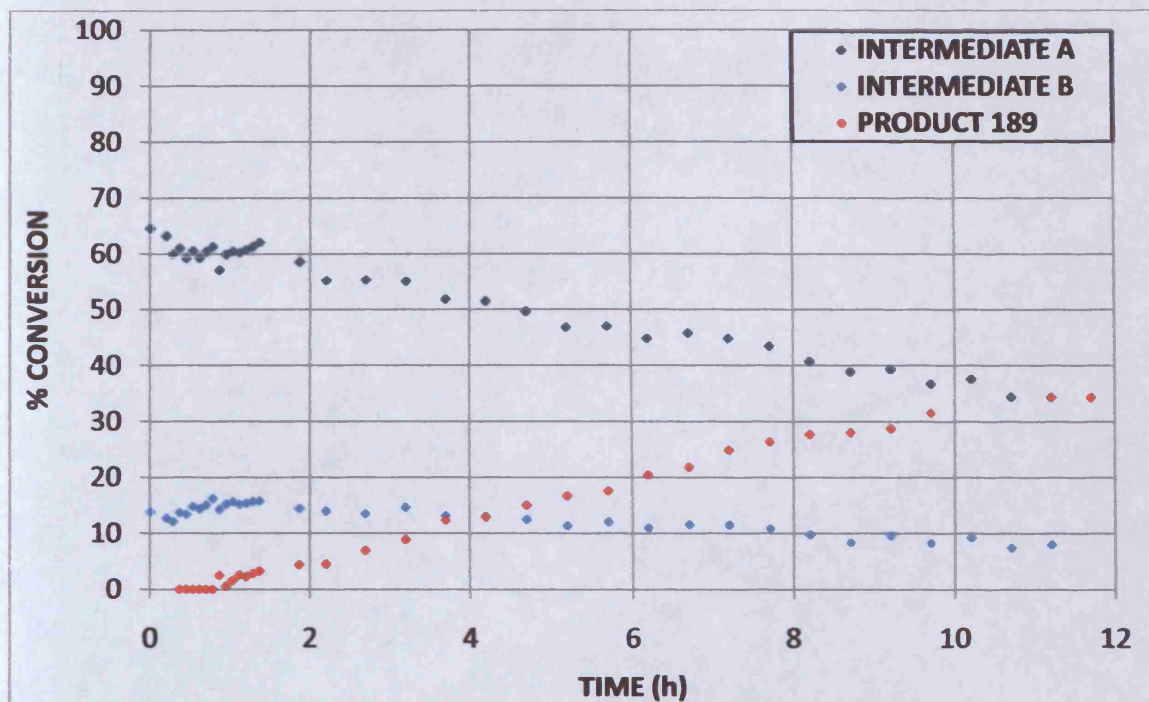


Figure 21: ^1H NMR reaction monitoring (298 K)

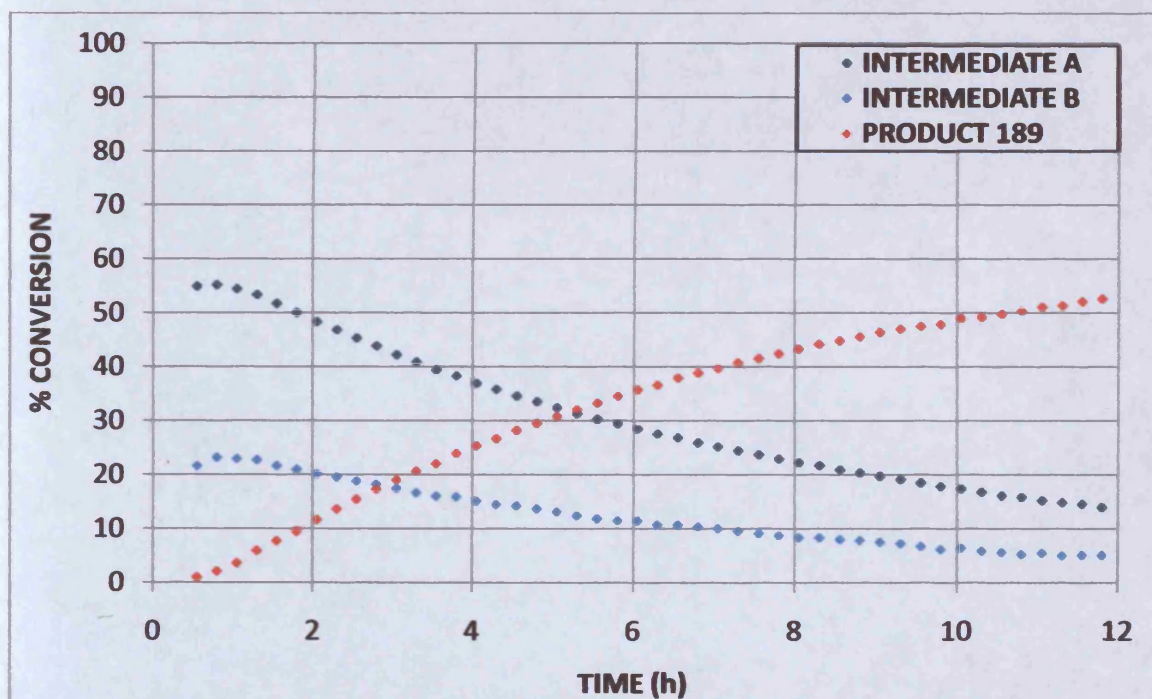


Figure 22: ^1H NMR reaction monitoring (303 K)

Figure 22 (at 303 K) showed a seemingly more reliable data set than the run at 298 K (Figure 21), with fewer and smaller deviations from smooth curves.

In previous experiments, the reaction mixtures were prepared by adding a solution of carbonyl compound in DMSO- d_6 (0.3 ml) to an NMR tube containing a solution of the hydroxylamine hydrochloride in DMSO- d_6 (0.3 ml). Prior to this, the solution in the NMR tube was scanned once in a 250 MHz spectrometer in order to determine a value for receiver gain prior to mixing, i.e. commencement of the reaction. The NMR tube therefore contained insufficient solution in the preparatory stage of the experiment, resulting in poor lock and shim. This was perpetuated in the kinetic run of the reaction; and perhaps strongly contributed to error when the areas under the peaks of interest were calculated. Once again, thought was given to improving the experimental procedure, and this resulted in the acquisition of data of higher quality. This same protocol was reproduced for reactions at 298 (therefore a good opportunity to repeat one of our runs) and 308 K (Figures 23 and 24).

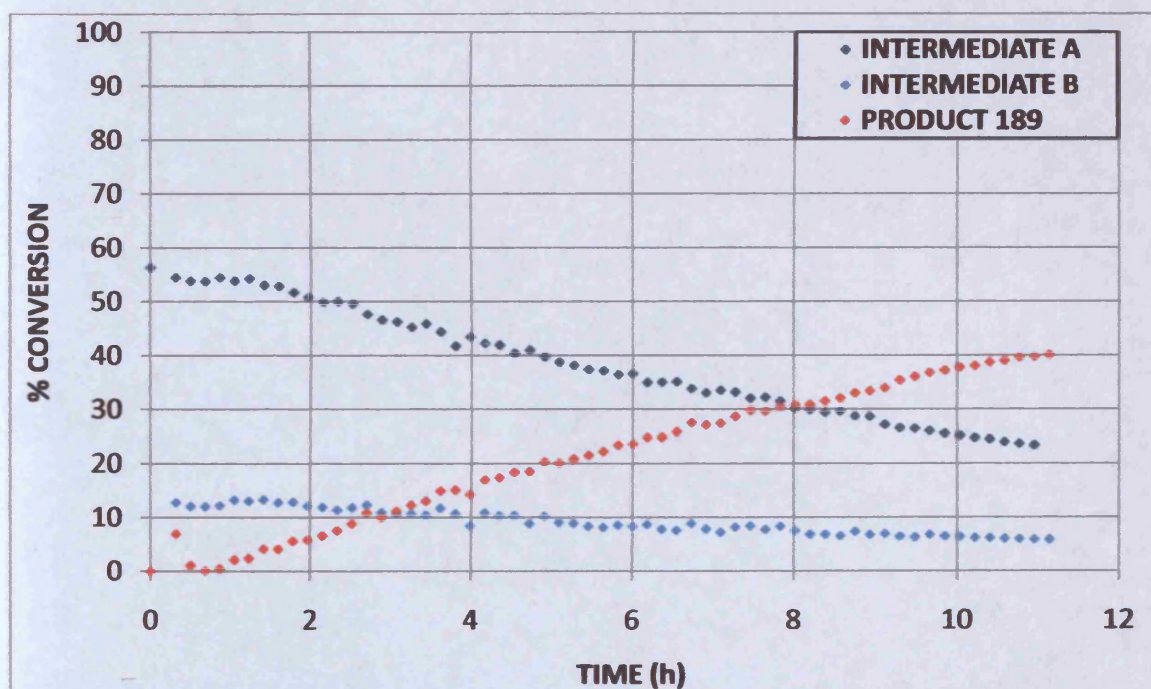


Figure 23: ^1H NMR reaction monitoring (298 K repeated)

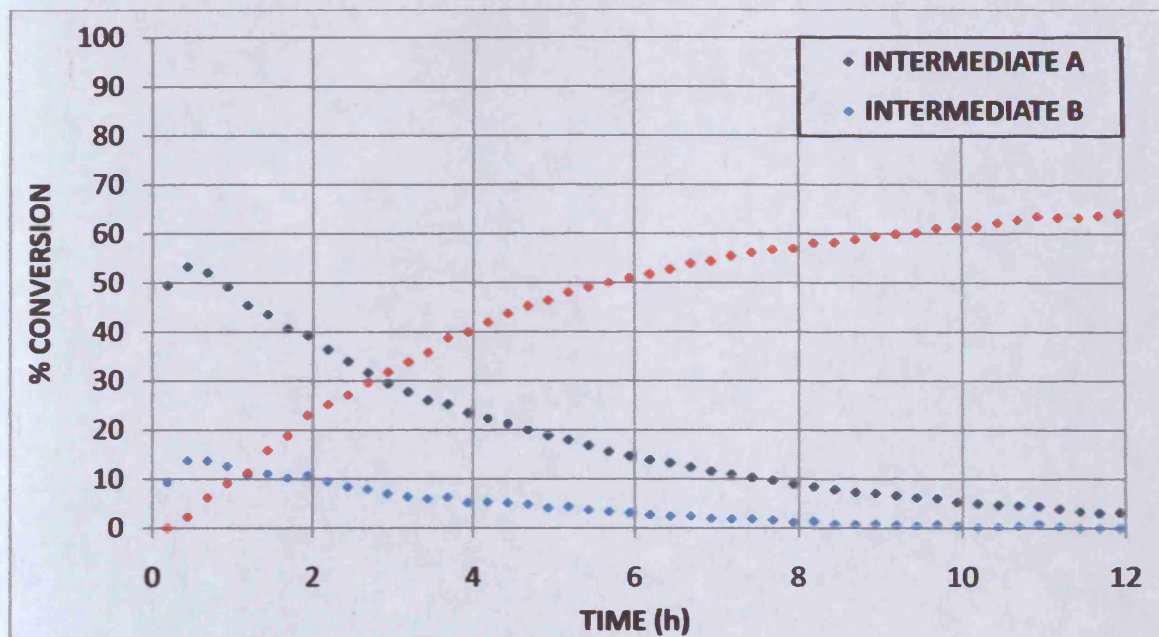


Figure 24: ^1H NMR reaction monitoring (308 K)

Overlaying the data series from the two runs at 298 K showed that the experimental procedure was reproducible, but only to a limited extent at this stage (Figure 25).

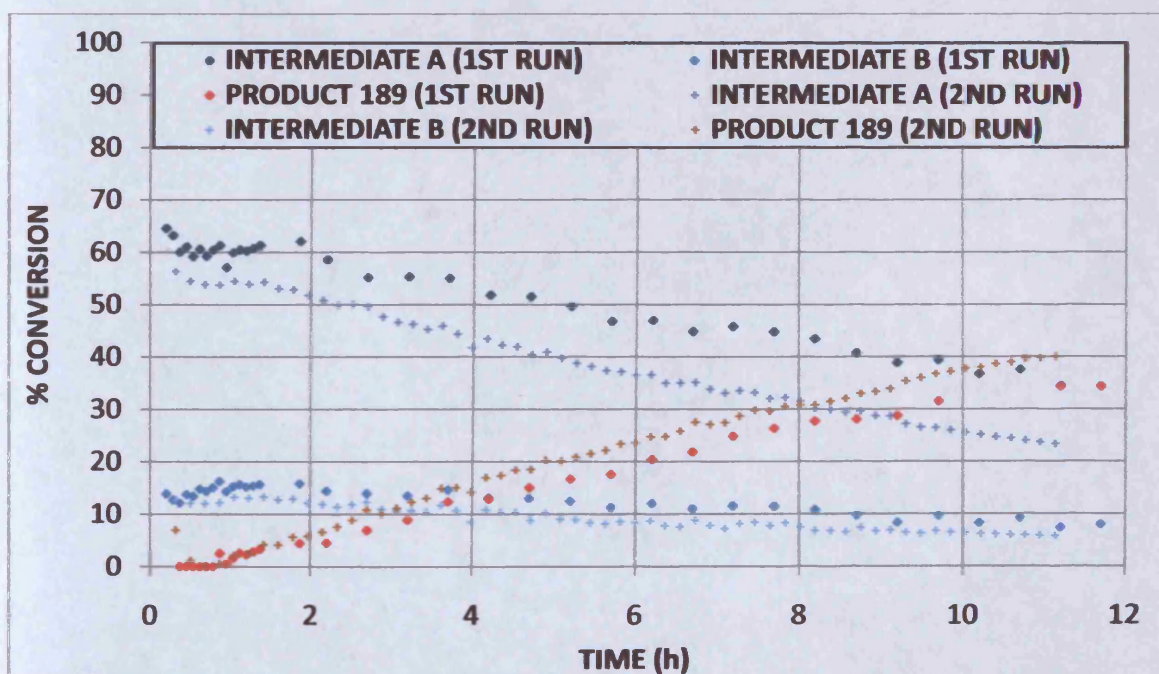


Figure 25: Data series at 298 K overlaid

5.2.3 Relationship between temperature and rate of reaction

The overlaid data series revealed maximum deviations of between 10–15% between the two runs. While the second data set had been obtained under an improved experimental method – and this had resulted in more consistent data and a smoother reaction profile – we reasoned that the discrepancies between the two runs could not be accounted for solely by the changes we had made to the protocol. Ideally, the proper course would have been to repeat the experiment several times under rigorously identical conditions; however both the finite time available for these experiments, and the realisation that we may not have developed the method fully; meant that further duplicate experiments were not conducted at this time. Nevertheless, we felt that the data that we had collected could be used to our benefit, provided that the appropriate consideration was given to the error contained therein.

Observing the increase in reaction rate as temperature increased was of immediate interest. This was highlighted by overlaying the plots of product formation at each of these temperatures (Figure 26).

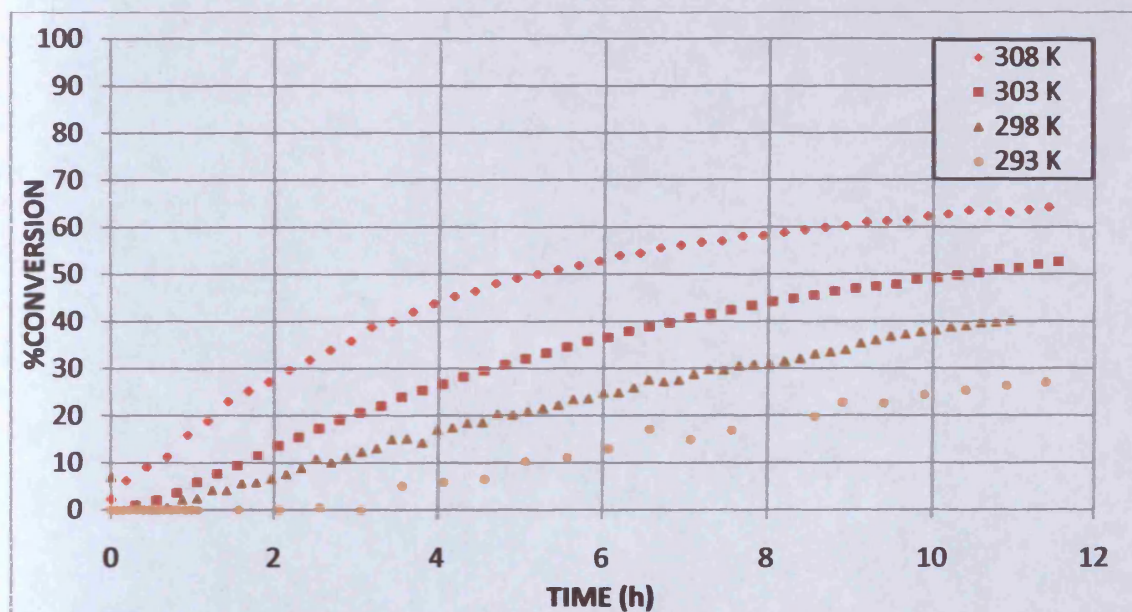


Figure 26: Overlay of product formation at various temperatures

In an admittedly crude approximation, rate constant values at each temperature were determined using the method of initial rates (the gradients of the curves were measured at the early stage of the reaction, i.e. when product was first being formed), and this data fed into the Arrhenius equation by plotting $\ln k$ against $1/T$ (Figure 27).

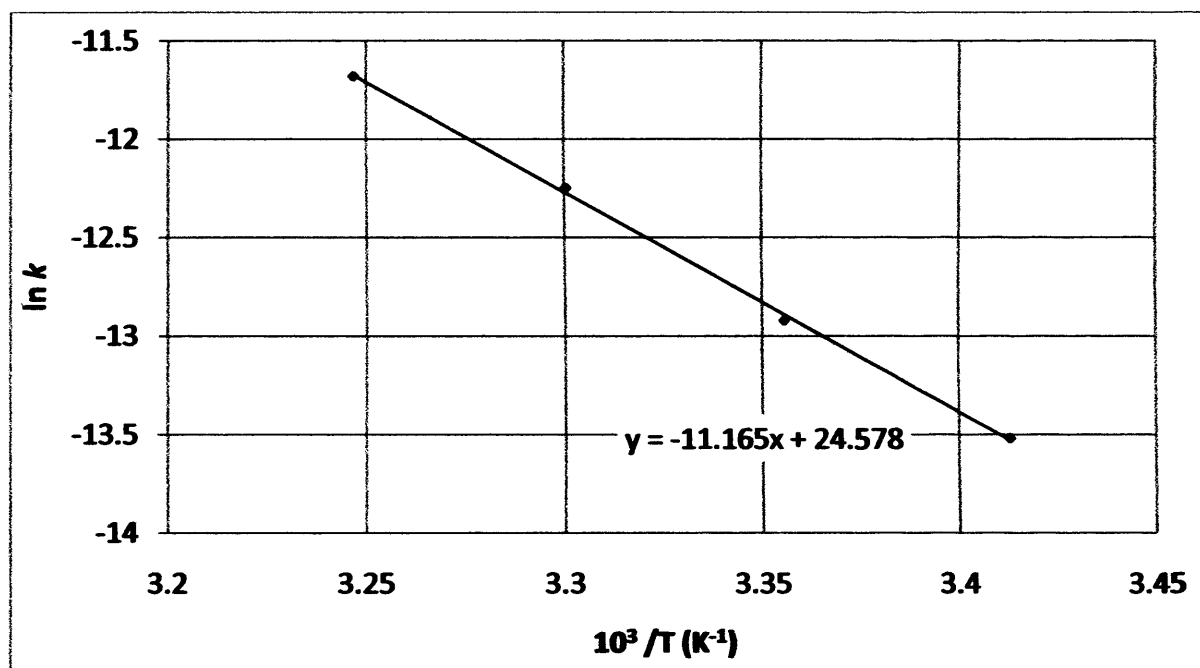


Figure 27: Arrhenius plot for reaction

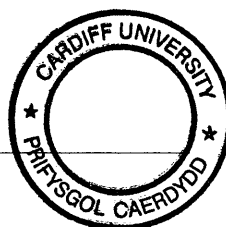
The Arrhenius equation states that:

$$\ln k = \ln A - \frac{E_a}{RT}$$

Under the acknowledged limitations of the original data series, the straight line form of the graph was a remarkable (and perhaps fortuitous) result, which showed that the rate of reaction varied with temperature according to the Arrhenius equation. Further, the activation energy for the reaction, E_a was given by the slope of the graph multiplied by $-R$, i.e. 93 kJ mol^{-1} . The value of A , the pre-exponential factor was calculated as $4.7 \times 10^{10} \text{ s}^{-1}$.

The inherent drawbacks of this approach were made evident by the early progress of the reaction, which in all cases and particularly at lower temperatures, showed a lag between mixing of the starting materials and formation of the product **189**. At this stage (the first hour), the intermediates were still being formed, and so in terms of the reaction kinetics, it was incorrect to think of starting materials forming two distinct intermediates (perhaps related to each other) followed by a stepwise conversion to the final product. Since the two processes were synchronous (i.e. concentration of the intermediates increased *whilst* product was being formed), we knew it would be necessary to ignore the early part of the curves when measuring the rate constants. The issue then was at what time point in the reaction coordinate it was valid to take a measurement of initial rate, a question which was complicated further by the observation that the reactions at lower temperature took a longer time to get underway in terms of product formation than in the experiments at higher temperature – this meant that it would be incorrect to take a time, t at which all the initial rates should be measured. We were therefore left with the somewhat arbitrary approach of taking the ‘initial’ time point in each case as being approximately one hour after the maximum concentration of intermediate species was observed.

The fact that these approximations – along with underlying experimental error arising from measurements of concentration, supposed purity of starting material and internal standard, integration and data processing – gave numbers strongly indicative of Arrhenius behaviour, perhaps owed more to our being fairly consistent in each experiment and in the treatment of each data series than to any serendipitous accuracy in the measurements. In all probability, the approximate initial rates method gave numbers which were proportional to the real rate constants, and hence gave a straight line Arrhenius plot.



5.2.4 Examination of the intermediates

On the NMR timescale, and using 3,3,5,5-tetramethylcyclohexanone **188** as the carbonyl compound in the α -oxygenation reaction, only two distinct intermediates were clearly visible and quantifiable in the reaction mixture. This was a greatly simplified picture in terms of the proposed reaction mechanism, and indicated that the reaction pathway was proceeding swiftly through a number of possible intermediate species up to the decay of the two visibly apparent species in the ^1H NMR. We hypothesised that the rate-determining part of the mechanism was therefore the consumption of the two intermediates.

This being the case, identification of these two species became a priority. Without having isolated any of these from the reaction mixture, and with GC-MS analysis having proven to be ambiguous, it was becoming clear that a more indirect approach and/or combination of techniques would be required.

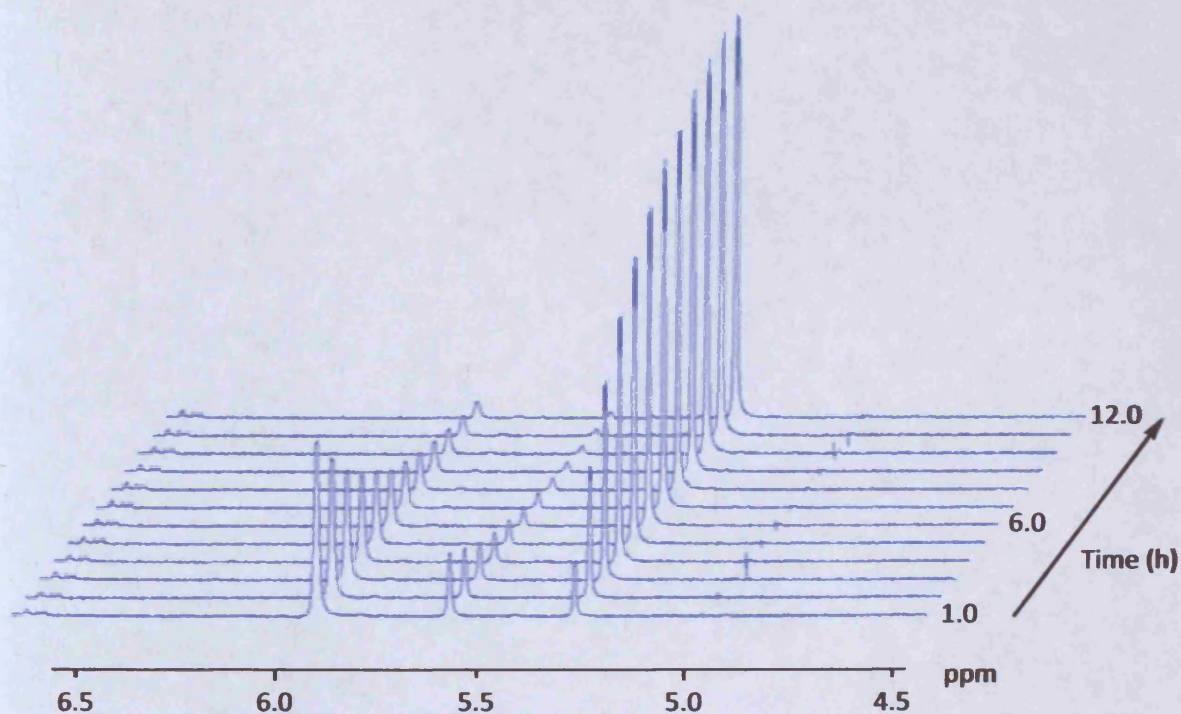
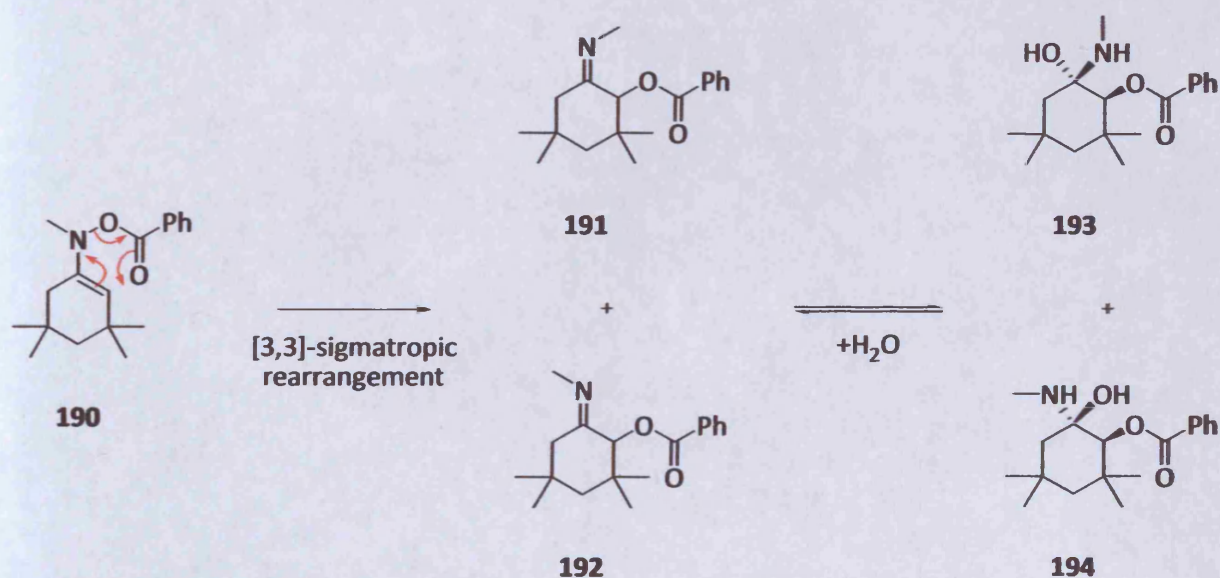


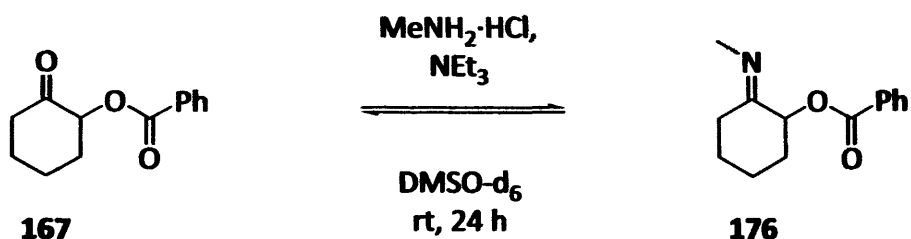
Figure 28: Overlay of ^1H NMR spectra showing diagnostic region

The de-cluttering of the ^1H NMR spectra which had been achieved by the use of 3,3,5,5-tetramethylcyclohexanone **189** as the carbonyl substrate meant that 2D NMR, specifically HMBC, was now able to furnish concrete information. The diagnostic α -hydrogens of the two intermediates were found to have a multi-bond coupling with the ester carbon, and this strongly suggested that these two signals belonged to intermediates occurring after rearrangement of the enamine **190** (see Appendix). Correlation was also noted to methyl resonances at around 3 ppm. If the proposed mechanism was correct, the observed intermediates could then be either α -functionalised imines **191** and **192** (geometric isomers giving rise to different chemical shifts for the diagnostic α -protons), or the aminol species **193** and **194** (*cis* and *trans* diastereoisomers) (Scheme 59).



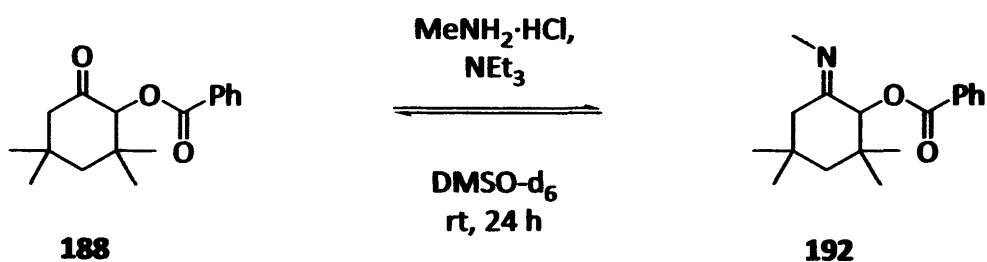
Scheme 59

In a further experiment towards identifying possible intermediate species within the reaction mixture, we had previously observed the equilibrium of the reaction between 2-benzoyloxycyclohexanone **167** and methylamine hydrochloride in DMSO-d_6 in the presence of a base by thoroughly mixing these substrates in an NMR tube and acquiring ^1H NMR spectra at intervals over a period of 48 hours (Scheme 60). The resulting spectra suggested that a signal at 5.13 ppm was the α -hydrogen of the α -benzoyloxy imine **176**.



Scheme 60

Repeating the experiment with the gem-dimethyl analogue **188** gave a similar picture, this time with an α -proton signal apparent at 5.05 ppm (Scheme 61). This somewhat lower chemical shift than those seen for the two major intermediates in the ^1H NMR monitoring work suggested that the intermediates which were prominent in the α -oxygenation reaction were not the α -oxy imines **191** and **192**.



Scheme 61

At this time, we favoured the two aminol diastereoisomers **193** and **194** as being the identity of the only two intermediates observed in this particular reaction sequence to any measurable extent. If correct, this assignment had interesting consequences for our understanding of the reaction. In seeking to make the transformation simpler in terms of the ^1H NMR, we had used starting materials which gave only two intermediate species within the reaction mixture. If these were the aminols from the latter part of the reaction sequence, and no other intermediates were present to any meaningful extent, expulsion of methylamine seemed to be the rate-limiting step for the reaction, when conducted using 3,3,5,5-tetramethylcyclohexanone **188** and *N*-methyl-*O*-benzoyl hydroxylamine hydrochloride **100-HCl**.

Looking at the kinetics of the consumption of the two intermediates provided further information which appeared to support this assignment (aminols **193** and **194**). As a unimolecular process, we expected the expulsion of methylamine to be a first order process (i.e. independent of concentration).

The integrated rate law for a first order consumption of a reactant, A is given by the equation:

$$\ln \frac{[A]}{[A_0]} = -kt$$

where $[A_0]$ is the concentration of A at time, $t = 0$; so that if $\ln [A]/[A_0]$ is plotted against t , a first order reaction will give a straight line going through the origin and a slope equal to $-k$, from which the rate constant can be obtained.

Thus, in a first order reaction, the concentration of reaction decreases exponentially with time with a rate, determined by the rate constant, k . Figures 29 and 30 show the plots of $\ln [A]/[A_0]$ against t for the decay of intermediates A and B respectively.

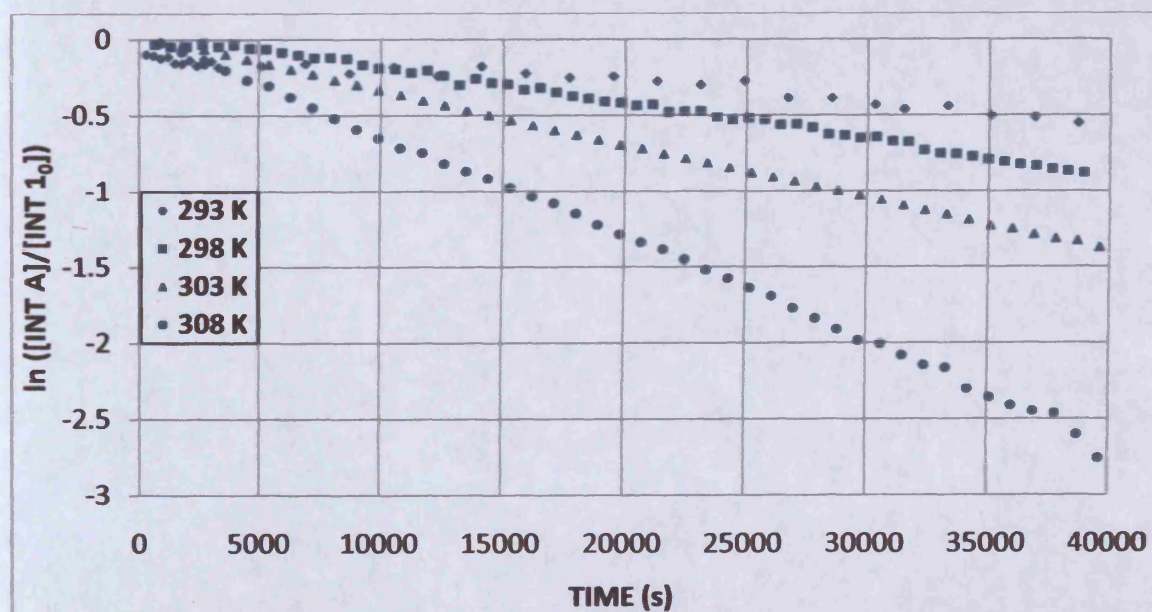


Figure 29: First order kinetics for intermediate A

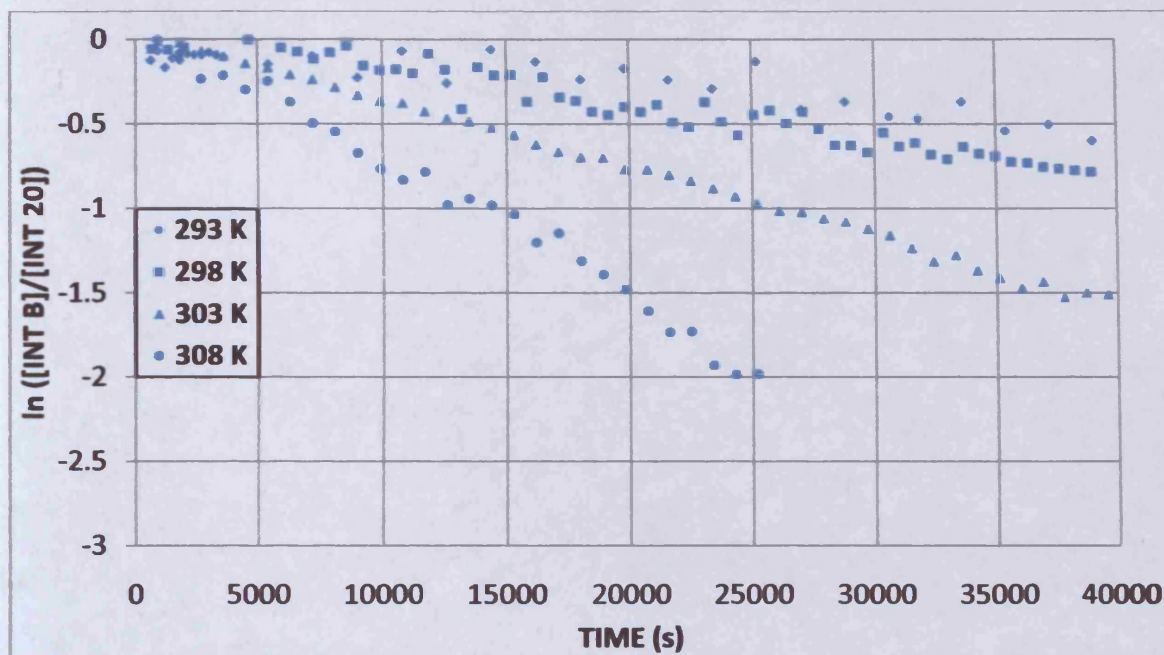


Figure 30: First order kinetics for intermediate B

Particularly in the case of the dominant species, intermediate A, applying the integrated rate law for a first order reaction appeared to give straight lines at all 4 temperatures. This lent credence to our hypothesis that the intermediates were the aminols **193** and **194**, or at any rate some species which underwent first order decay to give product **189**. This tentative identification of the key intermediates would later turn out to be erroneous, our thinking having been heavily influenced by what we observed as first order kinetics.

However, we were convinced that the two species were isomeric rather than chemically distinct; also that these two intermediates belonged towards the end of the reaction sequence, mechanistically speaking due to the evidence from 2D NMR (see Appendix).

This was borne out by the fact that the rate constants for both of the intermediates – when extracted by taking the gradient of the line of best fit in each case – were quite similar for both intermediates at each different temperature (Table 5).

Temperature (K)	k (Intermediate A) (s^{-1})	k (Intermediate B) (s^{-1})
293	1.42×10^{-5}	1.42×10^{-5}
298	2.17×10^{-5}	1.97×10^{-5}
303	3.47×10^{-5}	3.87×10^{-5}
308	6.63×10^{-5}	7.56×10^{-5}

Table 5: Rate constants for consumption of intermediates A and B

Aware that the previous method of deriving rate constants by the method of initial rates had serious limitations, we were cautious in our interpretation of these numbers. In order to plot the kinetic behaviour of the intermediates in terms of first order kinetics, we were obliged to ignore the early stages of the reaction. Here, we reasoned that the transformation proceeded with step(s) dominated by second order kinetics, e.g. the addition of the carbonyl compound **188** to the nucleophilic α -oxygenating reagent **100**·HCl. Hence, it would have been incorrect to assign purely first order kinetics across the entire reaction sequence, and so the portion of the data used in applying the integrated rate law for first order kinetics would necessarily need to comprise that part of the reaction where the decay of the intermediate (as a first order process) was dominant. Even with this correction having been applied, it was noted that the integrated rate law plots consistently showed deviations from straight line fits early in the reaction timeframe – indicative of the fact that ignoring much of the early data (and starting from a new time, $t = 0$) did not fully eliminate second order kinetics from our analysis.

This was thought to be a more reliable tool than the method of initial rates, so that having performed the integrated rate law calculations, it was a valid exercise to construct an Arrhenius plot, using the data from the consumption of the major unknown species, intermediate A (Figure 31).

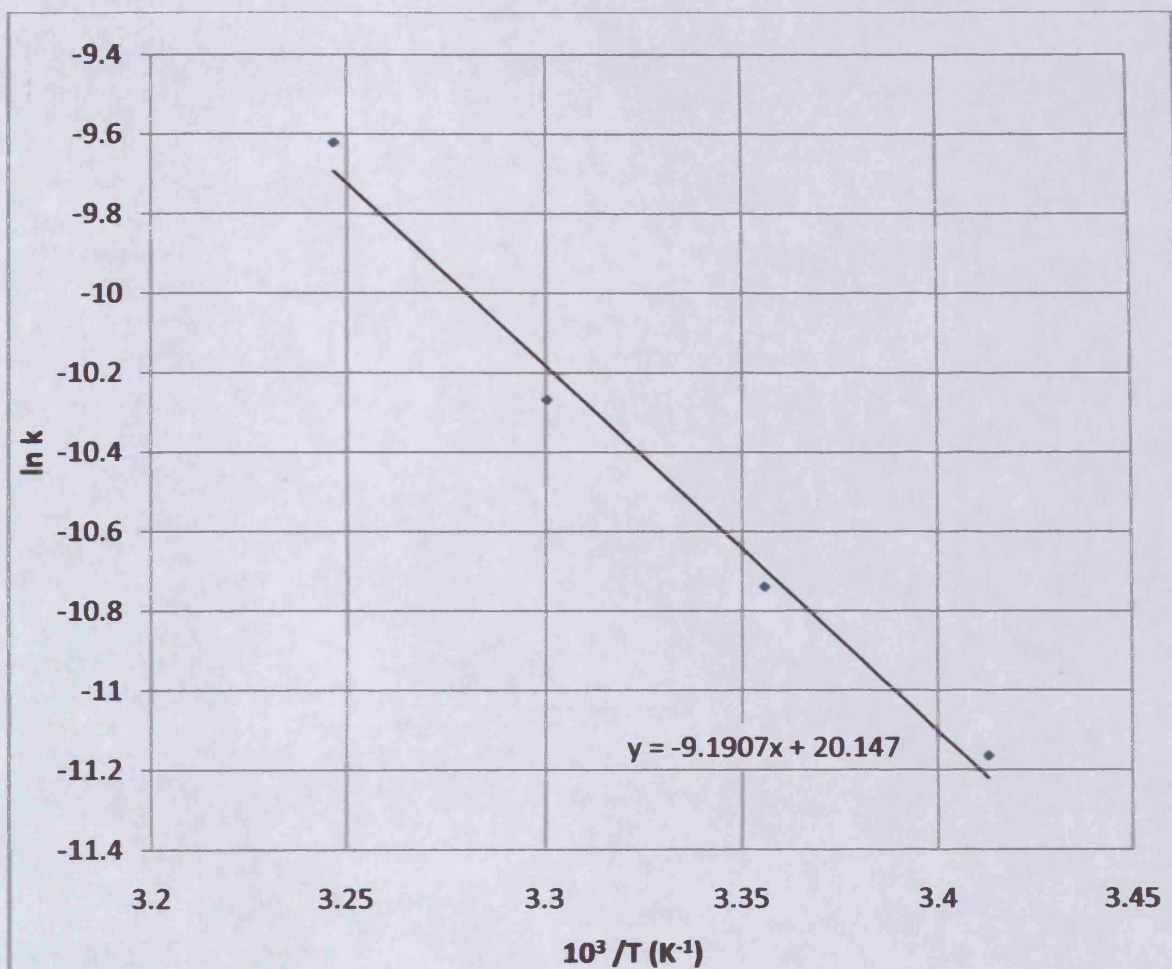


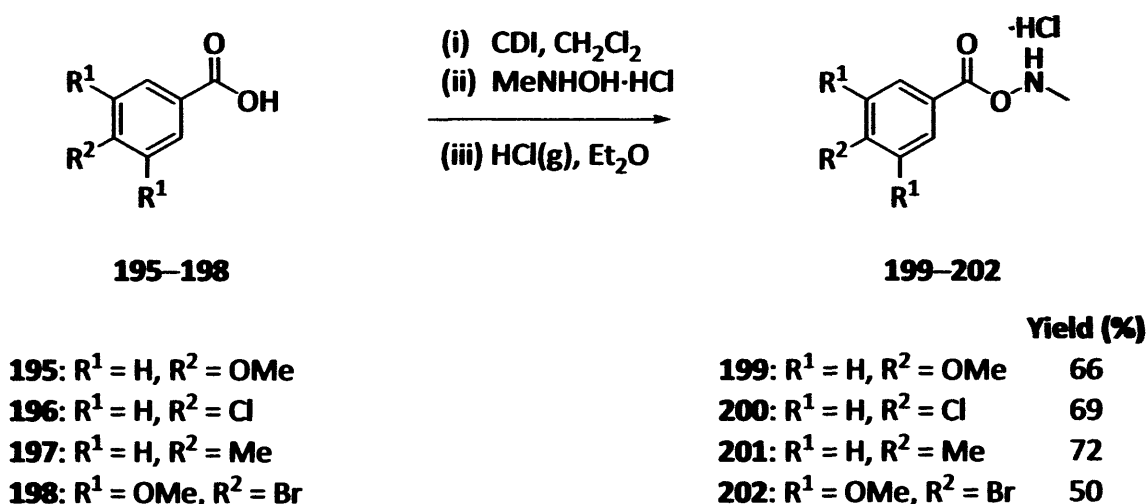
Figure 31: Arrhenius plot for consumption of intermediate A

From the Arrhenius plot, the activation energy was calculated to be 76 kJ mol^{-1} , and the pre-exponential factor, A was $5.6 \times 10^8 \text{ s}^{-1}$. These values made some sense and corresponded roughly to the values calculated from the whole reaction by the method of initial rates. To some extent, this result validated the practical procedure and the data processing which followed. However, the initial rates method did involve making major assumptions in determining the rate constants, while those derived from the decay of intermediates A and B were less ambiguous, albeit with inherent flaws.

5.3 Further variables in ^1H NMR work

5.3.1 Aromatic substituents

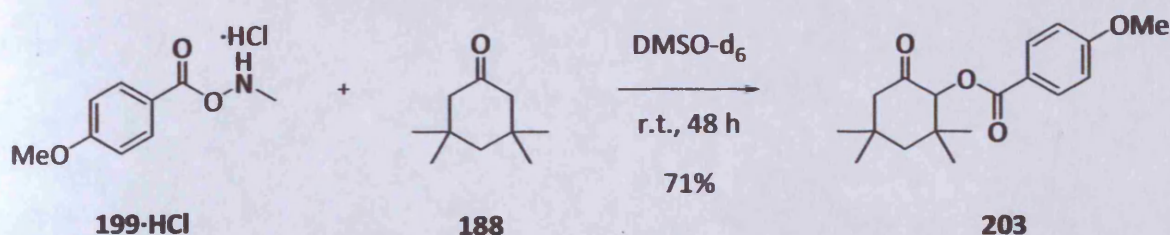
There was thought to be some further scope as far as simplifying the ^1H NMR spectra was concerned; namely by introducing substituents to the aromatic ring of the hydroxylamine reagent. It was hoped that even clearer spectra could be obtained; the absence of one or more hydrogen atoms on the ring would bring about a corresponding loss in resonances in the ^1H NMR in the aromatic region, as well as simplifying the coupling patterns due to the remaining protons. Synthesis of reagents **199–202** was therefore accomplished by the CDI-promoted coupling of *N*-methylhydroxylamine hydrochloride with the parent benzoic acids **195–198** (Scheme 62).



Scheme 62

A further purpose in preparing these new species was to test the effect of the *p*-substituent on the aromatic ring on the rate of reaction as well as the overall yield obtained under our ^1H NMR experimental conditions. We were hoping for an improvement upon the previous maximum conversion in the NMR work (64%), which curiously fell far short of the isolated yield (86%) for the same reaction when performed in the laboratory over the same timeframe.

In order to make the most efficient use of NMR machine time, this series of experiments was not performed by the continuous method we had developed. Instead, each reaction was conducted in the laboratory at ambient temperature (298 K) using dry DMSO- d_6 as the solvent; after 2 days the reaction mixtures were subjected to aqueous work-up and the product isolated by column chromatography. In conjunction with the bench experiment, a separate reaction was run within an NMR tube and this was analysed at known time intervals. Figure 32 shows the progress of the reaction with 3,3,5,5-tetramethyl cyclohexanone **188** over 2 days when *N*-methyl-*O*-4-methoxy-benzoyl hydroxylamine hydrochloride **199-HCl** was used as the α -oxygenating substrate (Scheme 63).



Scheme 63

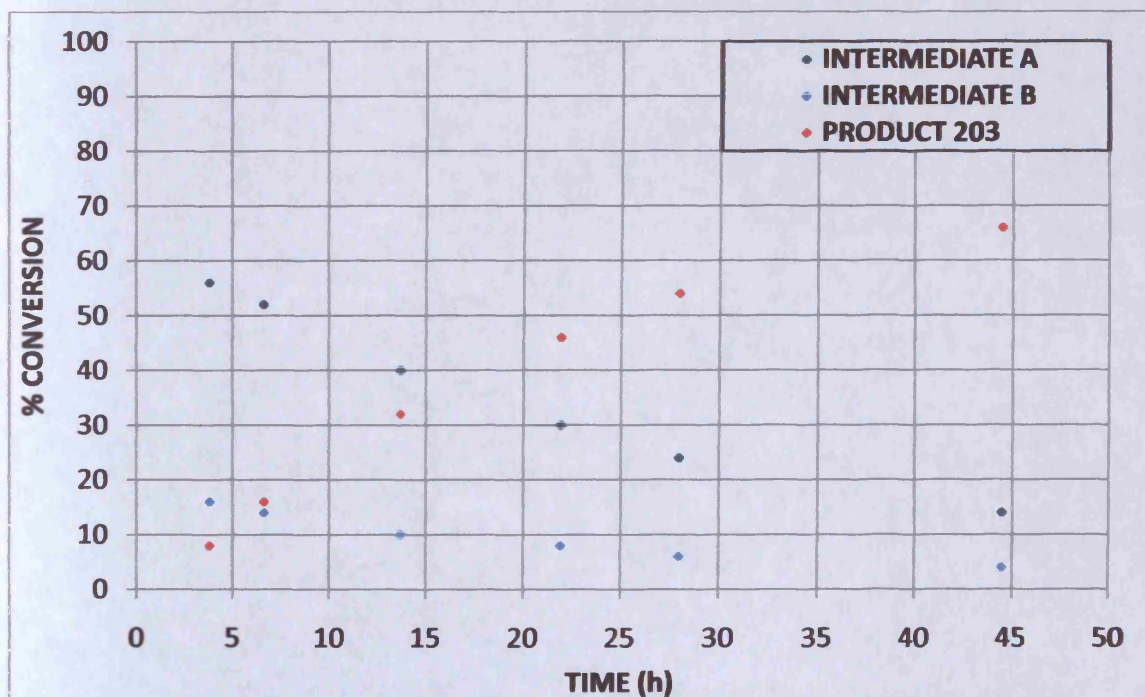
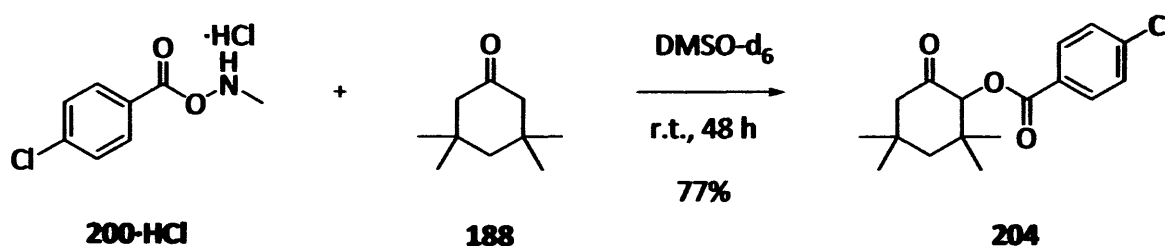


Figure 32: Reaction progress with 199-HCl

Compared with the usual *N*-methyl-*O*-benzoyl hydroxylamine hydrochloride species **100-HCl** which was our standard reagent for this transformation, the profile of the reaction with substrate **199-HCl** showed a few differences in terms of product formation and intermediate consumption. In the case of the methoxy *p*-substituted reagent **199-HCl**, there appeared to be an increased concentration of intermediates A and B present after 12 hours reaction time, and correspondingly less product **203**. However, after 2 days, we were able to measure a maximum conversion to product of 66% by ^1H NMR; furthermore we believed that formation of product was not yet complete by this point.

The procedure was repeated with *N*-methyl-*O*-4-chloro benzoyl hydroxylamine hydrochloride **200-HCl** (Scheme 64, Figure 33).



Scheme 64

This gave a broadly similar picture to that found with the previous substitution pattern, showing that neither the presence of an electron-donating methoxy group, nor a formally electron-withdrawing chlorine atom affected the rate of the formation of product to any significant extent, although there was less of the intermediate species remaining after 2 days in the case of the *p*-chloro reagent **200-HCl**.

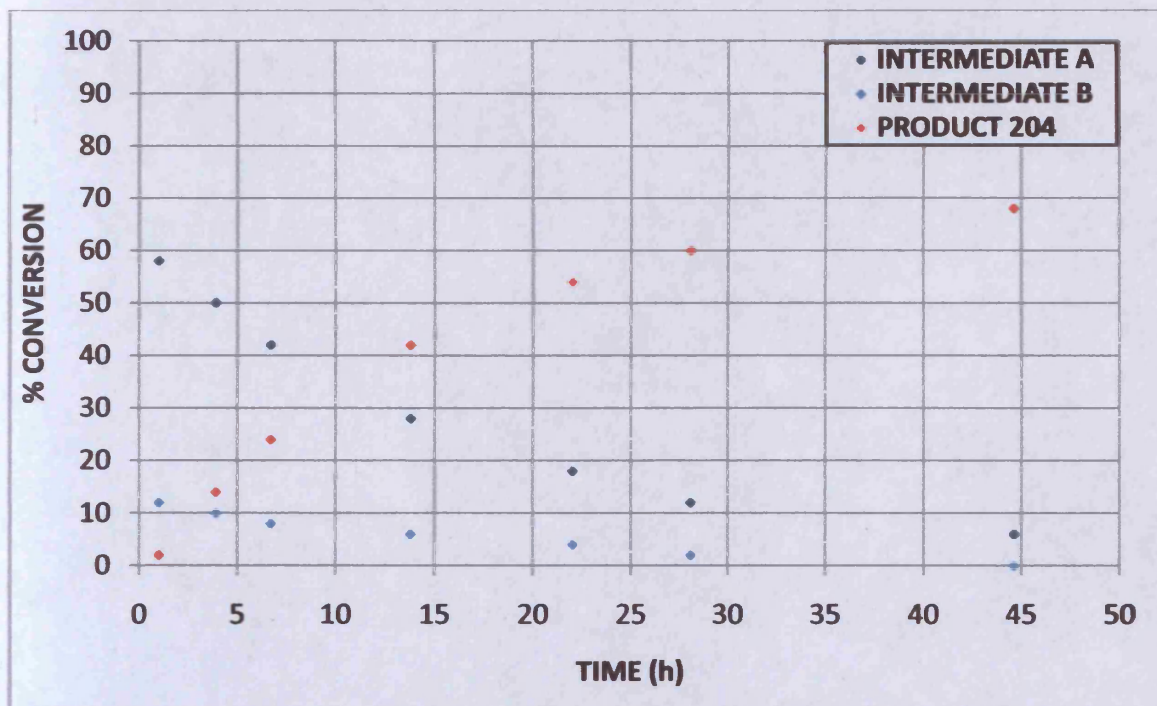
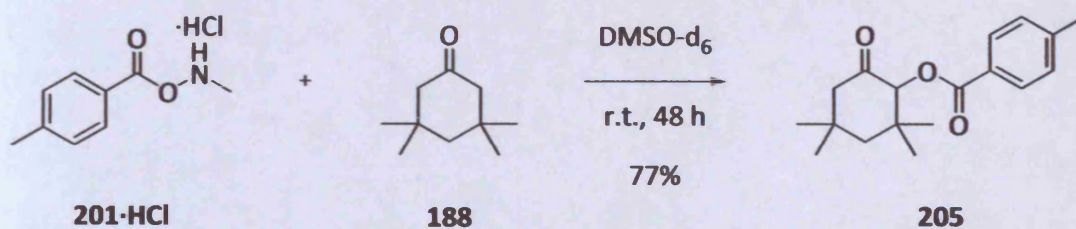


Figure 33: Reaction progress with 200-HCl

Broadly similar results were obtained using *N*-methyl-*O*-4-methyl-benzoyl hydroxylamine hydrochloride **201-HCl** (Scheme 65, Figure 34) and *N*-methyl-*O*-4-bromo-3,5-dimethoxy-benzoyl hydroxylamine hydrochloride **202-HCl** (Scheme 66, Figure 35).



Scheme 65

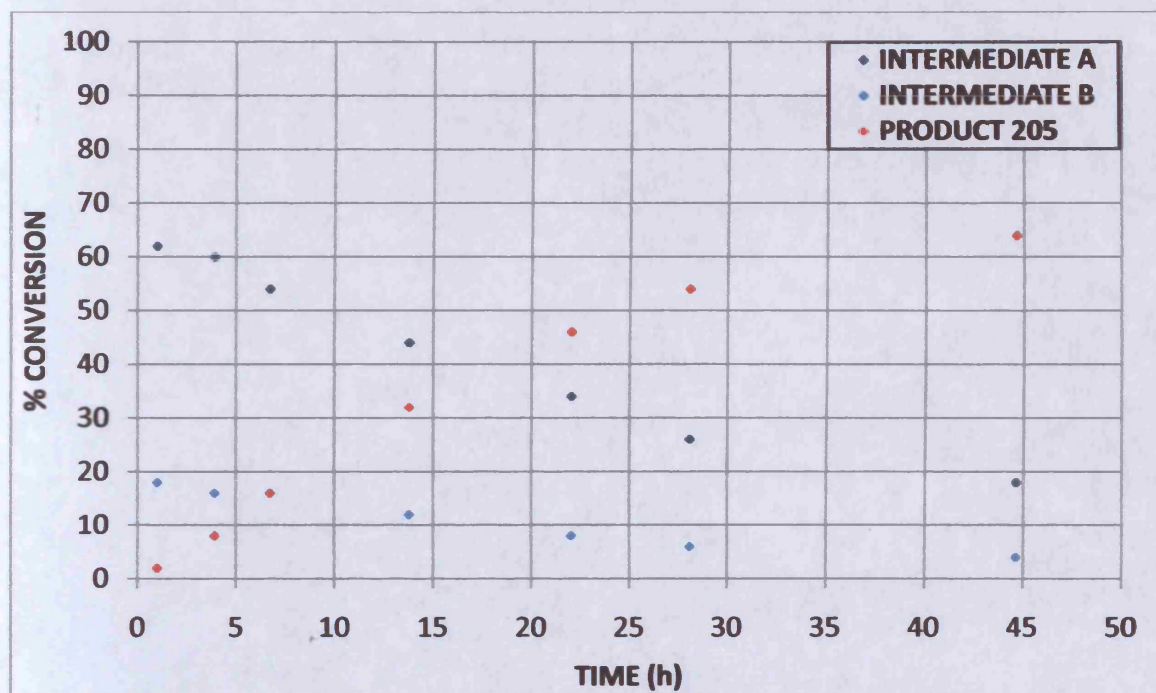
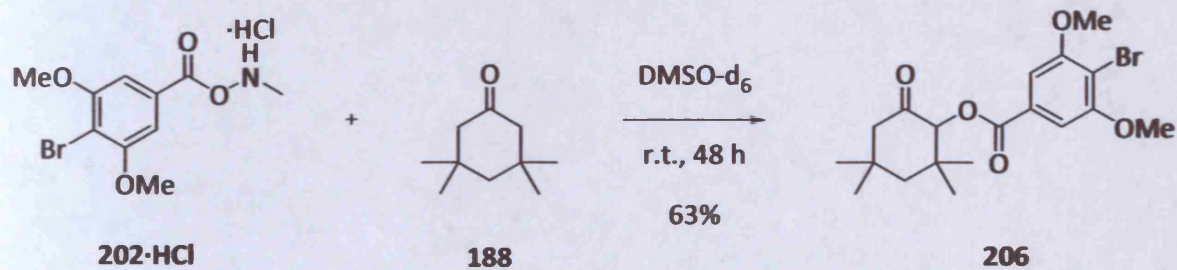


Figure 34: Reaction progress with 201-HCl



Scheme 66

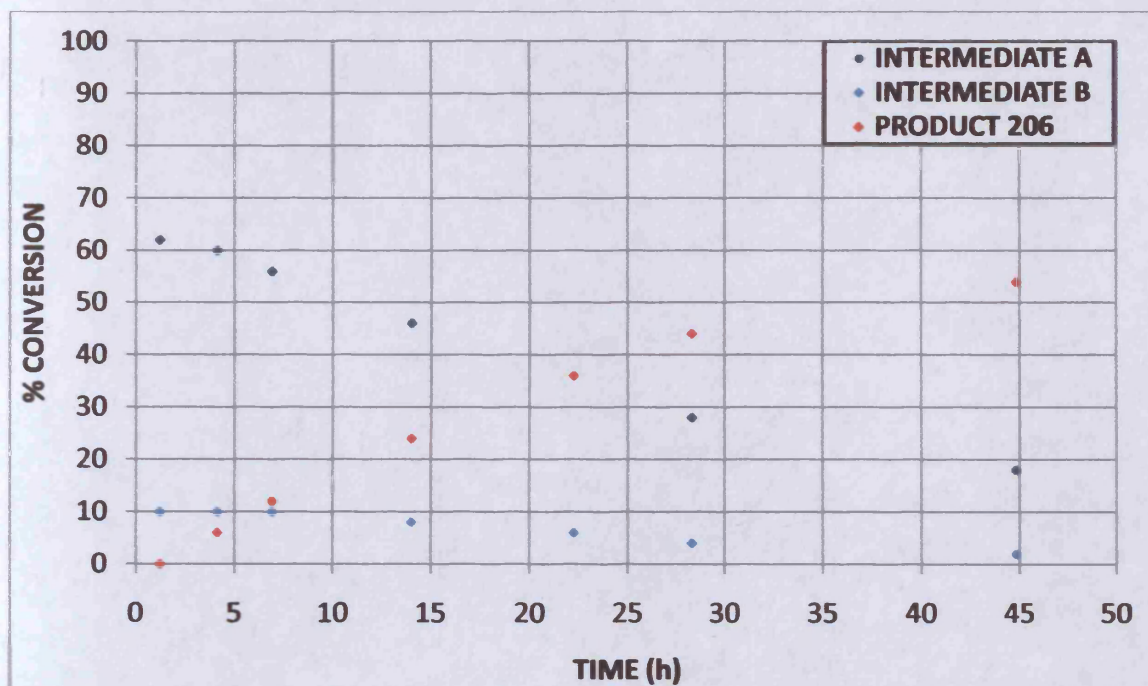


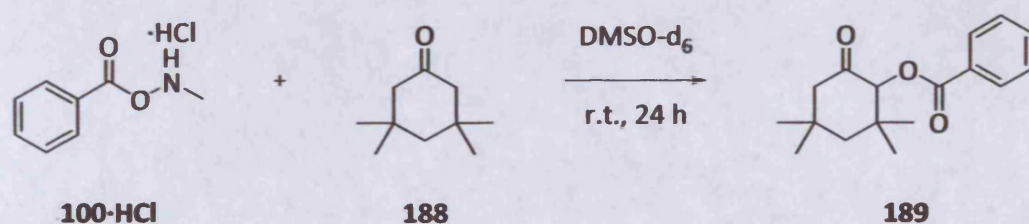
Figure 35: Reaction progress with 202-HCl

The latter result, with the tri-substituted phenyl ring within reagent **202-HCl**, was the only instance where a highly noticeable drop in reaction rate was observed by ^1H NMR monitoring; indicating that the reaction was potentially sensitive to changes in the steric or electronic nature of the ring substituents.

In terms of simplifying the ^1H NMR spectra, which was one of the reasons we undertook this series of experiments, the outcome was a successful one in that the loss of at least one peak and a simplification in the splitting patterns did simplify the spectra to a significant extent. However, there were no further discrete species detected as a result, either from elsewhere in the proposed reaction sequence or as a result of side reactions and/or product decomposition. Crucially, none of the new reagents gave any increase in isolated yield of product.

5.3.2 Stoichiometry

Returning to the standard reagent *N*-methyl-*O*-benzoyl hydroxylamine hydrochloride **100-HCl**, and its reaction with 3,3,5,5-tetramethylcyclohexanone **188**, we briefly examined the effect of varying the equivalents of both reactants. From the inception of the methodology, it was known that a 1:1 ratio of starting materials was optimal for most ketone substrates. In the first experiment, an excess of reagent **100-HCl** was used (1.2 eq., Scheme 67, Figure 36).



Scheme 67

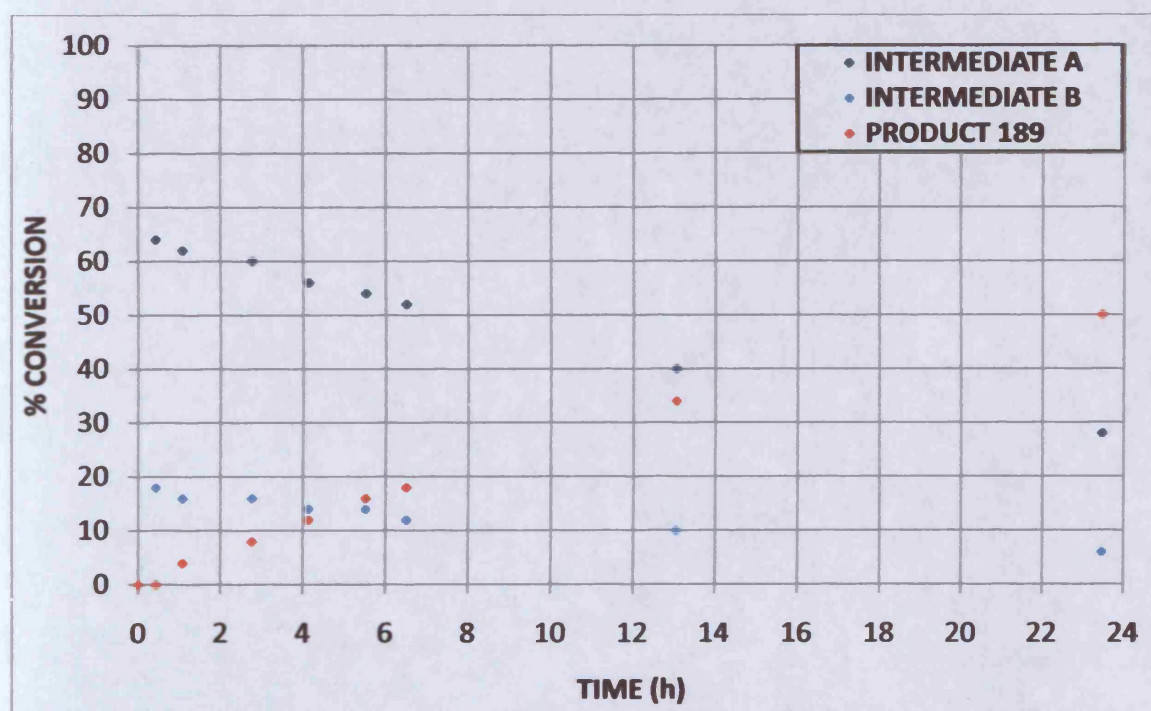


Figure 36: Reaction progress with 1.2 eq. **100-HCl**

Under the temperature controlled ^1H NMR experiments at 298 K, the reaction had progressed to roughly the same extent after 12 hours (approximately 30% conversion to product **189**) as in the current experiment with an excess of reagent **100-HCl**.

When a slight excess of ketone substrate **188** was employed, the reaction progressed slightly better (just over 40% conversion to product **189** after 12 hours) at 298 K over 24 hours; however this was not deemed a particularly dramatic improvement and therefore gave little grounds for re-inventing the entire methodology as far as stoichiometry was concerned (Figure 37).

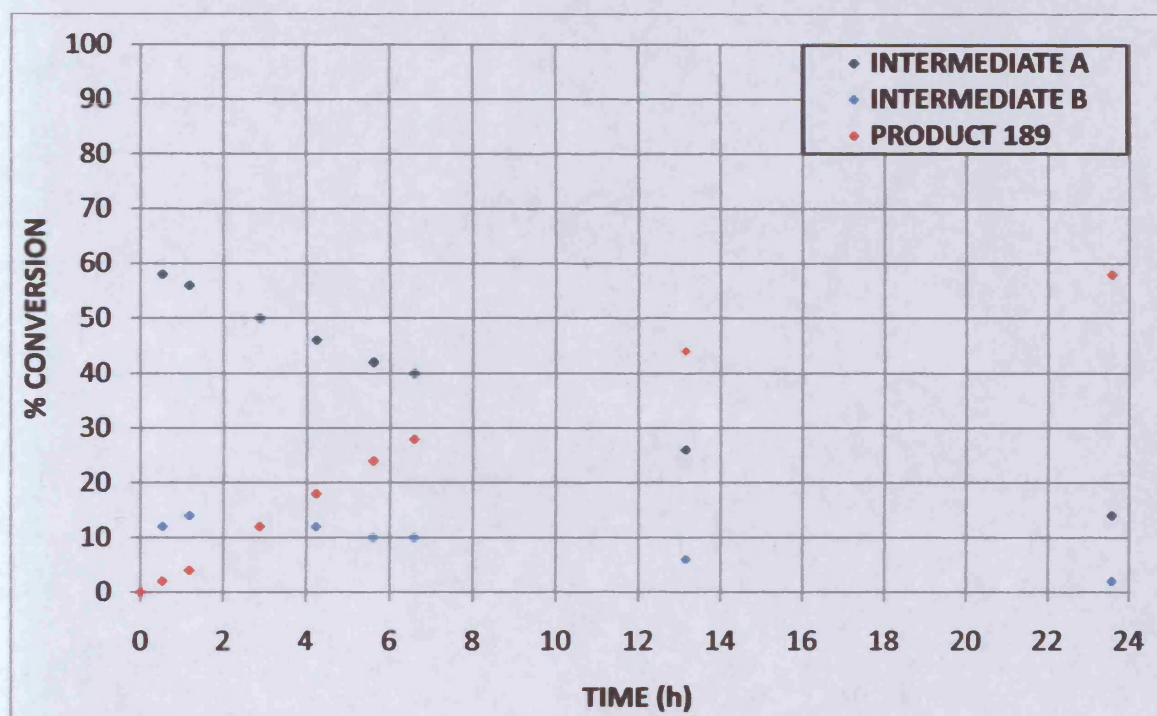


Figure 37: Reaction progress with 1.2 eq. 3,3,5,5-tetramethylcyclohexanone **188**

5.3.3 Solvent water content

We had for some time been interested in the possible effect of added water in the reaction mixture. The transformation gave an isolated yield of 86% in the laboratory when conducted at room temperature, after aqueous work-up and column chromatography; compared with a maximum conversion of only 63% when conducted in the NMR tube. We strongly wished to resolve this discrepancy, and reasoned that the only appreciable difference between the two reaction mixtures was the presence of water during work-up.

The deuterated DMSO used in the timed NMR work was labelled at 99.9 % purity and stored in sealed ampoules (and opened immediately before use). At the time, the moisture content of both the DMSO-d₆ and the solvent used in the laboratory work was not known; and we did not have any means of measuring this quantitatively. In testing the effect of added water, we made the assumption that the ampoules contained deuterated DMSO which was reasonably anhydrous.

The starting materials were 3,3,5,5-tetramethylcyclohexanone **188** and *N*-methyl-*O*-benzoyl hydroxylamine hydrochloride **100-HCl** in DMSO-d₆, and the reactions were conducted at 298 K, so as to replicate the earlier experiments as closely as possible.

The experiments were carried out using ampoules whose contents were doped with known amounts of water immediately prior to mixing of the starting materials (Figures 38 and 39 denote the progress of the reaction with 10 and 20 equivalents of added water respectively).

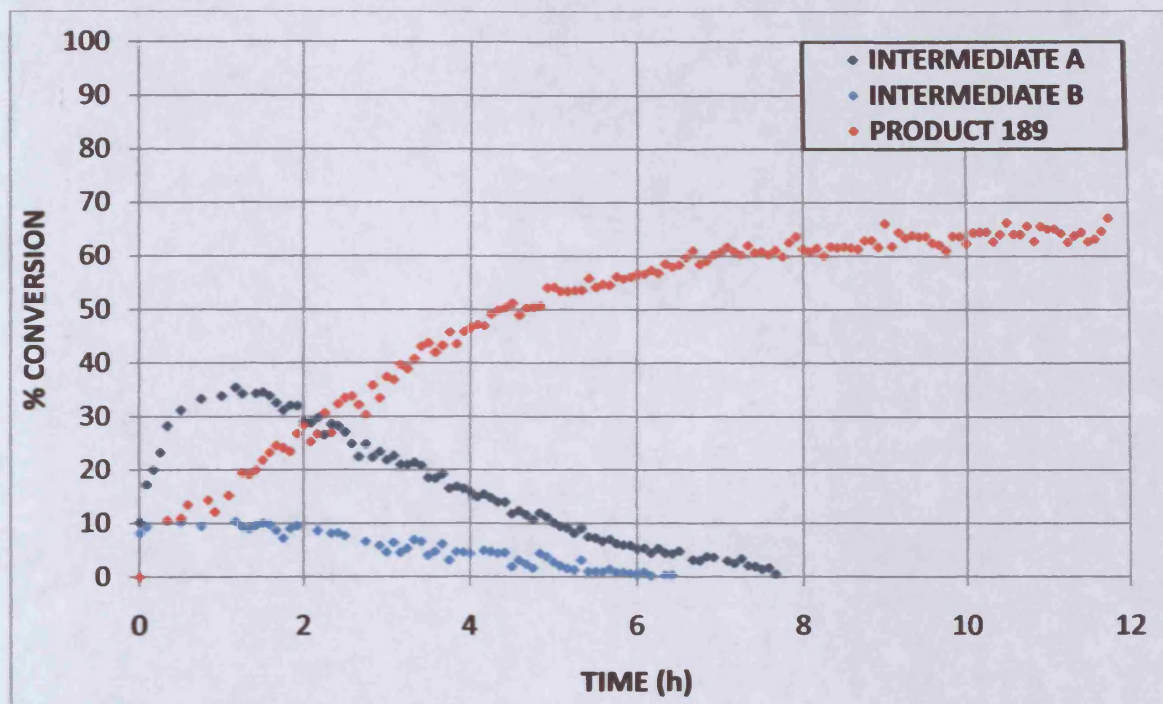


Figure 38: Reaction progress with 10 eq. added water

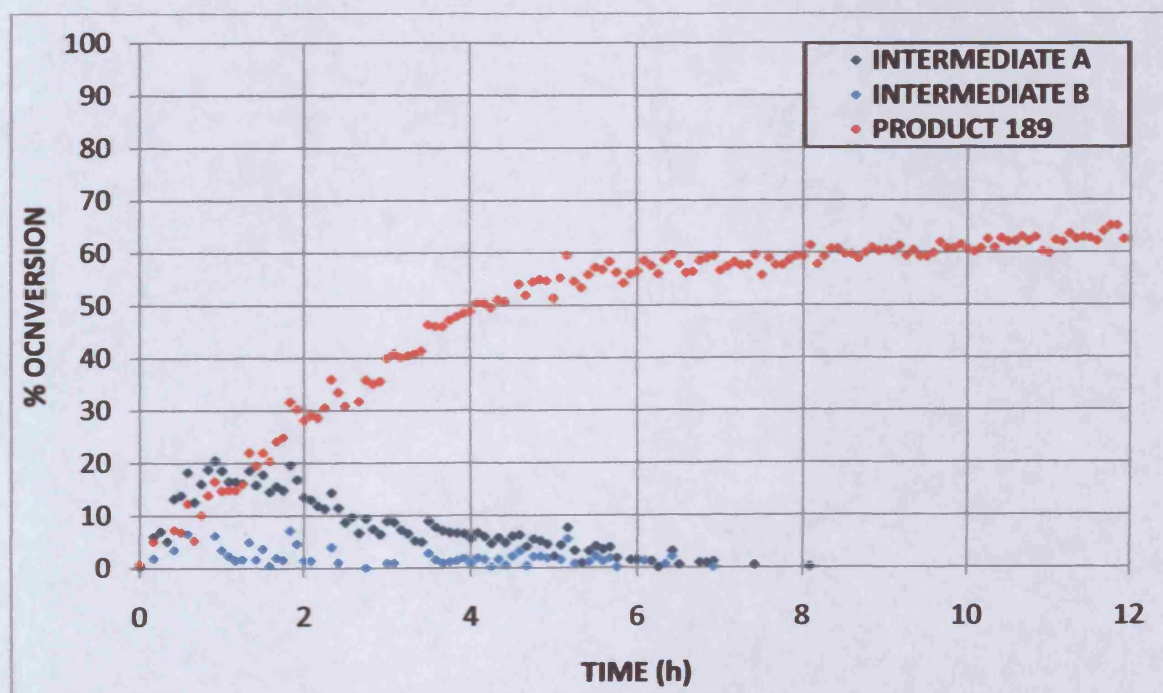


Figure 39: Reaction progress with 20 eq. added water

With excess water within the reaction mixture from the start, a notable increase in the rate of product formation was observed (Figure 40 is an overlay of product formation with no added water compared with 10 equivalents added water), along with a decrease in the concentration of the intermediate species in the early stages of the reaction. Additionally, the intermediates were both completely consumed long before the end of the monitoring period, and this had not been observed in any previous NMR monitoring experiment.

The presence of water was expected to have a retarding effect on the first phase of the reaction pathway, namely condensation of the amine with the ketone with the expulsion of an equivalent of water. It was possible this effect was overridden by the overall effect of accelerating the rate-limiting step for the process; however we believed at the time that the key intermediates were the diastereomeric aminols **193** and **194**, so it was difficult to envisage how their collapse (essentially the expulsion of methylamine) could be accelerated by the presence of extra water. Despite this concern, the positive result was that the behaviour of the reaction under the NMR conditions had more closely resembled that obtained in the laboratory.

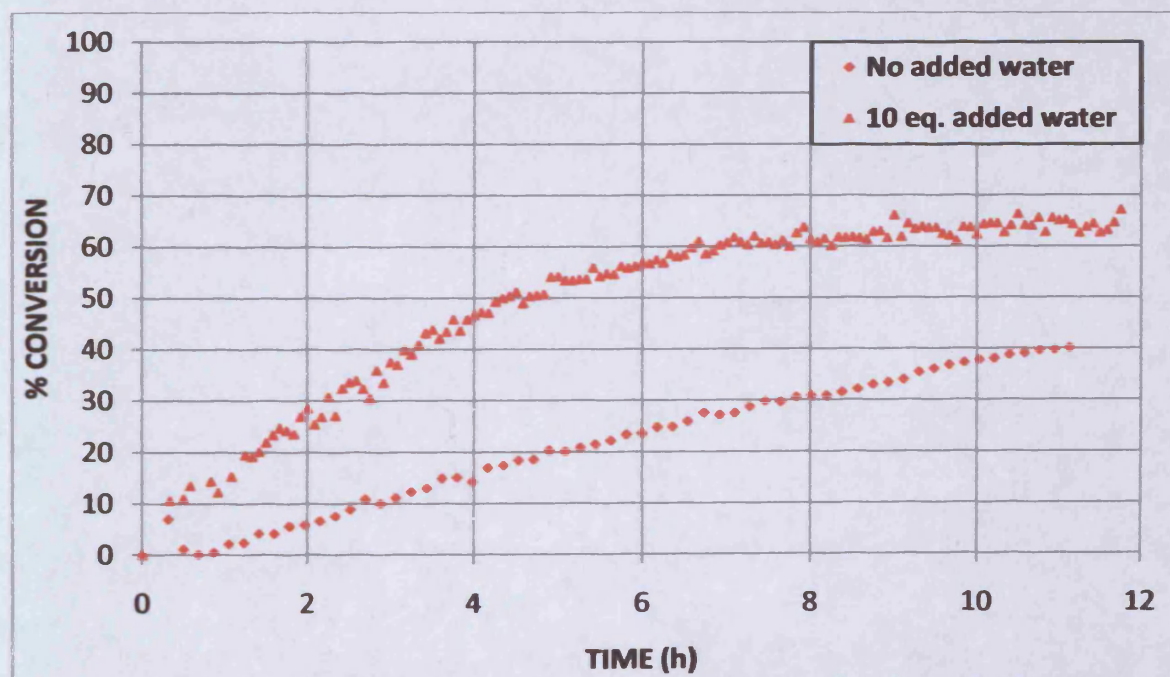
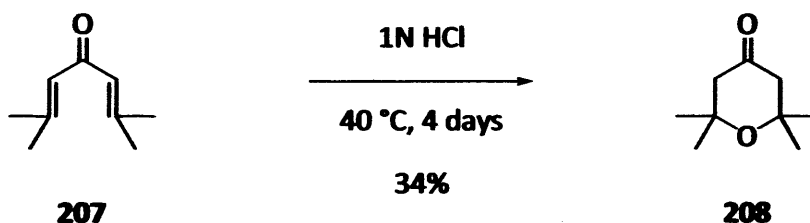


Figure 40: Overlay of product conversion with varied moisture level

5.3.4 A further ketone substrate

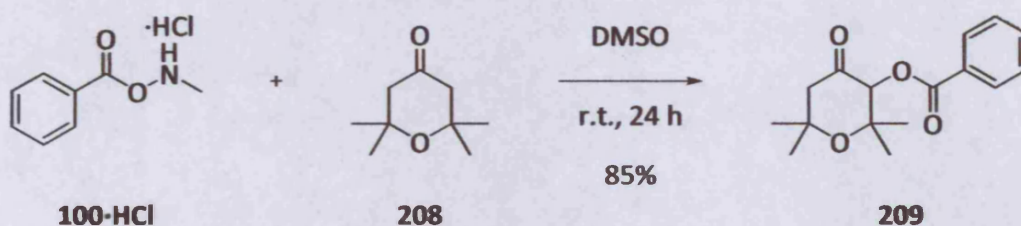
Finding another suitable ketone substrate was considered useful, not only in terms of validating the work we had carried out with 3,3,5,5-cyclohexanone **188**, but also because this material gave evidence for the presence of only 2 intermediate species in the NMR spectra; and we believed that the reaction mechanism included several other species. Evidence for the presence of any further intermediates could provide further confirmation for the mechanism of the transformation.

Stirring 2,6-dimethyl-2,5-heptadione-4-one **207** in 1N HCl at 40 °C over 4 days, gave after purification by column chromatography, tetrahydro-2,2,6,6-tetramethylpyran-4-one **208** in moderate yield (Scheme 68).⁷⁵ We hoped this would furnish a material which would be suitable for the NMR work for the reasons already described, as well as being a good partner for *N*-methyl-*O*-benzoyl hydroxylamine hydrochloride **100-HCl** in the α -oxygenation procedure.



Scheme 68

At room temperature, mixing *N*-methyl-*O*-benzoyl hydroxylamine hydrochloride **100-HCl** with the pyranone **208** in DMSO gave the desired product **209** in 85% isolated yield (Scheme 69).



Scheme 69

When this reaction was repeated under our NMR monitoring protocol at 303 K, at least two other peaks were evident in the diagnostic region of the spectra (6.3–5.0 ppm) (Figure 41).

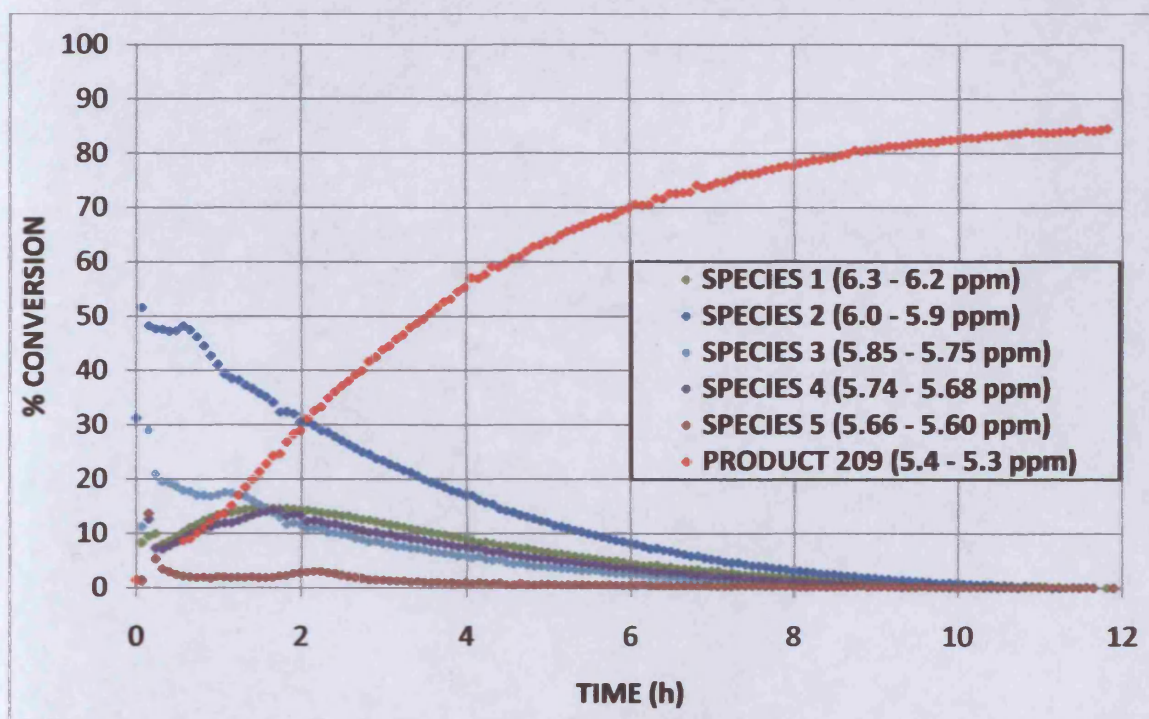


Figure 41: α -Oxygenation of pyranone 208 at 303 K

The addition of further peaks in the diagnostic region may have related to the presence of further intermediate species from within the reaction sequence. However, the additional complexity generated by this being a mixture of more components meant that running a 2D NMR did not furnish any additional meaningful information which could be used to identify any of the separate species within the reaction mixture.

On a positive note, the conversion measured by ^1H NMR in this transformation closely matched the isolated laboratory yield (86%); however it was not immediately obvious why a closely related analogue should produce such a highly differentiated data set to our previous substrate in this work, 3,3,5,5-tetramethylcyclohexanone **188**.

Examining the behaviour of the pyranone **208** gave an increase in the rate of product formation at elevated temperatures (Figure 42); this matched the findings with the previous ketone substrate **188**, although in general the transformation proceeded much more quickly with tetrahydro-2,2,6,6-tetramethylpyran-4-one **208** than with the commercially available 3,3,5,5-tetramethylcyclohexanone **188**.

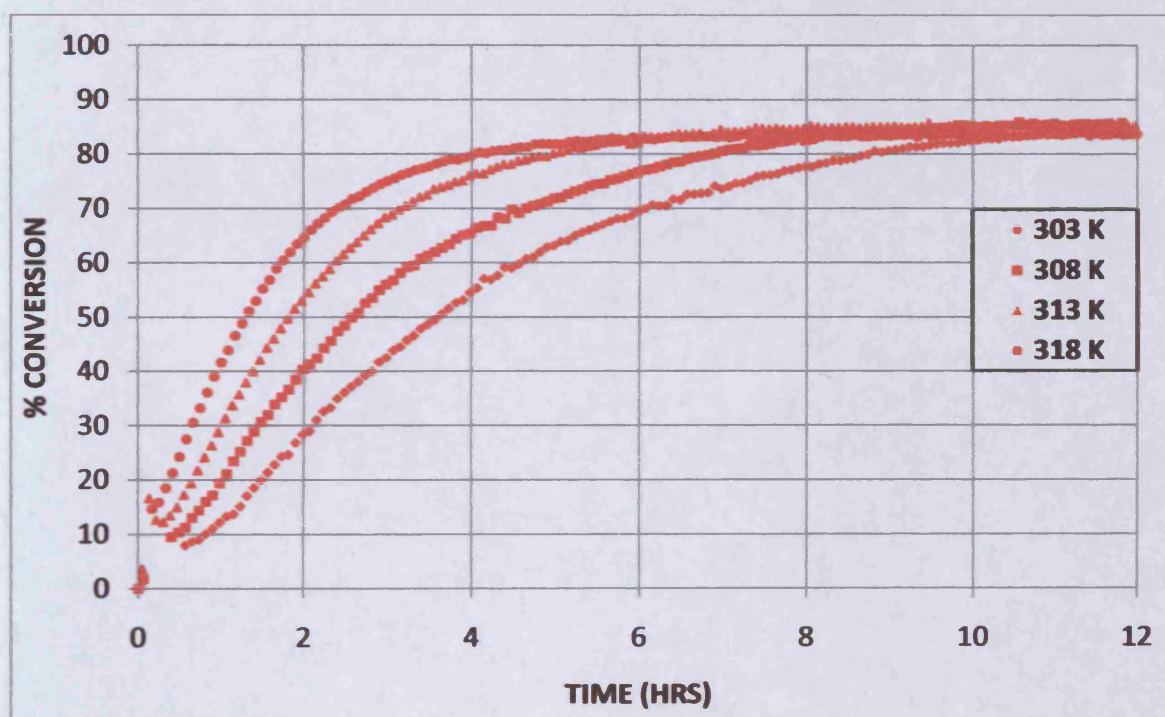


Figure 42: Formation of product **209** at various temperatures

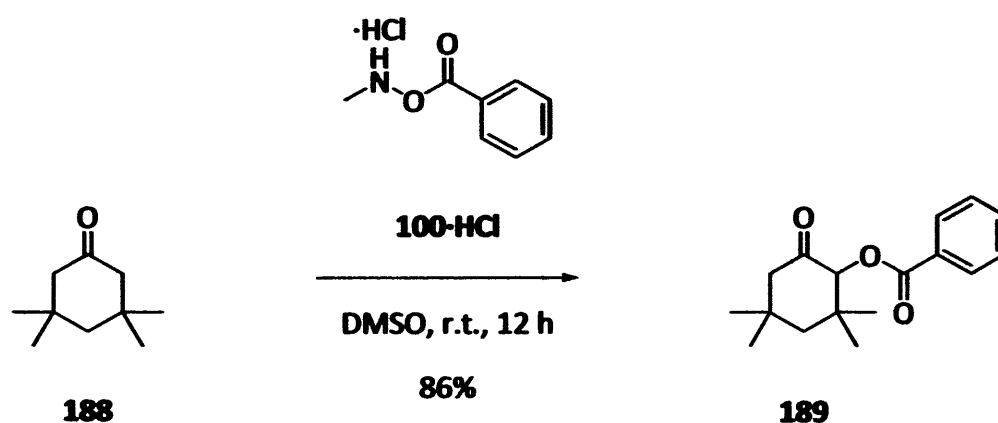
During this phase of the project, we successfully initialised a mechanistic investigation into the α -oxygenation reaction by developing a set of conditions and reactants conducive to quantitative *in situ* monitoring by ^1H NMR spectroscopy.

Having examined the effects of temperature, stoichiometry, the structure of the α -oxygenating reagent and moisture content in the reaction, we had uncovered some intriguing and useful information regarding the transformation. We wished therefore, to examine the mechanism in yet more detail, with a particular focus on definitive identification of the key intermediate species which were observed.

Chapter 6: Reaction Monitoring – Refinements and Further Techniques

A three month placement within the laboratories of the Process R & D group at the AstraZeneca site in Macclesfield, UK afforded the opportunity for the method of continuous reaction monitoring to be further explored. This continuing evolution of our science would take the form of further refinements to our *in situ* ^1H NMR method, and would additionally invoke further analytical techniques which were previously unavailable to us.

So that our limited time in this environment could be best exploited, it was decided to focus the majority of our experimental efforts on a single transformation, namely the already familiar reaction between commercially available 3,3,5,5-tetramethylcyclohexanone **188** and the hydroxylamine salt **100-HCl** (Scheme 58).



Scheme 58

We envisaged and hoped that it would be possible to:

- Identify the 2 observed intermediates for the reaction between these substrates.
- Quantitatively measure the effect of water on the transformation.
- Explore the effect of altering the reaction stoichiometry.
- Acquire accurate kinetic and thermodynamic parameters for the transformation.

Data from a variety of sources could then be used to unravel the key facets of the α -oxygenation, with the aim of not only to attaining a deeper fundamental mechanistic understanding, but also to use this knowledge on a practical level.

6.1 Reaction monitoring by ^1H NMR

A few further and final modifications to the experimental set-up were made, so that the data gathered would be of the highest quality achievable. For example, a plentiful supply of starting materials was secured, such that we would be able to analyse an aliquot of the reaction rather than the entire reaction mixture as had been the case up to this point. In performing the reaction on a rather larger scale than usual (i.e. 10 times, 2.5 mmol), experimental error due to the weighing and measuring of starting materials and reaction solvent would be reduced.

Furthermore, we planned to take a much more rigorous approach to the presence of water within the reaction mixture. This was obviously an aspect in which we were very interested – while we had previously taken all due care to exclude extraneous water from the analyte, the fact remained that we had no real quantitative idea as to how much – if any – water was present in the solvent or starting materials. Within the context of the placement at AstraZeneca however, we would for the first time have access to equipment which could accurately measure water levels within the reaction solvent. In hindsight, this would prove to be a crucial facility to have at this point, particularly since the reaction medium of choice, namely DMSO, is a very hygroscopic material. Clearly, any analytical results had the potential to be skewed by variable and unknown water content, and it was thought of paramount importance that we be particularly meticulous in this respect. The ability to measure the water content would mean in turn, that the water content at the start of reaction monitoring could be *controlled*.

For the first time, we were able to measure and therefore guarantee solvent water content of less than 50 ppm prior to the addition of carbonyl compound, and this proved to be an informative experimental variable. Accordingly, the first variable to be explored in this setting was the reaction temperature. Unless otherwise stated, all experiments were carried out on a 2.5 mmol scale, concentration 0.25 M, and integrals measured against 1,4-dimethoxybenzene as an internal standard.

6.1.1 The effect of temperature

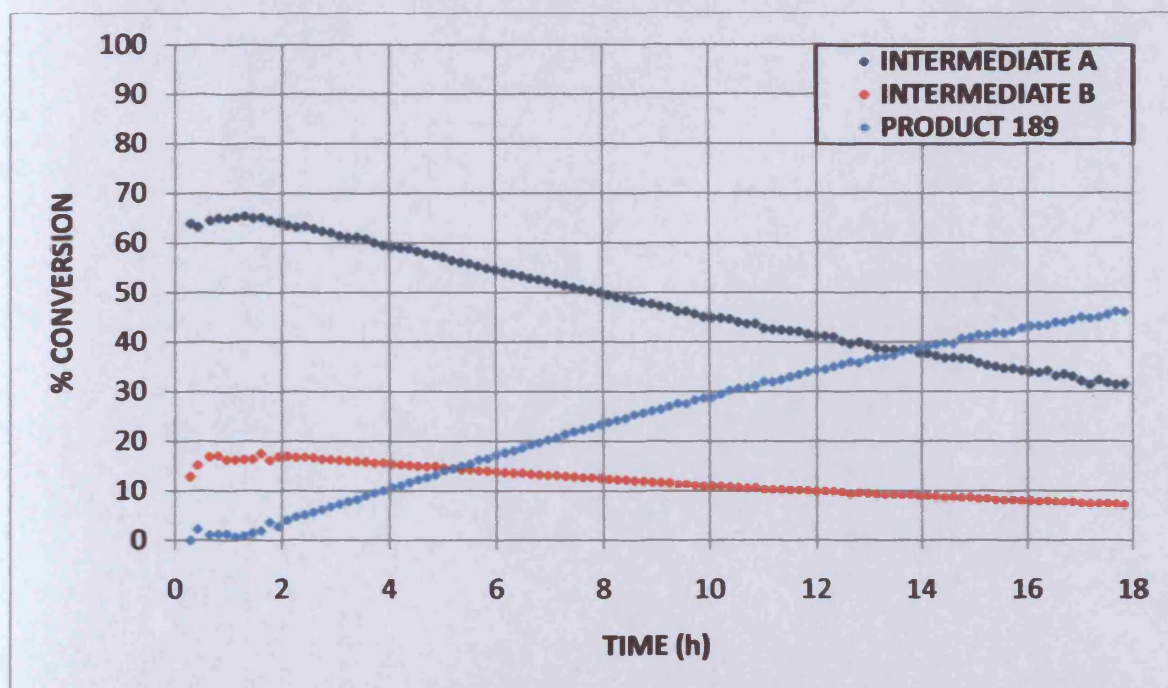


Figure 43: Product and intermediates at 300 K

It was possible to monitor the formation of product **189** and consumption of Intermediates **A** and **B**, with a degree of confidence in the data that had not yet been achieved. As before, the formation and decay of the two intermediates, **A** and **B**, as well as the formation of product **189** over the course of time was quantitatively determined by calculation against the internal standard, and the results plotted as in Figure 43.

We were encouraged to see similar behaviour as had previously been observed in earlier experiments. This indicated that although the techniques may have been somewhat cruder than the eventual experimental iteration that the reaction-monitoring methodology had evolved into, the reactivity profile of these substrates remained essentially the same. We could consistently observe the rapid formation of the two intermediate species **A** and **B**, and their subsequent slower decay, which was accompanied by steady formation of product **189**.

It appeared that the two intermediates shared a broadly similar kinetic profile in that the concentrations of both reached a maximum approximately 1 hour after the start of the reaction, after which they were both consumed in a similar fashion.

This was borne out by repetitions of the reaction, and its monitoring, at 305 K (Figure 44).

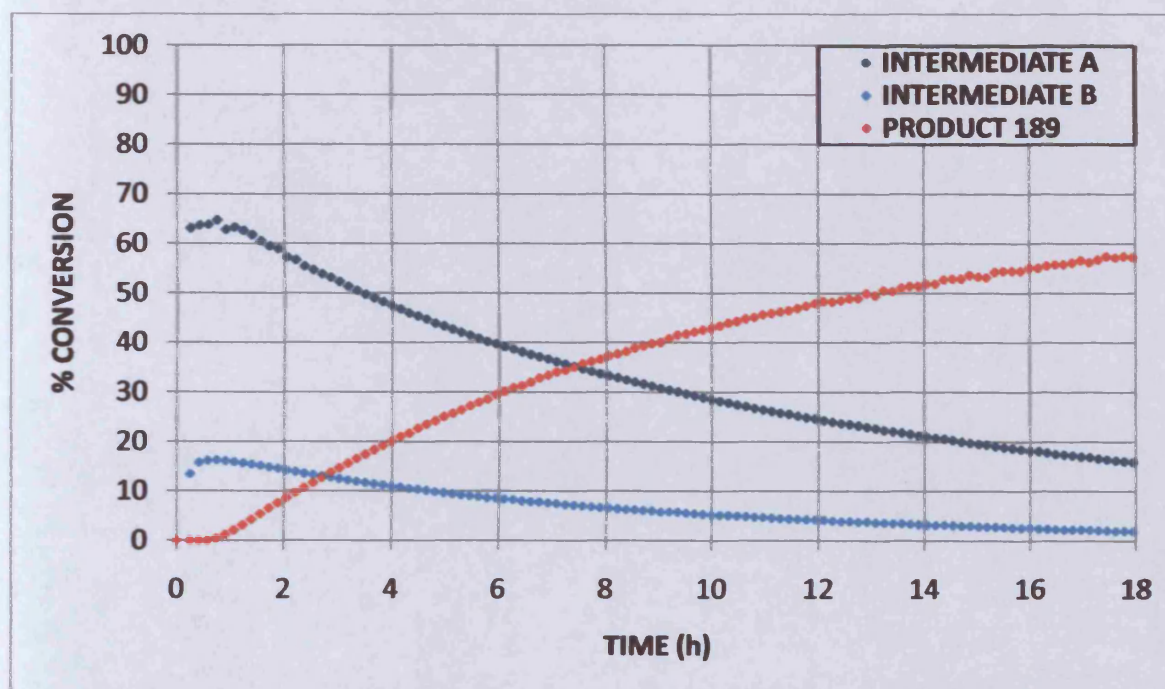


Figure 44: Products and intermediates at 305 K

We noted from the first couple of experimental runs that the data quality had been enhanced still further. This was due to further modifications made to the practical procedure; for this series of experiments we had access to a 500 MHz spectrometer (previous reaction monitoring had been performed on a 250 MHz instrument). Of greater significance was the fact that the reaction was conducted on a larger scale in the laboratory (10 x previous experiments), and a 1 ml sample withdrawn for ^1H NMR monitoring. This step therefore reduced experimental error arising from dispensing reactants on a smaller scale. The data quality remained consistently high for the reaction-monitoring at 310 K (Figure 45).

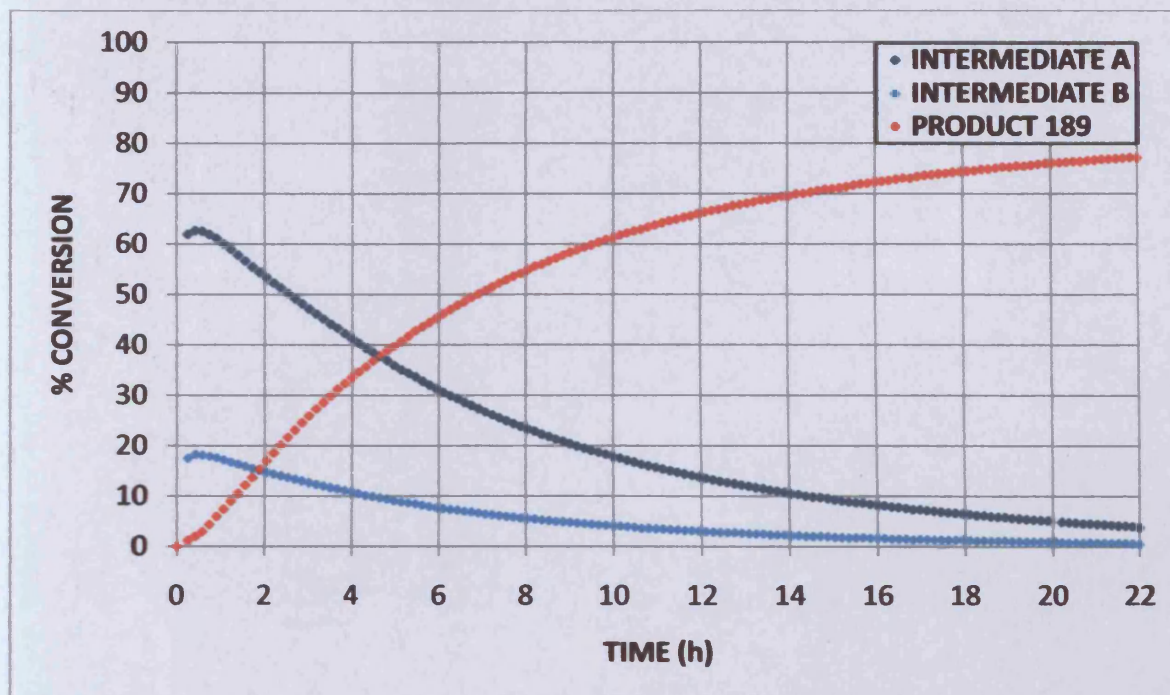


Figure 45: Product and intermediates at 310 K

Due to the improvements in the quality of the data, it was now possible to definitely conclude that the product **189** and two intermediates, A and B, taken together could not account for all the species present in the reaction mixture as the experiments proceeded. This was made evident by a mass balance calculation (Figure 46).

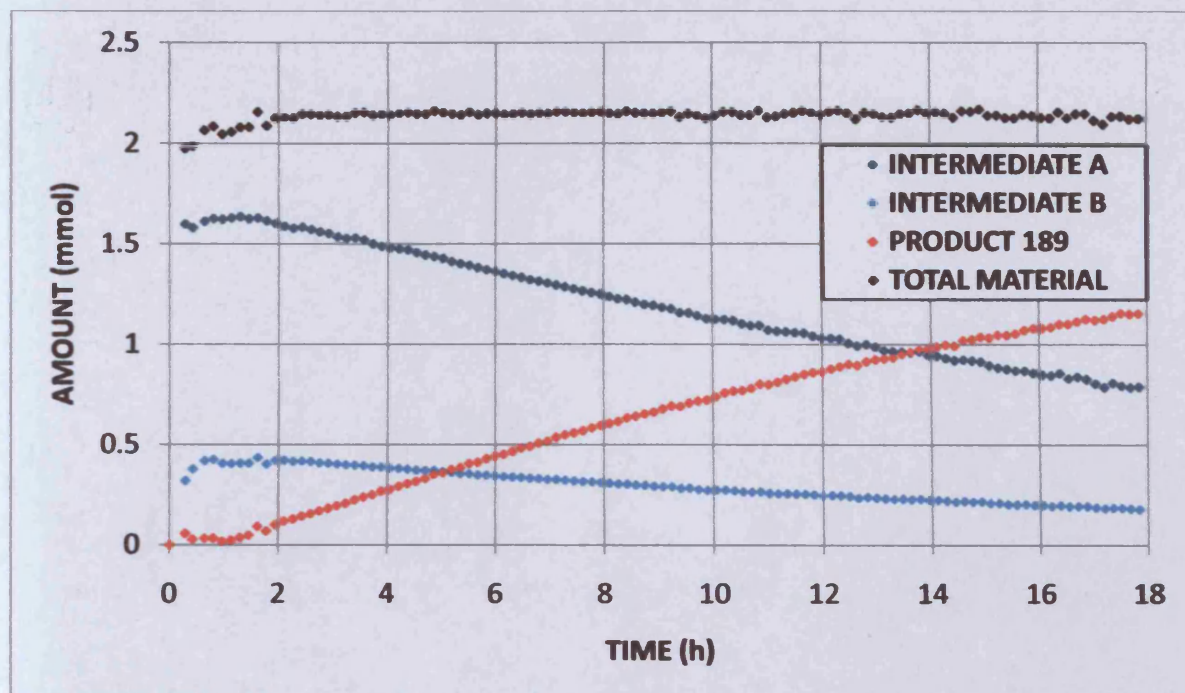


Figure 46: Mass balance for the reaction at 300 K

Plotting the results as a total figure allowed the 'missing mass' to be observed fairly dramatically, and this phenomenon was repeated for the experiments conducted at 305 and 310 K (Figures 47 and 48). For each temperature, addition of the respective amounts of product **189** and Intermediates A and B across the data series gave a total up to 86% of the material actually known to be present (i.e. 2.5 mmol in total). This could have arisen due to side reactions to give species which were not apparent by ^1H NMR (e.g. present in concentrations too low to be detected, or giving chemical shifts in the non-diagnostic region and obscured by other signals); incomplete conversion of starting material; or some combination of both. At higher temperatures, a decrease in total material over the course of the reaction became apparent, suggesting that any side reaction(s) that were taking place became more prevalent as the reaction temperature was elevated. This correlated with our own empirical observation, namely that the α -oxygenation reaction was not particularly viable at temperatures greater than 50 °C.

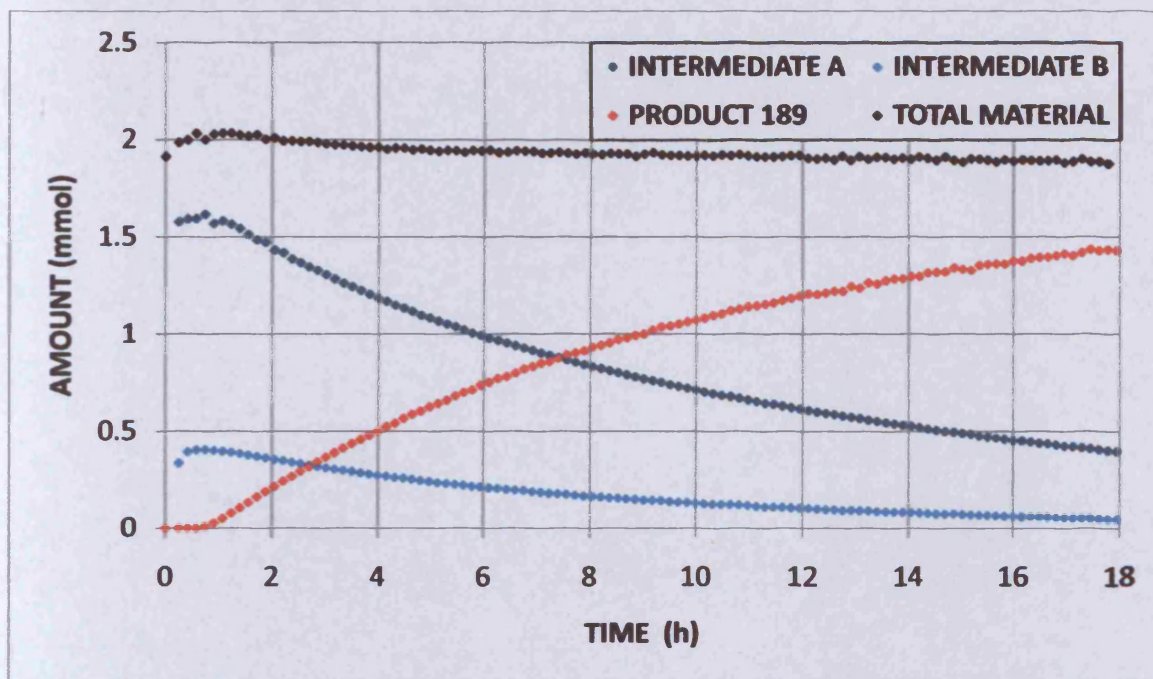


Figure 47: Mass balance for the reaction at 305 K

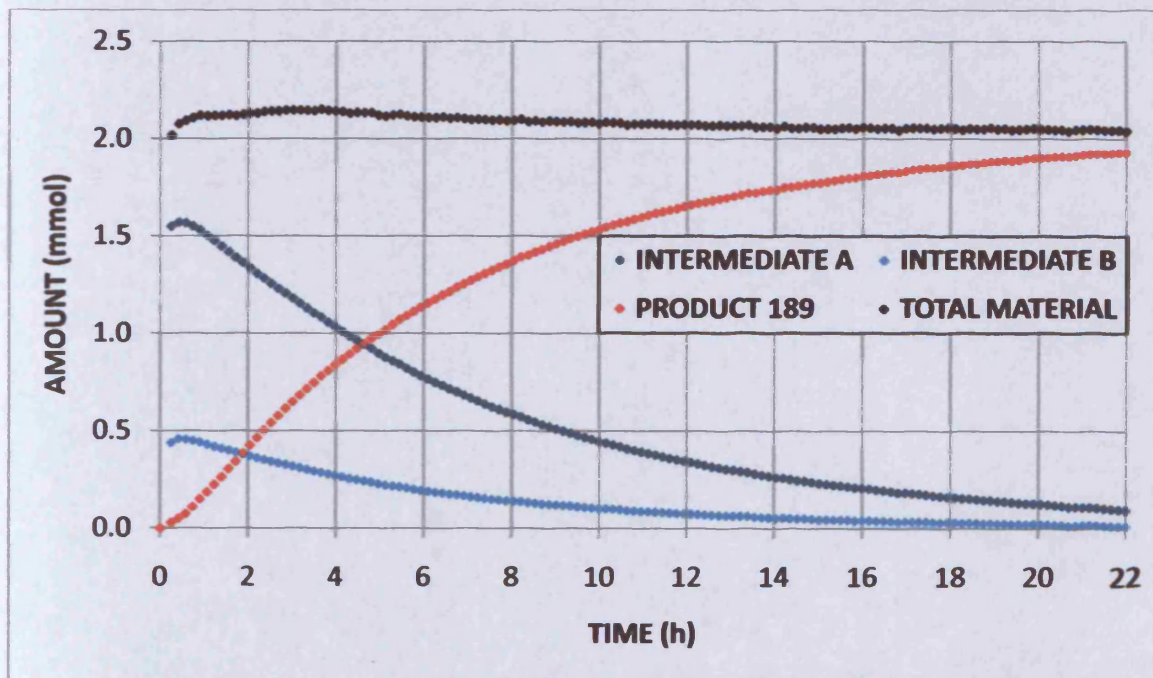


Figure 48: Mass balance for the reaction at 310 K

Inspection of a typical ^1H NMR spectrum for the reaction (in DMSO-d_6) taking place *in situ* underlined the difficulty of attempting to unravel all the signals present – apart from the diagnostic peaks we had easily associated with the product (5.3 ppm) and two intermediates (5.6 and 5.9 ppm) – this task being even more troublesome for peaks in the aliphatic region (Figure 49).

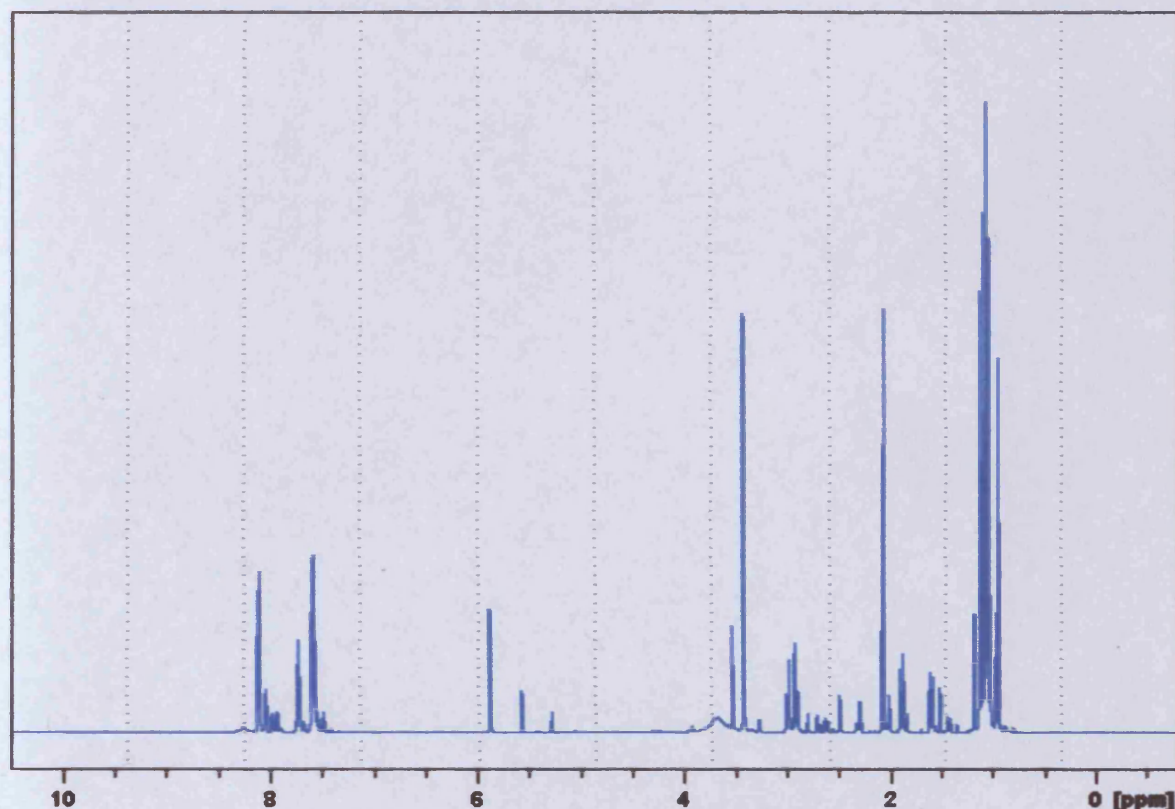


Figure 49: ^1H NMR spectrum for the reaction in DMSO-d_6 at 305 K (~1 hour reaction time)

However, we were for the first time running the experiments on a 500 MHz spectrometer, and this meant that in tandem with ^1H – ^{13}C correlation spectroscopy, it was possible to discern without any doubt the presence of ketone starting material within the reaction mixture (Figures 50 and 51).

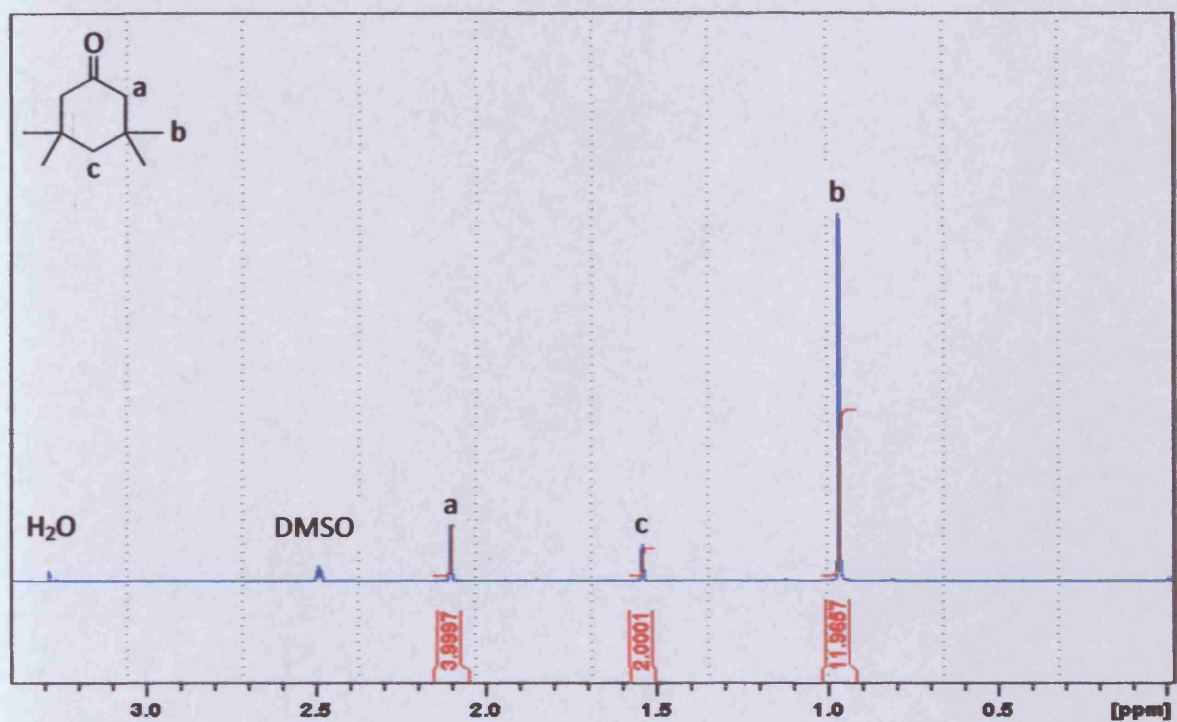


Figure 50: ^1H NMR spectrum of ketone starting material in DMSO-d_6

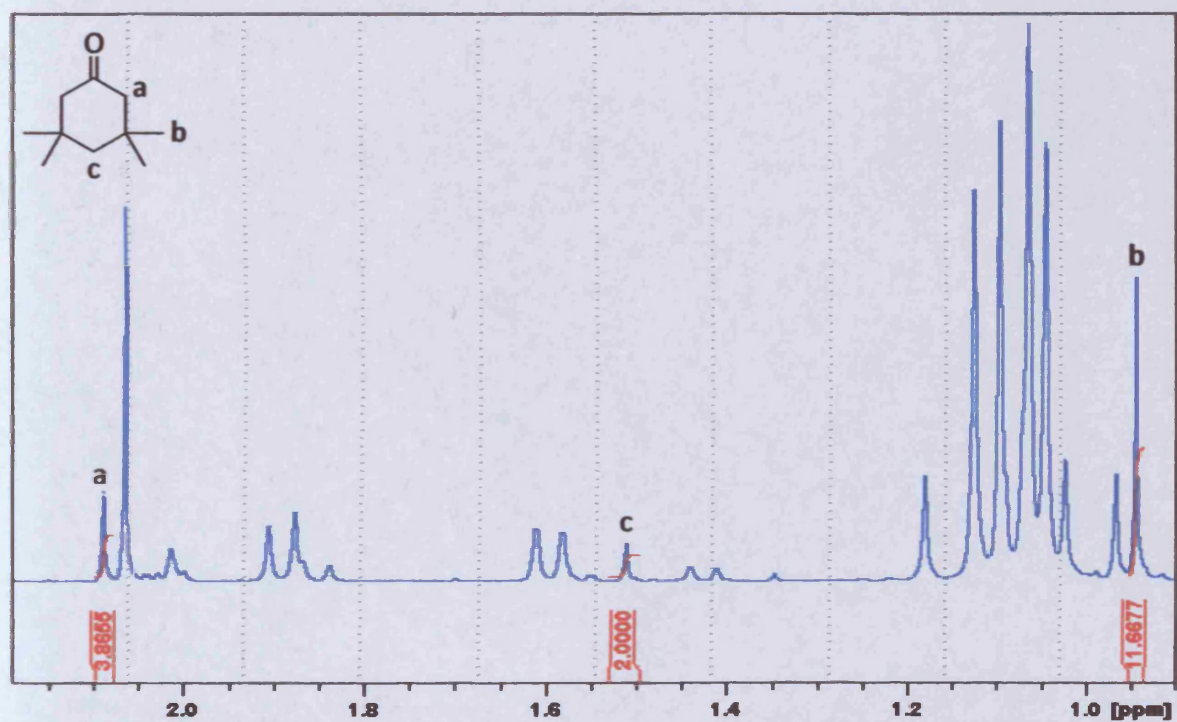


Figure 51: ^1H NMR spectrum of reaction mixture in DMSO-d_6 , $t = 1$ h

Furthermore, we were able to define several of the peaks due to starting material over the entire duration of the reaction with sufficient resolution so as to generate meaningful integrals for these. Therefore, not only did we now know that starting material was definitely present, but were also able to make quantitative measurements and incorporate this into our existing data sets (Figures 52, 53 and 54).

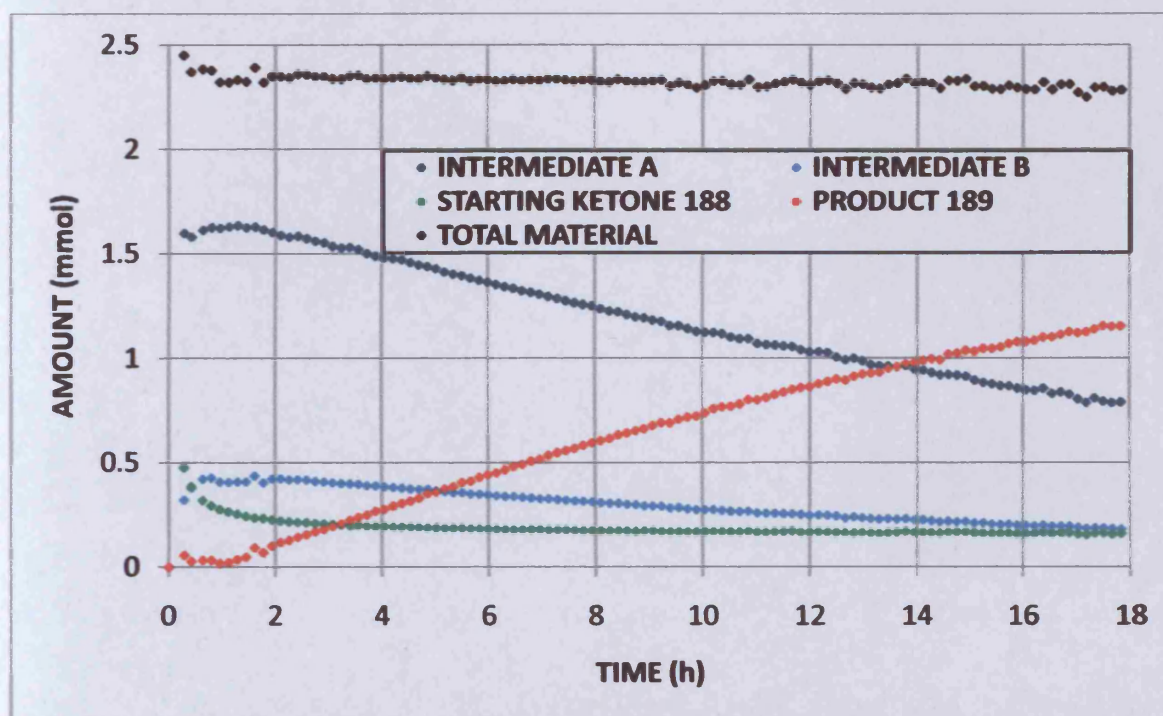


Figure 52: Product 189, starting material 188 and intermediates at 300 K

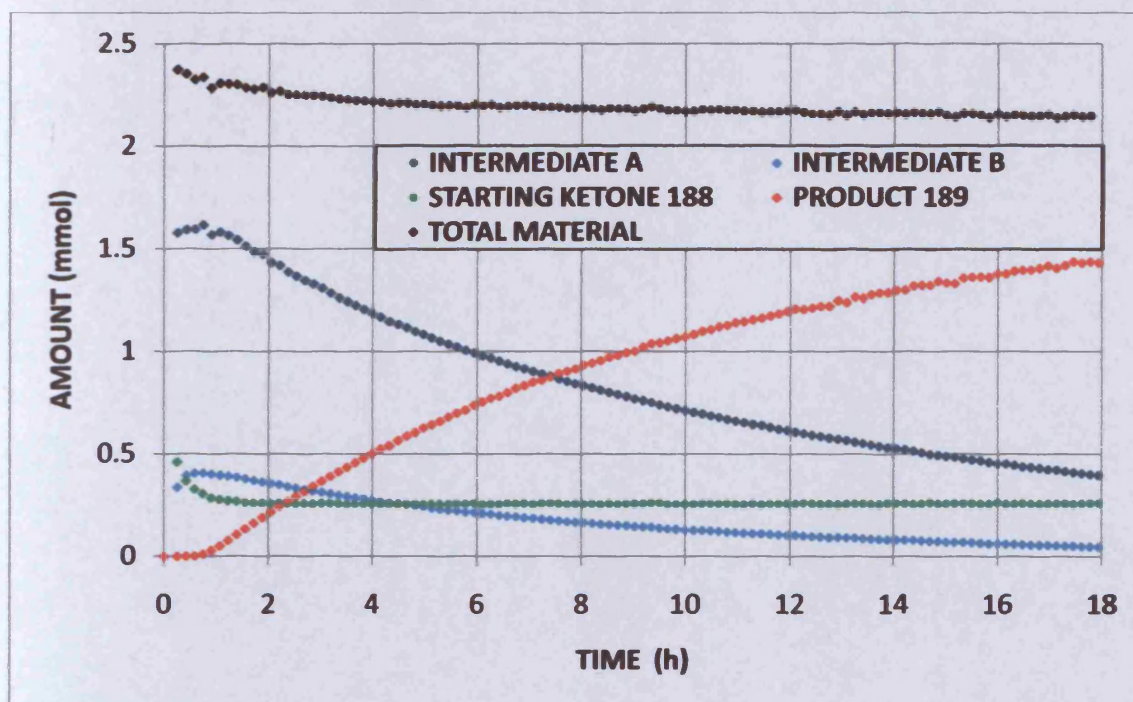


Figure 53: Product 189, starting material 188 and intermediates at 305 K

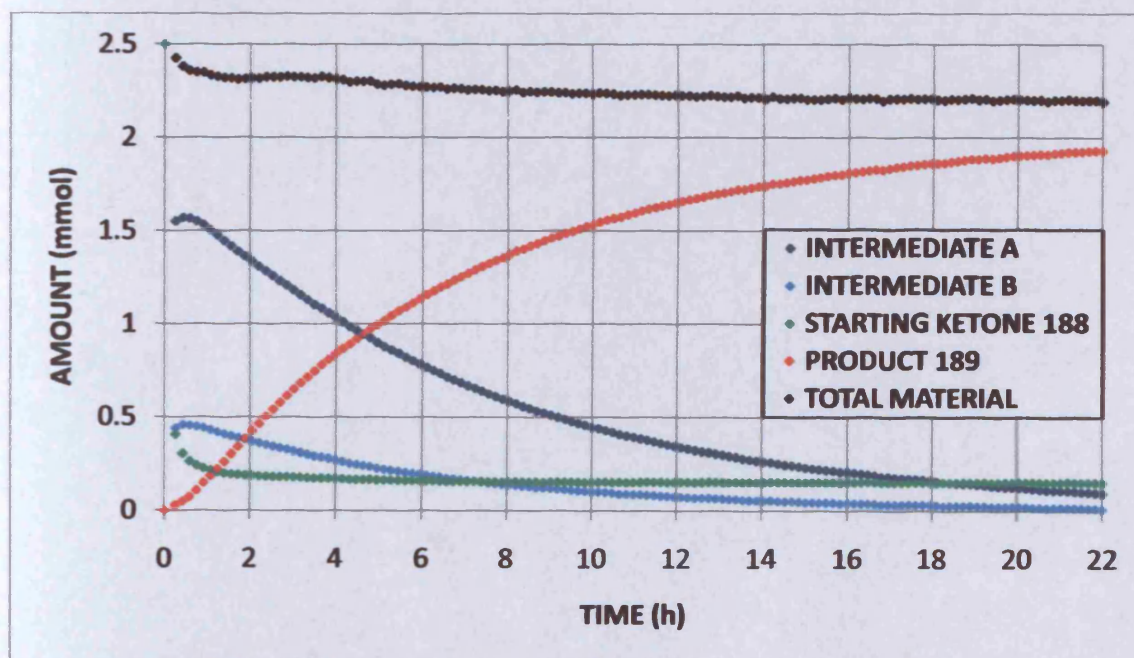


Figure 54: Product 189, starting material 188 and intermediates at 310 K

It was apparent that detecting and quantitatively accounting for the presence of starting material within the reaction mixture did not entirely explain the differing mass balance. However, the fact that starting material was observed at all was an unexpected bonus, since this meant we could potentially use consumption of starting ketone as a further tool for unravelling the kinetics of the transformation.

This was tantalising, since we had not previously been able to pin down the presence of either starting material previously – so much so that the assumption had been made that the first part of the reaction was simply too rapid for starting material consumption to be observed and measured. This data set the scene for the next series of experiments we had planned to carry out within the ^1H NMR methodology.

As a priority however, it was necessary to make a definitive identification of the two observed intermediates within the reaction. NMR was to have a crucial role in this determination.

6.1.2 Identification of intermediates

It became clear that in order to effectively probe the kinetics of the reaction and make mechanistic determinations, it was necessary to correctly identify the two intermediate species observed in the reaction. Whilst we had previously made tentative suggestions as to their identity (see Chapter 5), the opportunity was taken to repeat the 2D NMR experiments. The fact that the two intermediate species gave rise to signals in the ^1H NMR with chemical shifts of 5.6 and 5.9 ppm was strongly suggestive of hydrogens α - to a carbonyl group and a heteroatom, as we were already familiar with this chemical shift signature for the α -proton of the product at 5.3 ppm. HSQC (Figure 13) together with ^{13}C DEPT 135 (Figure 14) spectroscopy showed these protons were both bonded to methine carbon atoms (relative intensities).

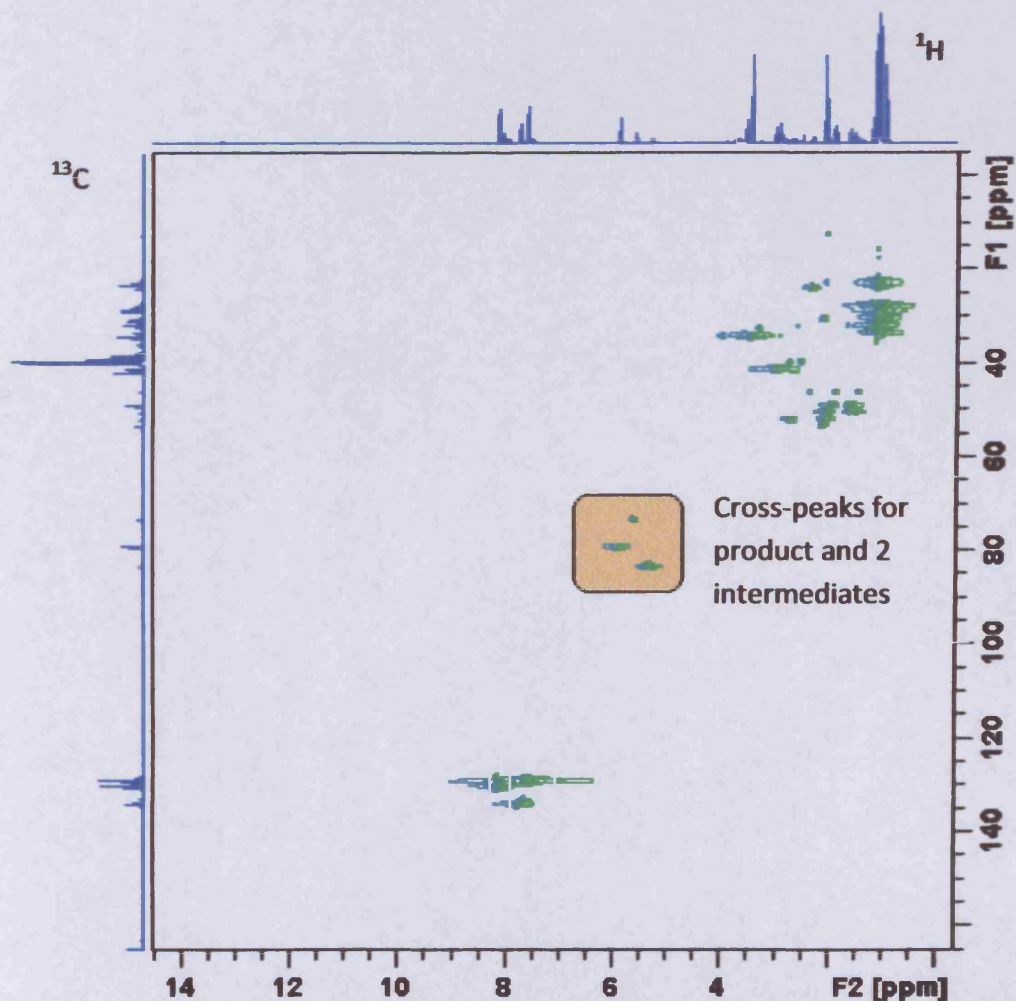


Figure 55: HSQC spectrum of reaction mixture in DMSO-d_6

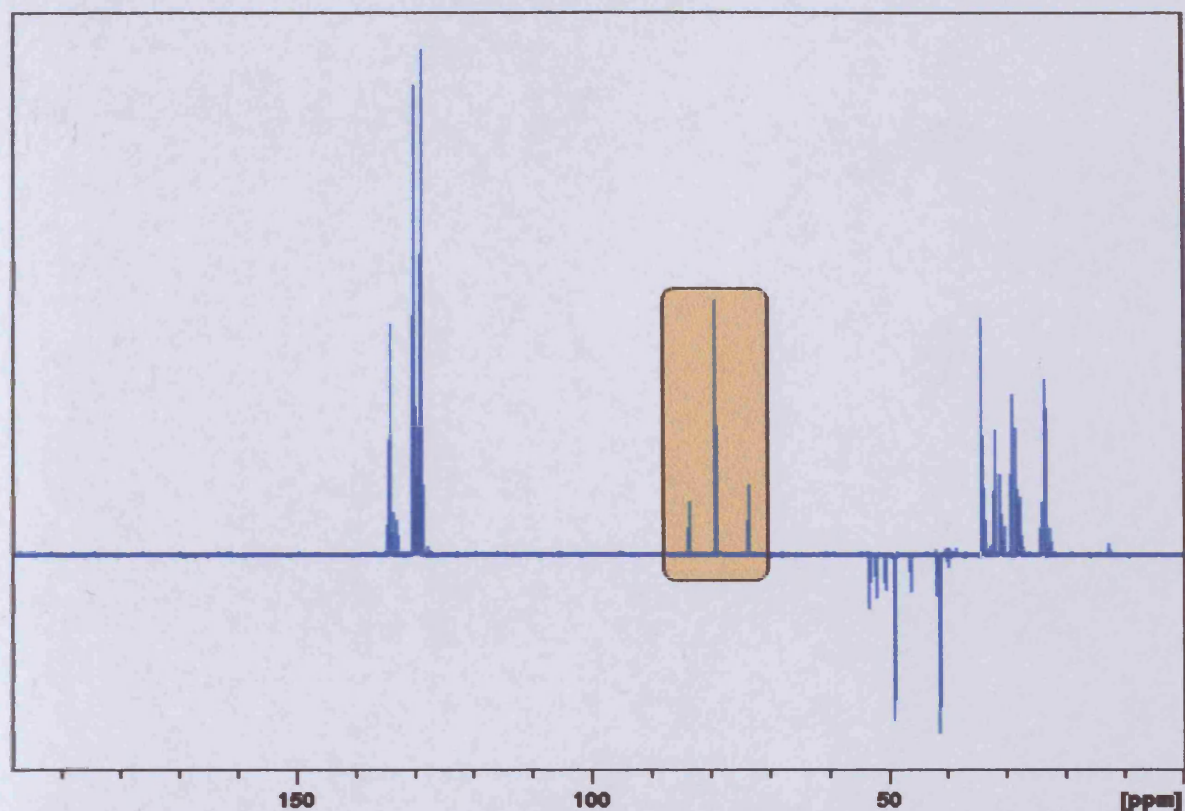
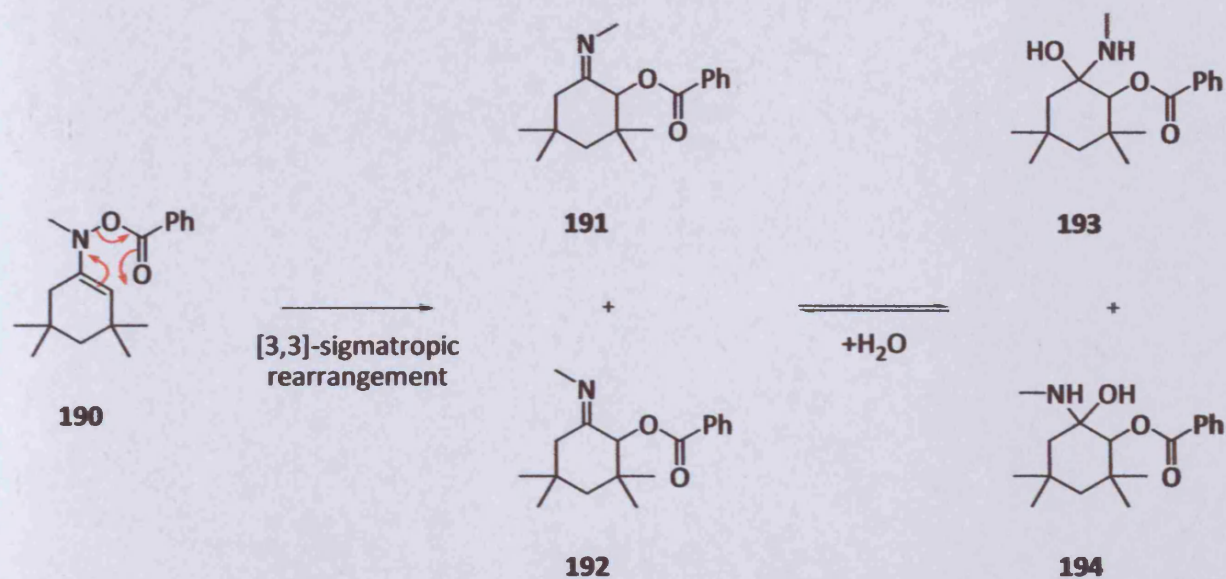


Figure 56: DEPT 135 ^{13}C NMR spectrum of reaction mixture in DMSO-d_6

The only way such a carbon multiplicity could be reconciled with the proposed mechanism would be to suggest that the intermediates A and B were either the enamine **190**, imine species **191** and **192** or aminols **193** and **194**. Owing to the similar kinetic profile of the two intermediates, our thinking was that these two may well be isomeric forms (Scheme 59).



Scheme 59

We were fairly certain, however, that the process followed swift kinetics in the early part of the reaction sequence, namely addition of the hydroxylamine to the ketone and subsequent deprotonation to form the enamine, with the rate-determining step occurring later in the hypothesised mechanism.

Acquiring further 2D NMR spectra provided further vital clues to the identity of the intermediates. Figure 57 shows the HMBC spectrum of the reaction mixture, taken 2 hours after mixing of the starting materials. To recap, we initially knew of 3 major species, namely the product **189** and two Intermediates A and B within the reaction mixture. We had furthermore recently detected starting ketone **188** by ^1H NMR. It was clear that the diagnostic peaks in the ^1H NMR spectra were the signals at 5.3 (product), 5.6 and 5.9 ppm (intermediates). These peaks were assigned as α -hydrogens on the C2 carbon, based on chemical shifts. Clearly, the ^{13}C and ^1H NMR spectra of the reaction mixture was hopelessly complicated in terms of unravelling all the information contained therein without considerable difficulty; however we approached the problem with the view that careful examination of the 2D spectra, in particular the cross peaks arising from the diagnostic signals, ought to give us at least some information as to the identity of the major intermediates we were consistently observing.

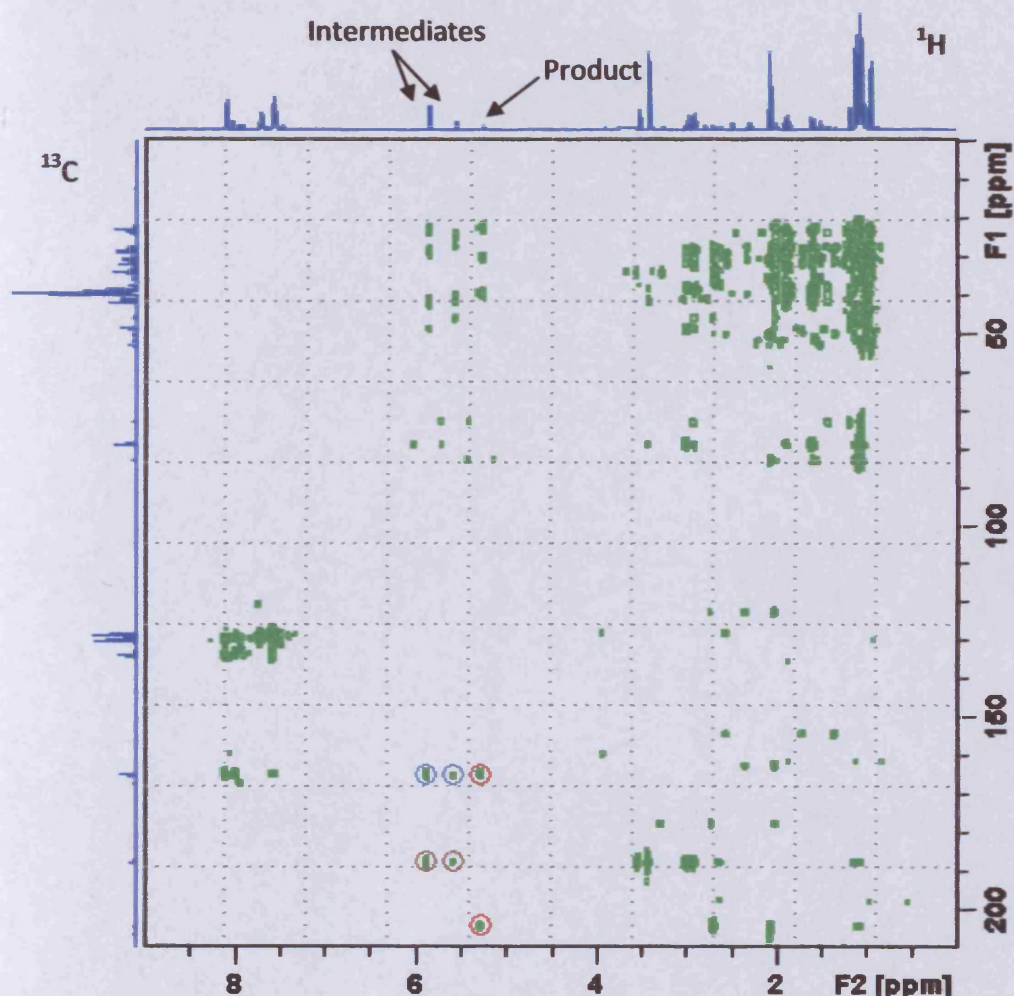


Figure 57: HMBC spectrum of reaction mixture in DMSO- d_6 , $t = 2$ h)

Multi-bond correlations were seen from the α -hydrogen of the product **189** at 5.3 ppm and the ketone and ester carbons at 204 and 164 ppm respectively (red circles). Both of the intermediates displayed coupling to an ester carbon (cross-peaks circled in blue), and so this eliminated the possibility of either of these species being the enamine **190**. Also, both intermediates correlated with carbon peaks at around 187 ppm (circled brown), and this chemical shift suggested sp^2 -hybridized carbon, i.e. the α -oxy imine **191** (or **192**) in the proposed mechanism. While imine carbons typically resonate at around 160 ppm in the ^{13}C NMR, it is difficult to imagine an aminol carbon with a chemical shift much greater than 100 ppm, so this possibility (**193** and/or **194**) was eliminated.

The somewhat high chemical shift for an imine carbon can be explained by the fact that protonated Schiff bases have a chemical shift around 20 ppm higher than their non-protonated counterparts.⁷⁶ Invoking the possibility of protonated imines as intermediates seemed a sensible deduction, particularly as there was an equivalent of HCl in the reaction mixture (pK_a in DMSO = 1.8). The pK_a of the imine **191** is about 5; we would therefore expect the reaction conditions to be sufficiently acidic so that these would exist primarily in the protonated form.

Further corroborative evidence for this assignment was provided by subjecting a small sample of the reaction mixture to analysis by LCMS (Figure 58).

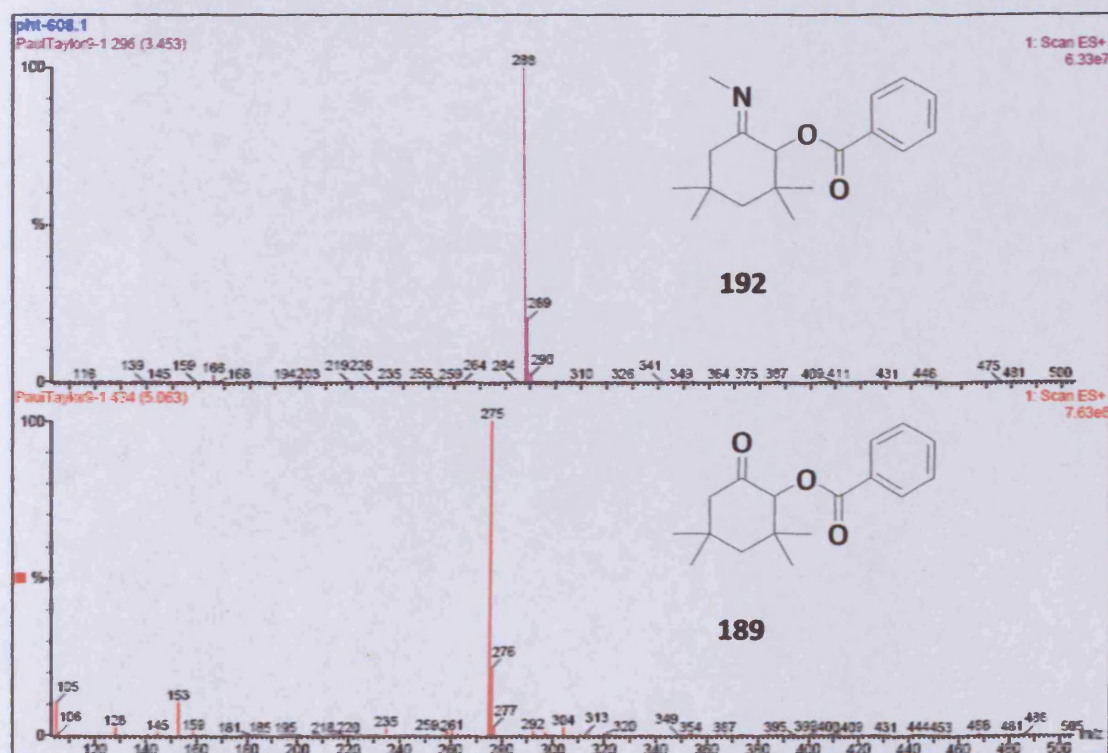


Figure 58: LCMS trace for product and major intermediate in reaction mixture

Species with m/z corresponding to parent ions for both the product **189** and the imine **191** were detected. Under the LCMS conditions, only one isomer with m/z 288 was observed, indicating that both intermediates co-eluted during the separation (however not discounting the possibility that the other isomer was unstable), and providing further indirect evidence for the isomeric nature of the two compounds. We therefore proposed that the two intermediates were the isomeric iminium ions **210** and **211** (Figure 59).

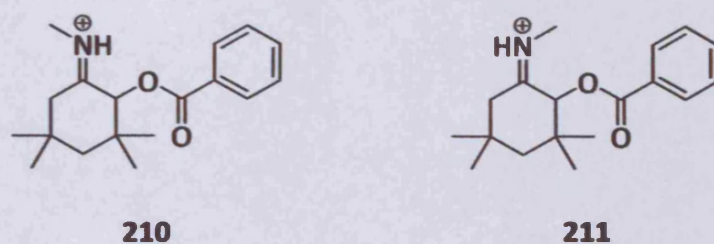


Figure 59

While they were not separable by LCMS, nor as yet isolable, the two intermediates were nonetheless distinguished by means of NOESY NMR spectroscopy (Figure 60).

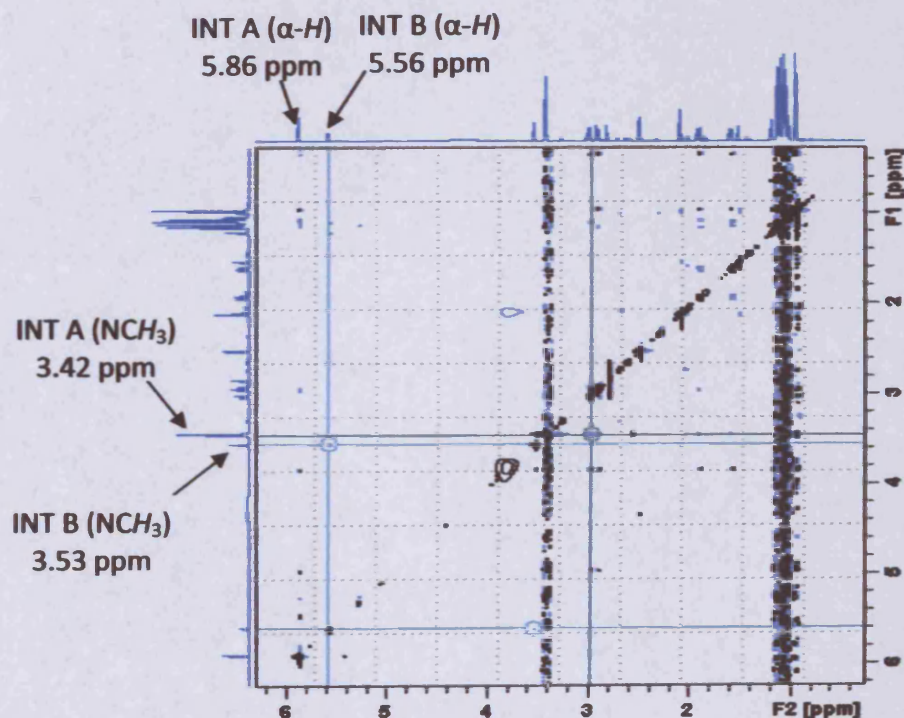


Figure 60: NOESY spectrum for the reaction mixture at 305 K in DMSO- d_6

The spectrum was taken 30 minutes after mixing of the starting materials, so as to obtain a snapshot of the reaction where the concentration of both Intermediates A and B was at a maximum, thereby optimising the chances of our being able to detect all the relevant couplings. This showed the minor Intermediate B, had a clear through-space coupling (highlighted light blue) from the α -proton to the protons of the methyl group. This nOe was lacking for the dominant Intermediate A, but crucially, a correlation was shown (highlighted dark blue) between the methyl hydrogens and the CH_2 protons on the other side of the carbonyl group.

These cross-peaks indicated that the major isomer, Intermediate A, was the *trans*-iminium species **210**, while the minor component, Intermediate B, possessed geometry consistent with the *cis*-iminium **211** (Figure 61).

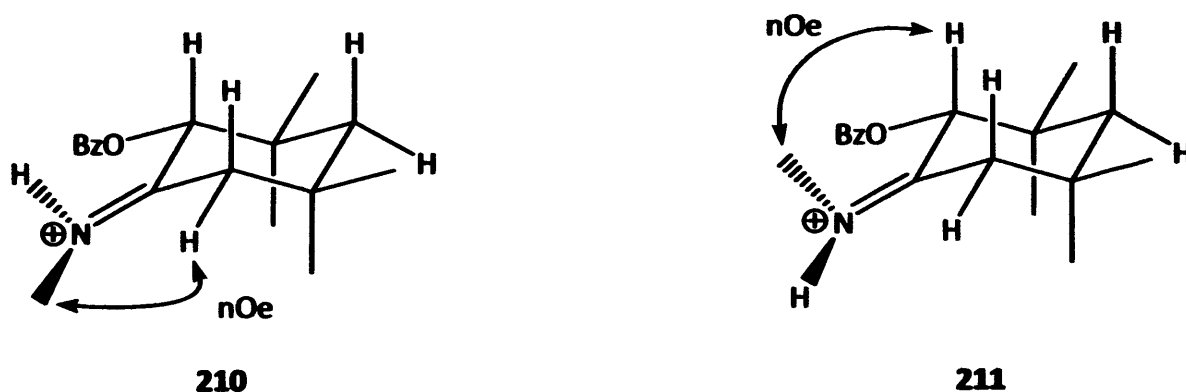
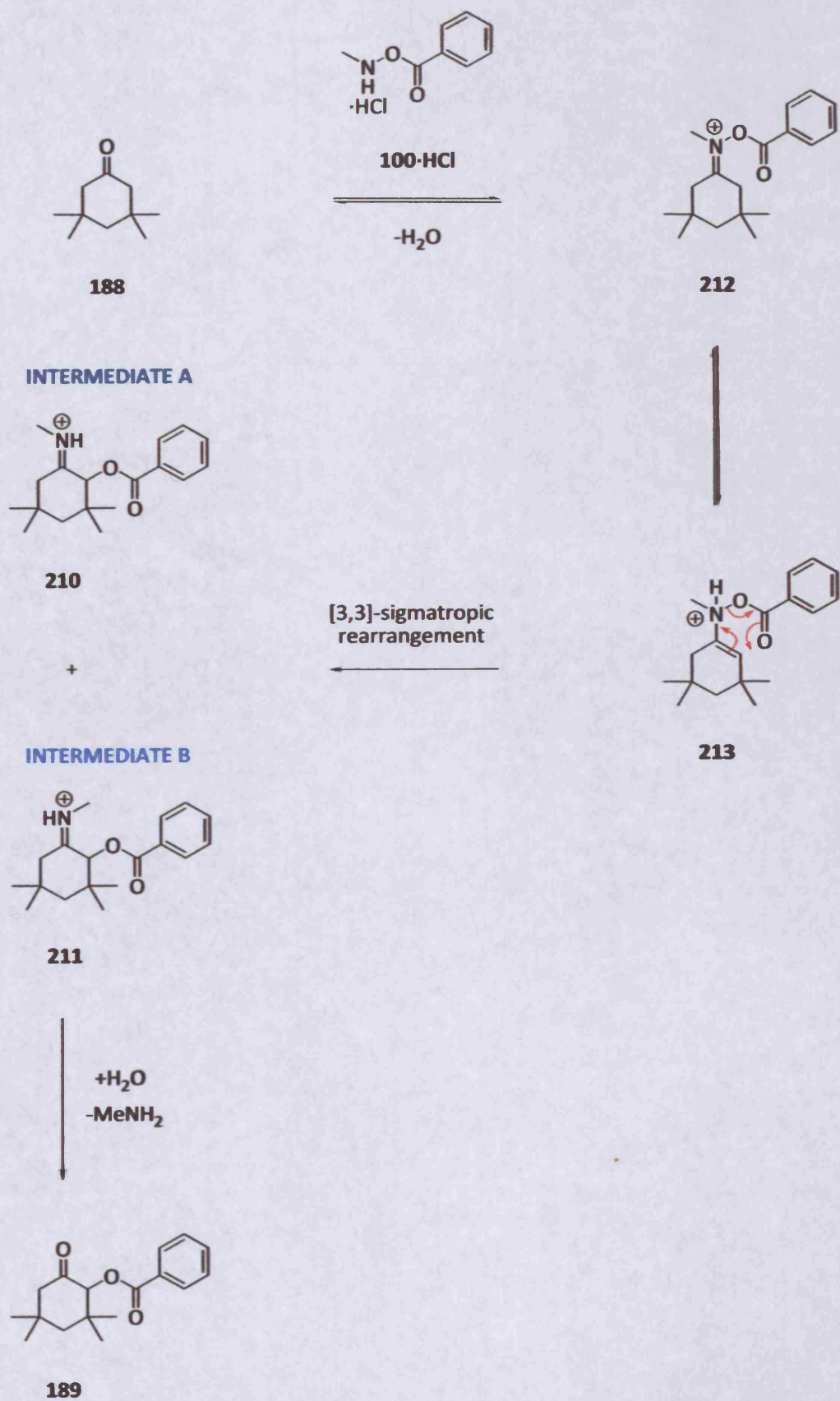


Figure 61

Deducing that the intermediates were the isomeric α -oxyiminium species **210** and **211** had profound ramifications on the proposed mechanistic pathway. If correct, and broadly applicable to other substrates, our assignments suggested that the α -oxygenation reaction proceeded swiftly through the early steps in the overall process, namely nucleophilic addition of the *O*-acyl hydroxylamine **100-HCl** onto the carbonyl compound **188**, loss of a proton from the iminium ion **212** to give the protonated enamine **213** with subsequent rearrangement to the α -oxyiminiums **210** and **211**; followed by rate-limiting iminium hydrolysis to give the product **189** (Scheme 70).



Scheme 70

6.1.3 Explaining the *cis:trans* ratio

It had been necessary to modify the model to invoke the α -oxyimines **210** and **211** in their protonated state. In turn, this led us to speculate on the fundamental process in the formation of these intermediates which led to the *trans*-isomer being the dominant species within this particular reaction. After all, if no viable explanation could be proposed, this could have had the potential to throw doubt on our hypothetical reaction mechanism.

Figure 62 provides a potential model of the C–O bond-forming step (i.e. the [3,3]-sigmatropic rearrangement).

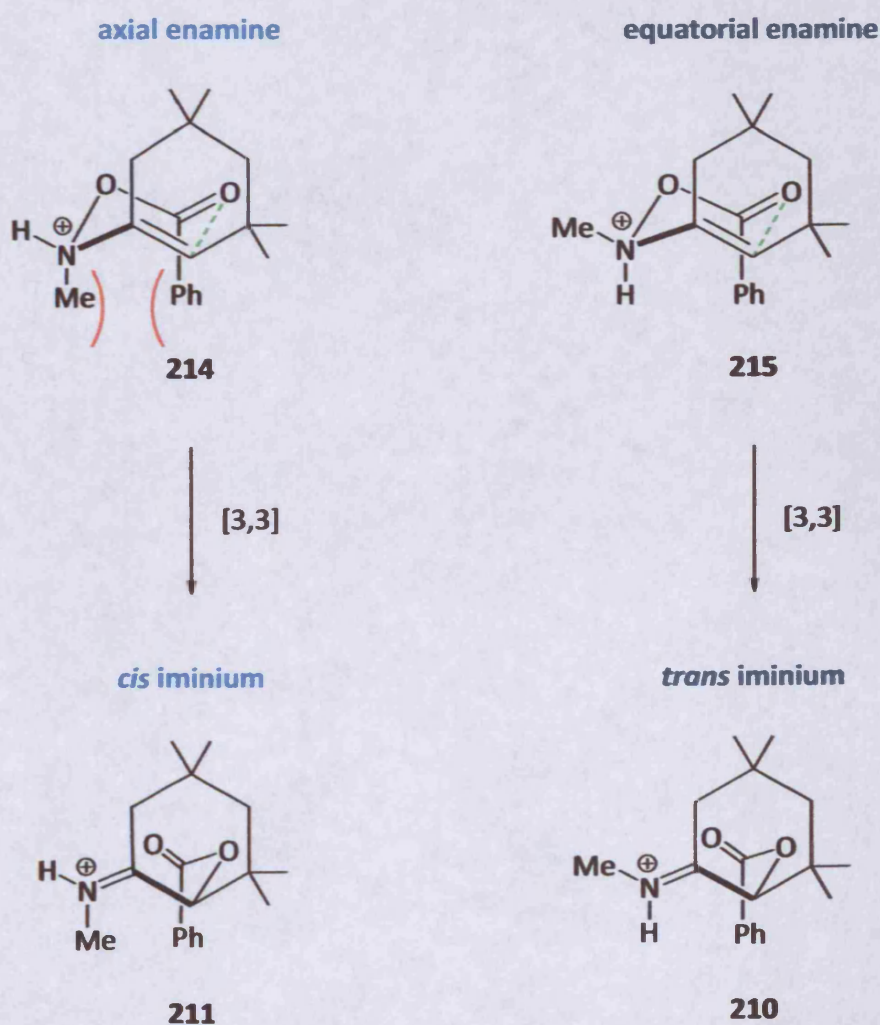


Figure 62

If the observed intermediates existed in their protonated form, then the preceding enamines would also be protonated. This invoked quaternised nitrogen centres in both cases with the possibility of axial or equatorial enamines **215** and **215** with respect to the *N*-methyl substituent.

In the model, a 1,3-diaxial interaction in disfavoured the formation of the axial enamine **214** and hence the *cis* iminium ion **211** which was formed thereafter. This contrasted with the equatorial enamine **215** and the *trans* species **210** which was the major rearrangement product.

It was therefore believed that the two observed intermediates had been identified, their two isomeric forms distinguished, and a working explanation for the observed *cis:trans* selectivity established.

6.1.4 The effect of water

Reaction monitoring by ^1H NMR, together with associated 2-D experiments had proved remarkably informative in terms of disassembling the reaction mechanism up to this point. Having identified the intermediates, the priority was to re-examine the reaction process in the light of our findings. We had shown that the two intermediates **210** and **211** were at their most abundant in the reaction mixture approximately 1 hour after the start of the reaction. Furthermore, one of our principal goals from the outset in undertaking this study, had been to achieve an enhanced understanding of the reaction mechanism; but then to make the procedure more efficient by applying this knowledge.

We were ideally placed to address this aspect by exploring the effect of water on the reaction kinetics; and reasoned that rate-limiting hydrolysis of the α -oxy iminium ions **210** and **211** could be accelerated by the presence of additional water in the reaction mixture. We therefore sought to determine the effect of water stoichiometry on the reaction.

With DMSO being a very hygroscopic material, we had carried out the initial kinetic runs using 3Å sieve-dried solvent in order to achieve a consistent set of results, unaffected by variable water ingress. Solvent water content was measured using a Mitsubishi CA100 Single Channel Coulometric Karl Fischer Titrator (Figure 63),⁷⁷ a moisture meter capable of measuring water content as low as 1 ppm by direct injection of samples into the titration cell.

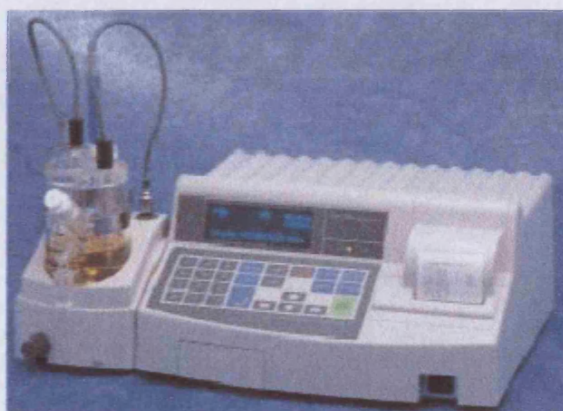
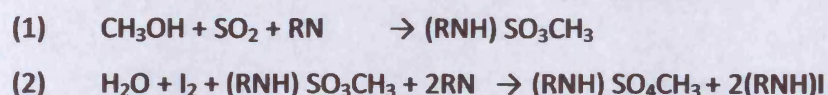


Figure 63: Coulometric Moisture Meter Model CA-100

Karl Fischer titration is a widely used analytical method for quantifying water content, fundamentally based on the Bunsen reaction between iodine and sulphur dioxide in an aqueous medium. In an industrial context, accurate determination of water content is crucial in terms of product quality and to ensure consistent physical and chemical properties.

In the coulometric method, the titration cell consists of two parts, an anodic (which contains the anode solution plus the analyte) and a cathodic compartment. The anode solution comprises an alcohol (typically methanol), a base (e.g. imidazole), SO_2 and I^- . The following reaction scheme has been proposed:⁷⁸



The alcohol reacts with sulphur dioxide and base to form an intermediate alkylsulphite salt (Equation (1)), which is then oxidised by iodine to an alkylsulphate salt (Equation (2)), consuming a molecule of water in the process. In coulometric Karl Fischer titration, iodine (I_2) is generated electrochemically from iodide (I^-). When iodine comes into contact with water in the sample, water is titrated according to Equations (1) and (2). The amount of water in the sample is calculated by measuring the current needed for the electrochemical generation of iodine from iodide according to equation (3):



Keeping the DMSO- d_6 over 3Å sieves gave a solvent with water content consistently less than 50 ppm when measured by the Karl Fischer titration method described above. Small variations in water content under these circumstances were ascribed to both normal experimental error and variable atmospheric humidity at the times of analysis. However, it turned out that measured water contents of less than 50 ppm were unimportant as far as the reaction kinetics were concerned; which was fortunate since there was no straightforward, practical means of eliminating or reducing these admittedly small disparities without substantially redesigning our experimental methodology. The reaction between 3,3,5,5-tetramethylcyclohexanone **188** and *N*-methyl-*O*-benzoyl hydroxylamine hydrochloride **100-HCl** was therefore repeated twice more at 305 K to test the reproducibility of the previous results at (more or less) negligible water content as measured in the DMSO- d_6 immediately prior to the start of the reaction (Figures 64 and 65).

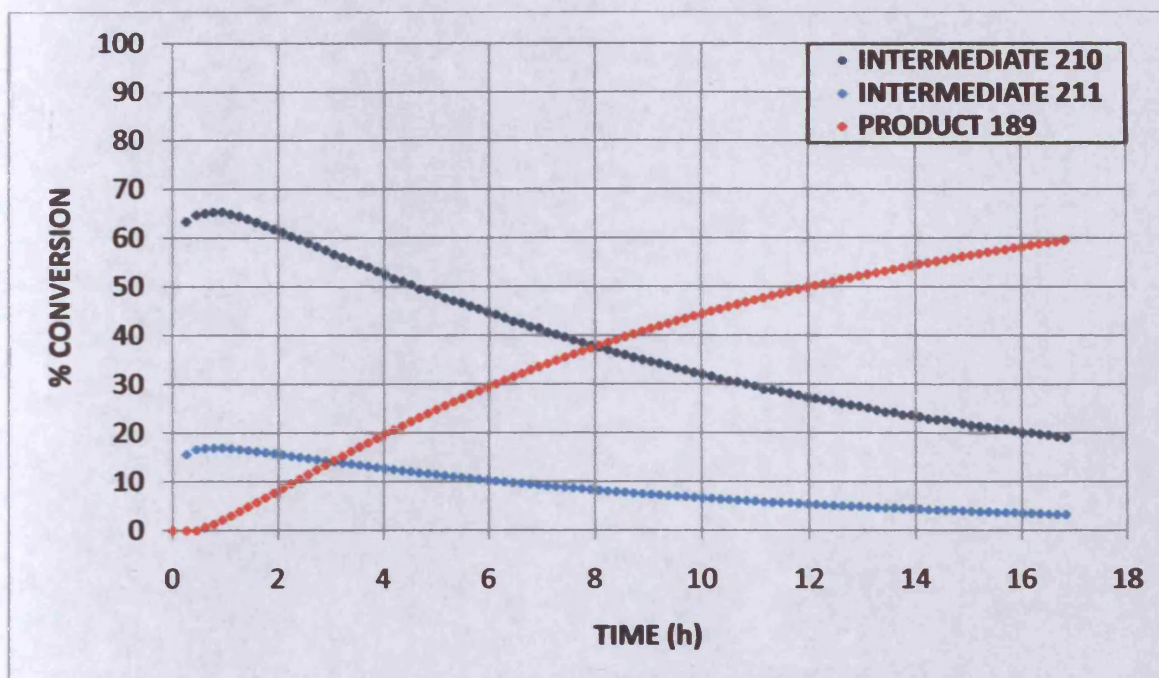


Figure 64: Product 189 and Intermediates 210 and 211 at 305 K (water content 4.8 ppm)

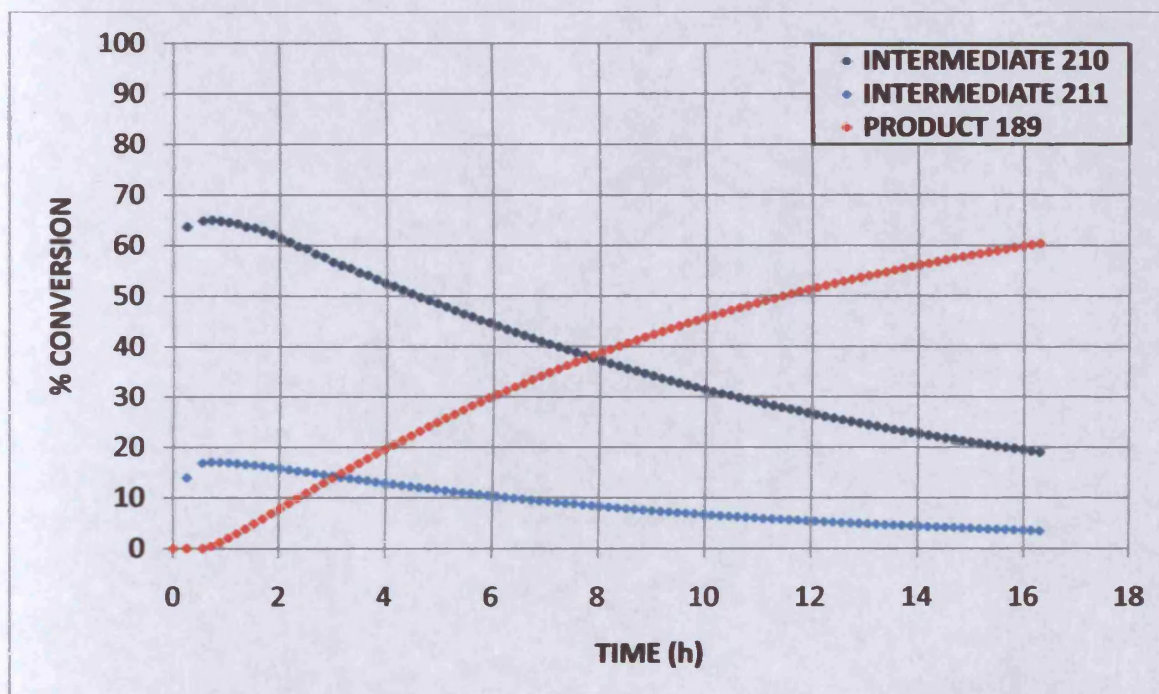


Figure 65: Product 189 and Intermediates 210 and 211 at 305 K (water content 20.4 ppm)

Taking the earlier data series into account, the reaction was conducted several times at 305 K, using DMSO- d_6 with three formally different measured moisture levels (4.76, 20.35 and 32.58 ppm). Figure 66 is an overlay of these three respective sets of results.

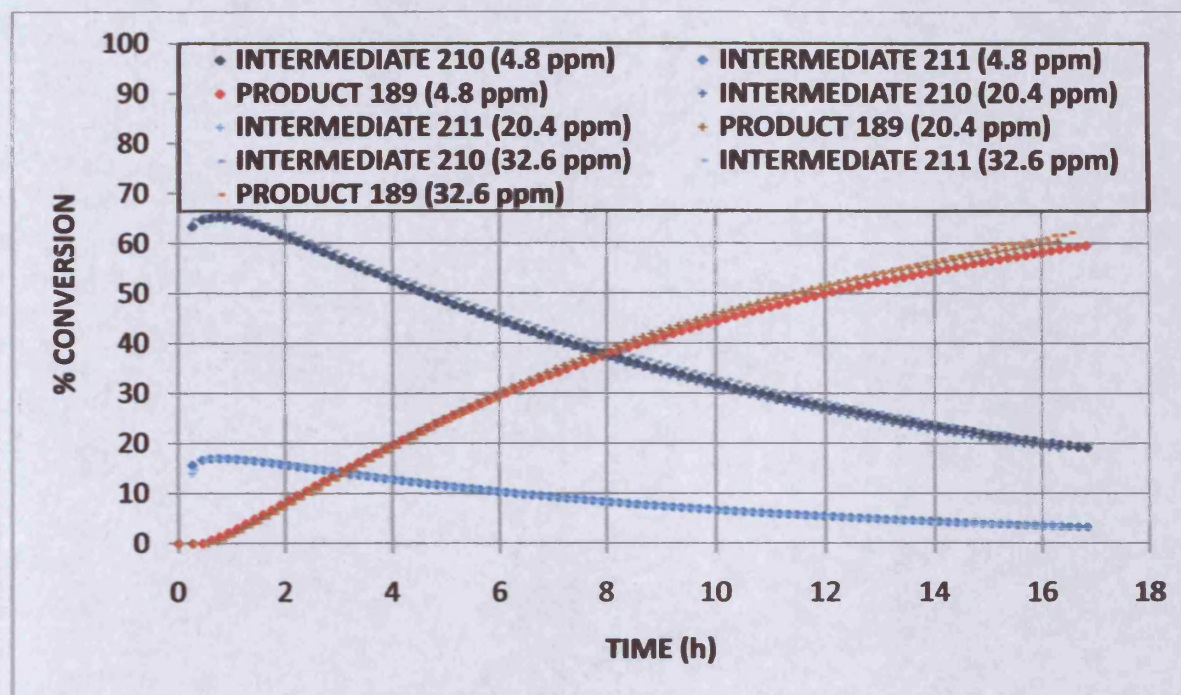


Figure 66: Product 189 and Intermediates 210 and 211 at 305 K (overlay of water contents)

In each case (moisture readings < 50 ppm), reaction to form product 189 took place with virtually identical kinetics, along with the decay of both Intermediates 210 and 211. In performing this comparison, it was possible to state that trace moisture did not either hamper or enhance reactivity, and that the methodology for obtaining data was reproducible and therefore robust.

Unfortunately, it was not possible to measure the water content of the reaction mixture after the addition of the substrates (the anode solution contained methanol and was therefore unsuitable for the analysis of samples containing ketones).

Further, as the reaction process released a stoichiometric equivalent of water during the formation of the iminium ion **212**, the only definite measurement available was the solvent water content prior to the addition of ketone.

The addition of more significant amounts of water to the reaction solvent resulted in highly altered kinetics for the reaction process at 305 K. Figures 67 and 68 are the reaction profiles when the measured water contents (just before mixing of starting materials) were 3315 and 3367 ppm respectively.

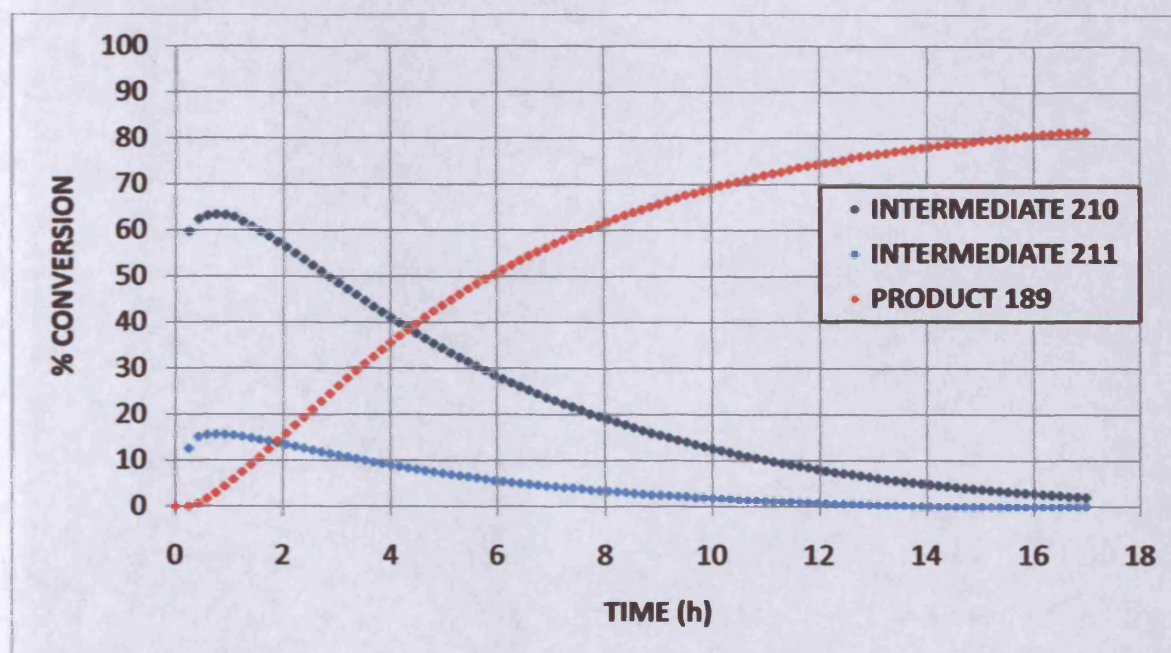


Figure 67: Product 189 and Intermediates 210 and 211 at 305 K (water content 3315 ppm)

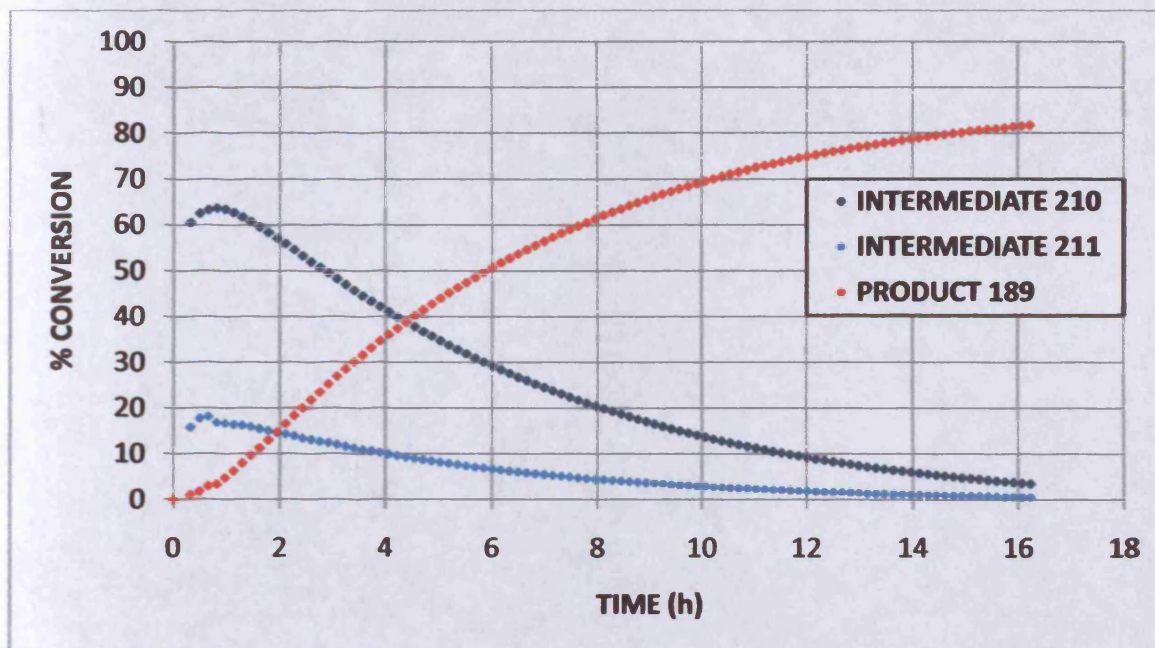


Figure 68: Product 189 and Intermediates 210 and 211 at 305 K (water content 3367 ppm)

Clearly, with increased water content, there was a pronounced enhancement in both the overall conversion to product **189** over the measured reaction timeframe, and the rate at which the product **189** was formed, together with an increased rate of consumption of both reactive intermediates **210** and **211**.

Furthermore, the two data sets were remarkably similar, indicating the reproducibility of the experimental procedure and thus adding further credibility to the results. Indeed, the purpose of running two experiments with as similar moisture levels as possible was to test the veracity of the results under duplicated experimental conditions. Figure 69 illustrates this by way of overlaying the data series from the two runs.

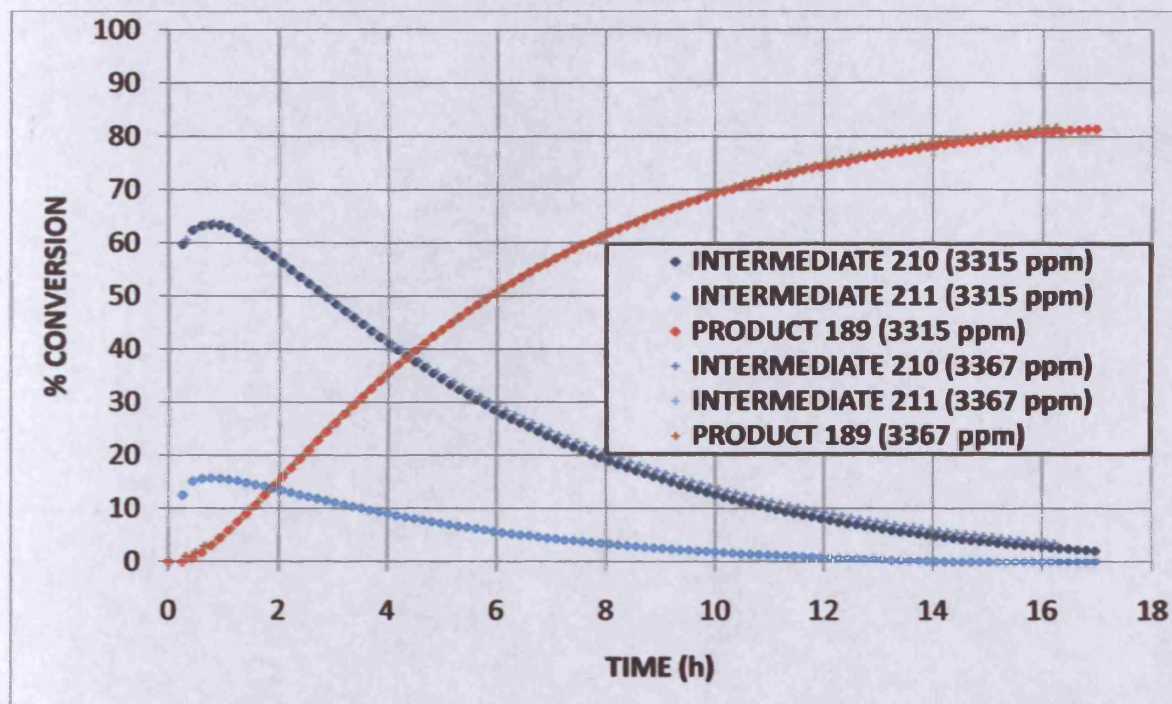


Figure 69: Overlay of Figures 67 and 68 (water contents 3315 and 3367 ppm)

Increasing the moisture level yet further – up to 26545 ppm (roughly equivalent to an extra 7 equivalents of water in terms of the stoichiometry of the starting materials) – resulted in still higher rates of product formation and intermediate consumption (Figure 70).

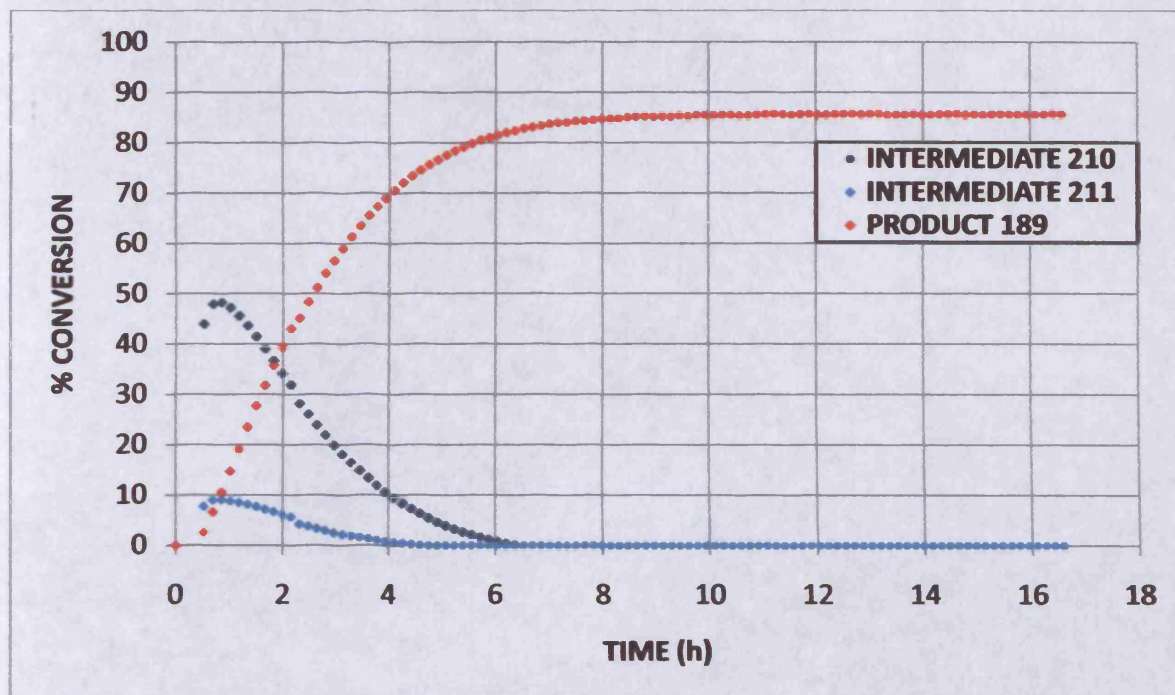


Figure 70: Product 189 and Intermediates 210 and 211 at 305 K (water content 26545 ppm)

A water content of 26545 ppm represented, to a good approximation, 7 extra equivalents of water in terms of the stoichiometry of the starting materials; and at this level of water doping, we observed for the first time a conversion to product which matched the isolated yield that had been achieved in the laboratory. This suggested that either the reaction solvent used 'on the bench' had rather excessive moisture content, or that aqueous work-up of the crude reaction mixture had effectively accelerated hydrolysis of the iminium ions **210** and **211**. At any rate, this result gave a possible explanation for the apparent contradiction in the isolated yield and the results from reaction monitoring.

The overall effect of water on the reaction, specifically with respect to formation of product, is illustrated to best effect by once again overlaying the results (Figure 71).

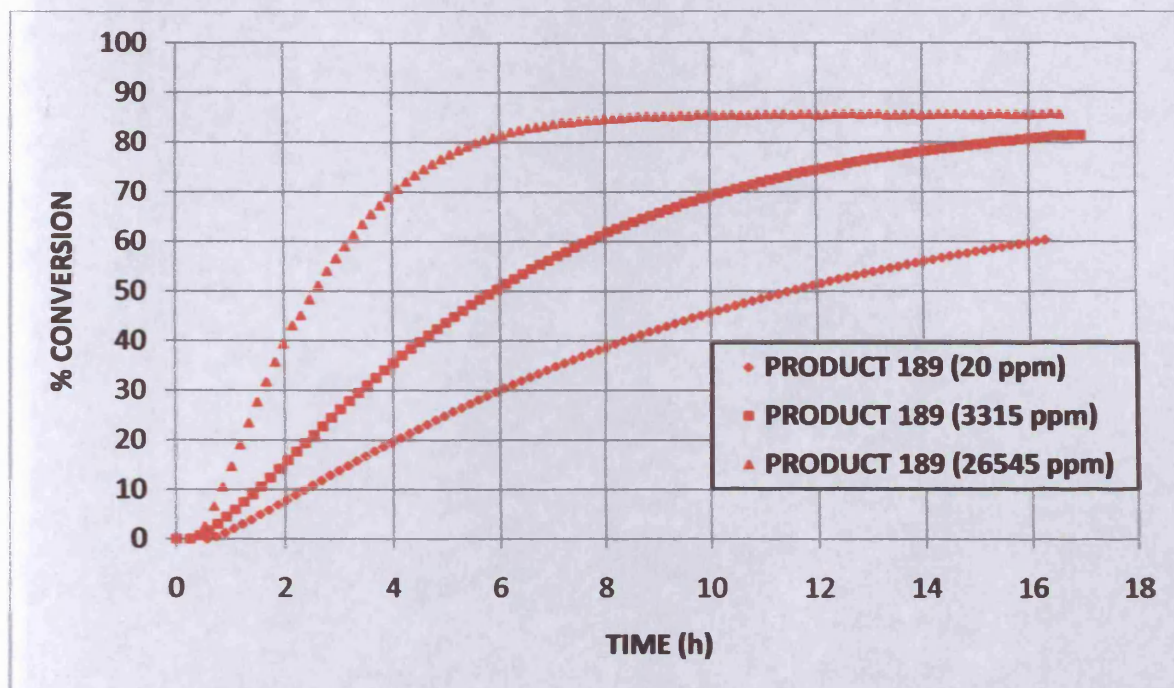


Figure 71: Formation of product 189 at 305 K (various water contents)

This set of results was in keeping with our proposed mechanism, in that the rate-limiting step was proposed earlier as the hydrolysis of α -oxy iminium ions **210** and **211** under quasi-anhydrous conditions. We had therefore speculated that increased water content should facilitate this process and this was borne out by the results obtained.

Perhaps surprisingly, formation of the intermediate species **210** and **211** was not significantly suppressed by additional water – one may have predicted that the initial equilibrium arising from the condensation between the starting ketone **188** and the nucleophilic *N*-benzoyl hydroxylamine **100**-HCl would disfavour formation of the initial iminium ion **212** to at least some extent. However, the α -oxygenation process had previously been successfully undertaken in water and solvent systems including water, perhaps indicating that the thermodynamically favourable [3,3]-sigmatropic rearrangement step provided a reaction pathway which overcame the deleterious effect of water on the ketone **188**/iminium **212** equilibrium.

Alternatively, each of the steps in the proposed reaction mechanism could be thought of as fast up until the hydrolysis of the products of the [3,3]-rearrangement, i.e. iminium ions **210** and **211**. This hydrolysis step could then be thought of as rate-determining, since it is the immediately preceding species which are the dominant feature in the ^1H NMR as far as reaction intermediates are concerned. This speculation was treated with some care, and always accompanied by the caveat that the discussion was strictly speaking only relevant to one pair of starting materials brought together under very specific reaction conditions.

6.1.5 Reaction stoichiometry

Figure 72 portrays the fate of the ketone starting material **188** at each different moisture level that was examined.

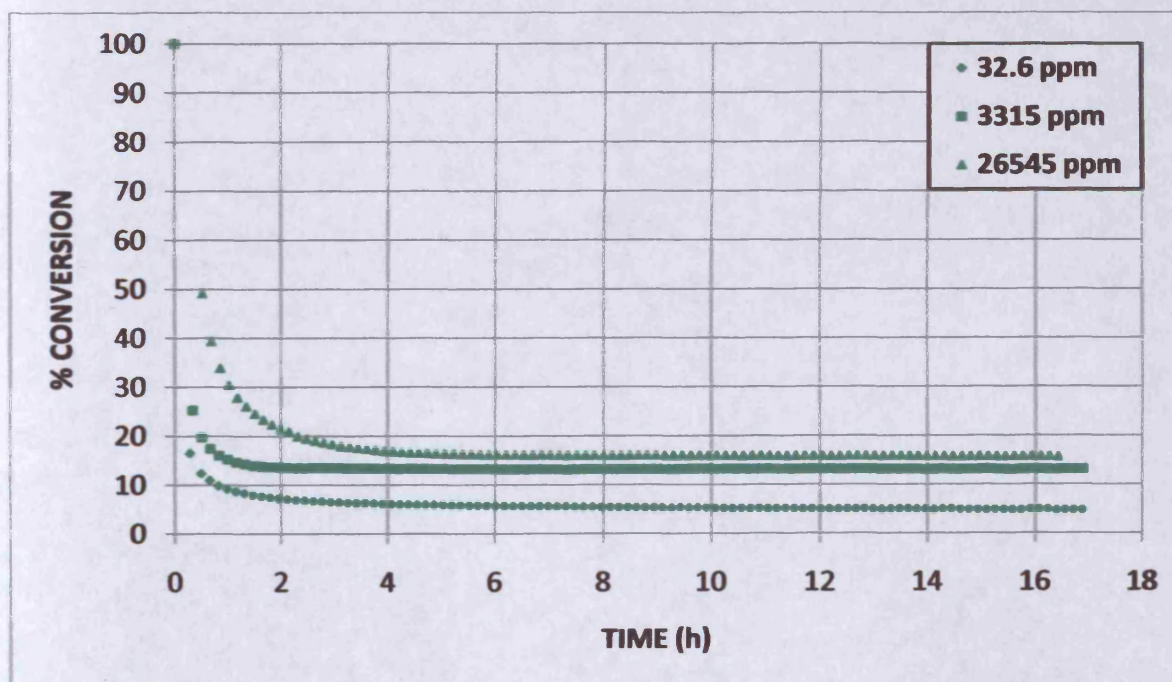


Figure 72: Consumption of starting ketone at 305 K (various water contents)

The conclusion from this data was that unreacted starting ketone **188** remained in solution right up until measurements were stopped. It appeared that this was the case at any moisture level, and that reaction between 3,3,5,5-tetramethylcyclohexanone **188** and the reagent **100-HCl** had slowed considerably after about 1 hour and had essentially ceased altogether after 3–4 hours.

With the apparent differences between the three data series, caution was required. It was tempting to immediately infer that significantly less ketone was being consumed overall as the moisture level was increased. However, the region of the ^1H NMR spectrum at which the amount of ketone was measured was between 1.54 and 1.45 ppm; which was in sufficiently close proximity to the water peak (3.30 ppm) to have its integral potentially skewed and thus give the misleading impression that more ketone was present than was actually the case.

Clearly, this effect was more significant as the water level increased (in fact, the moisture level of 26545 ppm, i.e. 3% was close to the limit at which meaningful data could be collected from any other region of the ^1H NMR spectrum). A brief look at the mass balance calculation between starting material **188**, the two iminium ion intermediates **210** and **211**, and the product **189** illustrated this point (Figure 73).

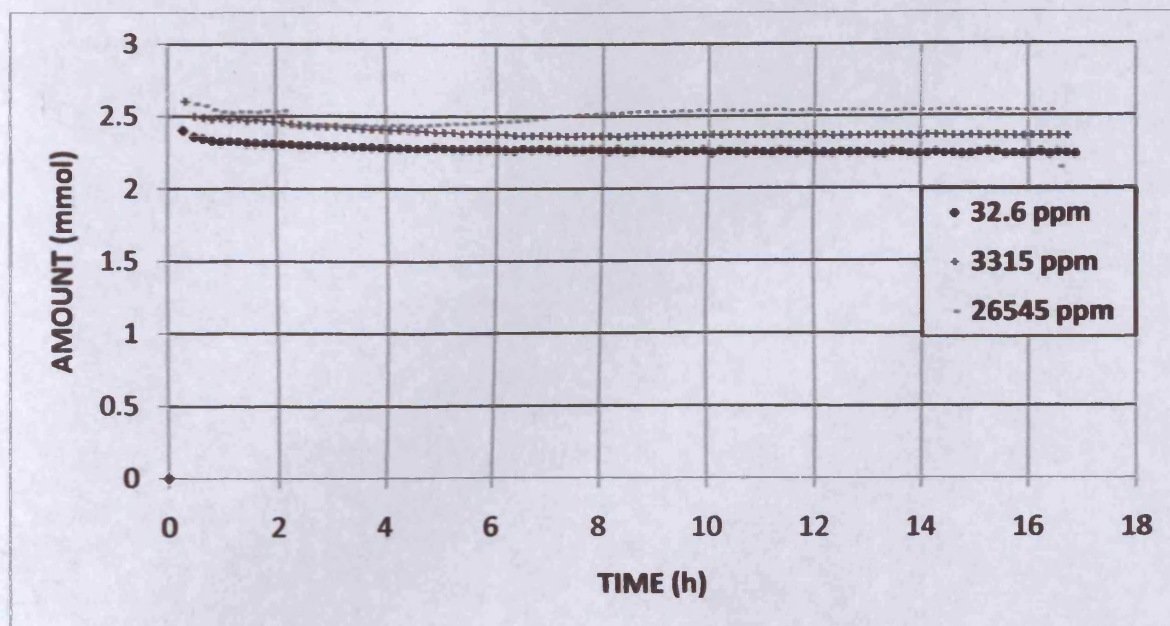


Figure 73: Mass balance calculation at 305 K (various water contents)

Therefore, it was deemed prudent at this point not to rely on the numbers generated for starting material in the water-doping experiments, but rather to focus solely on the fact that starting material *was* still present at the end of the reaction; this being contrary to all of our instincts concerning the reaction to date. This was not to altogether dismiss the possibility of the initial condensation between ketone and hydroxylamine being hindered where water is more prevalent – indeed it would be immensely foolish to suggest that this *was* categorically *not* the case. However, the reaction-monitoring experiments up to this point had strongly suggested that the initial nucleophilic addition/loss of water/iminium-forming sequence was not as kinetically significant as the apparently rate-limiting collapse of the iminium ions **210** and **211**.

The access to higher-powered NMR equipment had furnished data which showed starting material remained in the reaction mixture throughout the duration of the reaction time; this was observed consistently during each experiment, and was corroborated by 2-D NMR and LCMS.

The natural progression in the mechanistic work was therefore to attempt to find a set of reaction conditions which converted all of the available starting ketone **188** to product **189**.

Within the group, it had been reported that certain carbonyl compounds were less amenable to the α -oxygenation reaction, but that use of excess reagent addressed this problem with a degree of success.⁵⁰ Having studied the effect of added water on the reaction kinetics, the obvious next step was to monitor the reaction having altered the stoichiometry with respect to the reagent **100-HCl** (Figures 74, 75 and 76). For each of the following experiments, anhydrous DMSO- d_6 was used; for each separate run the water content did not exceed 50 ppm.

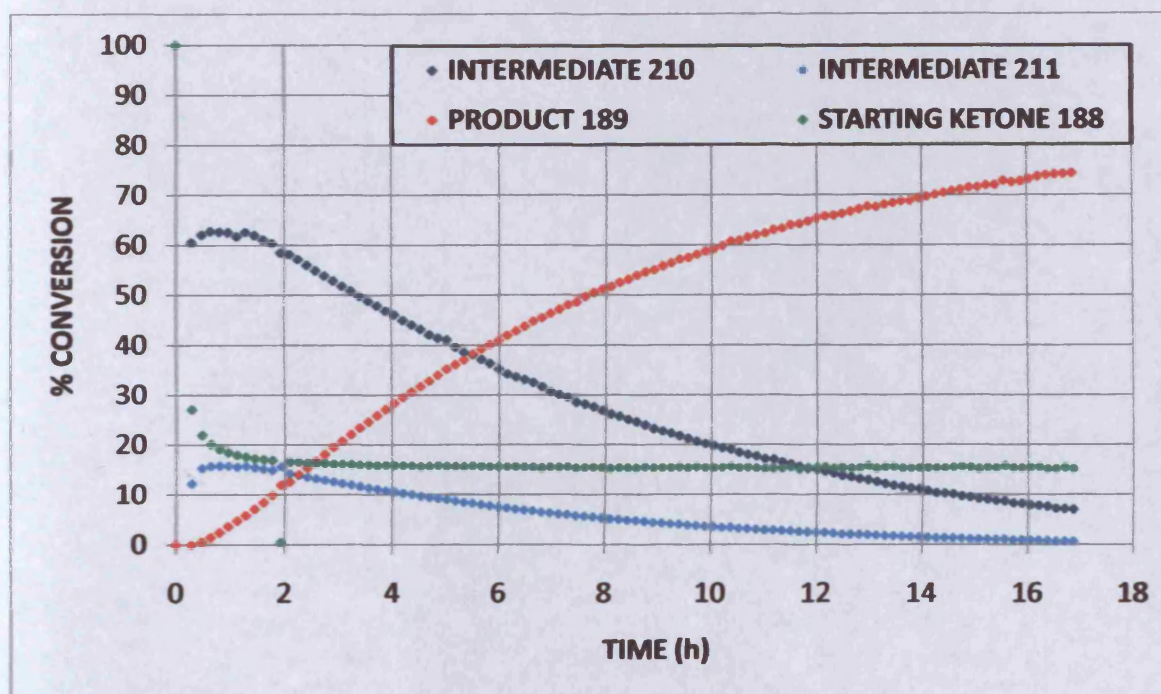


Figure 74: Product **189** and Intermediates **210** and **211** at 305 K (0.9 eq. w.r.t. **100-HCl**)

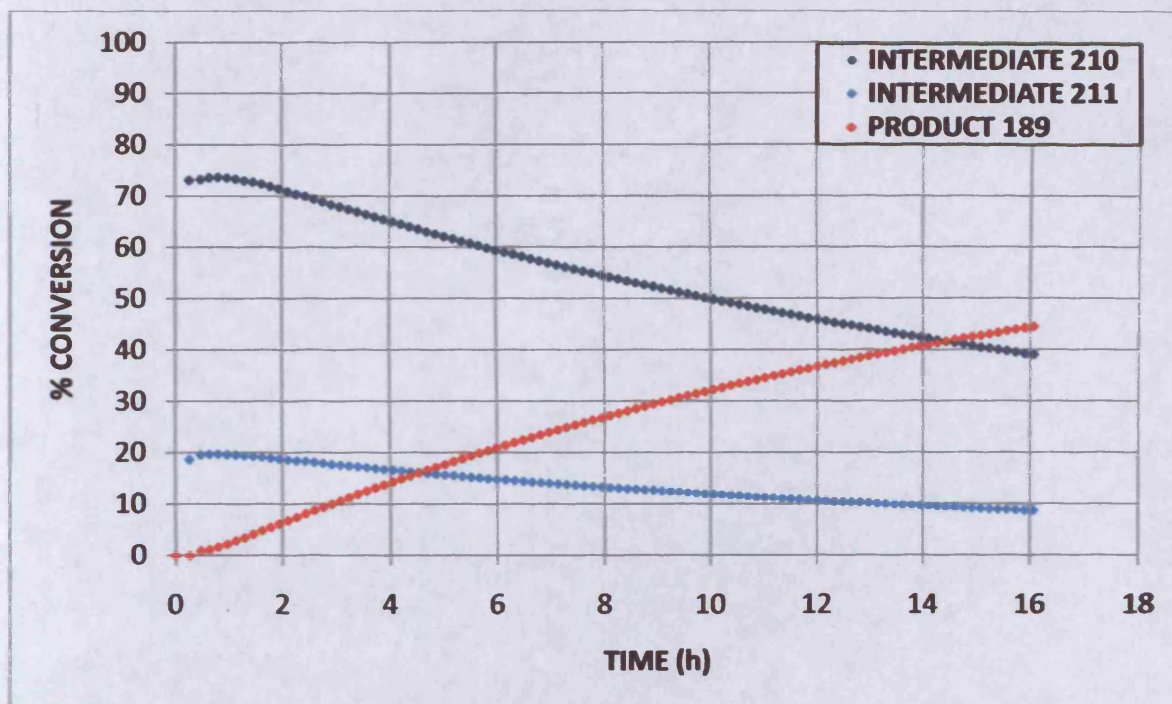


Figure 75: Product 189 and Intermediates 210 and 211 at 305 K (1.2 eq. w.r.t. 100-HCl)

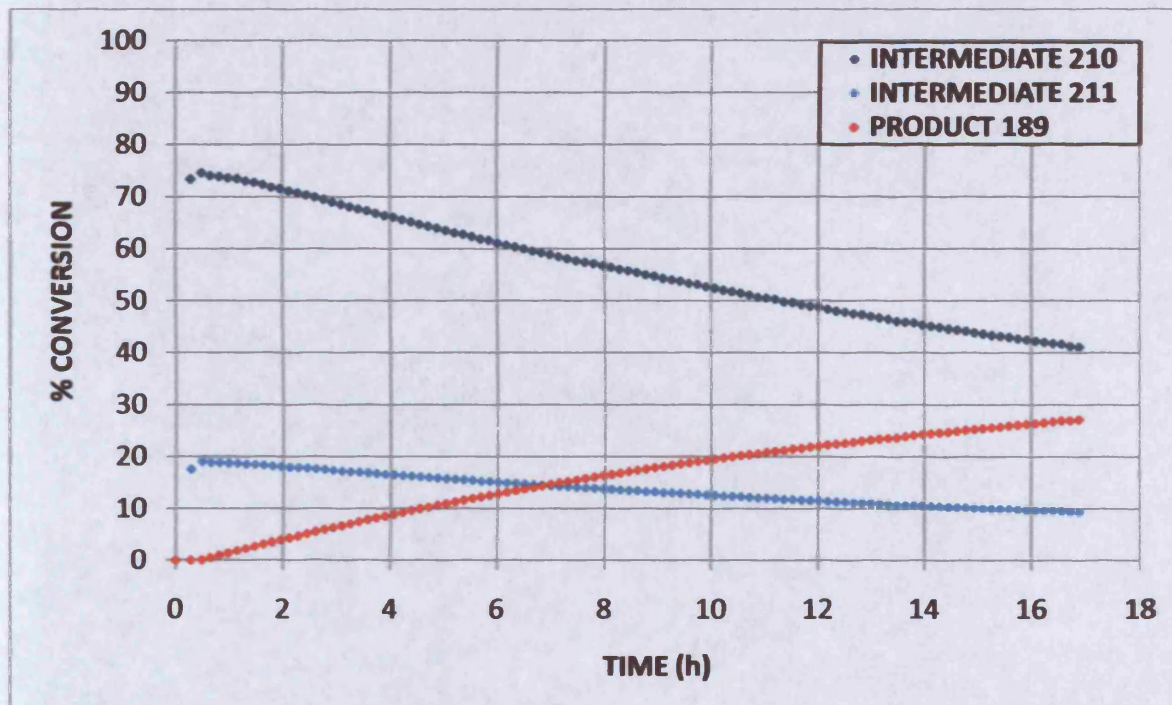


Figure 76: Product 189 and Intermediates 210 and 211 at 305 K (1.5 eq. w.r.t. 100-HCl)

For the data series where an excess of reagent **100-HCl** was employed, no starting material was detected over the course of the reaction time. This would have seemed to answer our question satisfactorily, were it not for the fact that apparent disappearance of starting material **188** did not correlate with the amount of product formed.

Figure 77 is an overlay for product formation under each reaction where the stoichiometry of the hydroxylamine species **100-HCl** was varied.

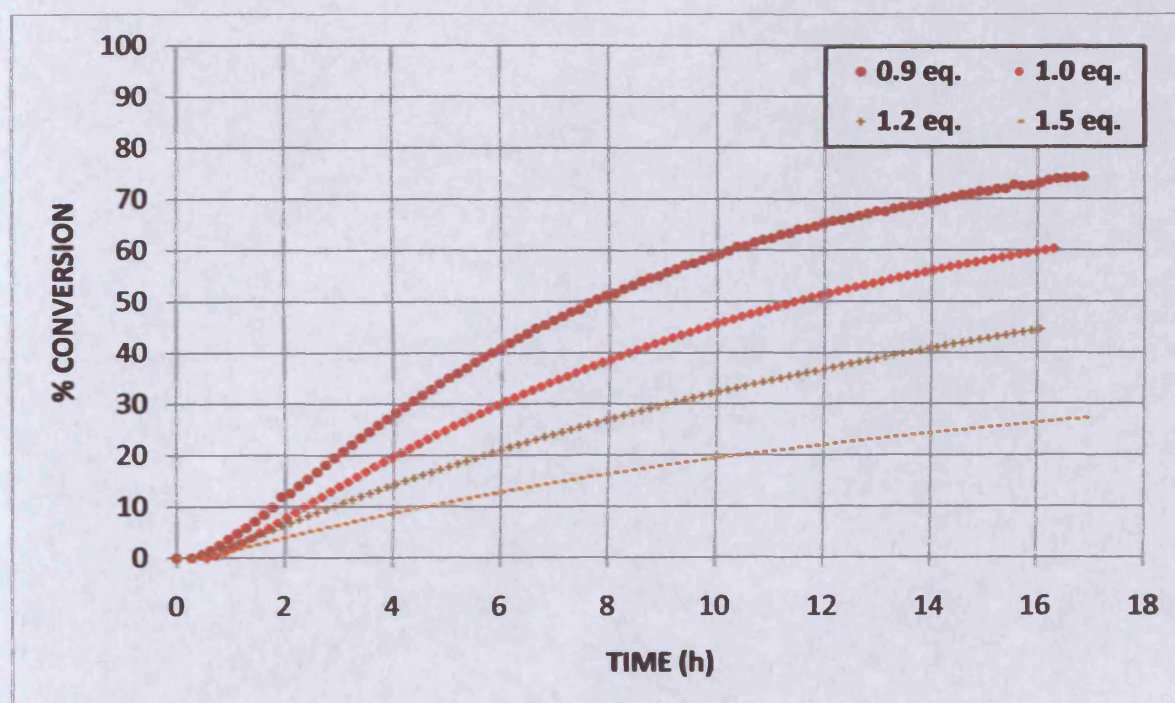


Figure 77: Overlay of formation of product 189 at 305 K (varying stoichiometry of 100-HCl)

Under the standard conditions for *in-situ* reaction monitoring – i.e. a temperature of 305 K and use of sieve-dried DMSO- d_6 (moisture content therefore < 50 ppm) – the somewhat surprising outcome was that an excess of *N*-methyl-*O*-benzoyl hydroxylamine hydrochloride **100-HCl** apparently suppressed the rate of formation of α -oxygenated adduct **189**. However, both of the expected intermediates were rapidly formed, and with conversions matching or exceeding the maxima that we had observed so far.

This set of results therefore did not entirely tally with the observations made within the group during the development of the methodology; namely, that when the reaction was performed in dry solvent with an excess of reagent, led to product being formed at an appreciably slower rate. Contrary to this finding, isolated yields were often known to increase in the laboratory as reagent stoichiometry was increased. It was noted, however, that the solvent moisture content during the NMR-based experiment may have differed substantially from the reactions conducted on the bench in the early days of the project.

During the time that was allotted to studying reagent stoichiometry, there did not evolve a wholly convincing rationale as to why an excess of reagent should have apparently suppressed the conversion to product **189** in dry solvent to the extent that was observed. It was felt that further, thorough experimental investigation – while desirable – carried with it the risk of overly digressing from the core aims of this part of the project overall.

6.2 Fate of reagent

Through deeper inspection of the ^1H and 2D NMR spectra, we started to suspect that benzoic acid was a common species to all of the reaction mixtures. This was supported by evidence from LCMS and HPLC experiments, in which a solution of *N*-methyl-*O*-benzoyl hydroxylamine hydrochloride **100-HCl** in DMSO-d_6 was stirred at 305 K. We theorised that the reagent was undergoing decomposition to a minor extent over a protracted time, and that this effect was more apparent at elevated temperatures.

Figure 78 is a HPLC trace of a solution of benzoic acid **117** in MeCN, showing that the retention time was 2.7 minutes.

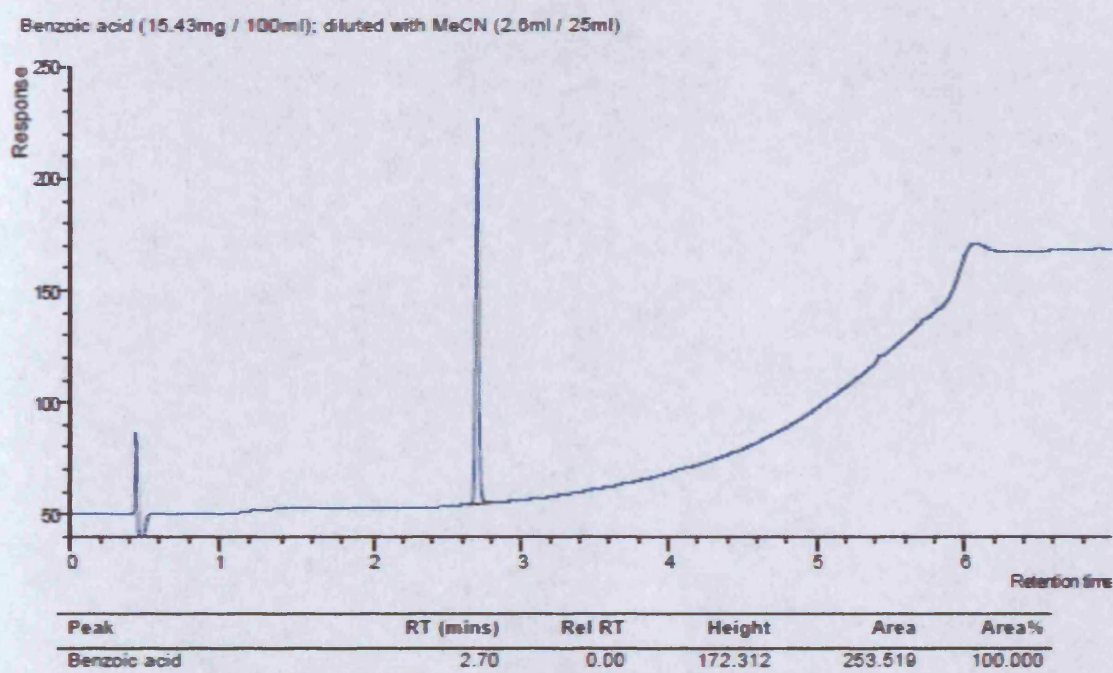


Figure 78: HPLC trace of benzoic acid

After 3 hours, the solution of reagent **100-HCl** in DMSO- d_6 was analysed by HPLC (Figure 79).

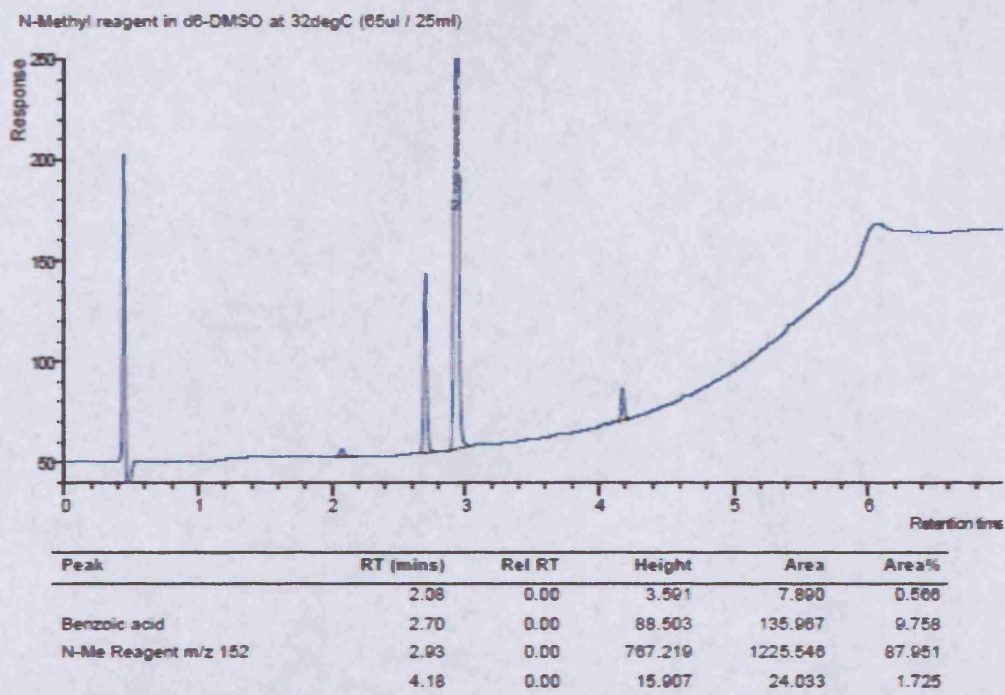


Figure 79: HPLC trace of reagent 100-HCl in DMSO- d_6 after 3 hours at 305 K

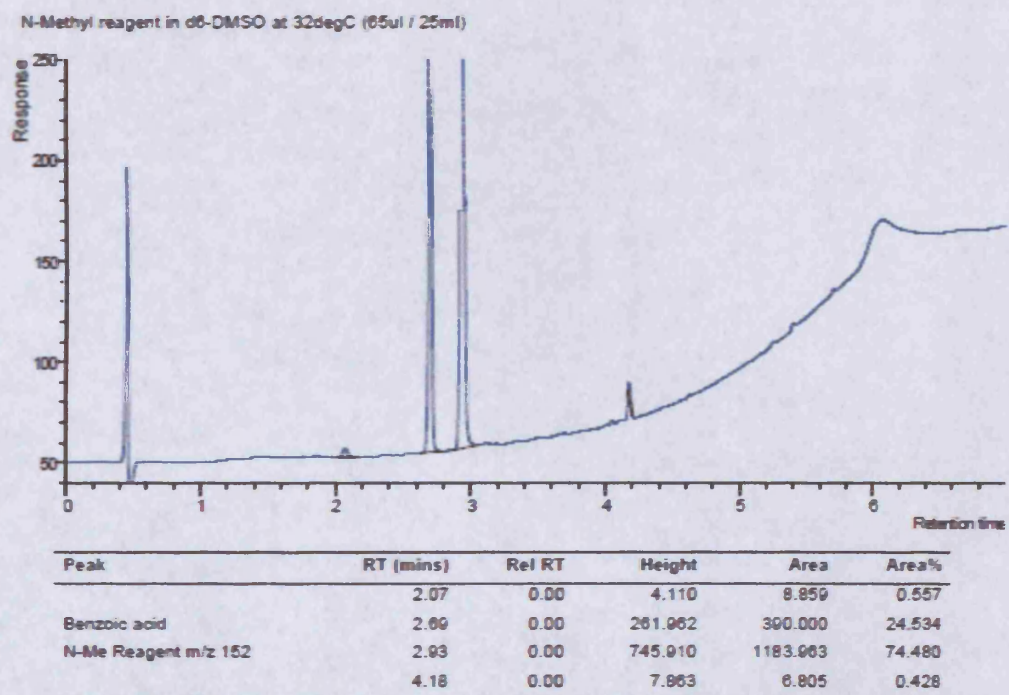


Figure 80: HPLC trace of reagent 100-HCl in DMSO- d_6 (spiked with BzOH solution)

As well as the peak corresponding to the reagent **100-HCl** with a retention time of 2.93 minutes, we also observed a peak with an almost identical retention time as benzoic acid **117**. To confirm the identity of this species, the solution was spiked with an aliquot of benzoic acid solution of known concentration, and this resulted in a quantitatively correct enhancement in the peak of interest in the HPLC trace (Figure 80).

This result was confirmed by ^1H NMR using the same conditions for the thermal decomposition of *N*-methyl-*O*-benzoyl hydroxylamine hydrochloride **100-HCl** in DMSO-d_6 . We therefore concluded that the benzoic acid observed in the reaction mixtures was a product of reagent decomposition, rather than any degradation of product or other side reaction arising from the presence of carbonyl compound.

With care, the amount of benzoic acid in the reaction-monitoring was determined retrospectively, and a new mass balance calculation performed (Figures 81 and 82).

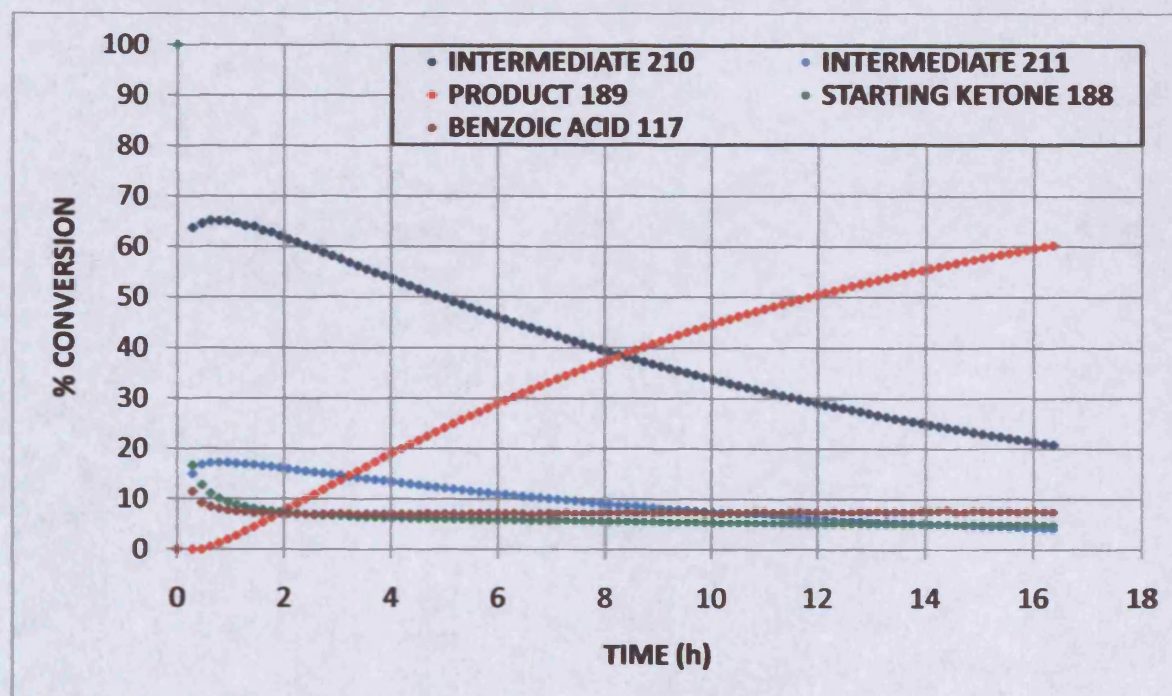


Figure 81: Reaction monitoring at 305 K (with starting ketone 189 and benzoic acid 117)

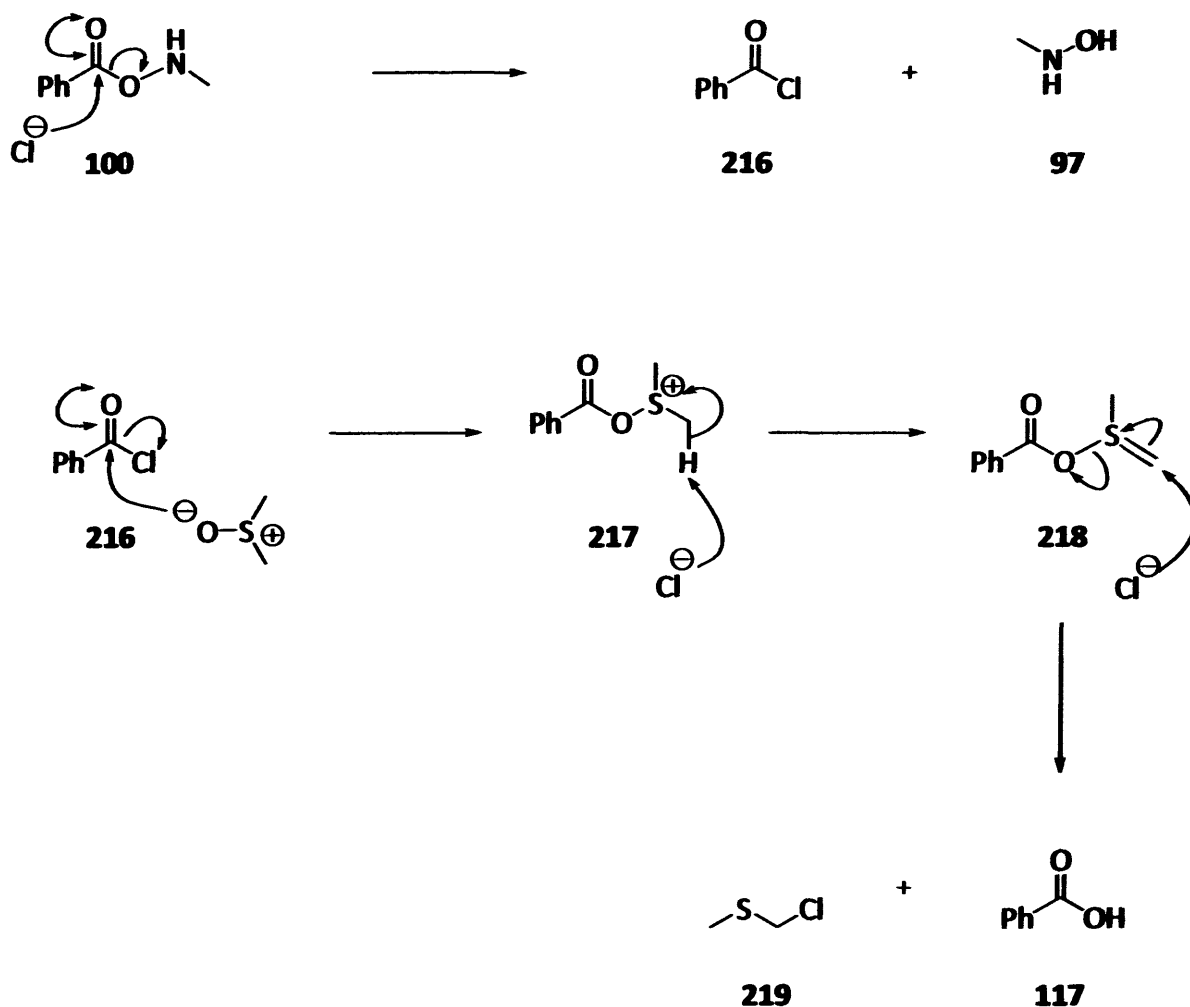


Figure 82: Mass balance calculation on Figure 81 data

Clearly, the mass balance problem we had been plagued with since the start was improved after benzoic acid **117** was taken into account, although it was acknowledged that we had been unable to detect and identify approximately 5% of the total material present within the reaction mixture. While this figure was within acceptable experimental error, the fact that the mass balance calculation was systematically less than expected suggested strongly that there was one or more species which was unaccounted for. It was suggested that this/these unknown species was/were best described as the products of unwanted side reactions rather than being intermediates in our proposed reaction pathway; this supposition being based on the fact that we did not see the total material 'recover', towards the true total of 2.5 mmol as the reaction progressed.

From a mechanistic point of view, the observations involving the presence of benzoic acid piqued our interest, because not only were these quantifiable and backed up with evidence from further experimental techniques (HPLC), but we now had the potential means to explain some of the apparently incongruous results from the ^1H NMR reaction-monitoring work. This led us to theorise about the possible decomposition pathway of the α -oxygenating reagent **100**·HCl.

Chloride anion is poorly solvated in DMSO, and therefore has more nucleophilic character than is usually observed. This enabled a model of reagent degradation to be constructed (Scheme 71).



Scheme 71

The products of nucleophilic attack by chloride anion on hydroxylamine species **100** were thought to be benzoyl chloride **216** and *N*-methyl hydroxylamine **97**. Acid chlorides readily react with DMSO to give chloromethyl methyl sulfide **219** and benzoic acid **117**.⁷⁹ Thus, we proposed a possible mechanistic pathway which explained the decomposition of the α -oxygenating reagent **100** in DMSO and the presence of benzoic acid **117** as a degradation product in the reactions with carbonyl compounds.

Returning to the 2D NMR analysis, our knowledge of the reaction up to this point enabled reasonably definite assignment of 56 of the 66 clear peaks present in the ^{13}C NMR of the reaction mixture, as collated in Table 6 (also see Figure 83).

$\delta\text{C}(\text{ppm})$	Carbon atom	$\delta\text{C}(\text{ppm})$	Carbon atom	$\delta\text{C}(\text{ppm})$	Carbon atom
211.21	1	128.82	12	36.06	5
206.41		128.72	12	35.68	3
204.37	1	128.52	10	34.16	14
187.95	1	128.49	5	33.81	14
187.81	1	128.02	10	33.51	8
167.16	1	127.61		32.64	8
165.31	9	83.26	2	31.84	8
164.87	9	78.98	2	30.95	5
164.84	9	73.24	2	30.81	
162.57		53.18	2	30.65	
134.26	13	51.89	4	30.25	7
133.97	13	50.55	4	28.86	7
133.51	13	50.22	6	28.31	8
133.43		48.79	4	27.66	
132.75	3	46.10		27.64	8
130.78	2	46.03	6	27.55	
130.03	11	41.87	3	27.28	7
129.61	11	41.73	4	23.89	7
129.36	10	41.13	6	23.87	
129.19	4	39.56	3	23.19	7
129.17	11	38.41	5	22.75	8
129.06	12	37.61	5	22.44	7

Table 6: Assignment of peaks in ^{13}C NMR

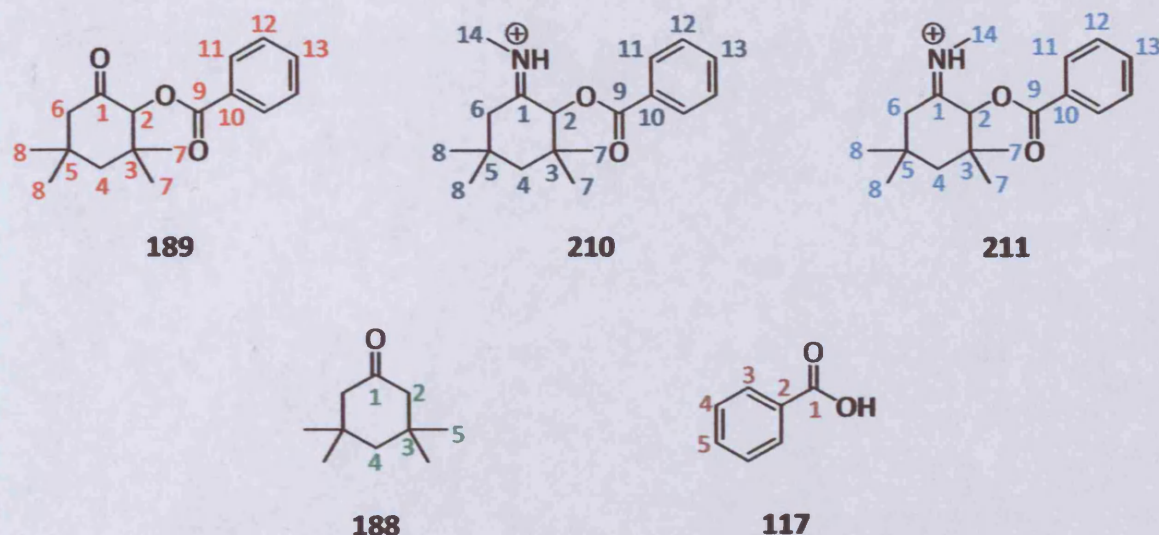


Figure 83

Assignment of the remaining 10 peaks proved impossible, either due to their being comparatively weak, and therefore no clear correlation present; or overlapping with nearby signals. We conjectured that these 10 peaks might represent one or more species present in only minor concentration, possibly relating to a side-product which had gone undetected in the ^1H NMR, or species from within the proposed decomposition pathway for the reagent **100-HCl**. Had assignment been possible, it seems likely that the mass balance calculation may have been improved further, i.e. we would have been able to account for 100% of the material present in the reaction mixture, detectable by NMR.

Nevertheless, it was possible to correlate the vast majority of the ^{13}C peaks to corresponding ^1H NMR signals; we therefore believed that we had substantially unravelled the workings of the reaction between the two substrates which we had examined extensively.

6.3 Reaction monitoring by ReactIR™

Although we had developed a methodology for ^1H NMR which allowed the reaction to be monitored *in situ*, it made good sense to explore at least one other analytical technique in order to try and find some complementarity within the results.

In the early stages of the project placement at AstraZeneca, calorimetry was discussed as a further means of probing the reaction; however a substantial hurdle was immediately apparent in that the available equipment required the reaction to be performed on an unfeasibly large scale. Even given the possibility of obtaining the necessary starting materials and solvent in an economically sensible fashion, the real possibility of an unwanted and potentially uncontrollable exotherm upon mixing of starting materials in DMSO meant that this technique was to all intents and purposes unavailable to us.

ReactIR™, however, provided a further means of studying progression of the reaction. Based on FTIR spectroscopy, ReactIR™ is a real-time *in situ* reaction analysis system in which a ReactIR™ probe is inserted directly into the reaction mixture, providing real-time information about chemical composition and information about the rate of change of concentration of all the key components of a reaction, thereby potentially furnishing useful information about reaction progression, mechanism and pathway.⁸⁰

Before the commencement of the reaction monitoring, sample spectra were recorded for the 3,3,5,5-tetramethylcyclohexanone **188**, *N*-methyl-*O*-benzoyl hydroxylamine hydrochloride **100-HCl** and the product ketone **189**. Figures 84 and 85 show an overlay of these IR spectra.

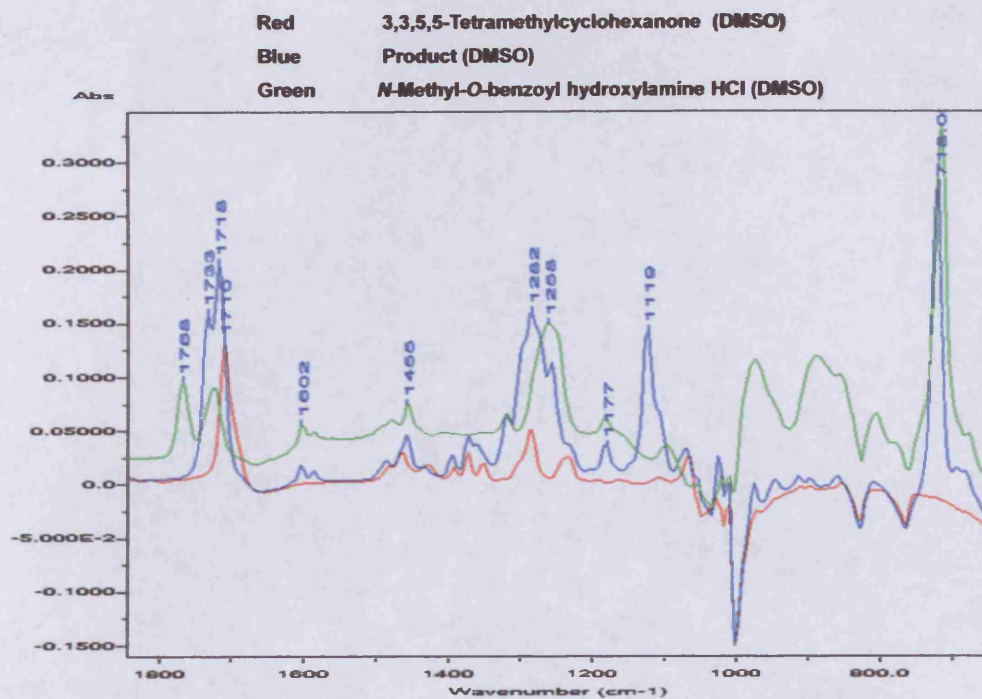


Figure 84: Overlaid IR spectra of starting materials 188 and 100-HCl and product 189
(1800-700 cm^{-1})

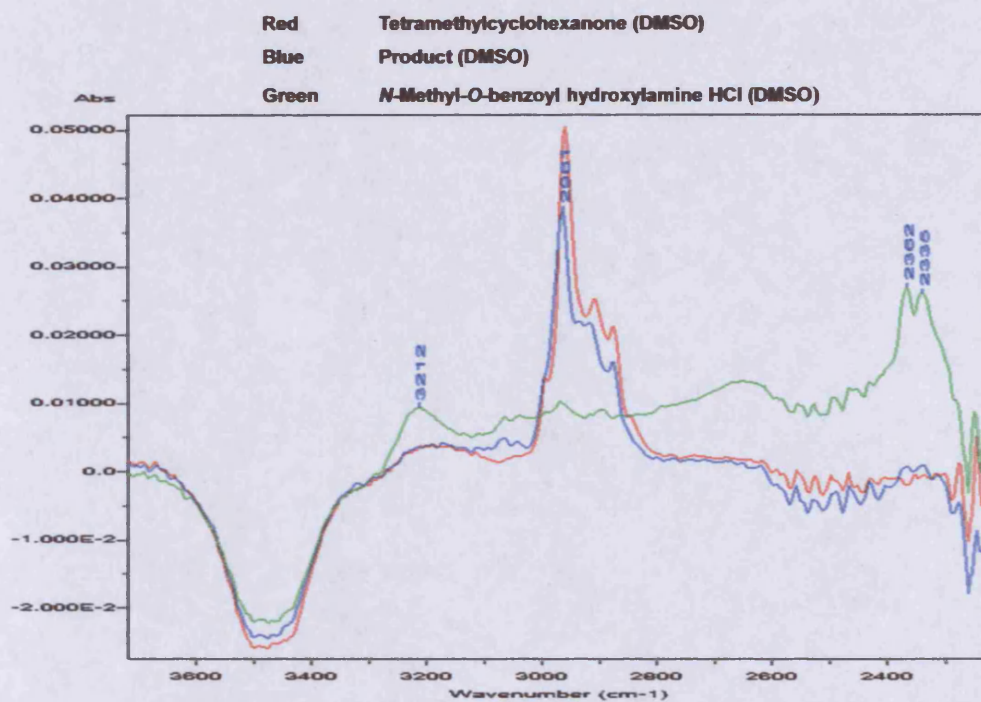


Figure 85: Overlaid IR spectra of starting materials 188 and 100-HCl and product 189
(3600-2300 cm^{-1})

In the experiment, a jacketed 80 ml vessel was equipped with a ReactIR™ probe, a thermocouple and a magnetic stirrer prior to the addition of DMSO- d_6 (in order to duplicate the conditions employed in the ^1H NMR reaction monitoring experiments as much as possible). The solvent was then warmed to 294 K and *N*-methyl-*O*-benzoyl hydroxylamine hydrochloride **100-HCl** added. Stirring was continued for 5 minutes, and then the ketone added in one portion. A small exotherm was observed (from 293.5 K up to 295 K) for 1 minute, after which the temperature started to drop back down to 294 K.

The first observation was that the intensity of the peak at 1769 cm^{-1} ($\text{C}=\text{O}$ for *N*-methyl-*O*-benzoyl hydroxylamine hydrochloride **100-HCl**) diminished with time after addition of the ketone (Figure 86).

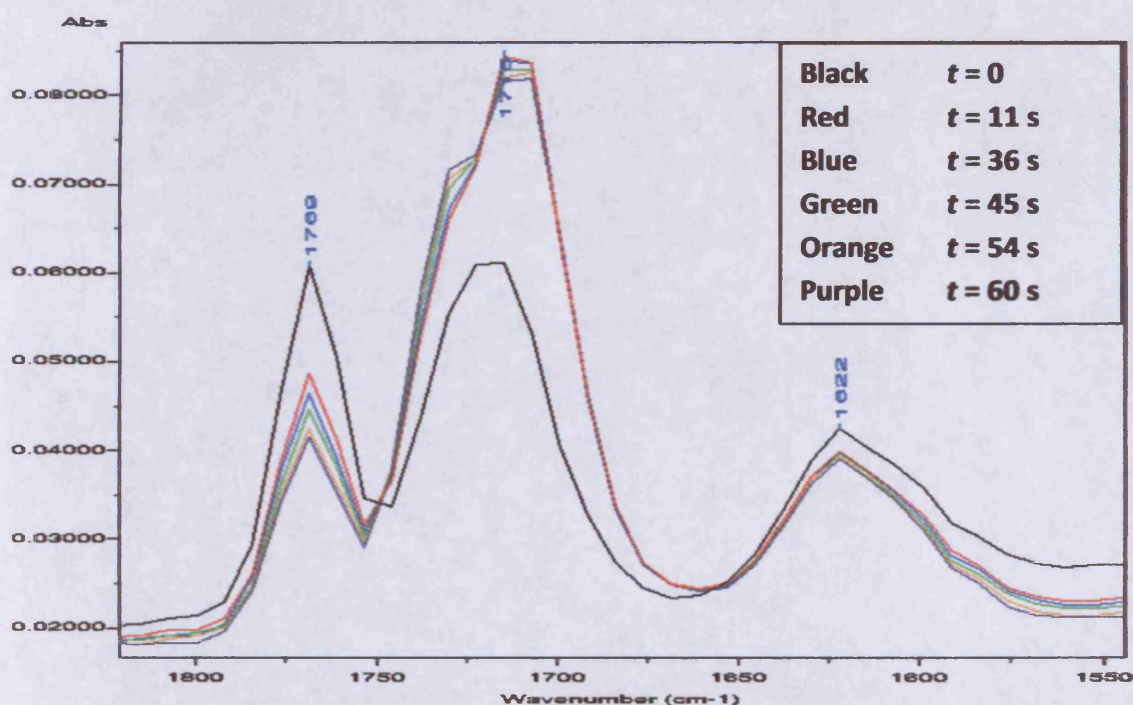


Figure 86: 2D IR spectra, 60 seconds after start of reaction

After 30 minutes had elapsed, this band had levelled off, and it was now also possible to see a new $\text{C}=\text{O}$ peak growing at 1730 cm^{-1} (Figure 87), along with peaks at 1259 cm^{-1} and 1104 cm^{-1} (Figure 88). Over time, a peak at 3507 cm^{-1} was also observed, and it was thought this could correspond to water, and the peak grew very slowly over time.

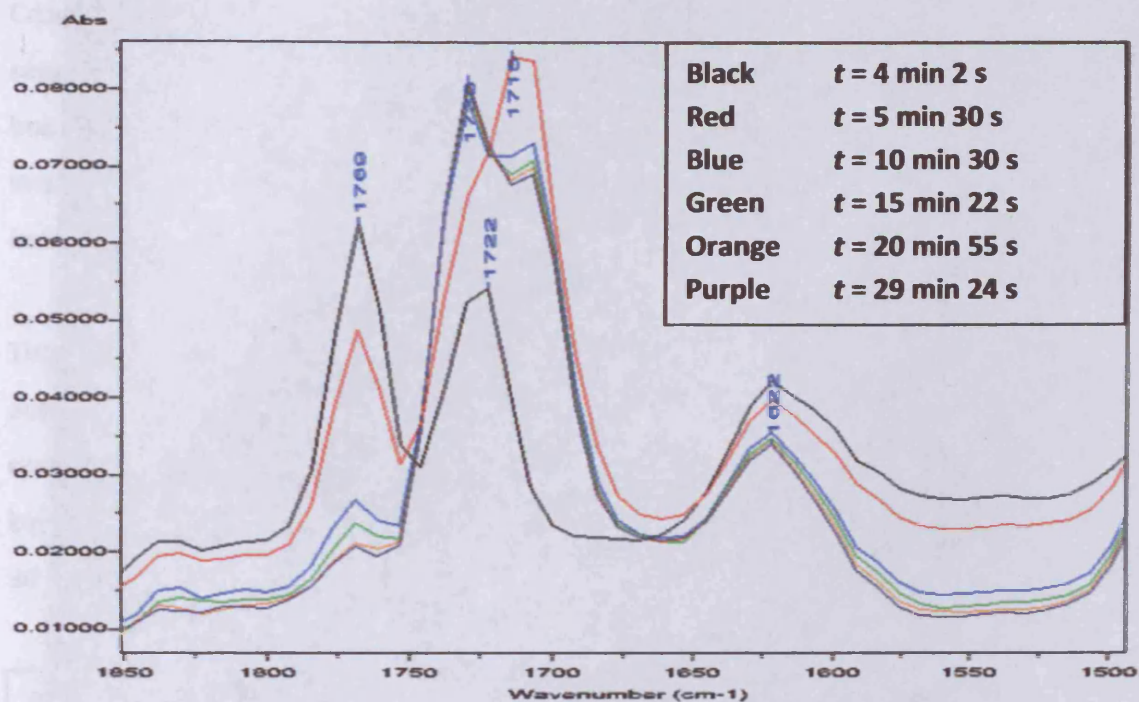


Figure 87: 2D IR spectra after 30 minutes reaction time

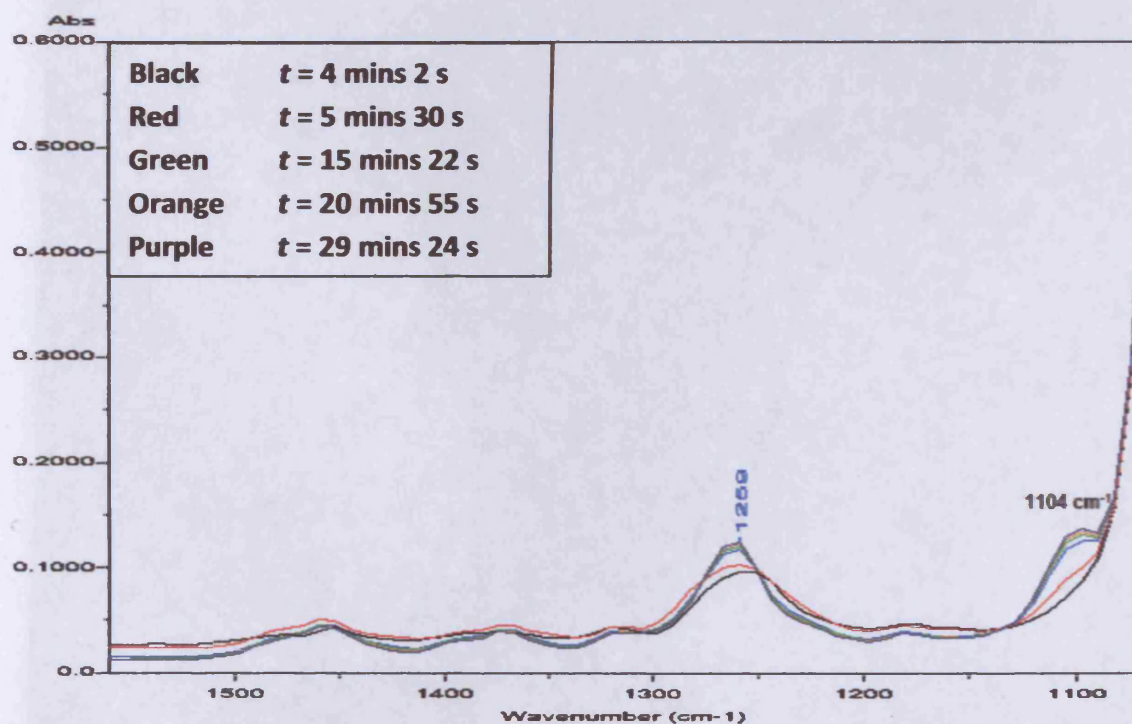


Figure 88: 2D IR spectra after 30 minute (growth of peaks at 1259 and 1104 cm⁻¹)

Crucially, a peak for C=N imine stretch was not seen between the expected wavenumber range of $1680 - 1640\text{ cm}^{-1}$. However, the deductions from the ^1H NMR work pointed to the iminium intermediates **210** and **211** existing as protonated species. If this was the case, the imine stretch could well have shifted over into the $\sim 1700\text{ cm}^{-1}$ region, particularly as the iminium ions also had electron-withdrawing groups in close proximity.

The reaction data thus far was then processed with ConclRTTM, a software package which automatically transforms spectroscopic data into reaction information; generating concentration profiles for each peak of interest across the reaction timescale, through which key reaction species can be identified and quantified. Figure 89 is the reaction profile after 30 minutes.

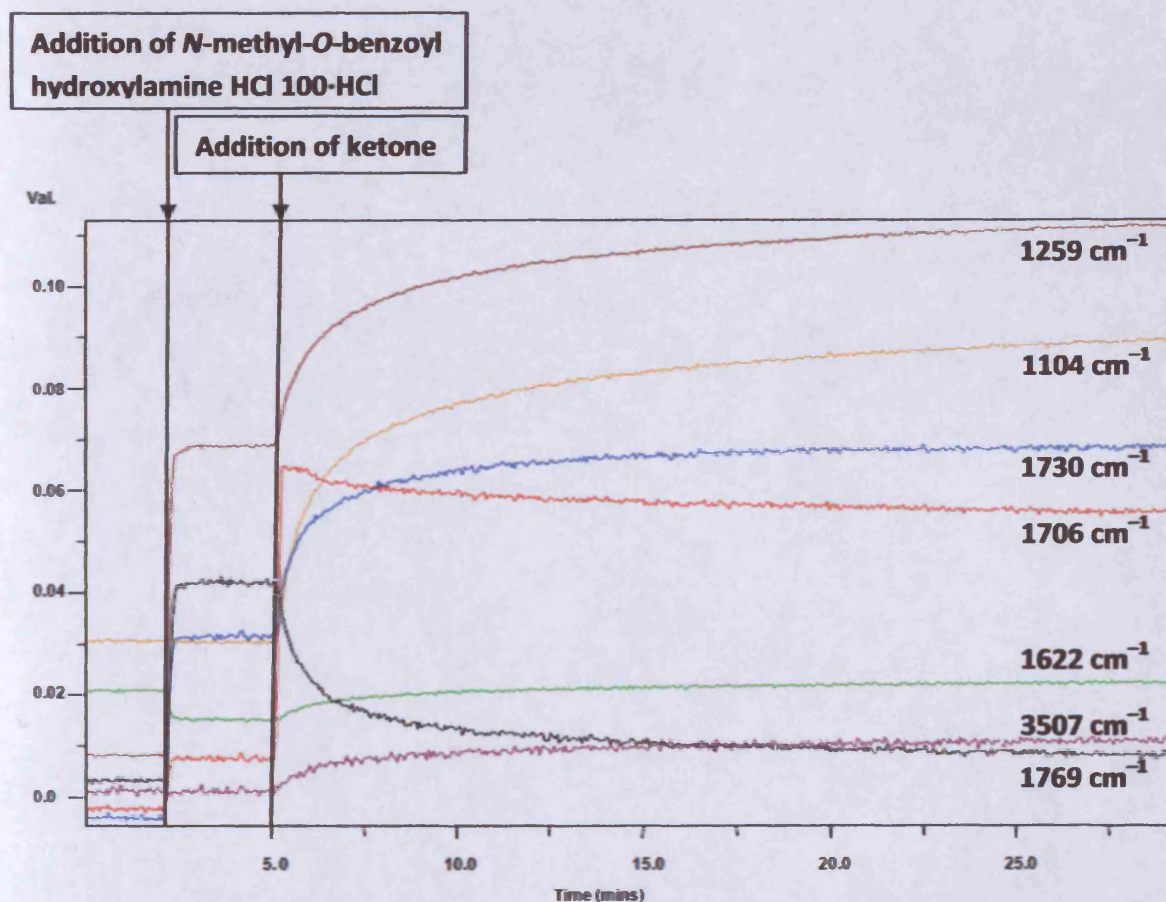


Figure 89: Reaction profile for first 30 minutes

In all, 5 components were identified by correlation with database of IR stretching frequencies:

- 3,3,5,5-Tetramethylcyclohexanone **188**, which was consumed over time, but (as with the NMR experiments) was not completely consumed.
- *N*-Methyl-*O*-benzoyl hydroxylamine hydrochloride **100-HCl**, which was again consumed over time.
- Intermediate **210** – increased over the 30 minutes; peak for C=O stretch at 1730 cm^{-1} , further peaks at 1452, 1259, 1104, 1004 and 718 cm^{-1} .
- Intermediate **211** – increased over the 30 minutes; peak for C=O stretch at 1707 cm^{-1} (with shoulder peak at 1730 cm^{-1} , further peaks at 1460, 1367, 1259, 1027, 888 and 718 cm^{-1} .
- DMSO

Figure 90 displays the reaction profile in terms of the 4 components of interest.

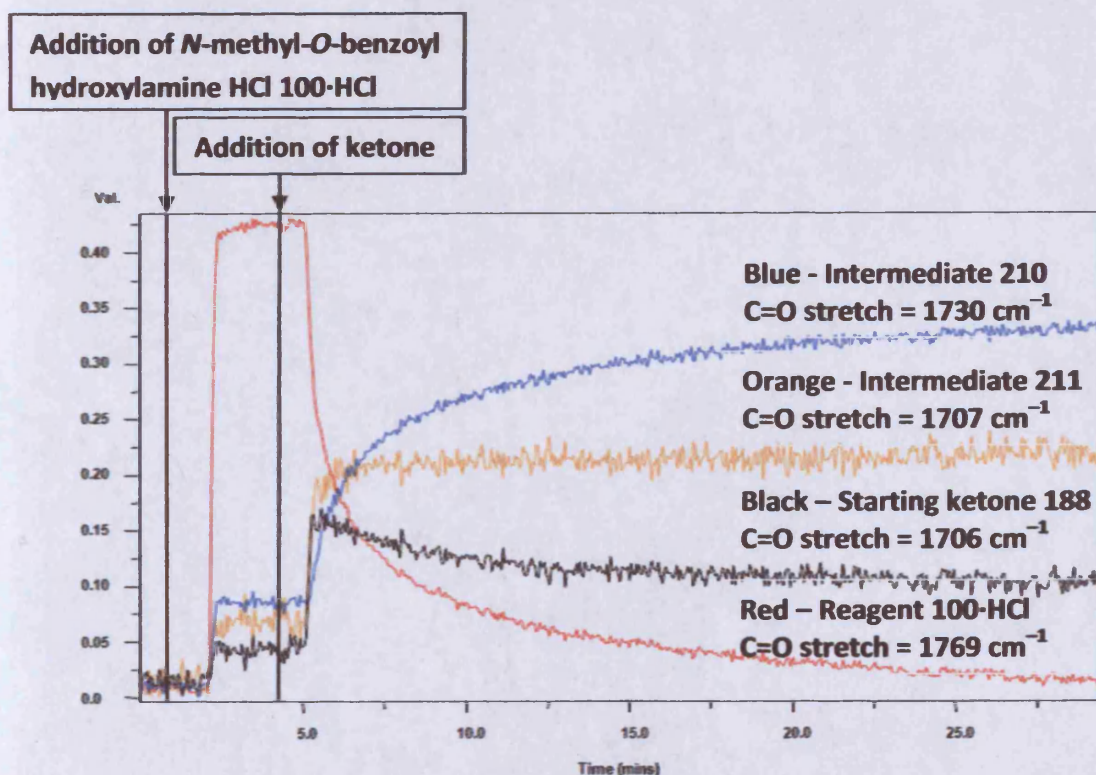


Figure 90: ConclRT™ profile for first 30 minutes of reaction

The peaks corresponding to Intermediate **211** were all smaller in intensity than those of Intermediate **210**, potentially analogous to the situation observed in the ^1H NMR. As a check, a sample was withdrawn from the reaction mixture at this point and submitted for analysis by ^1H NMR; the resulting spectrum displayed the 2 major intermediates as before. At this stage, the conclusions were consistent with previous observation, namely that *N*-methyl-*O*-benzoyl hydroxylamine hydrochloride **100-HCl** reacted swiftly with 3,3,5,5-tetramethylcyclohexanone **188** at 294 K to give 2 intermediates, **210** and **211**.

However, in terms of the IR monitoring, the reaction essentially came to a stop after 30 minutes. The reaction mixture was then warmed to 306 K over 10 minutes and the temperature held for 1 hour. From the real-time profile, it was seen that the peaks were not substantially changing in intensity with the increase in temperature (Figures 91 and 92).

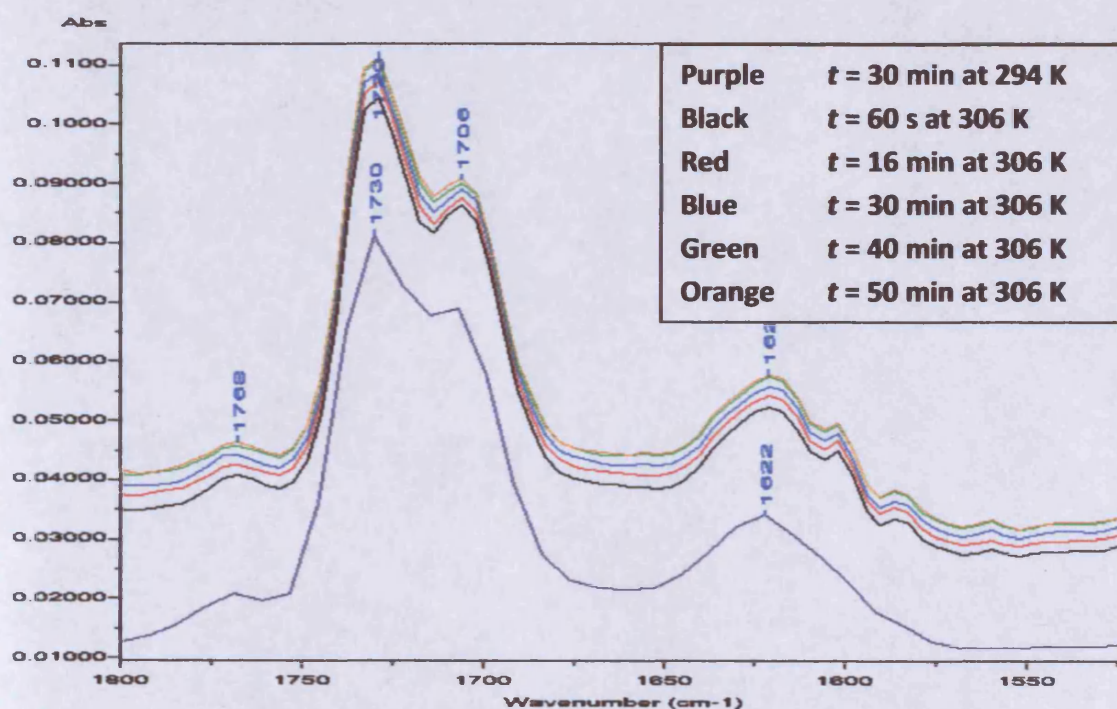


Figure 91: 2D IR spectra – reaction at 306 K for 1 hour ($1800\text{--}1530\text{ cm}^{-1}$)

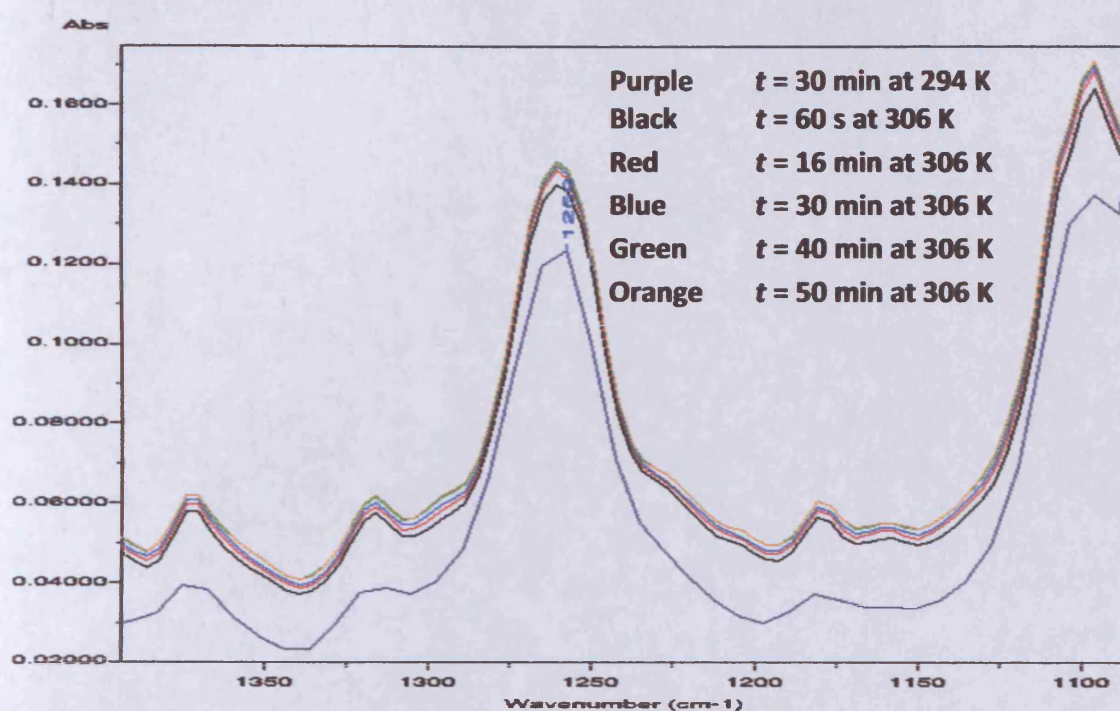


Figure 92: 2D IR spectra (1380–1090 cm^{-1}) – reaction at 306 K for 1 hour

At this stage water (~ 9 equivalents) was added, since we knew that the presence of water accelerated the consumption of the intermediates **210** and **211** to provide product **189**. Indeed, this seemed to kick-start the reaction again under the *in situ* IR conditions (Figures 93 and 94).

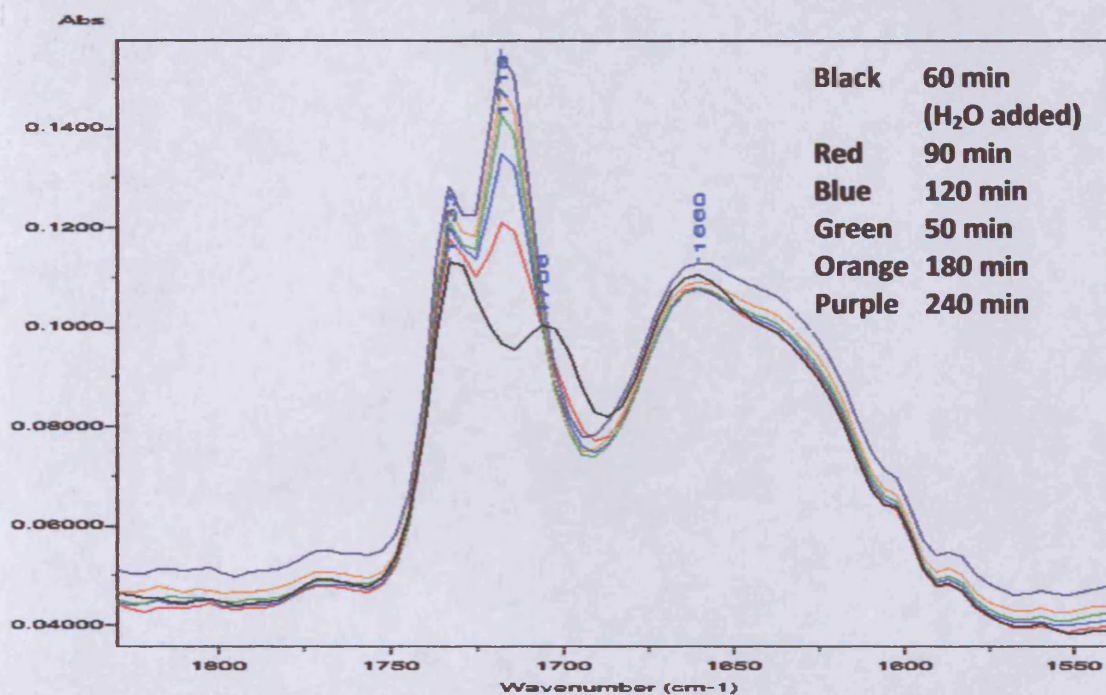


Figure 93: 2D IR spectra of reaction at 306 K for 4 h with added water (1800–1550 cm⁻¹)

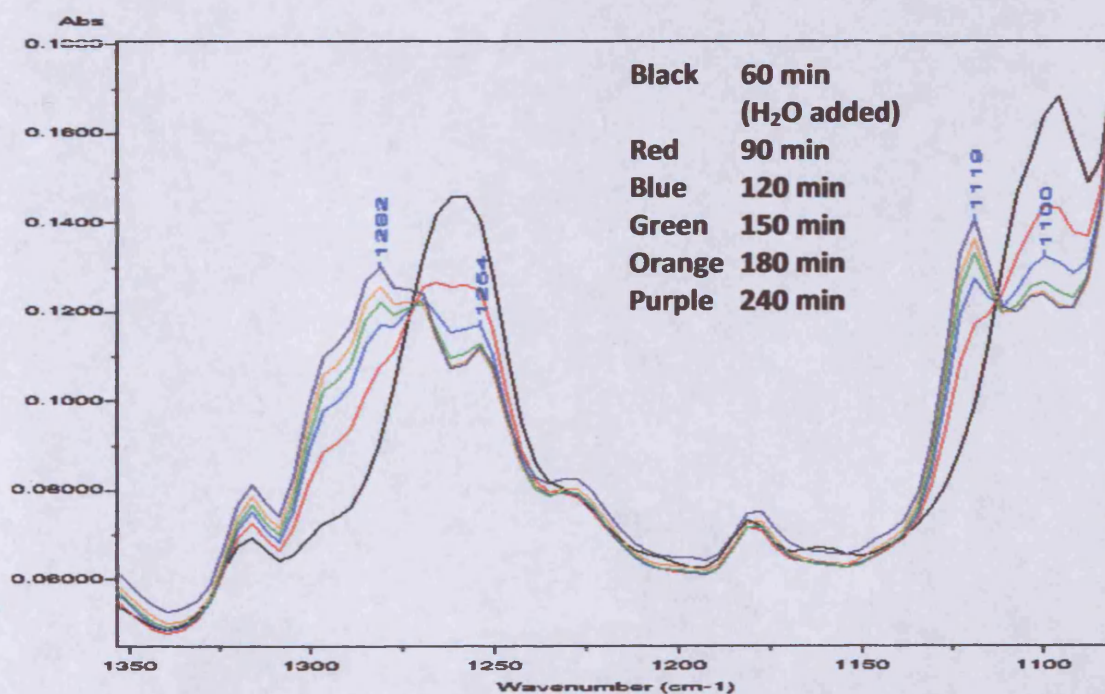


Figure 94: 2D IR spectra of reaction at 306 K for 4 h with added water (1350–1080 cm⁻¹)

On the addition of water, the intensity of the peaks at 1254 and 1100 cm^{-1} fell over time, whilst those at 1718 and 1733 cm^{-1} grew (accompanied by peak growth at 1316, 1297, 1282 and 1119 cm^{-1}). There was then very little change after 4 hours (Figures 95 and 96).

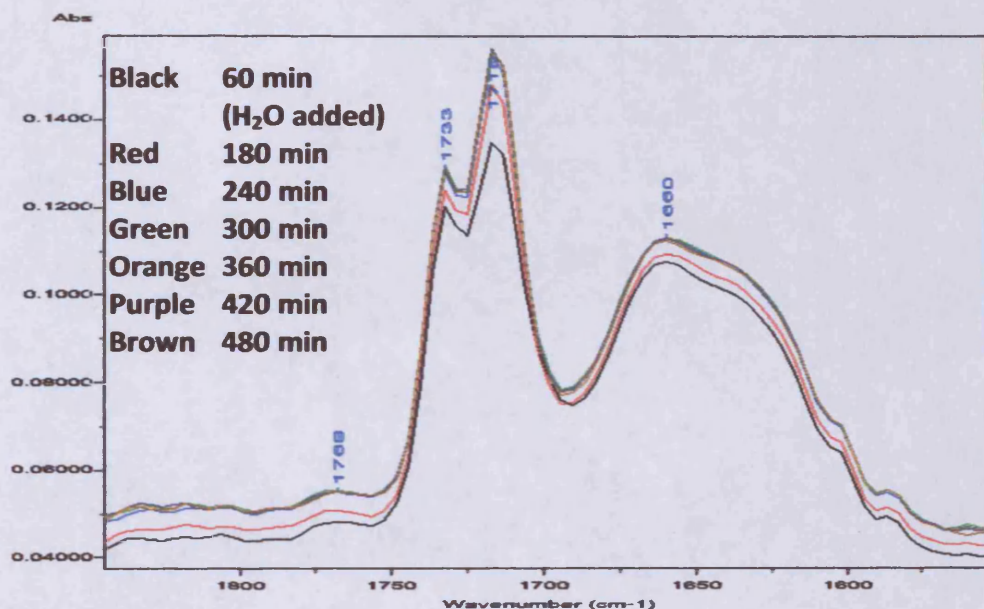


Figure 95: 2D IR spectra of reaction at 306 K for 8 hours (1800–1550 cm^{-1})

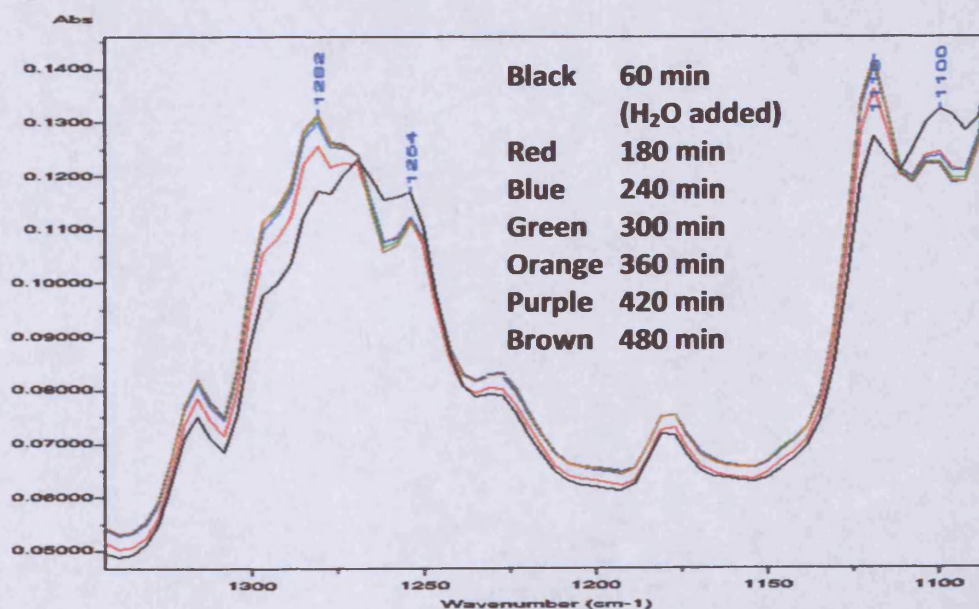


Figure 96: 2D IR spectra of reaction at 306 K for 8 hours (1300–1100 cm^{-1})

The new data was analysed with ConclRT™ (Figure 97).

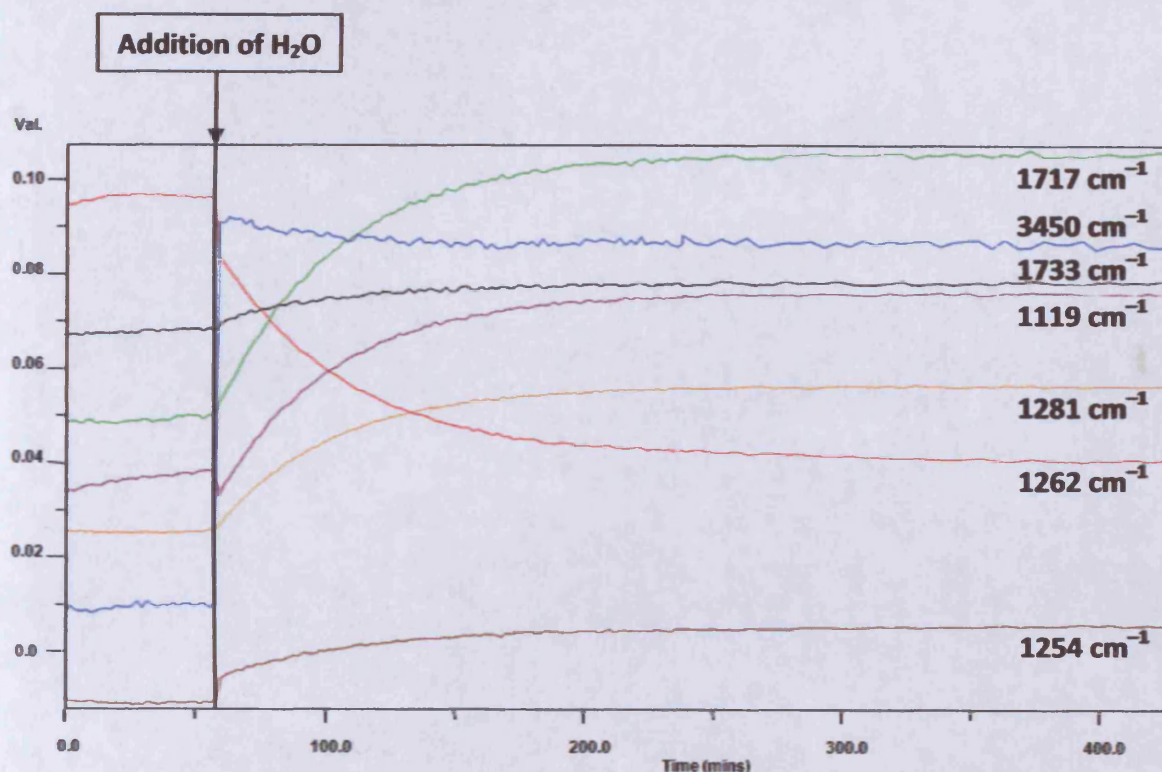


Figure 97: Reaction profile after 8 hours

4 components were identified:

- Water (broad peak at 1666 cm^{-1}).
- Intermediates **210/211** (with peaks at 1729 , 1702 , 1455 , 1262 and 1096 cm^{-1} – all diminishing with time).
- Product **189** (peaks at 1717 with shoulder at 1733 cm^{-1} , 1621 , 1281 and 1191 cm^{-1} – this component grows with time).
- Non-chemical variant (no distinguished peaks in the component spectrum).

Figure 98 displays the reaction profile in terms of the 4 components of interest.

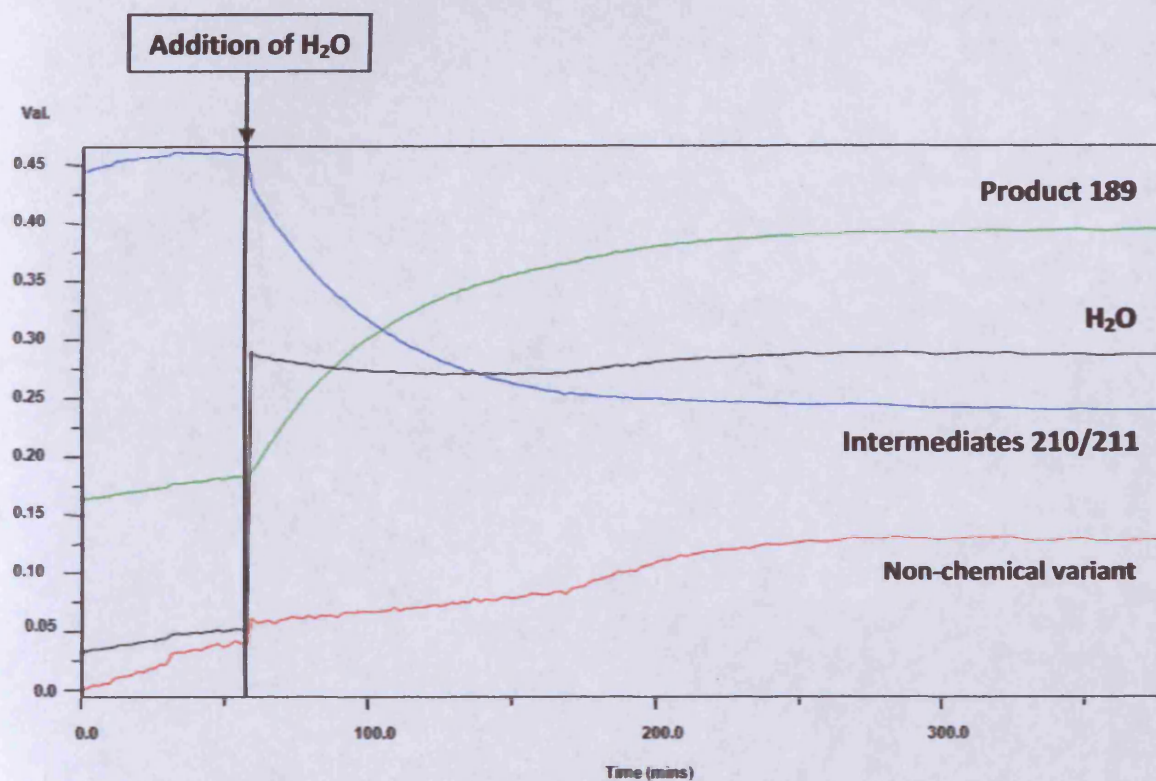
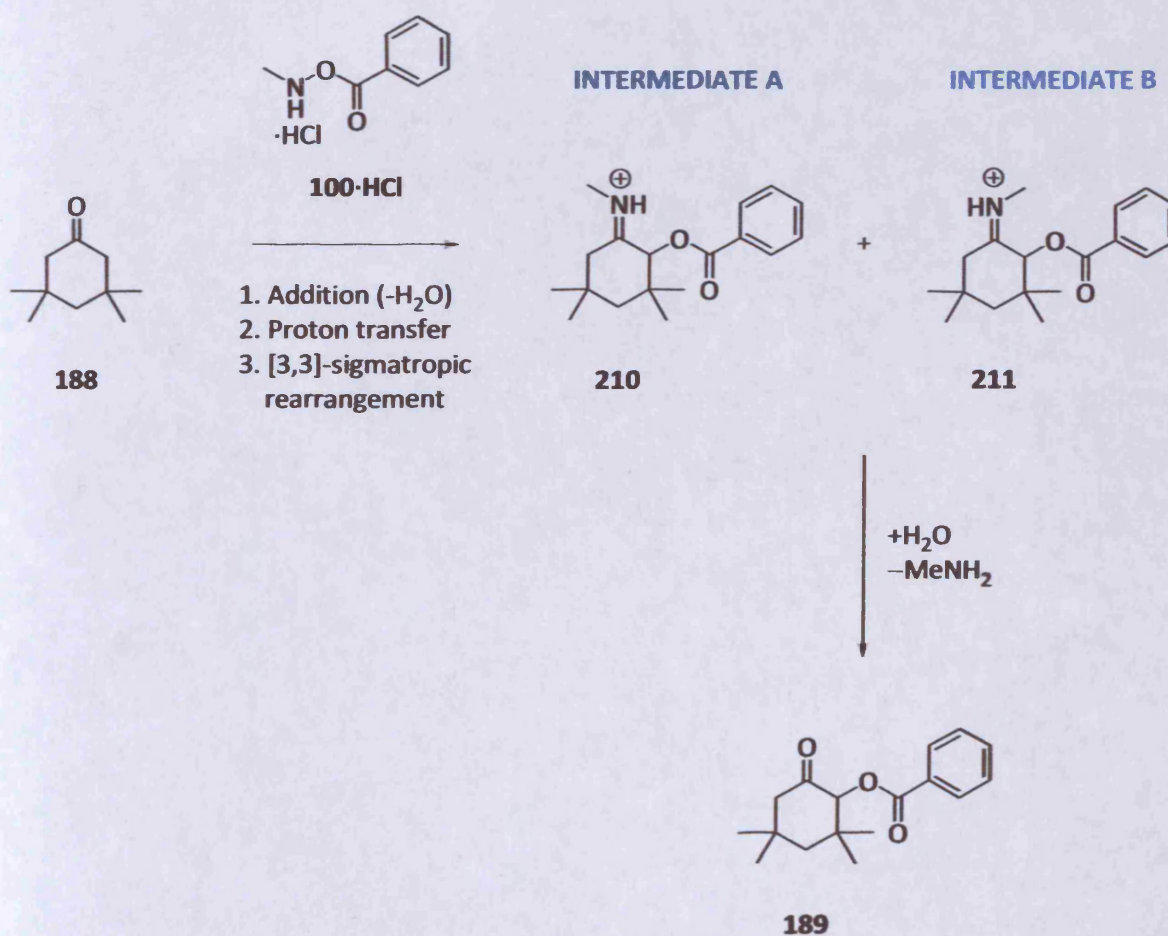
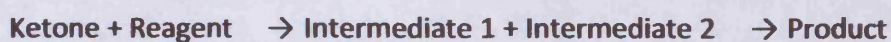


Figure 98: ConclRT™ profile for 6 hours reaction time

Broadly speaking, the results obtained appeared to back up the findings from the NMR work. In spite of the fact that time and practical considerations did not allow ReactIR™ to be explored more thoroughly (particularly with reference to quantifying the data), this technique stood as a suitable adjunct to the data we had accumulated by NMR.

6.4 Kinetic modelling

Having set as one of our goals the acquisition of kinetic and thermodynamic parameters for the transformation, we turned our attention to the problem of extracting rate constants of formation of product **189** from the data we had generated. This proved to be not entirely straightforward, as the process was essentially:



Scheme 72

Therefore, any analysis had to be undertaken allowing for the fact that in the early stages of the reaction, starting materials were being consumed at the same time as intermediates were both forming and decaying to product in two kinetically distinct steps. The simplest approximation would have been to simply take initial rates of product formation from the variable temperature series of experiments (Figure 99).

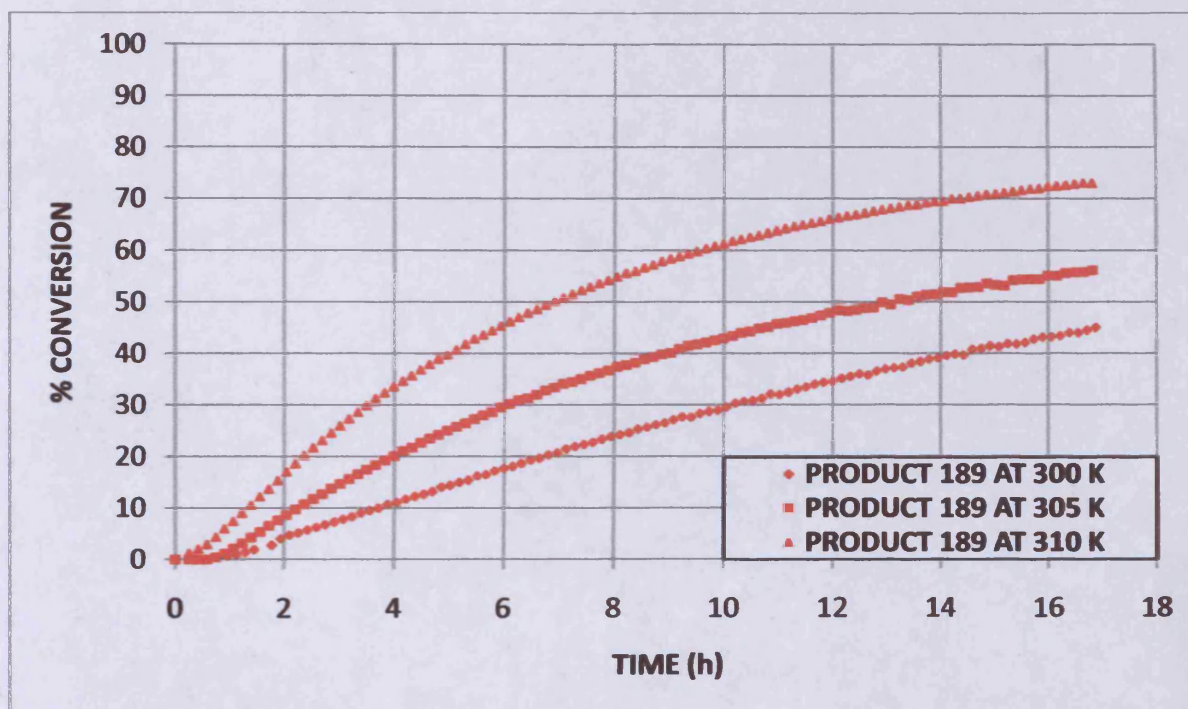


Figure 99: Product formation at various temperatures

However, it turned out to be very difficult to obtain rate constants by the method of initial rates, since to do so one would have had to ignore the earliest portion of the curve, where intermediates were still being formed. Hence, the method of initial rates, which was for a time considered as a method for extracting kinetic data, was discarded as inapplicable to our system (see Chapter 5, Section 5.2.3 for a detailed discussion).

As it was not possible to approach the problem by looking at the reaction as a whole by traditional methods, it was proposed that an analysis of the rate-determining step – namely hydrolysis of the iminiums **210** and **211** – could be undertaken using the integrated rate laws. The integrated rate law for a first order consumption of a reactant, A is given by the equation:

$$\ln \frac{[A]}{[A_0]} = -kt$$

where $[A_0]$ is the concentration of A at time, $t = 0$, so that if $\ln [A]/[A_0]$ is plotted against t , a first order reaction will give a straight line going through the origin and a slope equal to $-k$, from which the rate constant can be obtained.

Similarly, for a second order process:

$$\frac{1}{[A]} = kt + \frac{1}{[A]_0}$$

so that for a second order reaction, a plot of $1/[A]$ vs. t is a straight line with slope equal to k .

Figures 100 and 101 are the plots corresponding to the integrated rate laws for the 1st and 2nd order consumption of Intermediates **210** and **211** in the reaction at 305 K. For both plots, careful consideration was given to the reaction profile, such that starting points (i.e. new $t = 0$) were chosen sufficiently far along the reaction coordinate so that intermediates were no longer being formed. In so doing, the number of half-lives available for analysis was curtailed.

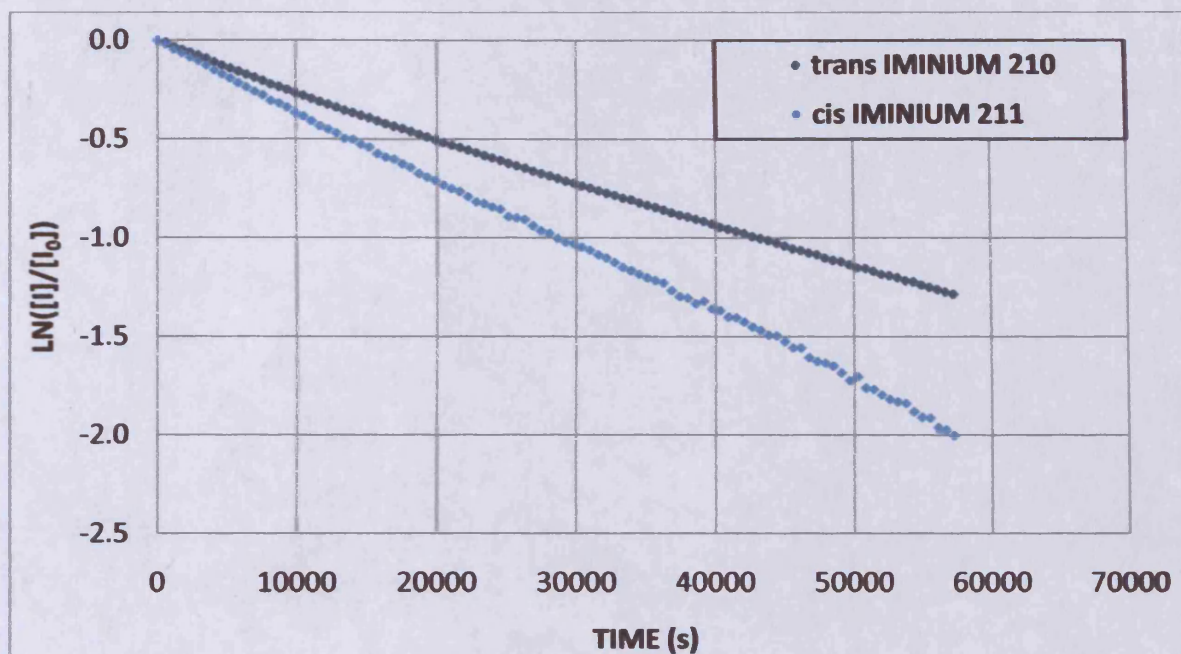


Figure 100: 1st order intermediate decay

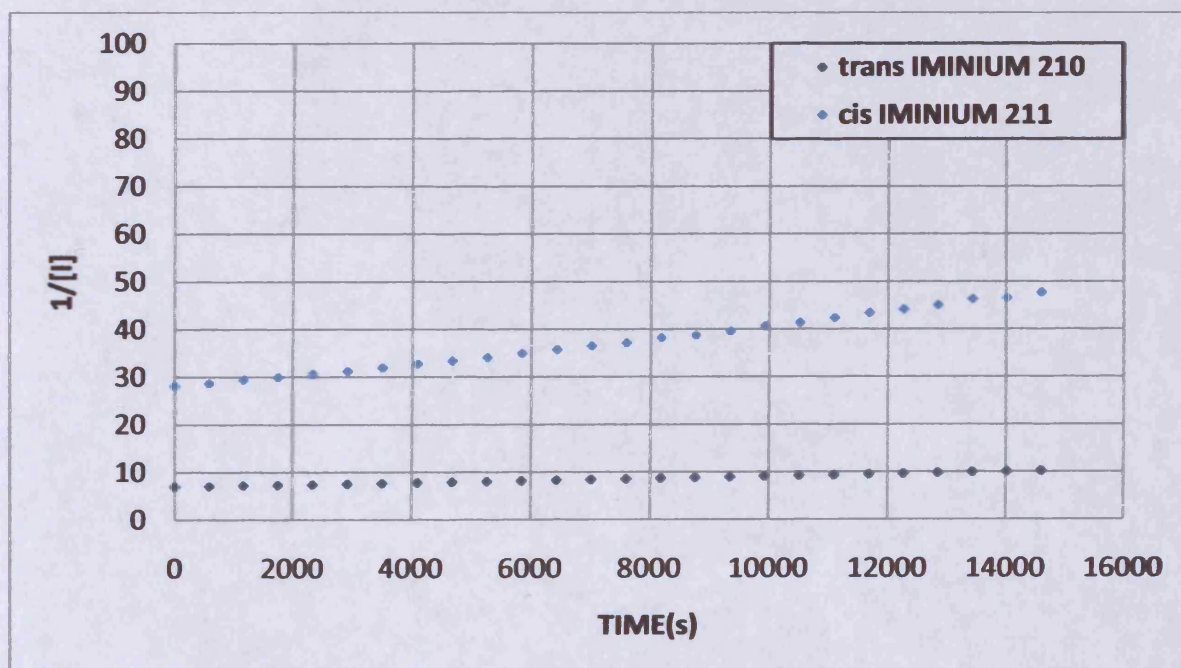


Figure 101: 2nd order intermediate decay

The net result of this exercise was a decidedly unclear outcome as to the order of intermediate decay. In Figure 100, Intermediate **210** had a clear straight-line form and this was initially indicative of first order reaction. However, the same could be said of the data series in Figure 101, i.e. Intermediate **210** apparently showed second order kinetics, as $1/[I]$ (where $[I]$ is the concentration of the Intermediate species) against time gave a straight line. For Intermediate **211**, a similar picture emerged, although the plot for second order reaction did take on a rather more curved form. Thus there was a distinct ambiguity in terms of performing the kinetic modelling by 'textbook' methods.

With the number of intermediates and equilibria within the reaction, together with the decomposition of reagent that had been uncovered, a more detailed level of chemical kinetic modelling was required. Modern computer applications, such as Micromath Scientist[®], are designed to provide solutions for the fitting of experimental data arising from complex chemical processes. Such programs allow the entry of a specific, hypothetical kinetic model, with a pre-defined set of experimental parameters. Subsequent analysis of the experimental data against the proposed model by sequential fitting iterations can then in theory provide a comprehensive solution to the model equations.

Such an analysis was undertaken with the experimental data from the reaction at 305 K.⁸¹ Within this study, two sets of kinetic models were programmed; both assumed that ketone **188** and hydroxylamine **100-HCl** reacted through to an enamine species. This initially formed enamine **190** was treated as a reactive steady state intermediate that reacted through to a pair of kinetically significant imine intermediates, **210** and **211**. Included in both models were the first order decomposition of the reagent **100-HCl** to benzoic acid **117**; this was to account for the incomplete consumption of the starting ketone **188** when using a 1:1 stoichiometry.

Model 1 treated the hydrolysis of the iminium ion intermediates, **210** and **211** as second order processes with kinetic dependencies upon both iminium ion and water (Figure 102).

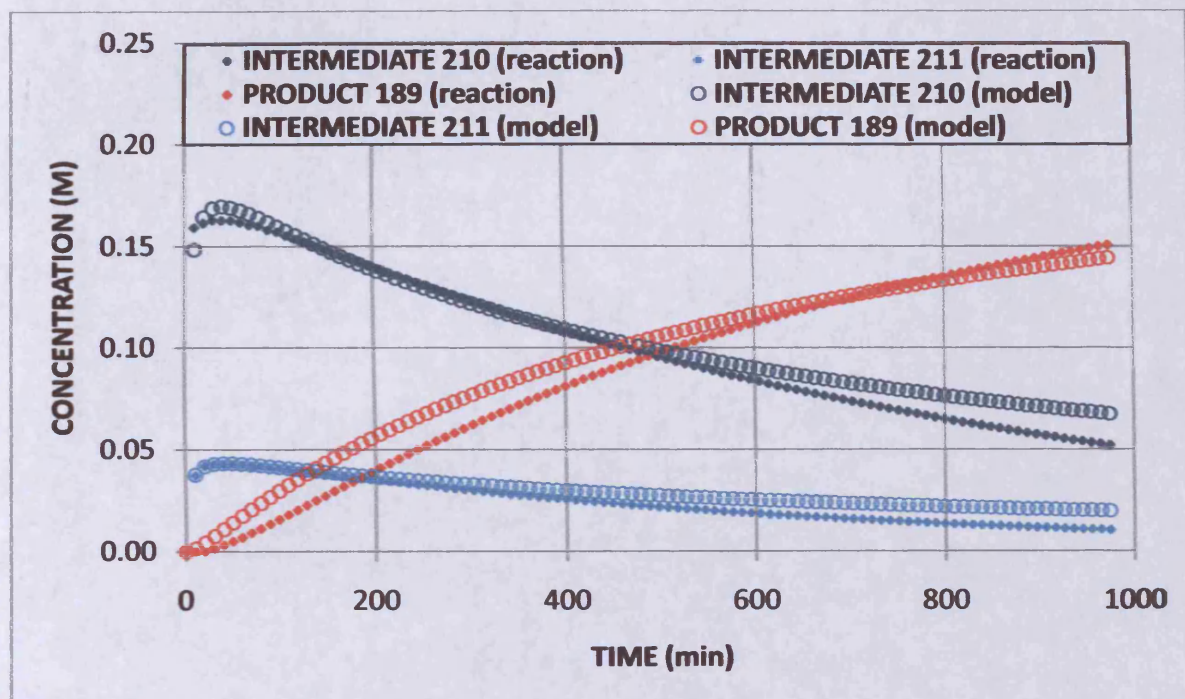


Figure 102: Kinetic model 1

Model 1 gave a very poor fit, which underestimated the amount of product 189 formed at the end of the reaction, overestimated the rate of product formation at the start, and did not describe the consumption of the two intermediates with the required accuracy.

Model 2 treated the iminium ion hydrolysis as a first order reaction, with no kinetic dependence on the concentration of water, although water was still consumed in the reaction (Figure 103).

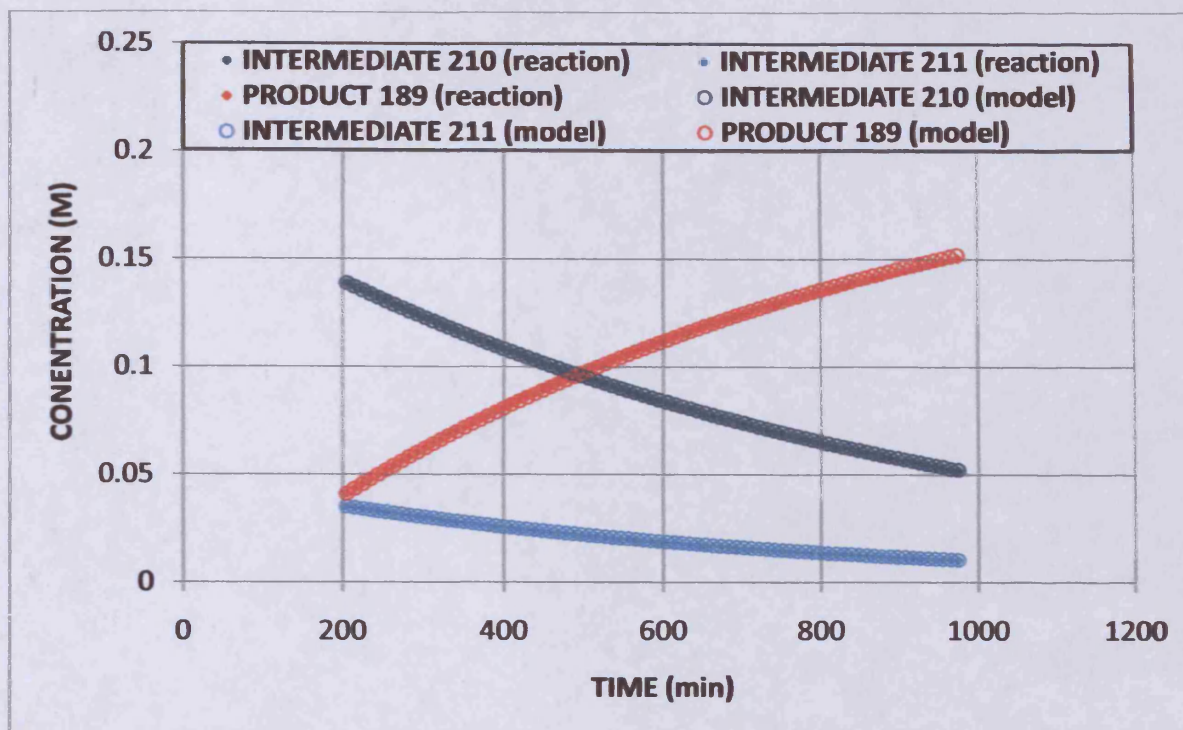
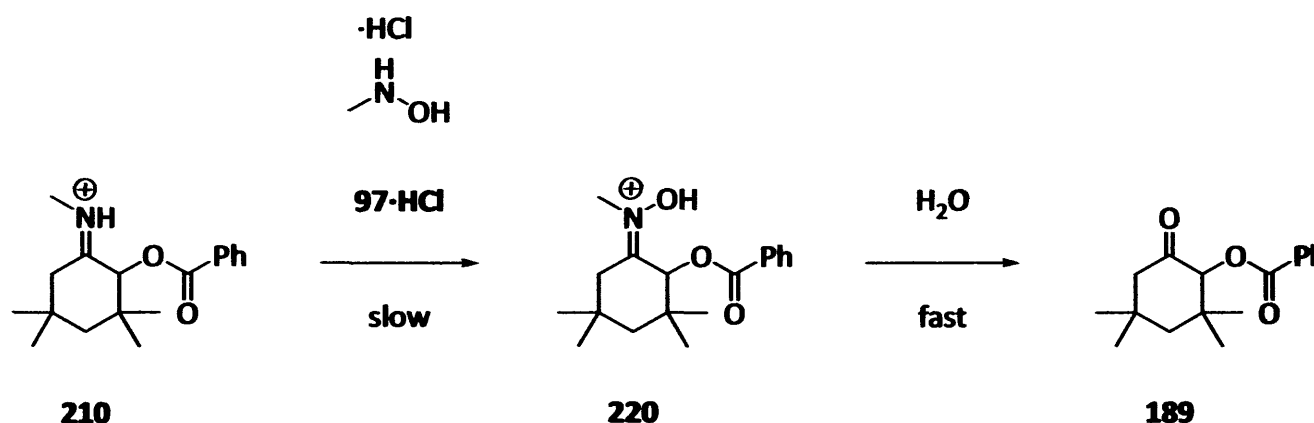


Figure 103: Kinetic model 2

In this much improved model, the data set was truncated and the initial parameter values modified to allow the program to fit data solely to iminium ion hydrolysis. In all cases where the entire dataset was analysed, the formation of product **189** predicted by the model commenced before product was actually observed. This possibly suggested the existence of another species between the iminium ions **210** and **211** and the product **189**, which does not accumulate to a sufficiently high level to be observed in the ^1H NMR data.

The kinetic modelling had ramifications to the proposed mechanism, in that we now had to think in terms of hydrolysis of iminium ions **210** and **211** under first order reaction kinetics. Clearly, hydrolysis is a bimolecular process, and we were accustomed to thinking of this in terms of a second order transformation – particularly as the earlier water-doping experiments had showed an increase in the rate of product formation as more water was added to the solvent.

An additional step was therefore postulated, in which iminium ion hydrolysis was catalysed by *N*-methyl hydroxylamine hydrochloride **97·HCl**, forming an intermediate *N*-alkyl oxime **220**, which is subsequently attacked by water to unmask the product ketone **189** (Scheme 73). By hypothesising that the nucleophilic catalysis step was rate-limiting, the concentration of water became irrelevant to the overall reaction kinetics, and therefore the iminium hydrolysis could follow first order kinetics.



Scheme 73

There was no direct evidence for this step, although rate enhancements were observed when the reaction was conducted (and once more monitored by ¹H NMR) with the addition of sub-stoichiometric quantities of *N*-methyl hydroxylamine hydrochloride **97·HCl**, 45 minutes after mixing of the starting materials in sieve-dried DMSO-d₆ (Figure 104).

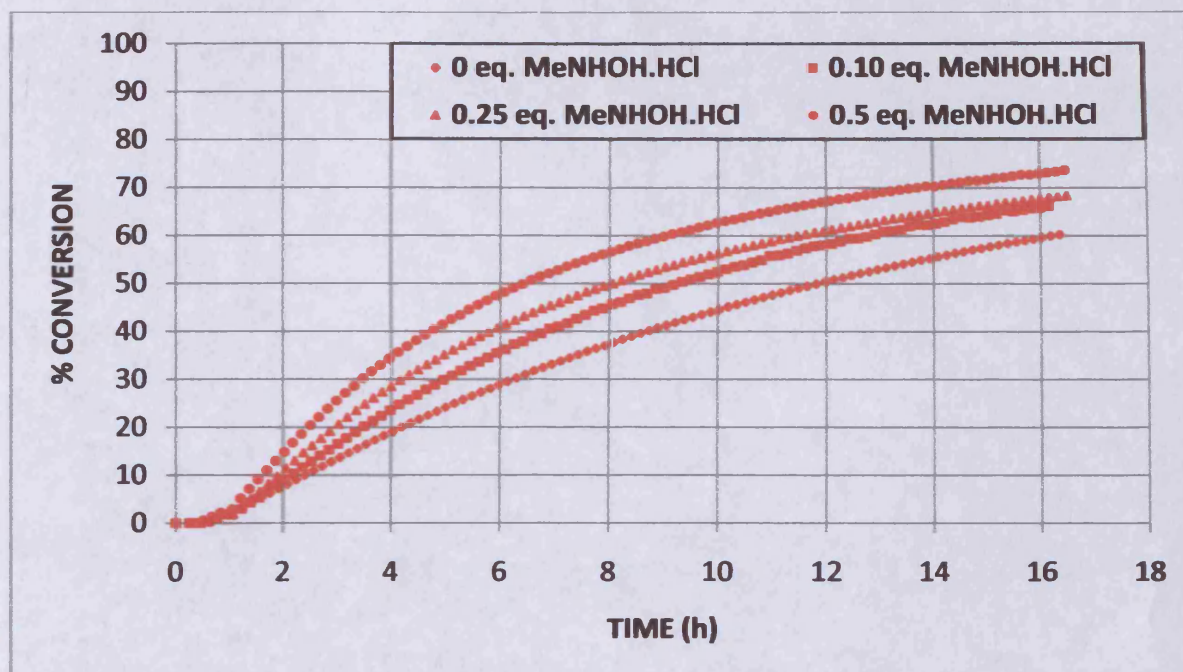


Figure 104: Rate enhancement in the presence of MeNHOH.HCl 97·HCl (reaction at 305 K)

The hydrolysis of the iminium ions **210** and **211** was therefore regarded as a first order process; the rate enhancing effect of additional water possibly a result of changes in the polarity/dielectric constant of the reaction medium as increasing amounts of water were doped into the DMSO.

The optimal outcome would clearly have been to repeat the modelling exercise with the data from the experiments conducted at several different temperatures, from which the respective rate constants could have been extracted. The values would then have been fed back into the Arrhenius equation, and thermodynamic parameters for the formation of product, and the consumption of the starting material and the two intermediates could then have been obtained. Analysing the reaction at a deeper level may have yielded quantitative information as to the rate of decomposition of reagent, and yielded more evidence in support of the proposed catalytic role of *N*-methyl hydroxylamine hydrochloride **97·HCl**, the proposed product of reagent degradation.

It was perceived that the numerical values obtained *via* the kinetic modelling treatment could have been regarded with a much higher degree of confidence than those obtained from either integrated rate laws (and these applied only to the two intermediates in any case), or from the method of initial rates (which while giving us information regarding the reaction as a whole, was deemed too crude to have real quantitative merit).

However, as with many other aspects of the work to date, time limitations were ultimately the deciding factor. Whilst a reasonable attempt was made to fit the working kinetic model to other data sets (the variations in temperature, water content and stoichiometry), this did not prove to be a trivial exercise. It was not thought that this apparent breakdown of the model invalidated the successful fitting; rather that the analytical process required in order to tweak the model successfully in each case exceeded the time available during the placement period.

At the end of this phase of the project, we lacked reliable numerical values for the thermodynamic parameters for all the experiments that were carried out.

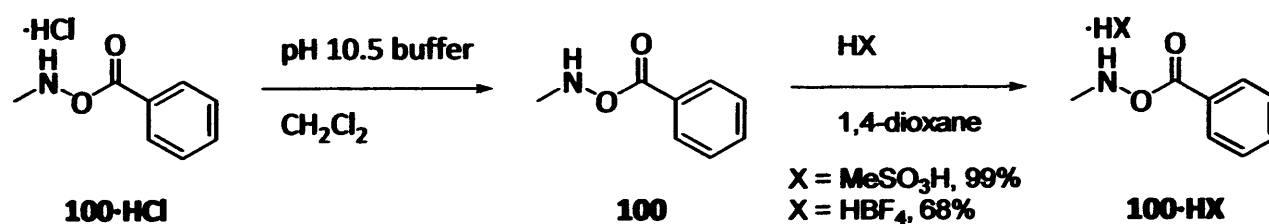
In spite of the admittedly incomplete result of the kinetic modelling work, the overall result, taking into account all of the experimental and analytical results, was that the fundamentals of the α -oxygenation reaction were explored in detail. Information was acquired which either confirmed our proposed mechanism, or enabled modifications to be made to the model. The effect of several variables was probed; namely temperature, water content, reaction stoichiometry and catalysis. Kinetic modelling software gave information regarding reaction order within the key step of the reaction, and also provided further mechanistic detail.

Chapter 7: Concluding NMR Experiments and Reaction Optimisation

7.1 Final ^1NMR reaction monitoring experiments

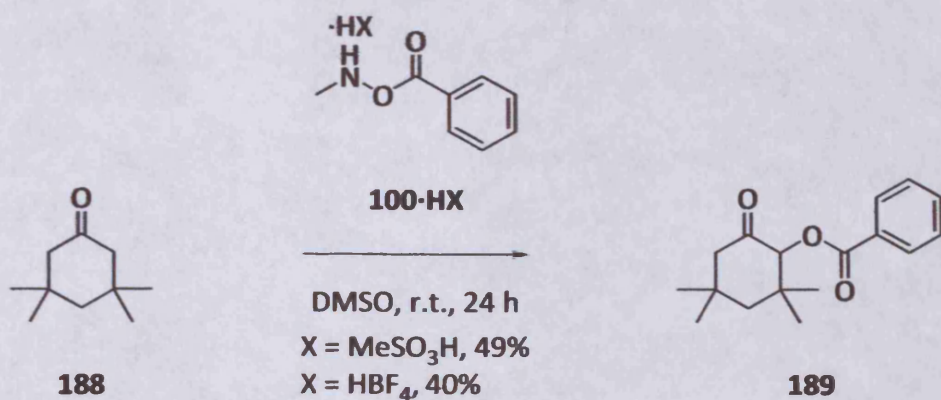
Whilst much information had been gained by the *in situ* monitoring work up this point, we decided that one variable which had been overlooked was the structure of the co-acid, HX within our family of α -oxygenating reagents. Whilst we did not necessarily expect dramatic changes to occur on changing this species, it was thought that briefly pursuing this would make a fitting counterpoint to the mechanistic study. We also hoped to isolate one or more of the intermediates from the reaction by precipitation of their iminium salts; characterisation of these species had the potential to provide further evidence in support of the findings from the preceding mechanistic work.

A sample of the standard reagent **100-HCl** was converted to its free base **100** by stirring for 1 hour in a mixture of aqueous pH 10.5 buffer and dichloromethane. After separation of the layers, removal of the solvent gave the free base as a yellow oil, which was then transformed into new reagents **100-MeSO₃H** and **100-HBF₄** by the addition of 5 equivalents of the corresponding acid to stirring solutions of the free base **100** in 1,4-dioxane (Scheme 74). In both cases, the new salts were collected as white solids after precipitation from solution.



Scheme 75

The reactivity of these new species with 3,3,5,5-tetramethylcyclohexanone **188** was tested under standard laboratory conditions; we were puzzled and disappointed at the comparatively low yields that were obtained (Scheme 75).



Scheme 75

To try and explain this dramatic fall in yield, the reactions of both salts **100-MeSO₃H** and **100-HBF₄** with the ketone **188** were repeated under ¹H NMR monitoring conditions at 298 K (Figures 105 and 106).

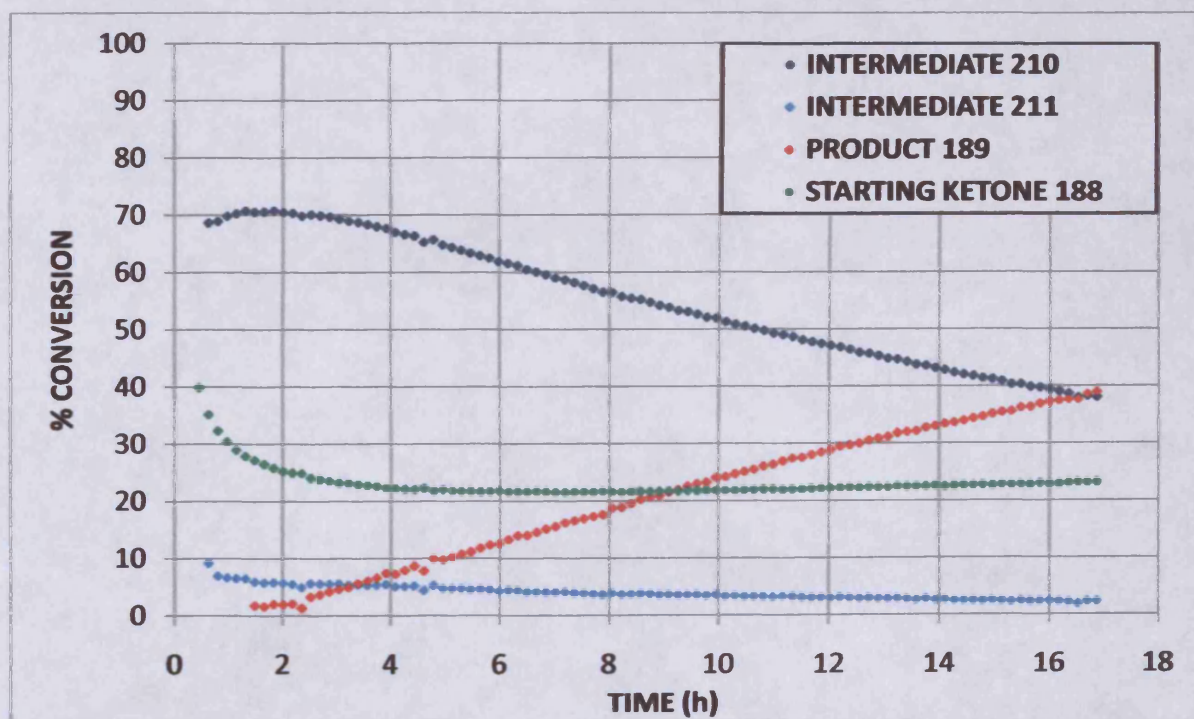


Figure 105: Reaction monitoring at 298 K (reagent 100-MeSO₃H)

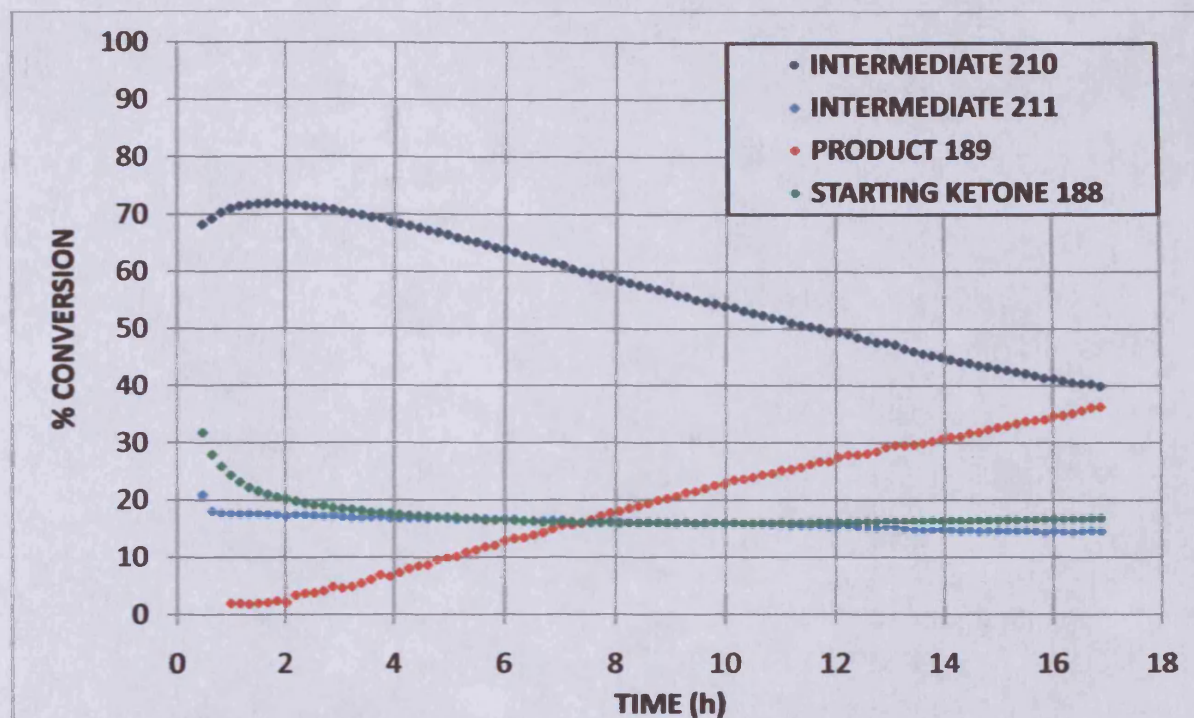


Figure 106: Reaction monitoring at 298 K (reagent 100-HBF₄)

On initial examination, these results were consistent with those from the laboratory. A significant quantity of starting material remained in the reaction mixtures after a lengthy reaction time (t.l.c. on the bench reaction mixtures had also indicated this). We speculated that decomposition of the reagents **100-MeSO₃H** and **100-HBF₄** may have been a greater contributory factor than for the **100-HCl** species, although our postulated mechanism for the decay of the latter implicated chloride ion. A further anomaly was that under the ¹H NMR monitoring conditions, the concentration of Intermediates **210** and **211** was still increasing towards the end of the analysis time. We expected that aqueous work-up should have accelerated the hydrolysis of the iminium ions **210** and **211**; however the isolated yields did not rise significantly beyond the conversions as plotted from the ¹H NMR data.

Clearly, this series of experiments had raised new questions regarding the transformation in general. However, with project time running short, it was reluctantly decided not to pursue this further – at this stage we prioritised experiments which we hoped would extend and optimise the methodology.

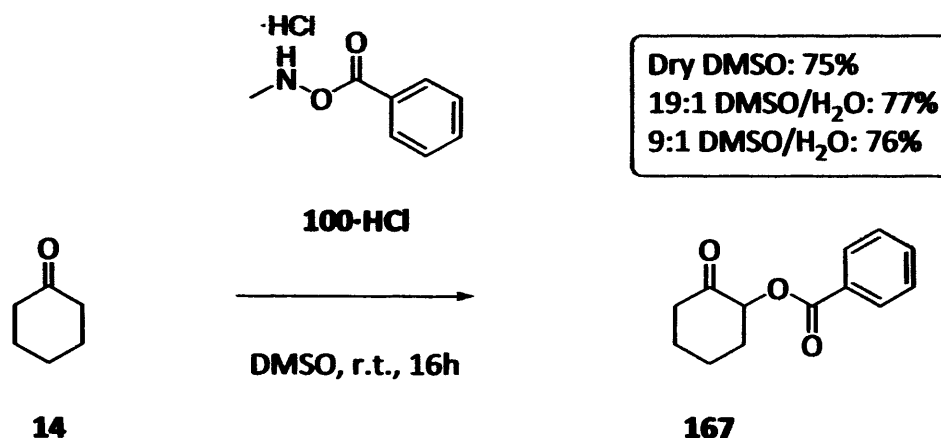
7.2 Reaction optimisation

During the mechanistic study, we learned that (at least for the substrates and under the reaction conditions that were thoroughly examined) the transformation proceeded comparatively swiftly through the early steps of the reaction sequence, followed by a rather slower hydrolysis of the major intermediates, the iminium ions **210** and **211**. Of the variables that were explored, the presence of additional water in the reaction mixtures led to the most dramatic increase in rate of conversion to product.

The key questions to be addressed in the final stages of the project were thought to be whether the effect of added water could be used to accelerate the general transformation across a range of ketone substrates. Of lesser significance, but considered important in terms of attaining a complete understanding, were the effects of concentration and structure of α -oxygenating species.

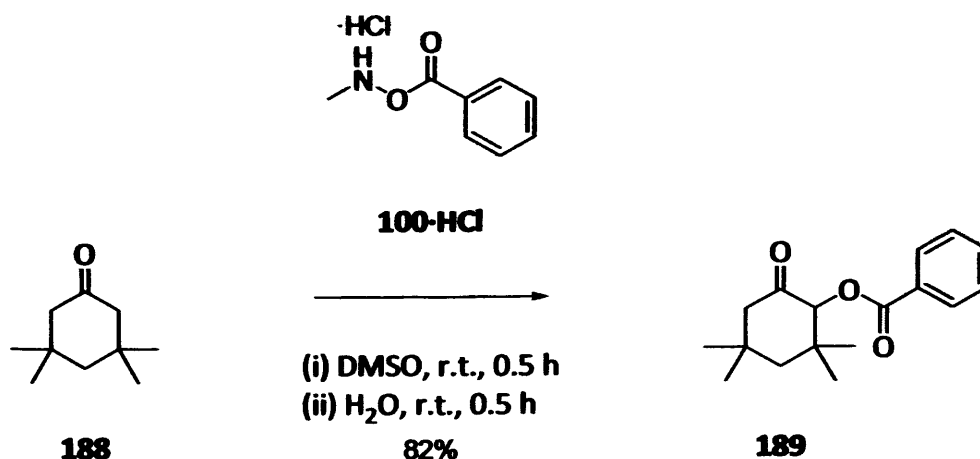
7.2.1 Additional water

It was speculated whether the presence of additional water from the start of the reaction would have any bearing on the final outcome in terms of the isolated yields. Using cyclohexanone **14** as the ketone substrate, and the standard reagent *N*-methyl-*O*-benzoyl hydroxylamine hydrochloride **100-HCl**, the reaction was conducted over 16 hours with mixed water/DMSO solvent systems (Scheme 76). It was shown to our satisfaction that additional water did not affect the final outcome of the reactions in terms of product yields. These were all consistent with the value of 80% which the group had previously reported.⁵⁰ This series of results seemed to bear out the conclusions from the mechanistic work, where the presence of water did not hinder the initial nucleophilic addition to any appreciable extent. We believed that acceleration of iminium hydrolysis with added water accelerated conversion to product, and that this process was dominant within the reaction sequence relative to the effect upon the initial condensation step.



Scheme 76

Given the conclusions from the reaction monitoring work, it seemed logical to attempt to shorten the procedure in the laboratory by means of added water. We therefore developed a new reaction protocol, in which the ketone and hydroxylamine species were stirred together for 30 minutes in dry (to all intents and purposes) DMSO; after this time had elapsed excess water (a volume equal to the original amount of DMSO, thereby giving a 1:1 DMSO/H₂O solvent system) was added and the reaction mixture stirred for a further 30 minutes prior to work-up and purification by chromatography. Scheme 77 shows the result when this new procedure was applied to 3,3,5,5-tetramethylcyclohexanone **188**.




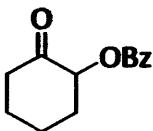
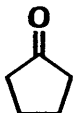
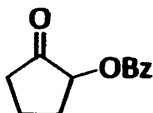
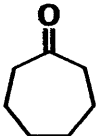
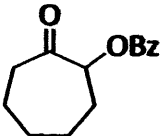
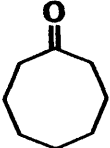
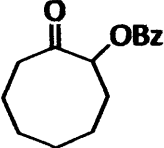
Scheme 77

Effectively the reaction time for this substrate had been shortened more than 10 fold, with a slight decrease in product yield (originally 86%), which was low enough to be attributed solely to experimental error.

The new conditions were found to be generally applicable to a range of cyclic ketones (Table 7, previous reported yields in parenthesis).⁵⁰

In terms of product yields, the results were mixed. Cycloheptanone **223** (Entry 3) and tetrahydro-4*H*-pyran-4-one **227** (Entry 5) gave the poorest performances when treated under the new conditions, while 1,4-cyclohexanedione-mono-ethylene ketal **229** (Entry 6) gave a dramatic increase in product yield. Outside of these extreme deviations from prior results, the remaining ketone substrates generally gave product yields either in excess or only slightly less than previously reported in the literature, where the reaction was conducted for at least 12 hours.

In the early days, the α -oxygenation of ketones was reported as often being substrate-specific in terms of the reaction time and temperature required to furnish the product in optimal yield. With this series of experiments, we did not therefore expect to observe dramatic increases in yield over the much shorter reaction timeframe. However, we did infer that the addition of excess water could provide a medium in which the reaction time was shortened and where the overall results were still acceptable by comparison with the original protocol.

Entry	Substrate	Product	Yield (%)
1	 14	 167	68 (80)
2	 221	 222	75 (73)
3	 223	 224	42 (69)
4	 225	 226	59 (n/a)


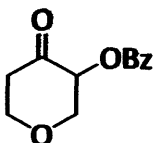
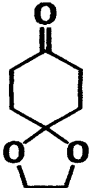
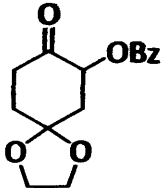
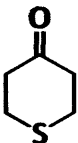
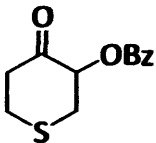
Entry	Substrate	Product	Yield (%)
5	 227	 228	56 (79)
6	 229	 230	90 (70)
7	 231	 232	65 (75)

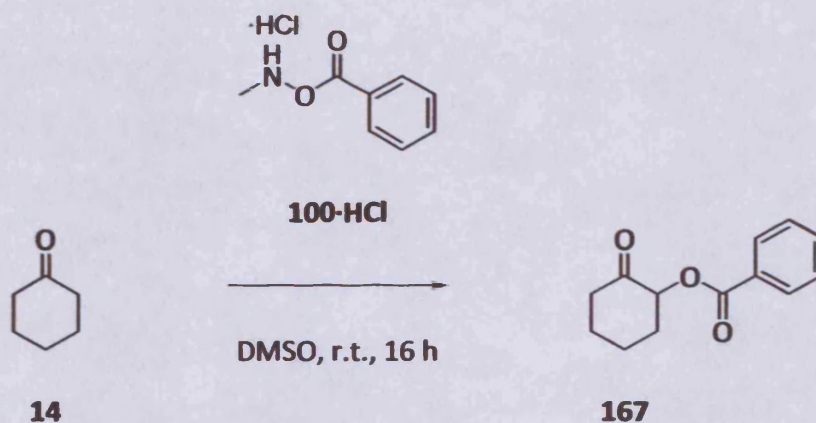
Table 7: α -Oxygenation of cyclic ketones under new conditions -

(i) ketone + 100-HCl, DMSO, r.t., 0.5 h; (ii) H₂O, r.t., 0.5 h

(previous yields reported by Tomkinson *et al* given in brackets)

7.2.2 Concentration

With cyclohexanone **14** as the ketone substrate, and *N*-methyl-*O*-benzoyl hydroxylamine hydrochloride **100-HCl** as α -oxygenating species in a 1:1 ratio, the effect of concentration was probed (Scheme 78).



Scheme 78

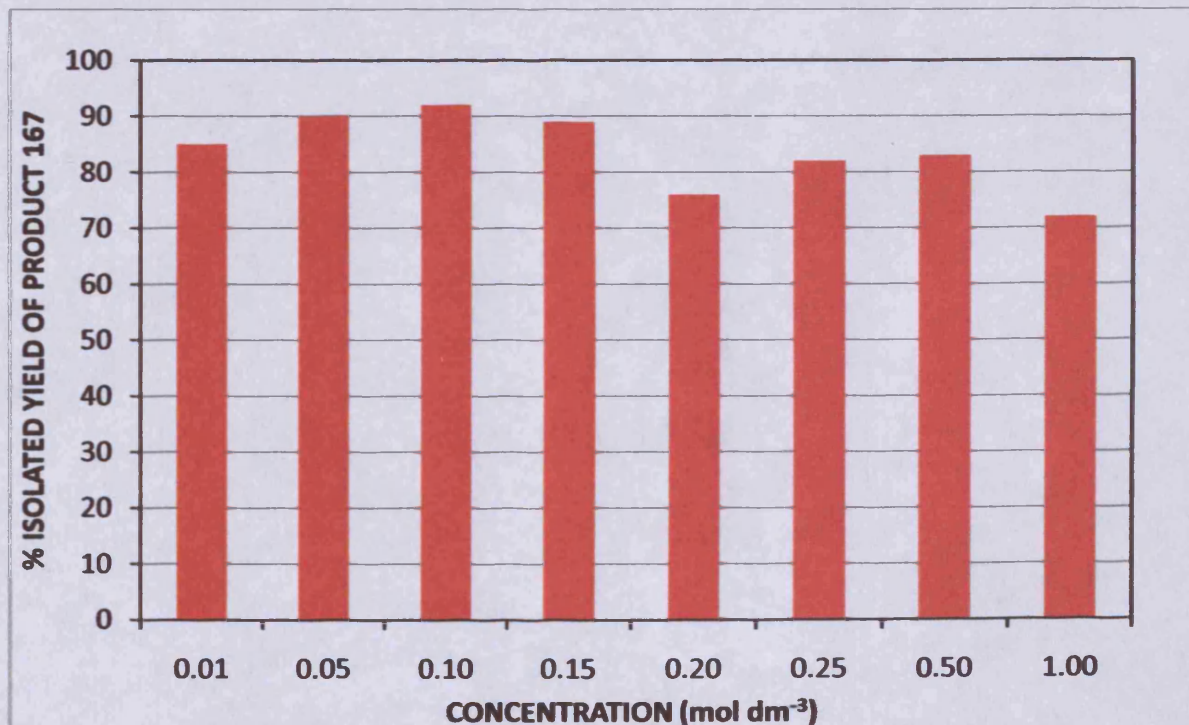


Figure 107: Product yield at variable reagent concentration

Reactions were conducted in DMSO (dry) at 30 °C for 16 hours in order to ensure maximum conversion to product for each experiment, following aqueous work-up and column chromatography (Figure 107).

The product yields fell within a range between 72% and 92% across the concentration range studied. While this would seem to imply a degree of sensitivity to concentration, we concluded that some of the variations must be accounted for in terms of general experimental error. A trend for declining yield with increasing concentration could be argued; however this effect became important only when concentration was increased tenfold (from 0.1 to 1.0 M), and perhaps could be ascribed to reagent decay.

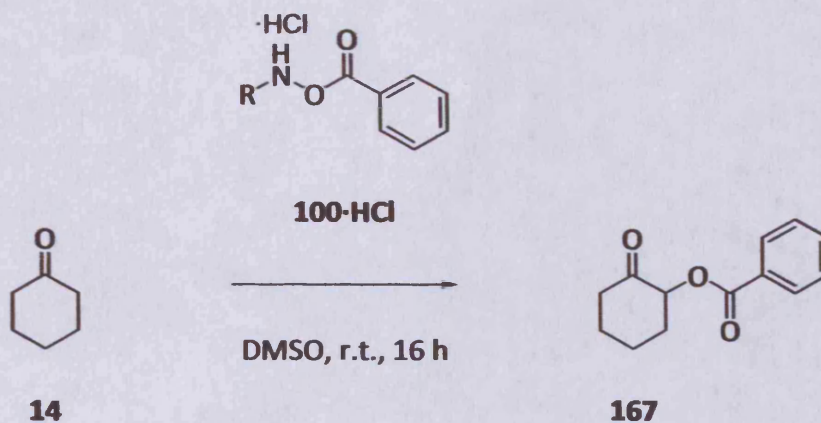
Further study of the heightened significance of reagent decomposition or possible side-reactions may have furnished a definitive answer to this question, particularly had we been able to repeat these reactions with ^1H NMR reaction monitoring as before.

We concluded that the transformation appeared to be tolerant over a fairly wide range of concentration values, giving fairly consistent and good yields for the substrates that were tested.

7.2.3 Structure of reagent

Over the course of the project, we had prepared a variety of α -oxygenating species, all theoretically capable of performing the transformation. The original purpose had been to test whether the structure of the reagent (particularly the nature of the *N*-substituent) had any bearing on the reaction outcome. This question had been thoroughly asked of the species as their free bases; nevertheless we wished to test their efficacy as their hydrochloride salts and allow a better evaluation of these compounds.

Each of the reactions was conducted with a stoichiometric ratio of cyclohexanone **14** and the requisite α -oxygenating species, at 0.1 M with respect to both starting materials, by stirring in DMSO at 30 °C for 16 hours. The crude reaction mixtures were subjected to standard work-up and chromatography to give the respective products in the yields described.



Scheme 79

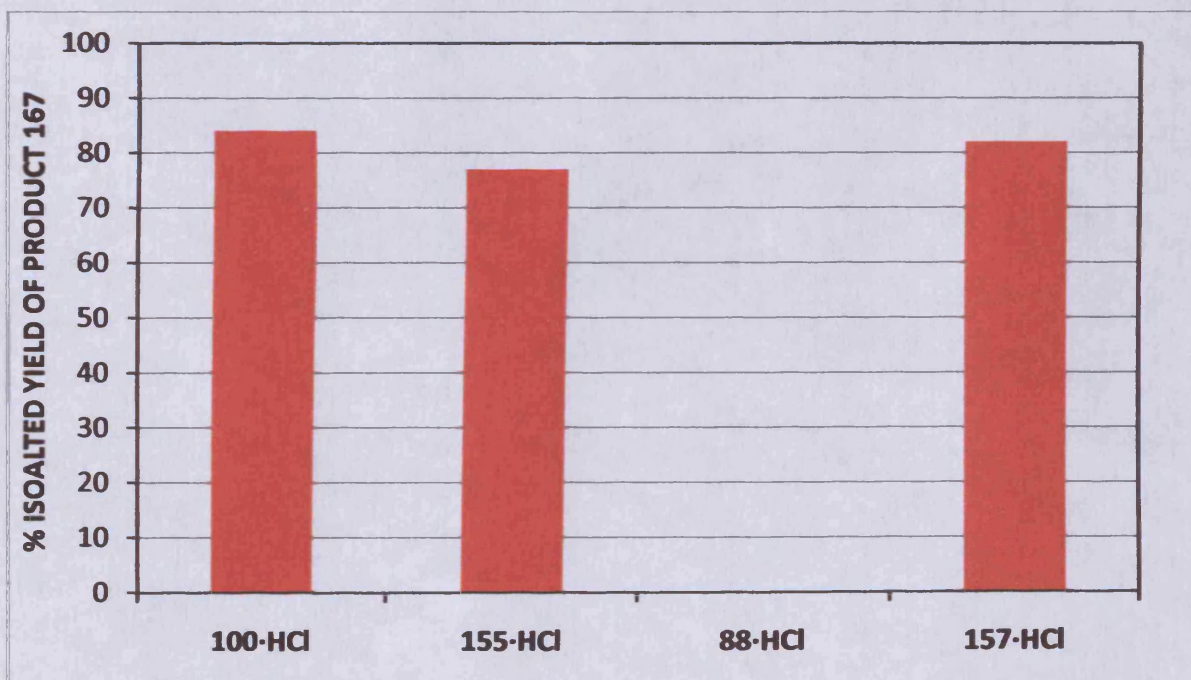


Figure 108: Product yield with various *N*-alkyl substituents

Figure 108 shows that the nature of the alkyl group on the nitrogen had little bearing on the reaction, with the exception of the sterically encumbered *N*-*t*-butyl species **88-HCl**, for which no product was detected; this was consistent with earlier reported observations (Figure 109).⁵⁰

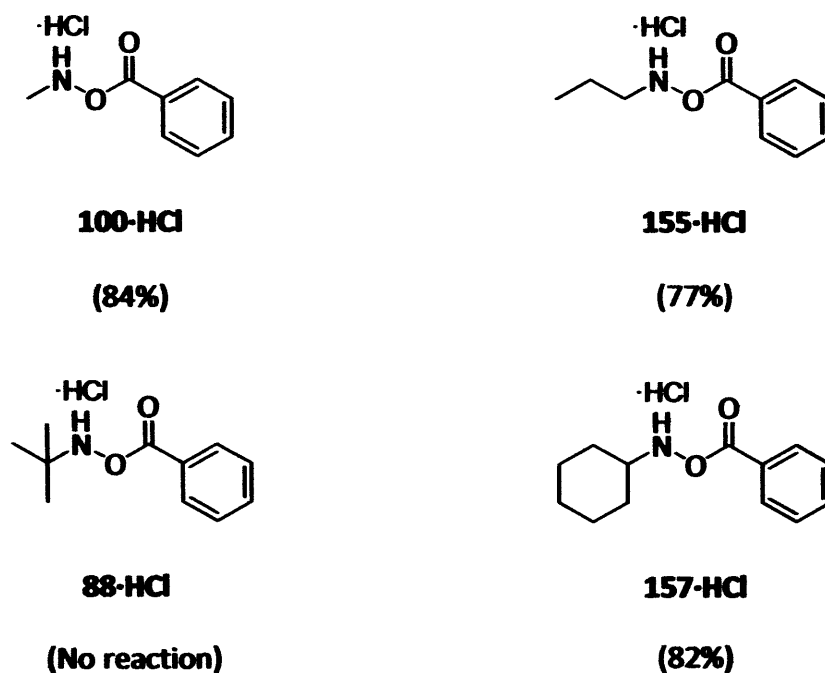
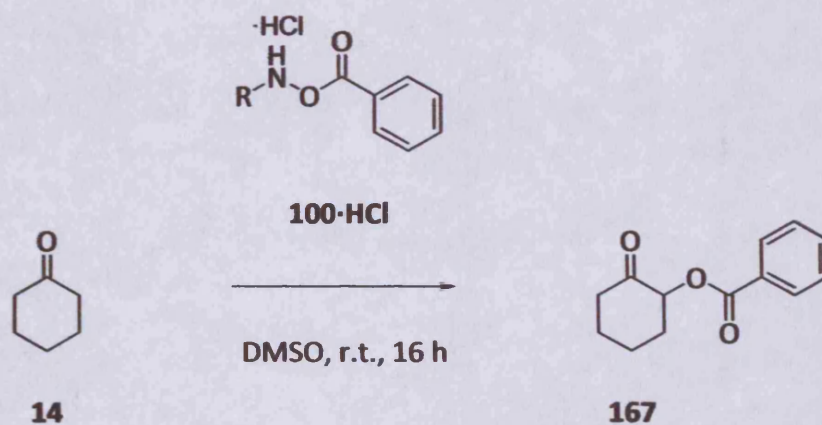


Figure 109

Introducing *N*-benzyl groups, a heteroatom and other aromatic groups also meant that the reaction outcome was virtually unchanged with respect to the standard *N*-methyl reagent **100-HCl** (Scheme 80, Figures 110 and 111).



Scheme 80

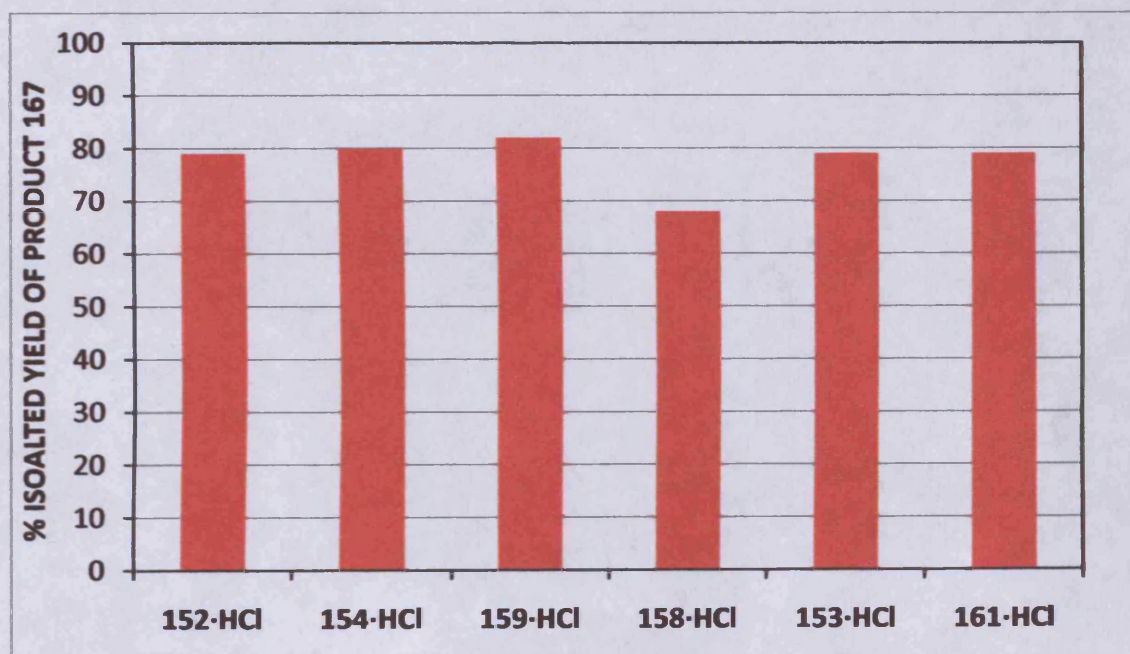


Figure 110: Product yield with further *N*-substituents

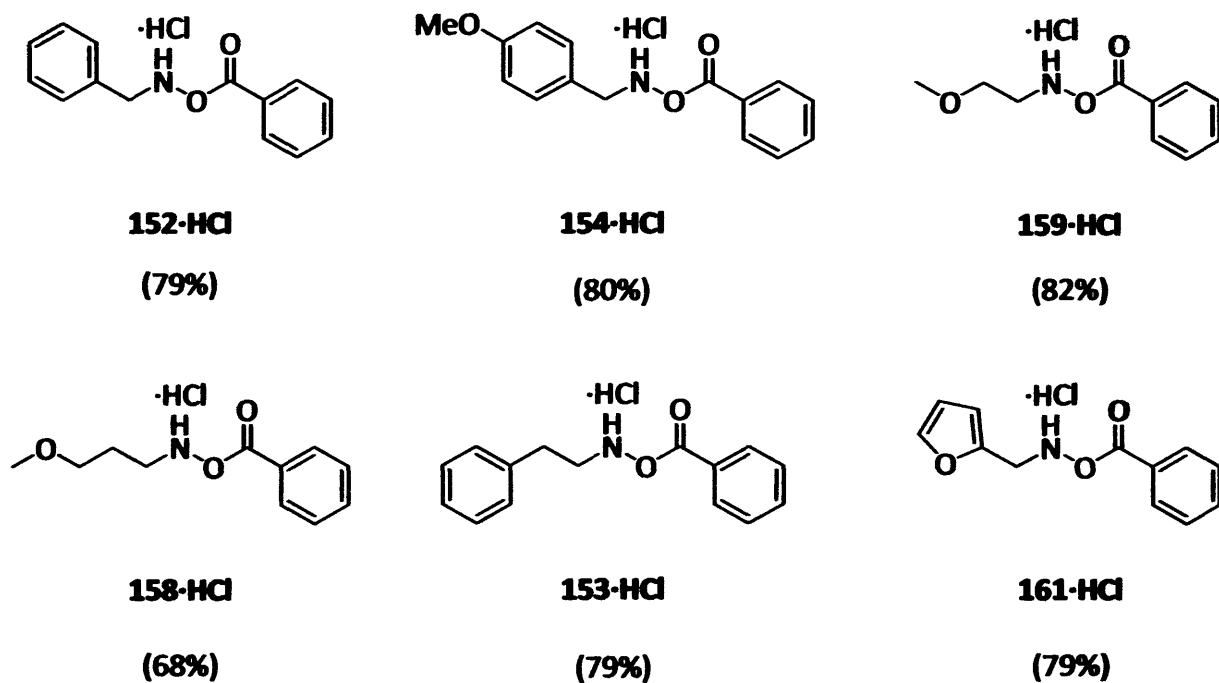
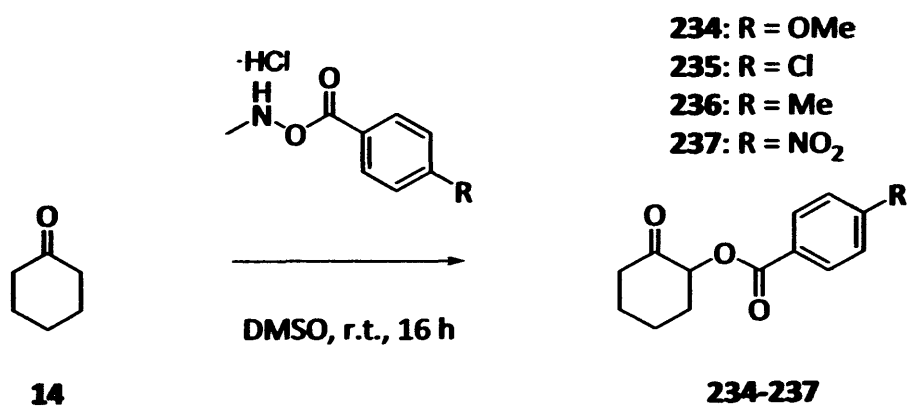


Figure 111

Finally for this investigation, the possible effect of *p*-groups on the phenyl ring of the *O*-benzoyl group was probed (Scheme 81, Figures 112 and 113).



Scheme 81

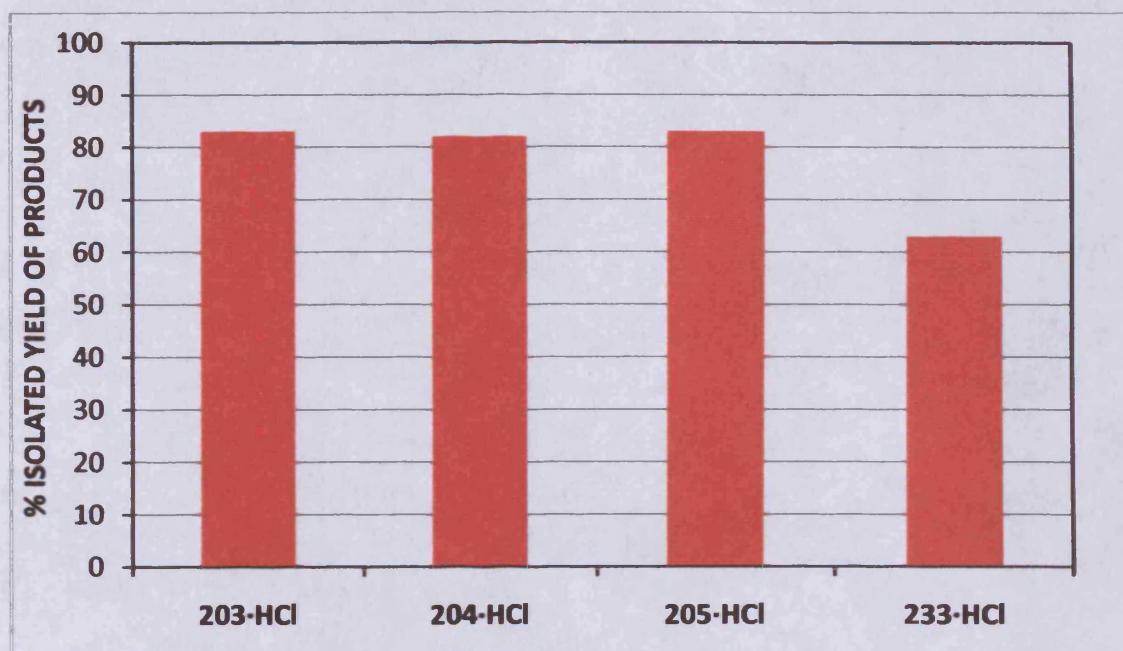
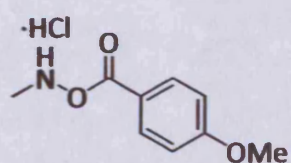
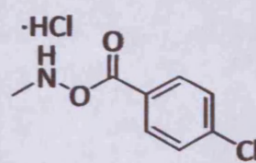


Figure 112: Product yield with *p*-substituents



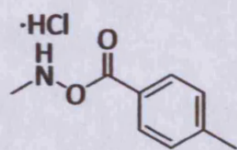
203-HCl

(83%)



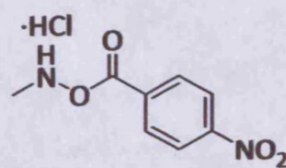
204-HCl

(82%)



205-HCl

(82%)

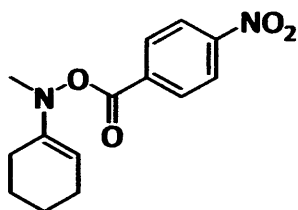


233-HCl

(63%)

Figure 113

Aside from an obvious drop in yield when the nitro group was present (an effect we attributed to the electron-withdrawing nature of this substituent), the yields showed a remarkable uniformity across the series. For the reaction with the nitro-bearing aromatic ring, we speculated that the enamine 238 may have been less disposed to rearrange due to the electron-withdrawing NO₂ group (Figure 114)



238

Figure 114

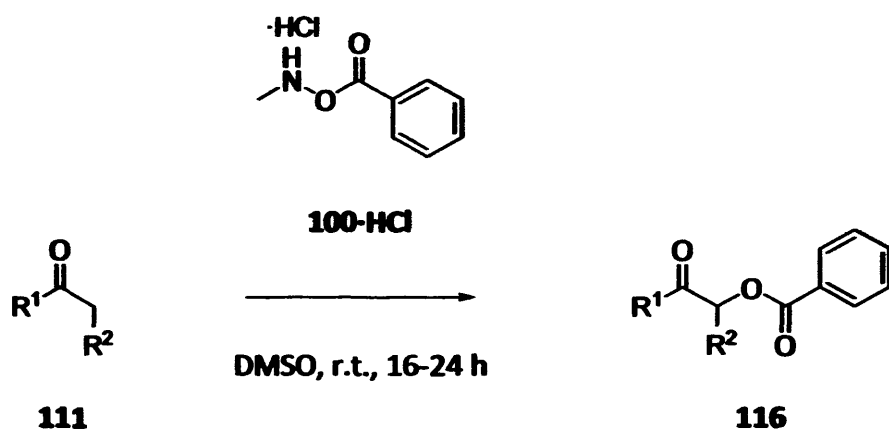
In summary, we had demonstrated that the transformation was generally applicable over several concentration profiles and that the structure of the reagent did not appreciably alter the course of the reaction.

The most encouraging aspect of these experiments was that the reaction, which had previously been carried out over a timeframe of up to 24 hours, could be brought to completion much sooner by the simple expedient of the addition of water. Although this finding was not universally true of all ketone starting materials, in general this represented a much more efficient protocol than originally described.

Chapter 8: Conclusion

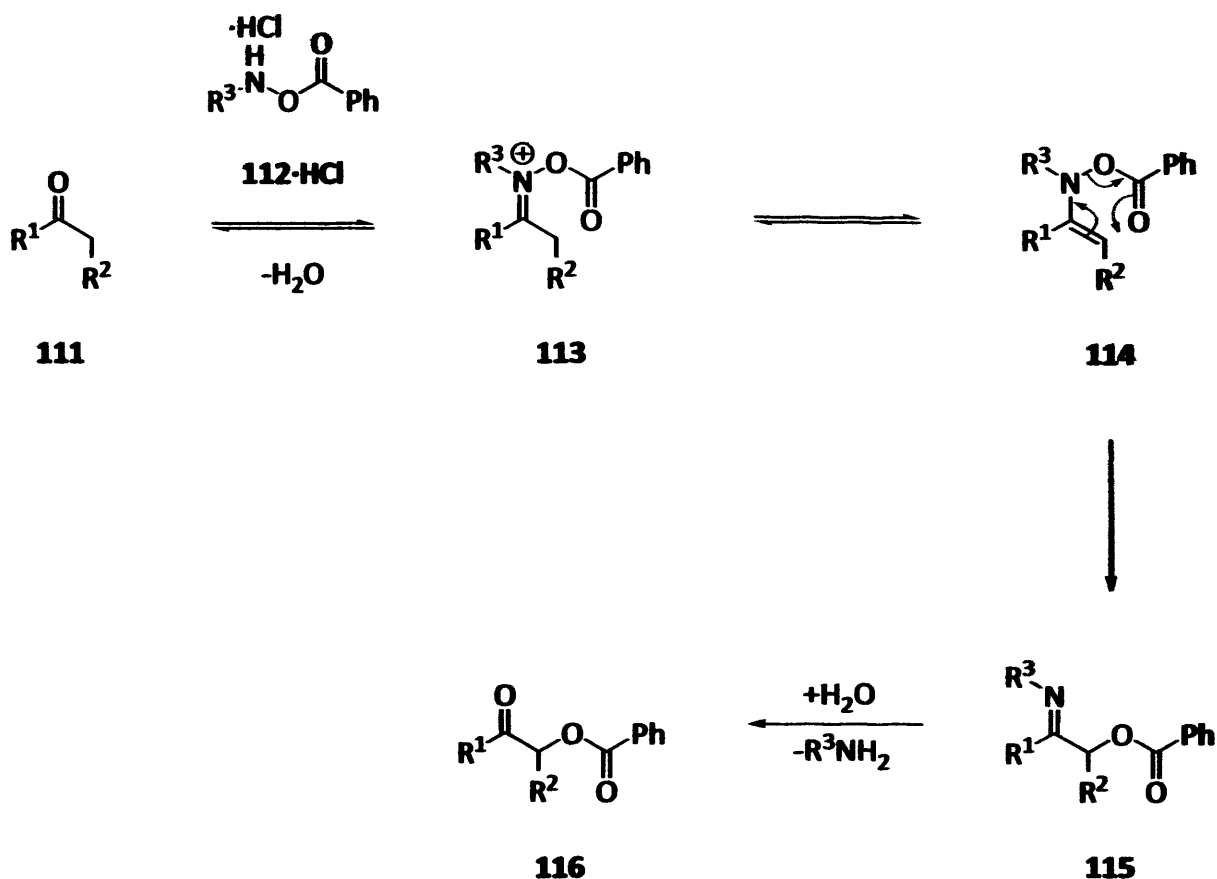
From the outset, the work described herein was to have a primarily investigative approach rather than be purely driven by synthetic targets. For this reason, it was almost inevitable that we would depart tangentially from the original aims of the project.

The established transformation was the general α -oxygenation of carbonyl compounds in good to excellent yields by reaction with hydroxylamine species such as **100-HCl** (Scheme 82).



Scheme 82

Mechanistically, we believed that the process proceeded *via* condensation of the reagents to give an iminium ion **113**, followed by loss of an α -hydrogen to give the enamine species **114**. Based largely on a wealth of literature precedent in favour of this pathway, our hypothesis was that the enamine **114** underwent a concerted, pericyclic rearrangement to give an α -benzoyloxy imine **115**, which was subsequently hydrolysed under the aqueous acidic reaction conditions to give the observed product **116** (Scheme 33).

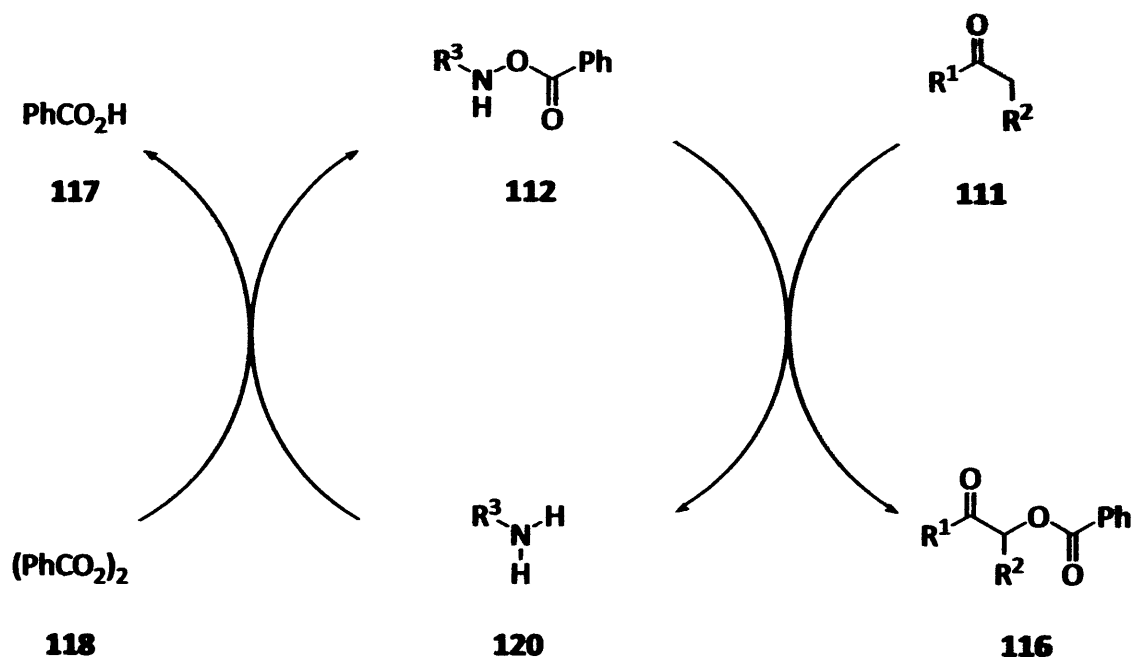


Scheme 33

We believed that the transformation in its then current form constituted a powerful piece of methodology for the following reasons:

- Clean reaction mixtures and generally good product yields
- A procedure which was general to aldehyde and ketone functionalities
- Toleration of a wide variety of functional groups, including hydrolytically sensitive esters and ketals
- The reaction worked well for cyclic or acyclic carbonyl compounds
- Toleration of the presence of moisture and air in the reaction mixture
- Proceeded without the need for potentially toxic metal-based catalysts/reagents

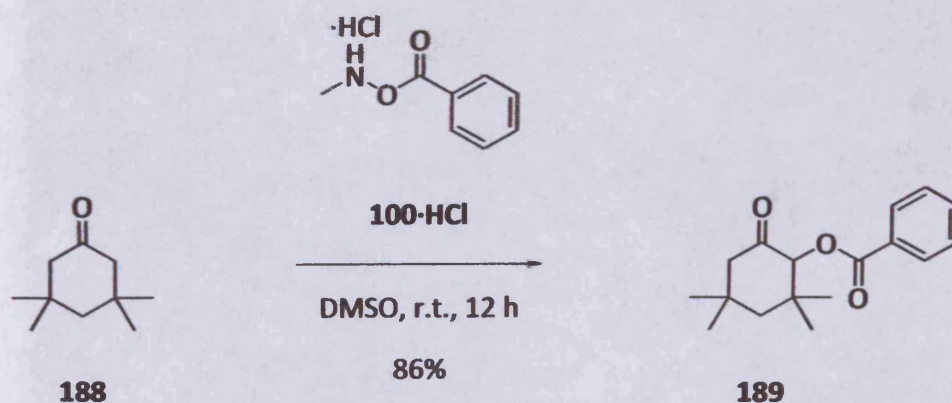
We commenced with the goal of extending a previously developed methodology for the α -oxygenation of carbonyl compounds into a fully catalytic process with respect to the parent amine **120** (Scheme 36).



Scheme 36

Unfortunately, our efforts in this regard (in conjunction with other group work) did not meet with success; rather than spend an undue amount of project time in what we reasoned may have been a fruitless endeavour, we decided to undertake a mechanistic investigation into the course of the reaction.

To that end, we deployed all the analytical techniques which were available, both in our home laboratory and in an industrial setting. Particularly with respect to NMR, we were able to develop and refine a method which eventually enabled us to quantify, with reasonable certainty, the consumption and formation of the major species within a reaction comprising representative starting materials (Scheme 58). A typical reaction profile obtained by these means is shown in Figure 45.



Scheme 58

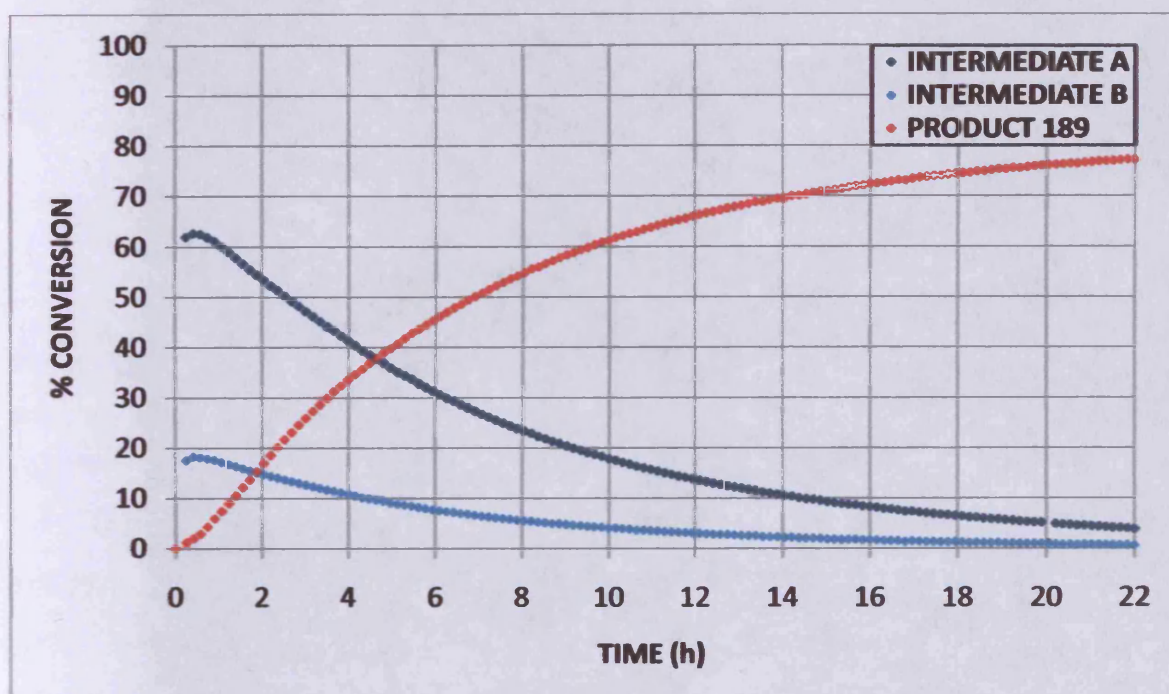
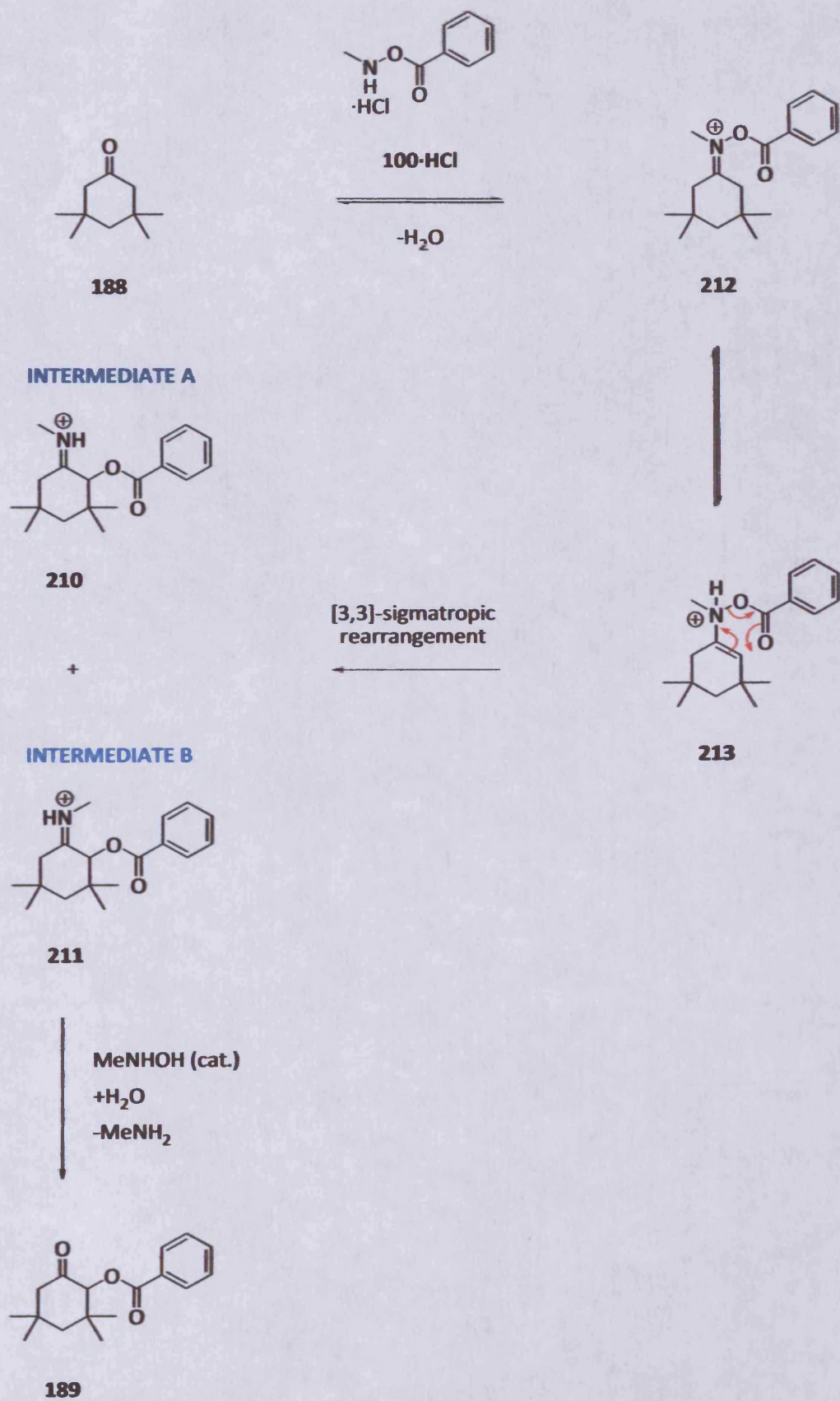
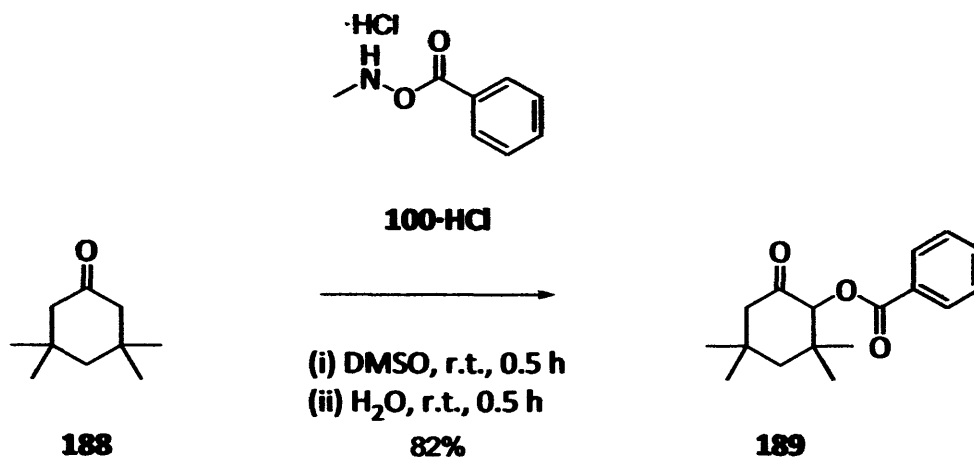


Figure 45: Products and intermediates at 310 K

Using this data, we explored the kinetic and thermodynamic parameters underlying the reaction, whilst acknowledging the limitations and approximations of each technique. The information obtained *via* NMR and a variety of other techniques led us to hypothesise a modified reaction mechanism (involving protonated iminium species **210** and **211**) which rationalised the findings from this study (Scheme 82).



The findings from the mechanistic study enabled the development of a modified protocol for the α -oxygenation procedure; the chief advantage of which was the drastic shortening of the reaction time with (in several cases) little or no drop in product yield relative to the earlier reported work (Scheme 77).



Scheme 77

Despite the fact that the original aims were not met, we were able to make considerable progress in our understanding of the reaction, and apply this knowledge in optimising the methodology.

We did not fully answer all the questions which arose during the project. There remain a good number of further experiments – especially within the mechanistic framework – which may yet serve to unravel this intriguing transformation. Perhaps more pessimistically, there were a good deal of reactions which did not drive the project forward in its principal aims; however such a statement is harsh and made very much in hindsight.

Our successes in this project derived from the fact that we undertook a rigorous, scientific approach to the discipline of Synthetic Organic Chemistry, and were ultimately rewarded with quantifiable data, an enhanced understanding of our chemistry, and perhaps most importantly the invaluable experience that arose from carrying out this work.

Chapter 9: Experimental

9.1 General

Reagents were obtained from Aldrich, Lancaster, Apollo and Fluka chemical suppliers. Anhydrous DMSO- d_6 was purchased from Aldrich. Solvents and reagents were purified according to the procedures of Perrin, Armarego and Perrin.⁸² Dichloromethane was dried by refluxing over, and distilling from calcium hydride. Ethanol was dried by refluxing over magnesium, followed by distillation. Toluene was dried over sodium wire for twenty-four hours prior to use. Petroleum ether refers to petroleum ether fraction 40–60 °C.

All reactions using air/moisture sensitive reagents were performed in oven-dried or flame-dried apparatus, under a nitrogen atmosphere. Multiple reactions were performed using a Radley's carousel, which consists of twelve test tubes with suba-seals and nitrogen inlets, a stirrer plate and a bath for heating. All reactions were followed and monitored by TLC, ^1H NMR, ^{13}C NMR and mass spectrometry as appropriate.

TLC analysis refers to analytical thin layer chromatography, using aluminium-backed plates coated with Merck Kieselgel 60 GF₂₅₄. Product spots were viewed either by the quenching of UV fluorescence, or by staining with a solution of 2% aqueous potassium permanganate. Chromatography refers to flash column chromatography using head pressure by means of compressed air according to the procedure of Still,⁸³ using Merck Kieselgel 60 H silica or Matrix silica 60.

Melting points were recorded using a Kofler Heated Stage Micro Melting Point Apparatus and are uncorrected.

Infra-red spectra were recorded in the range 4000–600 cm^{-1} using a Perkin-Elmer 1600 series FTIR instrument either as a thin film, a nujol mull or dissolved in chloroform between sodium chloride plates. All absorptions are quoted in wave numbers (cm^{-1}).

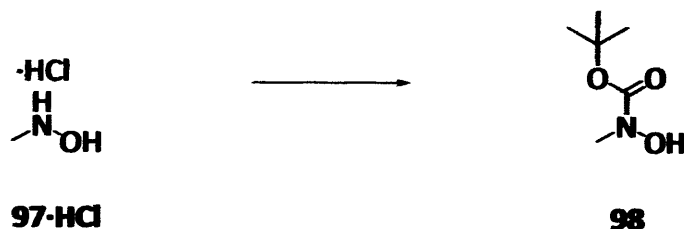
^1H NMR spectra (δ_{H}) were recorded using an Avance Bruker DPX 400 instrument (400 MHz) or an Avance Bruker DPX 500 (500MHz), with ^{13}C NMR spectra (δ_{C}) recorded at 100 MHz or 125 MHz respectively. Chemical shifts (δ_{H} and δ_{C}) were recorded in parts per million (ppm) from tetramethylsilane (or chloroform) and are corrected to 0.00 (TMS) and 7.27 (CHCl_3) for ^1H NMR and 77.30 (CHCl_3), centre line, for ^{13}C NMR. The abbreviations s, d, t, q, m, and br, denote singlet, doublet, triplet, quartet, multiplet and broadened resonances, respectively; all coupling constants were recorded in hertz (Hz).

Low resolution mass spectrometric data was determined using a Fisons VG Platform II Quadrupole instrument using atmospheric pressure chemical ionisation (APCI) unless otherwise stated. APCI refers to atmospheric pressure chemical ionisation, EI refers to electron ionisation and ES refers to electrospray. High resolution mass-spectrometric data was obtained courtesy of the EPSRC Mass Spectrometry Service at the University of Wales, Swansea, UK, using the ionisation methods specified. Calculated accurate masses are of the parent ion (exclusive of an electron, mass = 0.00055 Da).

9.2 Preparation of α -oxygenating reagents

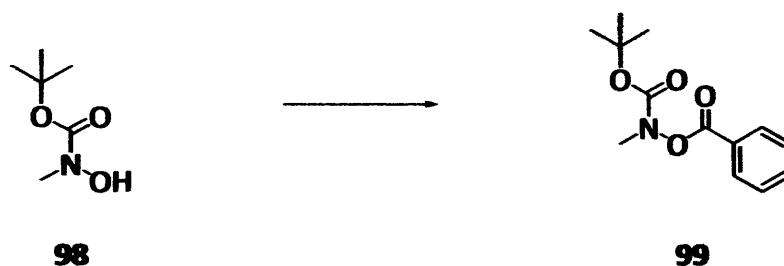
9.2.1 3-step method to reagent 100-HCl

N-Methyl-*N*-Boc hydroxylamine **98**²⁴



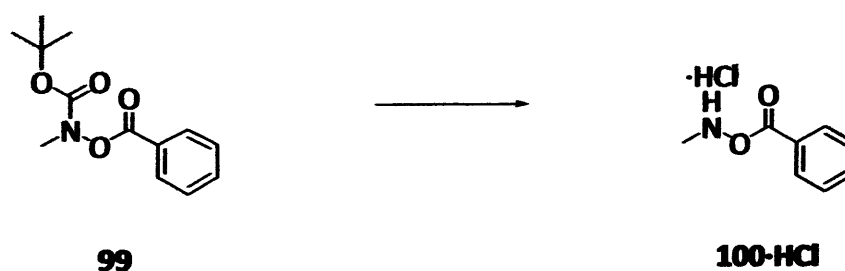
A solution of *N*-methylhydroxylamine hydrochloride (35.0 g, 0.42 mol) in a 1:1 mixture of THF/H₂O (200 ml) was cooled to 0 °C and potassium carbonate (28.2 g, 0.21 mol) was added portionwise. Following careful addition of di-*tert* butyl dicarbonate (100.0 g, 0.46 mol) the reaction was allowed to warm to room temperature and stirred for 24 h. The reaction mixture was evaporated under reduced pressure, extracted with ethyl acetate (100 ml), washed with water (3 x 50 ml), dried (MgSO₄), filtered and evaporated *in vacuo* to give the crude product as a salmon-pink oil. Purification by short-path distillation (62–64 °C, <1 mbar) afforded the *title compound* **98** (39.7 g, 64%) as a colourless oil; IR (thin film): 3262, 1704 cm⁻¹; ¹H NMR (400 MHz, CDCl₃): δ 8.00 (br, s, 1H, NOH), 3.14 (s, 3H, NCH₃), 1.45 (s, 9H, OC(CH₃)₃); ¹³C NMR (100 MHz, CDCl₃) δ 157.7, 81.7, 38.9, 28.3 ppm; MS (APCI) *m/z* 148 (M+H)⁺; HRMS (APCI) calculated for C₆H₁₄NO₃ 148.0973 [M+H]⁺, found 148.0974.

***N*-Methyl-*N*-Boc-*O*-benzoyl hydroxylamine 99⁸⁵**



A solution of *N*-Boc-*N*-methyl hydroxylamine **98** (4.05 g, 30 mmol), dimethyl amino pyridine (367 mg, 10 mol%) and triethylamine (4.16 ml, 30 mmol) in dichloromethane (70 ml) was cooled to 0 °C prior to slow addition of benzoyl chloride (3.5 ml, 30 mmol). The reaction mixture was allowed to warm to room temperature and stirred for 16 h. Evaporation under reduced pressure gave a yellow solid, which was triturated with petroleum ether 40–60 °C, filtered, dissolved in dichloromethane (100 ml), washed with saturated sodium hydrogen carbonate solution (2 x 30 ml), water (30 ml) and brine (30 ml). The organic layers were combined, dried over MgSO₄ and concentrated to give the *title compound* **99** (6.7 g, 89%) as a lime green oil without further purification; IR (thin film): 1763, 1721 cm⁻¹; ¹H NMR (400 MHz, CDCl₃) δ 8.01 (d, 2H, *J* 8.5 Hz, 2 x ArH), 7.61 (t, 1H, *J* 7.05 Hz, ArH), 7.46 (dd, 2H, *J* 8.5 & 7.0 Hz, ArH), 3.34 (s, 3H, NCH₃), 1.46 (s, 9H, OC(CH₃)₃); ¹³C NMR (125 MHz, CDCl₃) δ 164.7, 155.4, 133.9, 129.9, 128.6, 127.6, 82.4, 38.0, 28.1 ppm; MS (APCI) *m/z* 252 (M+H)⁺; HRMS (APCI) calculated for C₁₃H₁₈NO₄ 252.1230 [M+H]⁺, found 252.1236.

***N*-Methyl-*O*-benzoyl hydroxylamine hydrochloride 100-HCl⁸⁷**



Gaseous hydrogen chloride, generated from the reaction of concentrated sulfuric acid (ca. 50 ml) and ammonium chloride (ca. 50 g) was bubbled through a solution of *N*-Boc-*N*-methyl hydroxylamine **99** (6.7 g, 26.7 mmol) in 1,4-dioxane and the reaction mixture stirred at ambient temperature for 2 h. The resulting white precipitate was filtered and washed with cold ether and dried under vacuum to yield the *title compound* **100-HCl** (4.03 g, 21.6 mmol, 81%) as a colourless solid; Mp 127.5–129 °C (Lit. ref. 129–129.5 °C)⁵⁰; IR (CHCl₃): 3458 (br), 3056, 1759, 1712, 1600, 1550, 1422, 1264 cm⁻¹; ¹H NMR (400 MHz, DMSO-d₆) δ 11.95 (br, s, 2H, NH), 7.95 (d, 2H, *J* 7.0 Hz, 2 x ArH), 7.73 (t, 1H, *J* 7.5 Hz, ArH), 7.57 (dd, 2H, *J* 7.0 & 7.5, ArH) 2.93 (s, 3H, NCH₃); ¹³C NMR (100 MHz, DMSO-d₆) δ 163.9, 134.4, 129.2, 129.1, 126.7, 37.0 ppm; MS (APCI) *m/z* 252 (M+H)⁺; HRMS (APCI) calculated for C₈H₁₀NO₂ 152.0706 [M+H]⁺, found 152.0712.

9.2.2 General Procedure 1 – Hydroxylamine reagent synthesis by Phanstiel method⁵⁶

A solution of benzoyl peroxide 118 (70% in H₂O, 10.38 g, 30.0 mmol) in CH₂Cl₂ (75 ml) was added quickly to a mixture of amine (21.0 mmol) and pH 10.5 buffer solution (75 ml). Vigorous stirring was continued at r.t. overnight. The reaction mixture was then extracted with CH₂Cl₂ (2 x 50 ml), washed with saturated NaHCO₃ solution (100 ml), water (100 ml) and brine (50 ml), then dried over Na₂SO₄ and concentrated under reduced pressure to give the crude product, which was purified by column chromatography. When required, further purification was accomplished by conversion to the HCl salt (see General Procedure 2).

9.2.3 Preparation of pH 10.5 buffer solution⁵⁶

A 300 ml stock solution of aqueous pH 10.5 buffer was prepared by combining aqueous NaHCO₃ (222 ml, [0.75M]) with aqueous sodium hydroxide (78 ml, [1.5M]).

9.2.4 General Procedure 2 – Conversion of free base reagents to their hydrochloride salts

Gaseous hydrogen chloride, generated from the slow addition of concentrated sulfuric acid (ca. 50 ml) to ammonium chloride (ca. 50 g) was bubbled through a solution of hydroxylamine in 1,4-dioxane for 2 hours. The resulting white precipitate was filtered, washed with cold ether and dried under high vacuum to give the title compound as a colourless solid (90–99%).⁵⁰

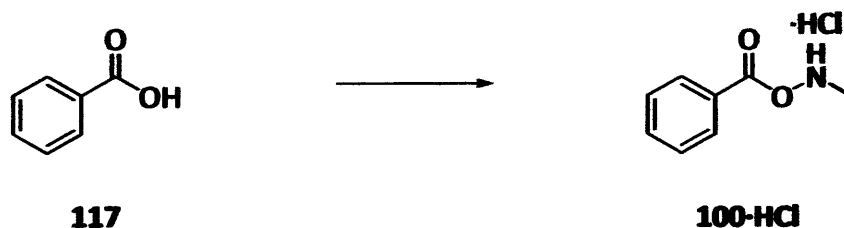
9.2.5 General Procedure 3 – Conversion of ·HCl salts to free base reagents

The requisite hydrochloride salt (10 mmol) was partitioned between pH 10.5 buffer (50 ml) and dichloromethane (50 ml) and the aqueous phase extracted with CH₂Cl₂ (2 x 50 ml). The organic layers were combined, washed with water (100 ml) and brine (100 ml); then dried over Na₂SO₄, filtered and evaporated to give the free base.

9.2.6 General Procedure 4 – Hydroxylamine reagent synthesis by Geffken method⁸⁷

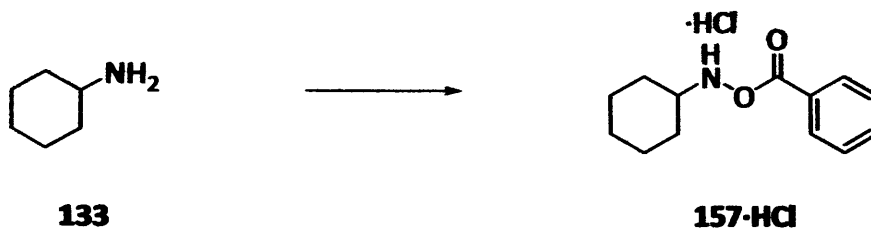
1,1'-Carbonyldiimidazole (2.59 g, 16.0 mmol) was added portionwise at ambient temperature over 15 min to a stirring solution of the requisite carboxylic acid (1.0 eq., 16.0 mmol) in CH₂Cl₂ (20 ml) and stirring was continued for a further 15–30 min until all effervescence had finished. The appropriate hydroxylamine (1.2 eq., 20.0 mmol) was then added quickly, and stirring at room temperature was continued for 1 hour. The reaction mixture was then diluted with CH₂Cl₂ (50 ml), washed with ice-cold 1M HCl (50 ml), saturated NaHCO₃ solution (50 ml) and brine (50 ml), dried (Na₂SO₄) and concentrated *in vacuo* to give the crude product, which was purified by column chromatography. When required, further purification was accomplished by conversion to the HCl salt (see General Procedure 2).

N-Methyl-*O*-benzoyl hydroxylamine hydrochloride 100-HCl⁵⁰



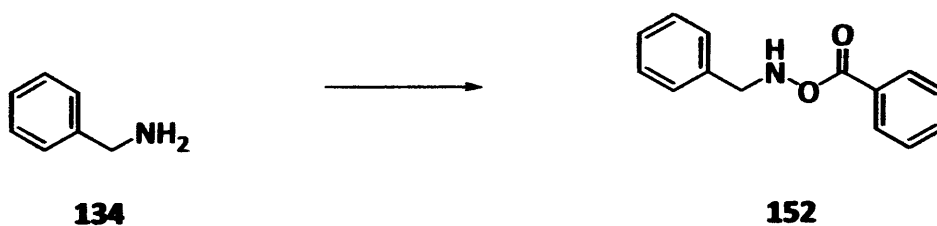
Compound **100-HCl** was prepared according General Procedure 4 (Geffken method) to give the free base as a colourless oil which was converted to **100-HCl** by General Procedure 2, providing the *title compound* as white crystals (1.59 g, 53%); Mp 129–129.5 °C (Lit. ref. 129–129.5 °C)⁵⁰; IR (CHCl₃): 3458 (br), 3056, 1759, 1712, 1600, 1550, 1422, 1264 cm⁻¹; ¹H NMR (400 MHz, DMSO-*d*₆) δ 7.94 (d, *J* 7.5 Hz, 2H, 2 x ArH), 7.70 (t, *J* 7.5 Hz, 1H, ArH), 7.56 (dd, *J* 7.5 Hz, 2 x ArH), 6.35 (s, br, 2H, NH), 2.84 (s, 3H, CH₃); ¹³C NMR (100 MHz, DMSO-*d*₆) δ 163.9, 134.4, 129.2, 129.1, 126.7, 37.0 ppm; MS (APCI) *m/z* 152 [M+H]⁺; HRMS (APCI) calculated for C₈H₁₀NO₂ 152.0706 [M+H]⁺, found 152.0706.

***N*-Cyclohexyl-*O*-benzoyl hydroxylamine hydrochloride 157·HCl**



Compound **157·HCl** was synthesised from cyclohexylamine **133** using General Procedure 1 (Phanstiel method). Conversion to the HCl salt (General procedure 2) gave *the title compound* **157·HCl** as a white solid (6.17 g, 74%), which was collected by filtration; Mp 145–147 °C (Lit. ref. 155 °C)⁸⁸; IR (CHCl₃): 2932, 2855, 1757, 1718, 1450, 1265, 1055, 704 cm⁻¹; ¹H NMR (400 MHz, DMSO-*d*₆) δ 9.20–9.40 (br, 2H, NH₂⁺), 7.95 (d, 2H, *J* 7.1 Hz, ArH), 7.65 (t, 1H, *J* 7.4 Hz, ArH), 7.50 (dd, 2H, *J* 7.4 & 7.1 Hz, ArH), 3.05–3.15 (m, 1H, CHN), 1.85–1.95 (m, 2H, CH₂), 1.50–1.80 (m, 2H, CH₂), 1.50–1.60 (m, 1H, CH), 1.05–1.30 (m, 5H); ¹³C NMR (100 MHz, DMSO-*d*₆), δ 165.3, 134.3, 129.5, 129.5, 128.2, 59.2, 29.4, 25.8, 24.4 ppm; MS (APCI) *m/z* 220 [M-Cl]⁺; HRMS (APCI) calculated for C₁₃H₁₈NO₂ [M-Cl]⁺ 220.1332, found 220.1331.

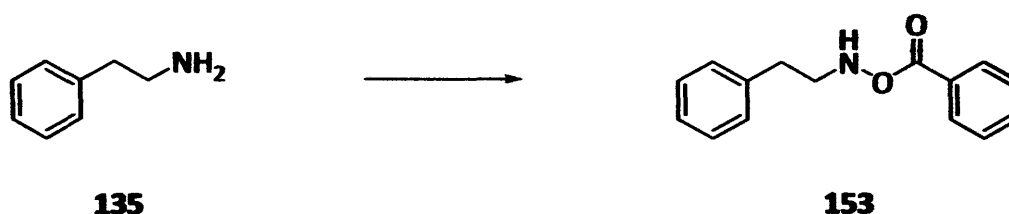
***N*-Benzyl-*O*-benzoyl hydroxylamine 152⁸⁷**



Compound **152** was synthesised from benzylamine **134** (4.0 g, 37 mmol) using General Procedure 1 (Phanstiel method). Purification by column chromatography, eluting with petroleum ether-ethyl acetate (4:1) gave *the title compound* **152** (5.70 g, 68%) as a white solid; Mp 25–28 °C; IR (CHCl₃): 3230, 3030, 1721, 1601, 1452, 1310, 1270, 1171, 1086, 1066, 1026, 750, 707 cm⁻¹; ¹H NMR (400 MHz, CDCl₃) δ 7.90 (d, 2H, *J* 7.1 Hz, ArH), 7.45 (t, 1H, *J* 7.5 Hz, ArH), 7.35 (dd, 2H, *J* 7.7 & 7.1 Hz, 2 x ArH), 7.20–7.30 (m, 5H, 5 x ArH), 4.20 (s, 2H, CH₂);

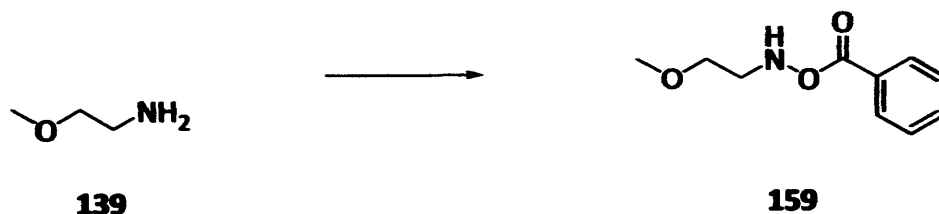
^{13}C NMR (100 MHz, CDCl_3), δ 166.9, 135.9, 133.4, 129.4, 129.1, 128.7, 128.6, 128.3, 128.0, 56.8 ppm; MS (ES) m/z 228 $[\text{M}+\text{H}]^+$; HRMS (ES) calculated for $\text{C}_{14}\text{H}_{14}\text{NO}_2$ $[\text{M}+\text{H}]^+$ 228.1019, found 228.1022.

***N*-Phenethyl-*O*-benzoyl hydroxylamine 153**



Compound **153** was prepared according to General Procedure 1 (Phanstiel method) to give the *title compound* **153** as a yellow oil (4.49 g, 62%); IR (thin film) 3235, 3063, 3028, 2933, 1720, 1601, 1496, 1452, 1316, 1271, 1178, 1093, 1067, 1025, 708 cm^{-1} ; ^1H NMR (400 MHz, CDCl_3) δ 8.07 (d, 2H, J 7.9 Hz, 2 x Ar-H) 7.91 (t, 1H, J 6.3 Hz, Ar-H), 7.65 (t, 1H, J 7.5 Hz, Ar-H), 7.55–7.49 (m, 2H, 2 x Ar-H), 7.41–7.36 (m, 2H, 2 x Ar-H), 7.33–7.28 (m, 3H, 3 x Ar-H), 3.55–3.46 (m, 2H, NCH_2), 3.03 (t, 2H, J 7.2 Hz, ArCH_2); ^{13}C NMR (100 MHz, CDCl_3) δ 165.1, 139.4, 134.3, 129.5, 129.4, 129.1, 128.9, 126.7, 126.6, 52.5, 32.9 ppm; MS (APCI) m/z 242 $[\text{M}+\text{H}]^+$; HRMS calculated for $\text{C}_{15}\text{H}_{16}\text{NO}_2$ 242.1178 $[\text{M}+\text{H}]^+$, found 242.1175.

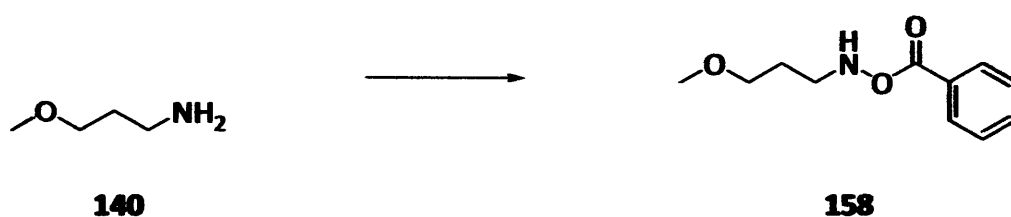
***N*-(Benzoyloxy)-2-methoxyethylamine 159**



Compound **159** was prepared according to General Procedure 1 (Phanstiel method) to give the *title compound* **159** as a yellow oil (1.98 g, 51%); IR (thin film) 3241, 3063, 2929, 2829,

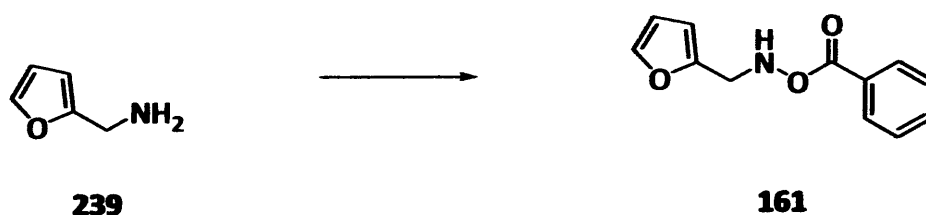
1722, 1601, 1451, 1270 cm^{-1} ; ^1H NMR (400 MHz, CDCl_3) δ 8.02 (d, 2H, J 8.0 Hz, 2 x ArH), 7.57 (t, 1H, J 8.0 Hz, ArH), 7.45 (dd, 2H, J 8.0 & 8.0 Hz, 2 x ArH), 6.32 (s, br, 1H, NH), 3.58 (t, 2H, J 5.0 Hz, OCH_2), 3.38 (s, 3H, OCH_3), 3.35 (t, 2H, J 5.0 Hz, NCH_2); ^{13}C NMR (100 MHz, CDCl_3) δ 166.5, 133.3, 129.3, 128.7, 128.3, 68.7, 53.5, 51.9 ppm; MS (APCI) m/z 218 $[\text{M}+\text{Na}]^+$; HRMS (APCI) calculated for $\text{C}_{10}\text{H}_{13}\text{NaNO}_3$ 218.0788 $[\text{M}+\text{Na}]^+$, found 218.0788.

***N*-(Benzoyloxy)- 3-methoxypropan-1-amine 158**



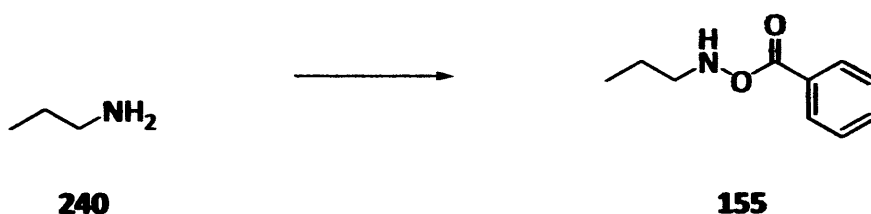
Compound **158** was prepared according to General procedure 1 (Phanstiel method) to give the *title compound* **158** as a colourless oil (3.20 g, 51%); IR (thin film) 3241, 3063, 2929, 2829, 1722, 1601, 1451, 1270 cm^{-1} ; ^1H NMR (400 MHz, DMSO-d_6) δ 7.95 (d, 2H, J 8.1 Hz, ArH), 7.49–7.45 (m, 1H, ArH), 7.40–7.30 (m, 2H, 2 x ArH), 3.40 (t, 2H, J 6.2 Hz, OCH_2), 3.21 (s, 3H, OCH_3), 3.12–3.07 (m, 2H, NCH_2), 1.80–1.76 (m, 2H, CH_2); ^{13}C NMR (100 MHz, DMSO-d_6) δ 164.5, 132.7, 129.3, 128.7, 128.3, 71.7, 59.3, 37.6, 26.3 ppm; MS (APCI) m/z 210 $[\text{M}+\text{H}]^+$; HRMS (APCI) calculated for $\text{C}_{11}\text{H}_{16}\text{NO}_3$ 210.1125 $[\text{M}+\text{H}]^+$, found 210.1126.

***N*-((Furan-2-yl)-methyl) benzoyloxyamine 161**



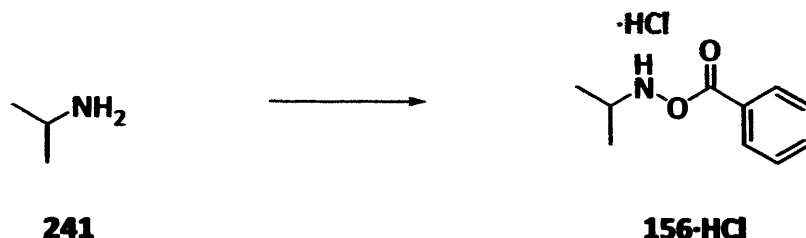
Compound **161** was prepared according to General Procedure 1 (Phanstiel method) to give the *title compound 161*, after purification by flash chromatography (4:1 petroleum ether/diethyl ether), as a yellow/green oil (3.96 g, 61%); IR (thin film) 3233, 3066, 2360, 2342, 1723, 1602, 1505, 1452, 1270, 1091, 1067, 1026, 1012, 742, 707 cm^{-1} ; ^1H NMR (400 MHz, CDCl_3) δ 8.02–7.99 (m, 2H, 2 x ArH), 7.62–7.58 (m, 1H, ArH), 7.52–7.42 (m, 3H, 3 x ArH), 6.34–6.32 (m, 2H, 2 x ArH), 4.31 (s, 2H, CH_2); ^{13}C NMR (100 MHz, CDCl_3) δ 166.6, 150.0, 142.7, 133.4, 129.4, 128.5, 128.3, 110.5, 109.0, 49.0 ppm; MS (APCI) m/z 218 $[\text{M}+\text{H}]^+$; HRMS (APCI) calculated for $\text{C}_{12}\text{H}_{12}\text{NO}_3$ 218.0812 $[\text{M}+\text{H}]^+$, found 218.0812.

***N*-(Propyl) benzoyloxyamine 155**



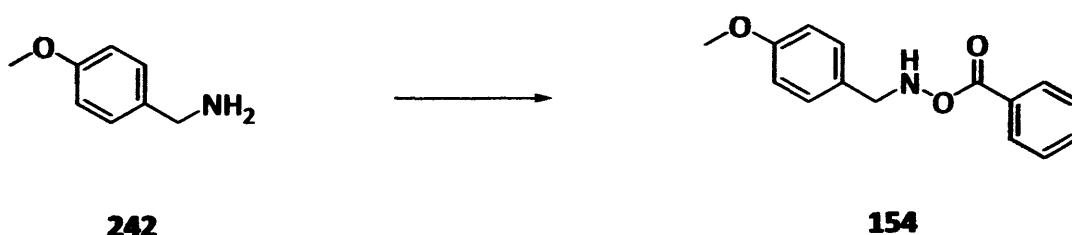
Compound **155** was prepared according to General Procedure 1 (Phanstiel method) to give the *title compound 155*, after purification by flash chromatography (4:1 petroleum ether/diethyl ether), as a yellow/green oil (3.14 g, 58%); IR (thin film) 3201, 2160, 1720, 1590, 1430, 1220, 1010, cm^{-1} ; ^1H NMR (400 MHz, CDCl_3) δ 7.95–7.93 (m, 2H, 2 x ArH), 7.83 (br, 1H, NH), 7.54–7.48 (m, 2H, 2 x ArH), 7.38–7.34 (m, 2H, 2 x ArH), 3.03 (t, 2H, J 7.1 Hz, NCH_2), 1.58–1.54 (m, 2H, CH_2), 0.92 (t, 3H, J 7.5 Hz, CH_3); ^{13}C NMR (100 MHz, CDCl_3) δ 164.5, 134.9, 129.8, 129.6, 128.9, 52.3, 19.0, 11.7 ppm; MS (ES) m/z 180 $[\text{M}+\text{H}]^+$; HRMS (ES) calculated for $\text{C}_{10}\text{H}_{14}\text{NO}_2$ 180.1019 $[\text{M}+\text{H}]^+$, found 180.1019.

***N*-(*iso*-Propyl) benzoyloxyamine hydrochloride 156-HCl**



Compound **156-HCl** was prepared according to General Procedure 1 (Phanstiel method) to give the *title compound*, after purification by flash chromatography (4:1 petroleum ether/diethyl ether), followed by conversion to the hydrochloride salt **156-HCl** as a white powder (3.26 g, 50%); Mp 120–121.5 °C; IR (CHCl₃): 2165, 1710, 1584, 1420, 1210, 1125, 1010, cm⁻¹; ¹H NMR (400 MHz, DMSO-d₆) δ 7.99–7.94 (m, 2H, 2 x ArH), 7.78–7.70 (m, 1H, ArH), 7.63–7.56 (m, 2H, 2 x ArH), 3.51–3.46 (m, 1H, CH), 1.18 (d, 6H, *J* 6.3 Hz, 2 x CH₃); ¹³C NMR (100 MHz, DMSO-d₆) δ 159.7, 134.7, 129.8, 129.4, 129.2, 50.8, 20.6 ppm; MS (APCI) *m/z* 180 [M-Cl]⁺; HRMS (APCI) calculated for C₁₀H₁₄NO₂ 180.1019 [M-Cl]⁺, found 180.1019.

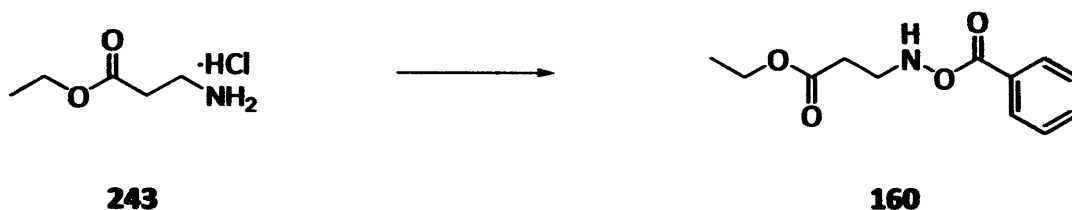
***N*-(4-Methoxybenzyl)-*O*- benzoyloxyamine 154**



Compound **154** was prepared according to General Procedure 1 (Phanstiel method) to give the *title compound* **154**, after purification by flash chromatography (4:1 petroleum ether/diethyl ether), as a colourless oil (4.51 g, 58%); IR (thin film): 3230, 2305, 1725, 1596, 1360, 1240, 1238, 1195, 1165, 1024, cm⁻¹; ¹H NMR (400 MHz, CDCl₃) δ 8.03–8.00 (m, 2H, 2 x ArH), 7.62–7.58 (m, 1H, ArH), 7.49–7.45 (m, 2H, 2 x ArH), 7.36 (d, 2H, *J* 8.6 Hz, 2 x ArH), 6.94–6.65 (m, 2H, ArH), 4.19 (s, 2H, CH₂), 3.82 (s, 3H, OCH₃); ¹³C NMR (100 MHz, CDCl₃) δ 164.5,

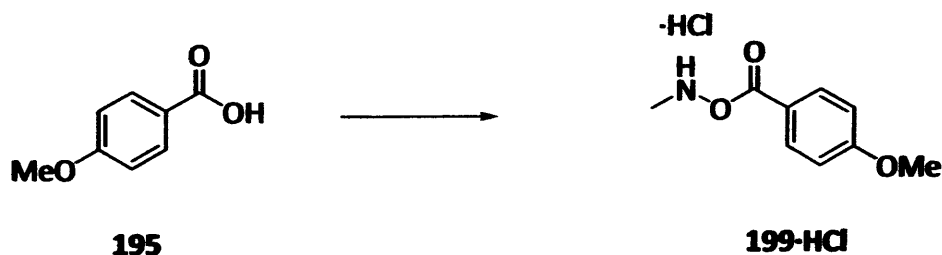
149.6, 134.7, 130.3, 129.8, 129.4, 128.7, 120.7, 52.6, 49.7 ppm (1 carbon missing); MS (APCI) m/z 180 $[M+H]^+$; HRMS (APCI) calculated for $C_{15}H_{16}NO_3$ 258.1125 $[M+H]^+$, found 258.1121.

***N*-(Ethyl-3-aminopropanoate)-*O*-benzoyloxyamine 160**



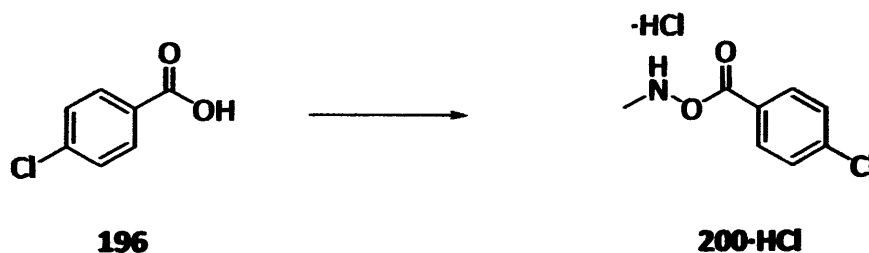
6-Alanine ethyl ester hydrochloride **243** (4.61 g) was converted to the free base by General Procedure 3 to give the desired amine as a colourless oil (3.50 g, 99%). Compound **160** was prepared according to General Procedure 1 (Phanstiel method) to give the *title compound* **160**, after purification by flash chromatography (1:1 petroleum ether/diethyl ether), as a colourless oil (2.96 g, 42%); IR (thin film): 3320, 1745, 1735, 1602, 1240, 1136, 1078, cm^{-1} ; 1H NMR (400 MHz, $CDCl_3$) δ 8.01–7.93 (m, 2H, 2 x ArH), 7.59–7.50 (m, 1H, ArH), 7.44–7.33 (m, 2H, 2 x ArH), 4.09 (q, 2H, J 7.1 Hz, OCH_2), 3.44–3.36 (m, 2H, NCH_2), 2.59 (t, 2H, J 6.5 Hz, $COCH_2$), 1.18 (t, 3H, J 7.1 Hz, CH_3); ^{13}C NMR (100 MHz, $CDCl_3$) δ 171.9, 166.5, 133.4, 129.3, 128.5, 128.3, 60.8, 48.9, 32.2, 14.1 ppm; MS (APCI) m/z 238 $[M+H]^+$; HRMS (APCI) calculated for $C_{12}H_{16}NO_4$ 238.1074 $[M+H]^+$, found 238.1074.

***N*-Methyl-*O*-(4-methoxy)benzoyloxyamine ·hydrochloride 199-HCl**



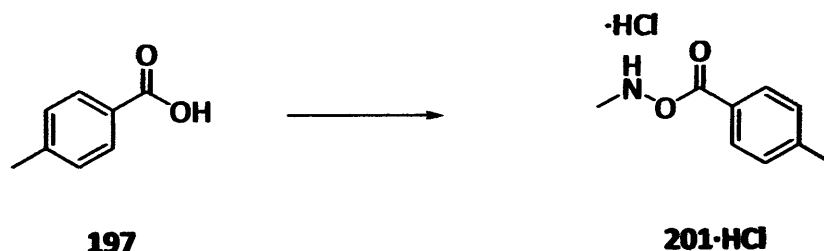
Compound **199-HCl** was prepared according to General Procedure 4 (Geffken method), followed by General Procedure 2 to give the *title compound* **199-HCl** as white microcrystals (4.66 g, 72%); Mp 130–132 °C; IR (CHCl₃): 3246, 2932, 1718, 1606, 1511, 1465, 1421, 1318, 1257, 1170, 1080, 1027, 846, 763 cm⁻¹; ¹H NMR (400 MHz, DMSO-d₆) δ 7.95 (d, 2H, *J* 15.2 Hz, 2 x ArH), 7.07 (d, 2H, *J* 15.1 Hz, 2 x ArH), 3.84 (s, 3H, OCH₃), 2.86 (s, 3H, NCH₃); ¹³C NMR (100 MHz, DMSO-d₆) δ 166.7, 163.7, 131.4, 120.6, 113.8, 55.5, 39.9 ppm; MS (APCI) *m/z* 182 [M-Cl]⁺; HRMS (APCI) calculated for C₉H₁₁NO₃ 182.0812 [M-Cl]⁺, found 182.0811.

N*-Methyl-*O*-(4-chloro)benzoyloxyamine hydrochloride **200-HCl*



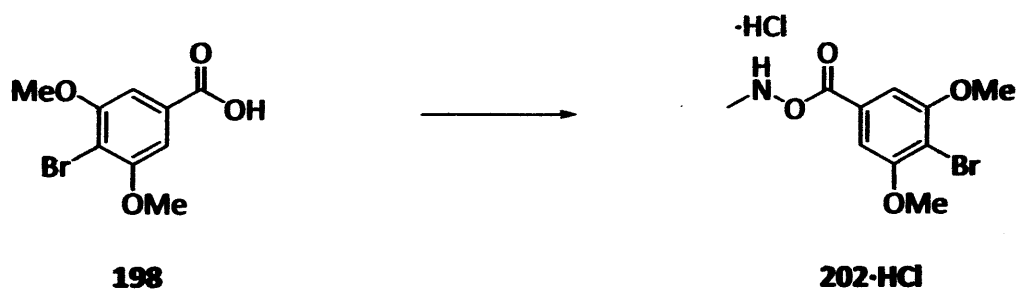
Compound **200-HCl** was prepared according to General Procedure 4 (Geffken method) to give the *title compound* **200-HCl** as white microcrystals (4.69 g, 66%); Mp 152–153 °C; IR (CHCl₃): 3246, 2969, 1724, 1603, 1508, 1474, 1436, 1414, 1272, 1239, 1156, 1080, 1014, 853, 760 cm⁻¹; ¹H NMR (400 MHz, DMSO-d₆) δ 8.15 (d, 2H, *J* 8.7 Hz, 2 x ArH), 7.64 (d, 2H, *J* 8.7 Hz, 2 x ArH), 2.92 (s, 3H, CH₃); ¹³C NMR (100 MHz, DMSO-d₆) δ 163.7, 139.6, 131.9, 131.6, 129.7, 37.8 ppm; MS (APCI) *m/z* 186 [M-Cl]⁺.

N*-Methyl-*O*-(4-methyl)benzoyloxyamine hydrochloride **201-HCl*



Compound **201-HCl** was prepared according to General Procedure 4 (Geffken method) to give the *title compound 201-HCl* as white microcrystals (4.40 g, 69%); Mp 145–147°C; IR (CHCl₃): 3280, 2950, 1726, 1610, 1454, 1429, 1258, 1209, 1166, 1007, 853, 760 cm⁻¹; ¹H NMR (400 MHz, DMSO-d₆) δ 12.20 (br, 1H, NH), 7.86 (d, 2H, *J* 8.2 Hz, ArH), 7.39 (d, 2H, *J* 8.0 Hz, 2 x ArH), 2.95 (s, 3H, NCH₃), 2.39 (s, 3H, ArCH₃); ¹³C NMR (100 MHz, DMSO-d₆) δ 164.2, 130.1, 130.0, 129.8, 129.6, 37.3, 21.7 ppm; MS (ES) *m/z* 166 [M-Cl]⁺; HRMS (ES) calculated for C₉H₁₂NO₂ 166.0863 [M-Cl]⁺, found 166.0864.

N*-Methyl-*O*-(4-bromo-3,5-dimethoxy)benzoyloxyamine hydrochloride **202-HCl*



Compound **202-HCl** was prepared according to General Procedure 4 (Geffken method) to give the *title compound 202-HCl* as white microcrystals (4.56 g, 50%); Mp 152–154°C; IR (CHCl₃): 3310, 1729, 1624, 1439, 1223, 1150, 1018, 867, 755 cm⁻¹; ¹H NMR (400 MHz, DMSO-d₆) δ 9.56 (br, 1H, NH), 7.25 (s, 2H, 2 x ArH), 3.92 (s, 6H, 2 x OCH₃), 2.89 (s, 3H, NCH₃); ¹³C NMR (100 MHz, DMSO-d₆) δ 166.4, 157.2, 128.4, 107.3, 105.3, 56.7, 40.0 ppm; MS (ES) *m/z* 312 [M-HCl+Na]⁺; HRMS (ES) calculated for C₁₀H₁₂BrNNaO₄ 311.9847 [M-HCl+Na]⁺, found 311.9842 (⁷⁹Br).

9.3 α -Oxygenated Carbonyl Compounds

9.3.1 General Procedure 5 – α -Oxygenation of ketones

A solution of ketone (1.0 eq., 0.5 mmol) and α -oxygenating species (1.0 eq., 0.5 mmol) in DMSO (1.0 ml) was stirred at ambient temperature for 12–24 hours, until TLC analysis indicated complete disappearance of the ketone substrate. At the end of the reaction time, the mixture was diluted with ethyl acetate (50 ml), then washed sequentially with saturated aqueous sodium chloride (50 ml), saturated sodium hydrogen carbonate solution (50 ml) and water (50 ml), dried over magnesium sulphate and concentrated *in vacuo* to give the crude product. Flash chromatography afforded the pure α -oxygenated species.

9.3.2 General Procedure 6 – α -Oxygenation of ketones in the presence of Lewis acids

The reaction was carried out with a mixture of *N*-phenethyl-*O*-benzoyl hydroxylamine **153** (140 mg, 0.64 mmol) and 1,4-cyclohexanedione-*mono*-ethylene ketal **131** (100 mg, 0.64 mmol), with a stoichiometric equivalent of Lewis acid in chloroform at 50 °C. Following standard aqueous work-up, 1,4-dimethoxybenzene (14 mg, 0.1 mmol) was added to the solution as an internal standard and the crude reaction mixture was analysed by ^1H NMR. Comparison of integrals gave approximate conversions to product.

9.3.3 General Procedure 7 – α -Oxygenation of ketones with free base reagents

The reaction was carried out with the relevant hydroxylamine reagent (140 mg, 0.64 mmol) and 1,4-cyclohexanedione-*mono*-ethylene ketal **131** (100 mg, 0.64 mmol), in the chosen solvent at 50 °C for 3 days. Following standard aqueous work-up, 1,4-dimethoxybenzene (14 mg, 0.1 mmol) was added to the solution as an internal standard and the crude reaction mixture was analysed by ^1H NMR. Comparison of integrals gave calculated product conversions.

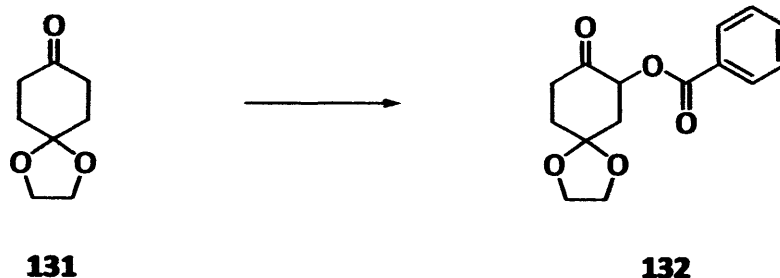
9.3.4 General procedure 8 – α -Oxygenation of ketones with thiourea catalyst

The reaction was carried out with a mixture of *N*-methyl-*O*-benzoyl hydroxylamine (45 mg, 0.3 mmol) and 1,4-cyclohexanedione-*mono*-ethylene ketal **131** (47 mg, 0.3 mmol), with 1,3-bis-(3,5-bis(trifluoromethyl)phenyl) thiourea **163** in the chosen solvent at 50 °C for 3 days. Following standard aqueous work-up, 1,4-dimethoxybenzene (14 mg, 0.1 mmol) was added to the solution as an internal standard and the crude reaction mixture was analysed by ^1H NMR. Comparison of integrals gave approximate conversions to product.

9.3.5 General procedure 9 – α -Oxygenation of ketones (optimised conditions)

A solution of ketone (1.0 eq., 0.5 mmol) and α -oxygenating species (1.0 eq., 0.5 mmol) in DMSO (1.0 ml) was stirred at 30 °C for 0.5 hours, at which time water (1.0 ml) was added and the reaction mixture allowed to stir at 30 °C for a further 0.5 hours. After this interval, TLC analysis indicated complete disappearance of the ketone substrate. At the end of the reaction time, the mixture was diluted with ethyl acetate (50 ml), then washed sequentially with saturated aqueous sodium chloride (50 ml), saturated sodium hydrogen carbonate solution (50 ml) and water (50 ml), dried over magnesium sulphate and concentrated *in vacuo* to give the crude product. Flash chromatography afforded the pure α -oxygenated species.

Benzoic acid 8-oxo-1,4-dioxaspiro[4.5]dec-7-yl ester 132



Benzoic acid 8-oxo-1,4-dioxaspiro[4.5]dec-7-yl ester **132** was prepared by General Procedure 5, to give the crude product as a brown oil. Purification by flash chromatography (5:1 petroleum ether/ethyl acetate) gave the desired product **132** as colourless crystals (148 mg, 84%); Mp 114–116 °C; IR(CHCl₃): 2915, 1714, 1448, 1260, 1101, 1036 cm⁻¹; ¹H NMR (400 MHz, CDCl₃) δ 8.01 (d, *J* = 8.0 Hz, 2H, 2 x ArH), 7.51 (t, *J* = 8.0 Hz, 1H, ArH), 7.38 (dd, *J* = 8.0 Hz & 8.0 Hz, 2H, 2 x ArH), 5.57–5.69 (m, 1H, CH), 3.95–4.11 (m, 4H, OCH₂CH₂O), 2.66–2.80 (m, 1H, CH), 2.35–2.49 (m, 2H, CH₂), 2.20 (t, *J* = 13.0 Hz, 1H, CH), 1.90–2.09 (m, 2H, CH₂); ¹³C NMR (100 MHz, CDCl₃) δ 203.4, 165.4, 133.3, 129.9, 129.4, 128.4, 107.3, 73.7, 65.0, 64.9, 40.3, 35.6, 34.6 ppm; MS (APCI) *m/z* 277 [M+H]⁺; HRMS (APCI) calculated for C₁₅H₁₇O₅ [M+H]⁺ 277.1071, found 277.1073.

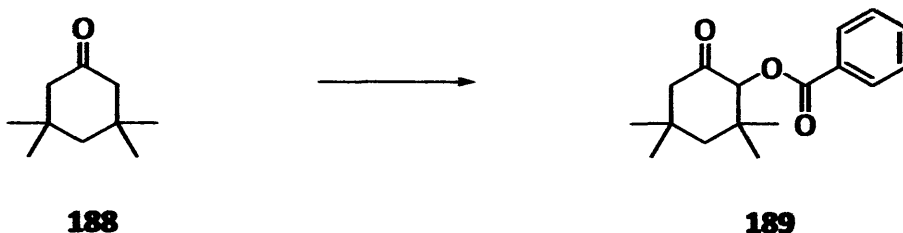
2-Benzoyloxy cyclohexanone 167⁵⁰



The α-oxygenated product was prepared according to General Procedure 5 to give the crude product which was purified on silica, eluting with petroleum ether/ethyl acetate (3:1) to give the *title compound* **167** (87 mg, 80%) as a white crystalline solid; Mp 81–81.5 °C (Lit. ref. 81–83 °C)⁵⁰; IR (CHCl₃): 2945, 2867, 1743, 1719 1603, 1451, 1316, 1271, 1177, 1112, 1071,

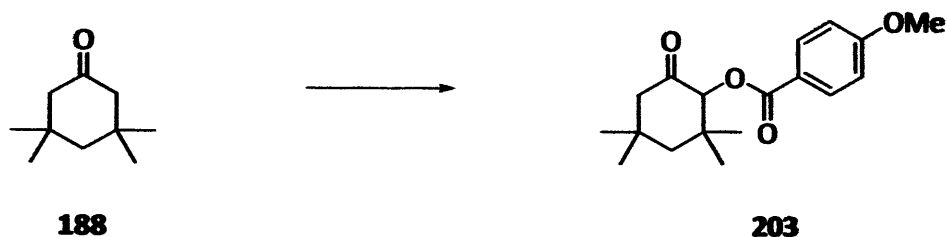
1034 cm^{-1} ; ^1H NMR (400 MHz, CDCl_3) δ 8.05 (d, 2H, J 8.3 Hz, 2 x ArH), 7.53–7.48 (m, 1H, ArH), 7.40–7.36 (m, 2H, 2 x ArH), 5.35 (dd, 1H, J 12.0 & 9.5 Hz, CHCO), 2.45–2.55 (m, 1H, CH), 2.30–2.45 (m, 2H, CH_2), 2.00–2.10 (m, 1H, CH), 1.90–2.00 (m, 1H, CH), 1.70–1.90 (m, 2H, CH_2), 1.55–1.70 (m, 1H, CH); ^{13}C NMR (100 MHz, CDCl_3), δ 204.4, 165.6, 133.2, 129.9, 129.7, 128.4, 77.0, 40.8, 33.2, 27.2, 23.8 ppm; MS (ES) m/z 219 $[\text{M}+\text{H}]^+$; HRMS (ES) calculated for $\text{C}_{13}\text{H}_{15}\text{O}_3$ $[\text{M}+\text{H}]^+$ 219.1016, found 219.1015.

2-Benzoyloxy 3,3,5,5-tetramethylcyclohexanone 189



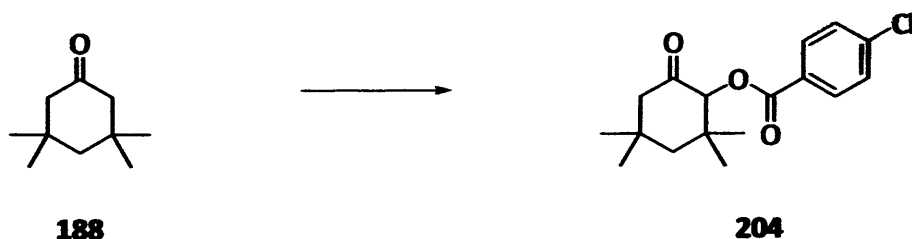
The α -oxygenated product **189** was prepared according to General Procedure 5 to give the crude product which was purified on silica, eluting with petroleum ether-ethyl acetate (3:1) to give the *title compound* **189** (118 mg, 86%) as a white crystalline solid; Mp 87–88 °C; IR (CHCl_3): 2887, 2797, 1753, 1731, 1605, 1432, 1295, 1136, 1092, 1053 cm^{-1} ; ^1H NMR (400 MHz, CDCl_3) δ 8.00 (d, 2H, J 8.0 Hz, 2 x ArH), 7.52–7.48 (m, 1H, ArH), 7.43–7.36 (m, 2H, 2 x ArH), 5.15 (s, 1H, CHCO), 2.45 (d, J 13.0 Hz, 1H, CH), 2.2 (dd, J 13.0 & 3.0 Hz, 1H, CH), 1.80 (d, J 15.0 Hz, 1H, CH), 1.60 (dd, J 15.0 3.0 Hz, 1H), 1.08–1.00 (m, 12H, 4 x CH_3); ^{13}C NMR (100 MHz, CDCl_3), δ 204.3, 164.9, 133.5, 129.4, 129.2, 128.8, 83.3, 51.9, 50.2, 39.6, 36.0, 33.5, 30.2, 27.6, 22.4 ppm; MS (ES) m/z 275 $[\text{M}+\text{H}]^+$; HRMS (ES) calculated for $\text{C}_{17}\text{H}_{23}\text{O}_3$ $[\text{M}+\text{H}]^+$ 275.1642, found 275.1642.

2-(4-Methoxy)benzoyloxy 3,3,5,5-tetramethyl cyclohexanone 203



Compound **203** was synthesised using General Procedure 5. Purification by column chromatography, eluting with petroleum ether/ethyl acetate (65:35), gave the *title compound 203* (108 mg, 71%) as a white crystalline solid; Mp 104–106 °C; IR (CHCl₃): 2944, 1727, 1702, 1604, 1511, 1320, 1280, 1260, 1173, 1109, 1038, 770 cm⁻¹; ¹H NMR (400 MHz, CDCl₃) δ 8.05 (d, 2H, *J* 8.8 Hz, 2 x ArH), 6.95 (d, 2H, *J* 8.8 Hz, 2 x ArH), 5.20 (s, 1H, CHCO), 3.90 (s, 3H, CH₃), 2.52 (d, 1H, *J* 12.8 Hz, CH), 2.30 (dd, 2H, *J* 12.8 & 2.5 Hz, CH₂), 1.92 (d, 1H, *J* 14.5, CH), 1.67 (dd, 1H, *J* 14.5 & 2.5 Hz, CH), 1.25–1.05 (m, 12H, 4 x CH₃); ¹³C NMR (100 MHz, CDCl₃) δ 204.3, 164.9, 133.5, 129.4, 129.2, 121.6, 114.6, 74.3, 55.4, 45.1, 39.6, 36.0, 32.7, 28.6, 27.4, 23.0 ppm; MS (APCI) *m/z* 305 [M+H]⁺.

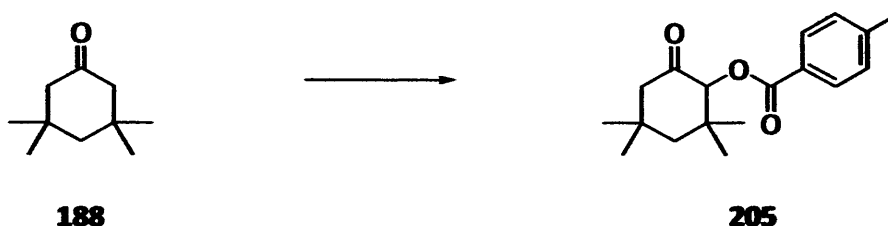
2-(4-Chloro)benzoyloxy 3,3,5,5-tetramethyl cyclohexanone 204



Compound **204** was synthesised using General Procedure 5. Purification by column chromatography, eluting with petroleum ether/ethyl acetate (80:20), gave the *title compound 204* (115 mg, 77%) as a white crystalline solid; Mp 112–115 °C; IR (CHCl₃): 2940, 1721, 1700, 1610, 1531, 1320, 1287, 1254, 1167, 1129, 1038 cm⁻¹; ¹H NMR (400 MHz, CDCl₃) δ 7.91 (d, 2H, *J* 8.2 Hz, 2 x ArH), 7.17 (d, 2H, *J* 8.2 Hz, 2 x ArH), 5.13 (s, 1H, CHCO), 2.52 (d, 1H,

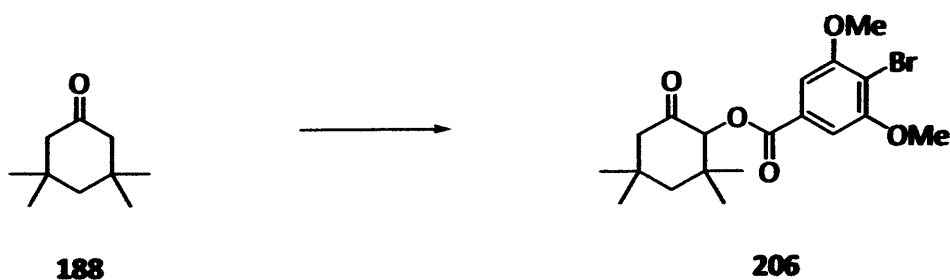
J 12.8 Hz, CH), 2.33 (s, 2H, CH₂), 2.19 (dd, 1H, J 12.9 & 2.7 Hz, CH), 1.83 (d, 1H, J 14.5 Hz, CH), 1.59 (dd, 1H, J 14.5 & 2.7 Hz, CH), 1.14–0.95 (m, 12H, 4 x CH₃); ¹³C NMR (100 MHz, CDCl₃), δ 204.4, 166.0, 143.9, 129.9, 129.1, 127.1, 83.5, 52.8, 51.9, 40.1, 36.4, 34.3, 30.9, 28.1, 22.8, 21.7 ppm; MS (APCI) m/z 309 [M+H]⁺.

2-(4-Methyl)benzoyloxy 3,3,5,5-tetramethyl cyclohexanone 205



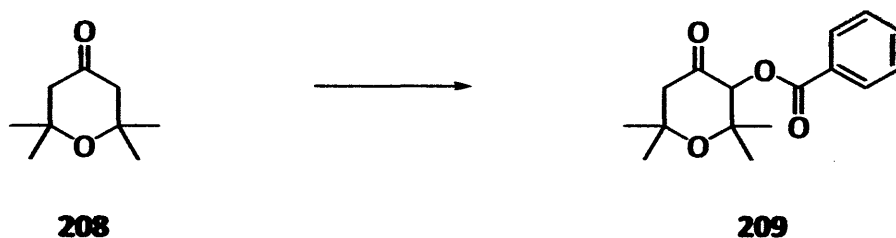
Compound **205** was synthesised using General Procedure 5. Purification by column chromatography, eluting with petroleum ether/ethyl acetate (80:20), gave the *title compound* **205** (107 mg, 77%) as a white crystalline solid; Mp 116–118.5 °C. IR (CHCl₃): 2930, 1716, 1690, 1625, 1511, 1320, 1285, 1253, 1159, 1134, 1038, 989 cm⁻¹; ¹H NMR (400 MHz, CDCl₃) δ 8.04 (d, 2H, J 8.6 Hz, ArH), 7.43 (d, 2H, J 8.6 Hz, ArH), 5.21 (s, 1H, CHCO), 2.51 (d, 1H, J 12.9 CH), 2.39 (s, 3H, CH₃), 2.30 (dd, 1H, J 2.7, 12.9 CH), 1.91 (d, 1H, J 14.6 Hz, CH), 1.68 (dd, 1H, J 2.7, 14.5, CH), 1.24–1.03 (m, 12H, 4 x CH₃); ¹³C NMR (100 MHz, CDCl₃), δ 204.0, 165.1, 139.6, 131.2, 128.8, 128.3, 83.9, 52.7, 51.9, 40.1, 36.4, 34.3, 30.9, 28.0, 22.7 ppm (1 carbon missing).

2-(3,5-Dimethoxy-4-bromo)benzoyloxy 3,3,5,5-tetramethyl cyclohexanone 206



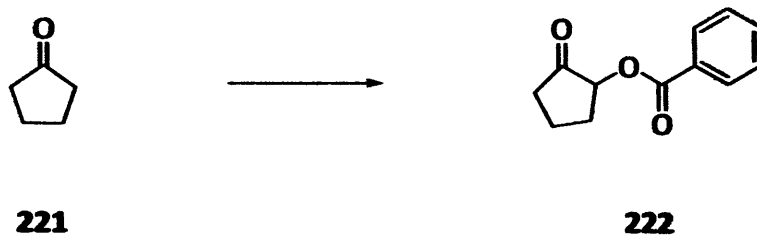
Compound **206** was synthesised using General Procedure 5. Purification by column chromatography, eluting with petroleum ether/ethyl acetate (60:40), gave the *title compound 206* (129 mg, 63%) as a white crystalline solid; Mp 116–118.5 °C; IR (CHCl₃): 2930, 1716, 1690, 1625, 1511, 1320, 1285, 1253, 1159, 1134, 1038, 989 cm⁻¹; ¹H NMR (400 MHz, CDCl₃) δ 7.20 (s, 2H, 2 x ArH), 5.13 (s, 1H, CHCO), 3.90 (s, 6H, 2 x ArOCH₃) 2.44 (d, 1H, *J* 12.9 Hz, CH), 2.21 (dd, 1H, *J* 12.9 & 2.7 Hz, CH), 1.85 (d, 1H, *J* 14.6 Hz, CH), 1.62 (dd, 1H, *J* 14.6 & 2.7 Hz, CH), 1.15–0.92 (m, 12H, 4 x CH₃); ¹³C NMR (100 MHz, CDCl₃), δ 207.3, 166.0, 146.4, 131.0, 118.8, 118.3, 83.9, 55.2, 52.7, 51.9, 40.1, 36.4, 34.3, 30.9, 28.0, 22.7 ppm.

2-Benzoyloxy 3,3,5,5-tetramethyl-1,2-tetrahydropyranone **209**



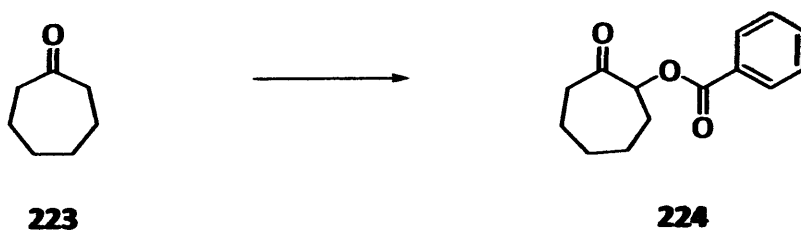
Compound **209** was synthesised using General Procedure 9. Purification by column chromatography, eluting with petroleum ether/ethyl acetate (70:30), gave the *title compound 209* (129 mg, 85%) as a white crystalline solid; mp 116–118.5 °C; IR (CHCl₃): 2843, 1732, 1680, 1619, 1512, 1320, 1301, 1273, 1229, 1038 cm⁻¹; ¹H NMR (400 MHz, CDCl₃) δ 7.99 (d, 2H, *J* 7.9 Hz, ArH), 7.56–7.48 (m, 1H, ArH), 7.44–7.36 (m, 2H, ArH), 5.24 (s, 1H, CHCO), 2.73 (d, 1H, *J* 13.3 CH), 2.56 (d, 1H, *J* 13.3 Hz, CH), 1.40–1.20 (m, 12H, 4 x CH₃); ¹³C NMR (100 MHz, CDCl₃), δ 207.4, 166.0, 133.1, 130.2, 129.9, 105.8, 74.9, 58.3, 52.7, 50.6, 38.4, 36.6, 35.3, 28.0 ppm; MS (APCI): *m/z* 277 [M+H]⁺. HRMS calculated for C₁₆H₂₀O₄ [M+H]⁺ 277.1434, found 277.1435.

2-Benzoyloxy cyclopentanone 222



Compound **222** was prepared using General Procedure 9. Purification by column chromatography, eluting with petroleum ether/ethyl acetate (7:3), gave the *title compound* **222** (79 mg, 75%) as a white crystalline solid; Mp 82–86 °C (Lit. ref. 88–91 °C)^x; IR (CHCl₃): 2915, 2846, 1751, 1716, 1451, 1287, 1269, 1117, 709 cm⁻¹; ¹H NMR (400 MHz, CDCl₃) δ 8.00 (d, 2H, *J* 7.1 Hz, ArH), 7.52–7.48 (m, 1H, ArH), 7.37–7.33 (m, 2H, 2 x ArH), 5.25 (dd, 1H, *J* 10.1 & 8.6 Hz, CHCO), 2.40–2.50 (m, 1H, CH), 2.20–2.40 (m, 2H, CH₂), 2.05–2.15 (m, 1H, CH), 1.80–2.00 (m, 2H, CH₂); ¹³C NMR (100 MHz, CDCl₃) δ 212.4, 165.8, 133.4, 130.0, 129.4, 128.4, 76.1, 35.0, 28.6, 17.2 ppm; MS (APCI) *m/z* 205 [M+H]⁺; HRMS (ES) calculated for C₁₂H₁₃O₃ [M+H]⁺ 205.0859, found 205.0861.

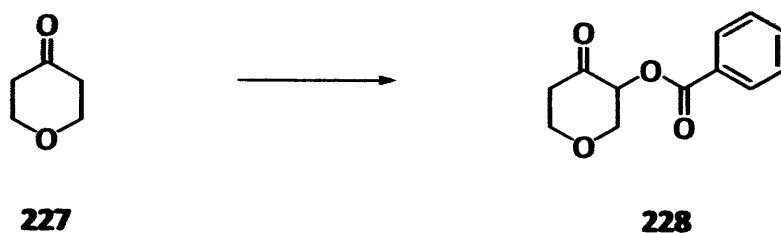
2-Benzoyloxy cycloheptanone 224



Compound **224** was prepared using General Procedure 9. Purification by column chromatography, eluting with petroleum ether/ethyl acetate (4:1), gave the *title compound* **224** (49 mg, 42%) as a white crystalline solid; Mp 52–56 °C (Lit. ref. 57–57.5 °C)⁸⁹; IR (CHCl₃): 2932, 2861, 1734, 1714, 1448, 1315, 1272, 1107, 850, 789 cm⁻¹; ¹H NMR (400 MHz, CDCl₃) δ 8.00 (d, 2H, *J* 7.1 Hz, ArH), 7.52–7.480 (m, 1H, ArH), 7.37–7.33 (m, 2H, 2 x ArH), 5.40 (dd, 1H, *J* 9.6 & 3.3 Hz, CHCO), 2.60–2.70 (m, 1H, CH), 2.35–2.50 (m, 1H, CH), 2.00–2.10 (m, 1H, CH),

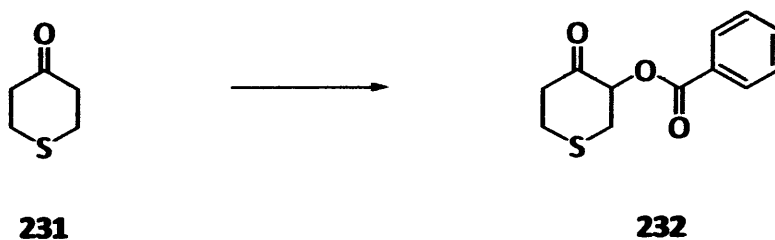
1.60–1.90 (m, 6H), 1.30–1.40 (m, 1H, CH); ^{13}C NMR (100 MHz, CDCl_3), δ 207.5, 165.8, 133.2, 129.9, 129.6, 128.4, 79.0, 40.8, 30.4, 28.4, 26.5, 23.0 ppm; MS (ES) m/z 233 $[\text{M}+\text{H}]^+$; HRMS (ES) calculated for $\text{C}_{14}\text{H}_{17}\text{O}_3$ $[\text{M}+\text{H}]^+$ 233.1172, found 233.1172.

2-Benzoyloxy tetrahydropyran-4-one 228



Compound **228** was prepared using General Procedure 9. Purification by column chromatography, eluting with petroleum ether/ethyl acetate (1:1), gave the *title compound* **228** (62 mg, 56%) as a white crystalline solid; Mp 76–79 °C; IR (CHCl_3): 2913, 2856, 1736, 1719, 1597, 1451, 1315, 1275, 1261, 1204, 1121, 1096, 760 cm^{-1} ; ^1H NMR (400 MHz, CDCl_3) δ 8.00 (d, 2H, J 7.2 Hz, ArH), 7.52–7.48 (m, 1H, ArH), 7.38–7.32 (m, 2H, 2 x ArH), 5.45 (dd, 1H, J 9.9 & 7.1 Hz, CHCO), 4.30–4.40 (m, 1H, CH), 4.20–4.30 (m, 1H, CH), 3.60–3.70 (m, 2H, CH_2), 2.70–2.85 (m, 1H, CH), 2.50–2.60 (m, 1H, CH); ^{13}C NMR (100 MHz, CDCl_3), δ 200.5, 165.1, 133.6, 130.0, 129.0, 128.5, 74.1, 70.6, 68.6, 42.3 ppm; MS (EI) m/z 221 $[\text{M}+\text{H}]^+$. HRMS calculated for $\text{C}_{12}\text{H}_{13}\text{O}_4$ $[\text{M}+\text{H}]^+$ 221.0808, found 221.0809.

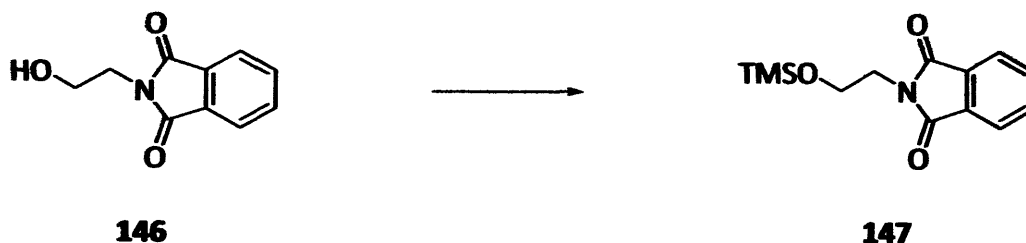
2-Benzoyloxy tetrahydrothiopyran-4-one 232



Compound 232 was prepared using General Procedure 9. Purification by column chromatography, eluting with petroleum ether/ethyl acetate (3:2), gave the *title compound* 232 (77 mg, 65%) as an off-white solid; Mp 73–78 °C; IR (CHCl₃): 2912, 1736, 1721, 1602, 1451, 1300, 1267, 1177, 1112, 1070, 1028, 772, 710 cm⁻¹; ¹H NMR (400 MHz, CDCl₃) δ 8.00 (d, 2H, *J* 7.1 Hz, ArH), 7.53–7.49 (m, 1H, ArH), 7.38–7.32 (m, 2H, 2 x ArH), 5.50 (dd, 1H, *J* 11.0 & 6.3 Hz, CHCO), 3.05–3.15 (m, 2H, CH₂), 2.85–2.95 (m, 4H, 2 x CH₂); ¹³C NMR (100 MHz, CDCl₃), δ 201.6, 165.2, 133.5, 130.0, 129.2, 128.5, 77.2, 44.8, 34.7, 30.4 ppm; MS (EI) *m/z* 236 [M+H]⁺; HRMS (EI) calculated for C₁₂H₁₃O₃S [M+H]⁺ 237.0580, found 237.0579.

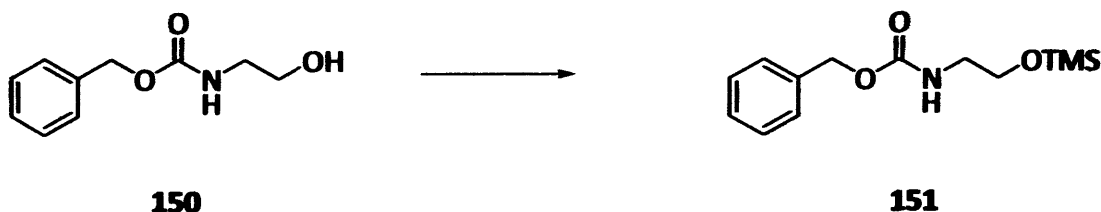
9.4 Miscellaneous compounds

N-(2-Trimethylsiloxyethyl)phthalimide **147**



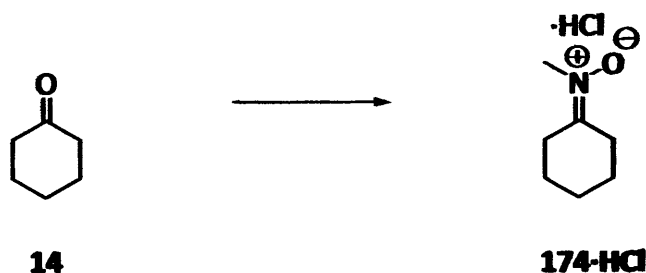
To a solution of *N*-(2-hydroxyethyl)phthalimide **146** (5.00 g, 26.15 mmol) and triethylamine (10 ml) in dichloromethane (75 ml) at ambient temperature, was added 1,1,3,3,3-hexamethyldisilazane (2.73 ml, 13.08 mmol) dropwise followed by trimethylchlorosilane (3.34 ml, 26.15 mmol). The mixture was stirred at reflux for 16 h, and the reaction quenched by adding the mixture to ice-cold water (200 ml). The organic layer was separated, washed with brine (100 ml), dried (Na_2SO_4), filtered and the solvent removed under reduced pressure to give the crude product as an orange oil. The residue was purified by flash column chromatography, eluting with 1:4 diethyl ether/ light petroleum ($R_f = 0.2$) to give the *title compound* **147** as a colourless oil (6.30 g, 91 %); IR(thin film): 3207, 1872, 1410, 1385, 1360, 1102, 987, 780 cm^{-1} ; ^1H NMR (400 MHz, CDCl_3) δ 7.77–7.73 (m, 2H, 2 x ArH), 7.65–7.61 (m, 2H, 2 x ArH), 3.89–3.82 (m, 4H, 2 x CH_2), 0.0 (s, 9H, $\text{OSi}(\text{CH}_3)_3$); ^{13}C NMR (100 MHz, CDCl_3) δ 168.3, 133.9, 132.1, 123.2, 59.5, 40.1, 0.6 ppm; MS (APCI) m/z 264 $[\text{M}+\text{H}]^+$; HRMS (APCI) calculated for $\text{C}_{13}\text{H}_{18}\text{NO}_3\text{Si}$ $[\text{M}+\text{H}]^+$ 264.1050, found 264.1051.

Benzyl *N*-(2-trimethylsiloxyethyl) carbamate **151**



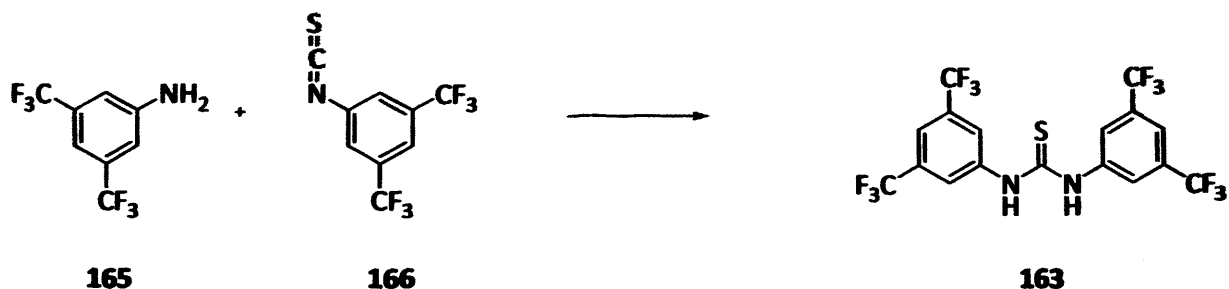
To a solution of benzyl *N*-(2-hydroxyethyl) carbamate (500 mg, 2.56 mmol) and triethylamine (1.0 ml) in dichloromethane (15 ml) at ambient temperature, was added 1,1,3,3,3-hexamethyldisilazane (270 μ L, 1.28 mmol) dropwise followed by trimethylchlorosilane (330 μ L, 2.56 mmol). The mixture was stirred at reflux for 16 h, and the reaction mixture was washed with ice-cold water (2 x 20 ml). The organic layer was separated and dried over Na₂SO₄, the solution was filtered and the solvent removed *in vacuo* to give the crude product as a salmon-pink oil. The residue was purified by flash column chromatography, eluting with 1:4 diethyl ether/ light petroleum (*R*_f = 0.15) to a colourless oil (389 mg, 57 %); IR(thin film): 3050, 1775, 1597, 1385, 1170, 1102, 1050, 962, 728 cm⁻¹; ¹H NMR (400 MHz, CDCl₃) δ 7.29–7.19 (m, 5H, 5 x ArH), 5.00 (s, 2H, ArCH₂), 3.57–3.44 (m, 2H, NCH₂), 3.27–3.16 (m, 2H, SiOCH₂), 0.0 (s, 9H, OSi(CH₃)₃); ¹³C NMR (100 MHz, CDCl₃) δ 165.2, 138.0, 130.5, 129.1, 128.6, 62.5, 61.3, 43.6, 0.9 ppm; MS (APCI) *m/z* 268 [M+H]⁺; HRMS (ES) calculated for C₁₃H₂₂NO₃Si [M+H]⁺ 268.1363, found 268.1360.

***N*-Methylcyclohexylnitronium hydrochloride 174-HCl²⁷**



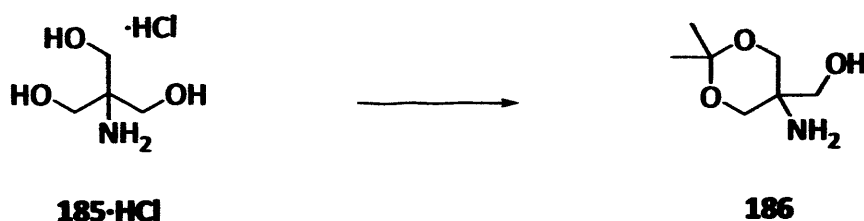
A mixture of *N*-methyl hydroxylamine hydrochloride 97-HCl (4.20 g, 0.05 mmol) and cyclohexanone 14 (15.0 ml, 0.14 mmol) was heated to 70 °C under a nitrogen atmosphere in a flame-dried 3-necked round-bottomed flask. After 3 hours, the flask was cooled in ice and the resulting pale brown precipitate was filtered rapidly, washing with cyclohexanone (10 ml) and dry ether (20 ml), and then dried overnight over P₂O₅ in a vacuum dessicator, to give the *title compound* 174-HCl as pale yellow crystals (7.05 g, 86 %); mp 128–130 °C (Lit. Ref. 138 °C)²⁷; IR (CHCl₃): 2938, 2861, 1452, 1367, 1163 cm⁻¹; ¹H NMR (400 MHz, CDCl₃) δ 3.63 (s, 3H, CH₃) 2.80–2.42 (m, 4H, 2 x CH₂), 1.20–1.88 (m, 6H, 3 x CH₂).

***N-N'*-Bis(3,5-bis(trifluoromethyl)phenyl) thiourea 163⁶⁷**



A solution of 3,5-bis(trifluoromethyl) phenyl isothiocyanate **166** (1.08 g, 4.0 mmol) and 3,5-bis(trifluoromethyl) aniline **165** (0.92 g, 4.0 mmol) in acetonitrile (30 ml) was stirred for 5 days at room temperature. The reaction mixture was then concentrated *in vacuo* to give a pale solid, which was recrystallised from CHCl_3 to give the *title compound* **163** as colourless needle-like crystals (1.89 g, 95 %); mp 171.5–173 °C; IR(KBr disc) 3207, 3051, 2360, 1799, 1627, 1556, 1467, 1376, 1287, 1133, 1005, 930, 904, 891, 849, 764, 702, 684, 620, 593, 571, 520, 408 cm^{-1} ; ^1H NMR (400 MHz, $\text{DMSO}-d_6$) δ 10.70 (br, s, 2H, 2 x NH), 8.24 (s, 4H, 4 x ArH), 7.91 (s, 2H, 2 x ArH); ^{13}C NMR (125 MHz, $\text{DMSO}-d_6$) δ 181.1, 141.6, 130.8, 124.6, 122.5, 118.2; MS (ES) m/z 501.2 $[\text{M}+\text{H}]^+$; HRMS (ES) calculated for $\text{C}_{17}\text{H}_9\text{N}_2\text{F}_{12}\text{S}$ $[\text{M}+\text{H}]^+$ 501.0289, found 501.0288.

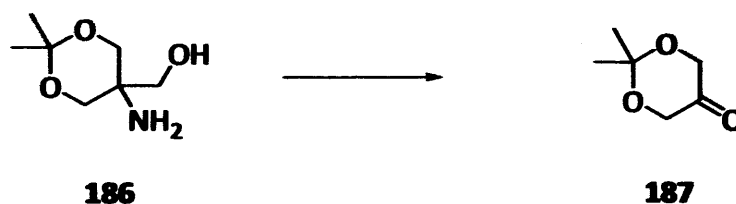
5-Amino-2,2-dimethyl-1,3-dioxane-5-methanol 186⁷⁴



p-Toluenesulphonic acid (603 mg, 3.17 mmol) was added to a solution of 2-amino-2-(hydroxymethyl) propane-1,3-diol hydrochloride **185-HCl** (10.0 g, 63.4 mmol) in dry DMF (70 ml) at ambient temperature, followed by the addition of 2,2-dimethoxypropane

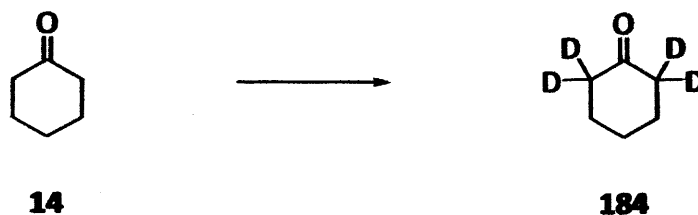
(8.55 ml, 69.7 mmol) in one portion. The resulting white suspension became clear and colourless after 45 minutes. The reaction mixture was stirred for 12 hours, after which time triethylamine (5.0 ml, 36.0 mmol) was added, and the mixture stirred for an additional 30 minutes. The mixture was then concentrated *in vacuo*, treated with further triethylamine (7 ml) and ethyl acetate (250 ml), filtered and the crude product purified by column chromatography (silica gel; CH₂Cl₂: MeOH 9:1) to give the *title compound 186* as a white solid (5.62 g, 55%); mp 68–70 °C (Lit. Ref. 67–69 °C)⁷⁴; IR (CHCl₃): 3401, 1600, 1455, 1377, 1199, 1037, 826 cm⁻¹; ¹H NMR (CDCl₃, 400 MHz): δ 3.80 (2H, d, *J* 12.0 Hz, CH₂), 3.54 (2H, d, *J* 12.0 Hz, CH₂), 3.50 (2H, s, CH₂OH), 2.55 (2H, br, s, NH₂), 1.46 (3H, s, CH₃), 1.42 (3H, s, CH₃); ¹³C NMR (CDCl₃, 125 MHz): 98.5, 66.9, 64.4, 50.4, 25.0, 22.0.

2,2-Dimethyl-1,3-dioxan-5-one **187**⁷⁴



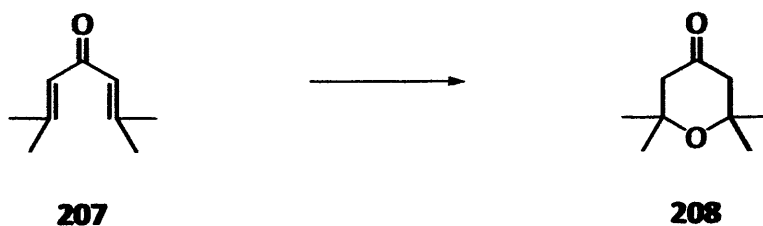
A solution of sodium periodate (2.79g, 13.0 mmol) in H₂O (40 ml) was added dropwise at 0 °C, over a period of 1.5 hours, to a slurry of **186** (2.10 g, 13.0 mmol) and potassium phosphate monobasic (1.77 g, 13.0 mmol) in H₂O (40 ml). The resulting mixture was stirred at 0 °C for 0.5 hours, then at room temperature for a further 5 hours to give a pale yellow mixture. Sodium thiosulphate (2.06 g, 13.0 mmol) was added, and the solution stirred for a further 15 minutes. The mixture was extracted with CH₂Cl₂ (10 × 20 ml), the organic fractions combined, dried over Na₂SO₄, filtered, concentrated *in vacuo*, and the resulting yellow oil purified by column chromatography (silica gel; EtOAc: light petroleum 3:1) to give the dioxane **187** (1.38 g, 82%) as a colourless oil; IR (thin film): 2991, 2942, 2890, 1753, 1424, 1377, 1221, 1092, 832 cm⁻¹; ¹H NMR (CDCl₃, 400 MHz): δ 4.20 (4H, s, 2 × CH₂), 1.41 (s, 6H, 2 × CH₃); ¹³C NMR (CDCl₃, 125 MHz): δ 208.0, 100.1, 66.8, 23.5; MS (ES) *m/z* 130 [M+H]⁺.

2,2,6,6-d-cyclohexanone **184**



A suspension of cyclohexanone **14** (30.0g, 0.31 mmol) and potassium carbonate (83.0 g, 0.62 mmol, 2.0 eq.) in D₂O (112 ml, 6.2 mol, 20 eq.) was stirred at reflux for 24 hours. The organic layer was separated and an aliquot analysed by ¹H NMR (CDCl₃). This was found to comprise 87% of the deuterated adduct, with 13% of unconverted starting material remaining, and so the material was subjected to the same procedure a further 2 times. This gave a product which was found to be >98% deuterated; therefore the organic layer was dried over MgSO₄ and purified by vacuum distillation (50–52 °C, 1 mbar) to give the *title compound* **184** as a colourless oil (13.67 g, 43%); ¹H NMR (CDCl₃, 400 MHz): δ 1.78–1.68 (4H, m, 2 x CH₂), 1.66–1.60 (2H, m, CH₂); MS (EI) *m/z* 102.

3,3,5,5-Tetramethyl-1,2-tetrahydropyranone **208**⁷⁵



A mixture of 2,6-dimethyl-2,5-heptadien-4-one **207** (25 g, 0.18 mmol) in 1N HCl was stirred at 40 °C for 4 days. The reaction mixture was extracted with Et₂O (5 x 50 ml), dried (MgSO₄), filtered and the solvent removed at atmospheric pressure to give a pale green oil. The crude product was subjected to column chromatography (Et₂O: light petroleum 3:1) to give the *title compound* **208** as a clear colourless oil (9.5 g, 34%); IR (thin film): 2978, 1721, 1303,

1230, 1009 cm^{-1} ; ^1H NMR (CDCl_3 , 400 MHz): δ 2.10 (s, 4H, 2 \times CH_2), 1.05–0.99 (m, 12H, 4 \times CH_3); ^{13}C NMR (CDCl_3 , 125 MHz): 208.5, 75.0, 51.5, 31.3.

9.5 Analytical experiments

9.5.1 General Procedure 10: ^1H NMR reaction monitoring (early protocol, Chapter 6)

A solution of *N*-methyl-*O*-benzoyl hydroxylamine hydrochloride **100-HCl** (39 mg, 0.25 mmol) and 1,4-dimethoxybenzene (21 mg, 0.15 mmol) in d_6 -DMSO (1.0 ml) was placed in an NMR tube. The NMR tube was loaded into a Bruker 250 MHz NMR spectrometer with the probe preset at the required temperature and allowed to equilibrate for 20 minutes, during which time the tube was allowed to shim and value for receiver gain noted. Immediately prior to the start of data collection, 3,3,5,5-tetramethylcyclohexanone **188** (44 μL , 0.25 mmol) was added to the solution via syringe, ensuring thorough mixing of the liquids. The NMR tube was replaced in the spectrometer for 16–24 hours, with spectra acquired at the set interval (5–30 minutes). At the end of the experiment, the raw data was processed by the XWin-NMR software package (multiple integration across pre-defined chemical shift ranges).

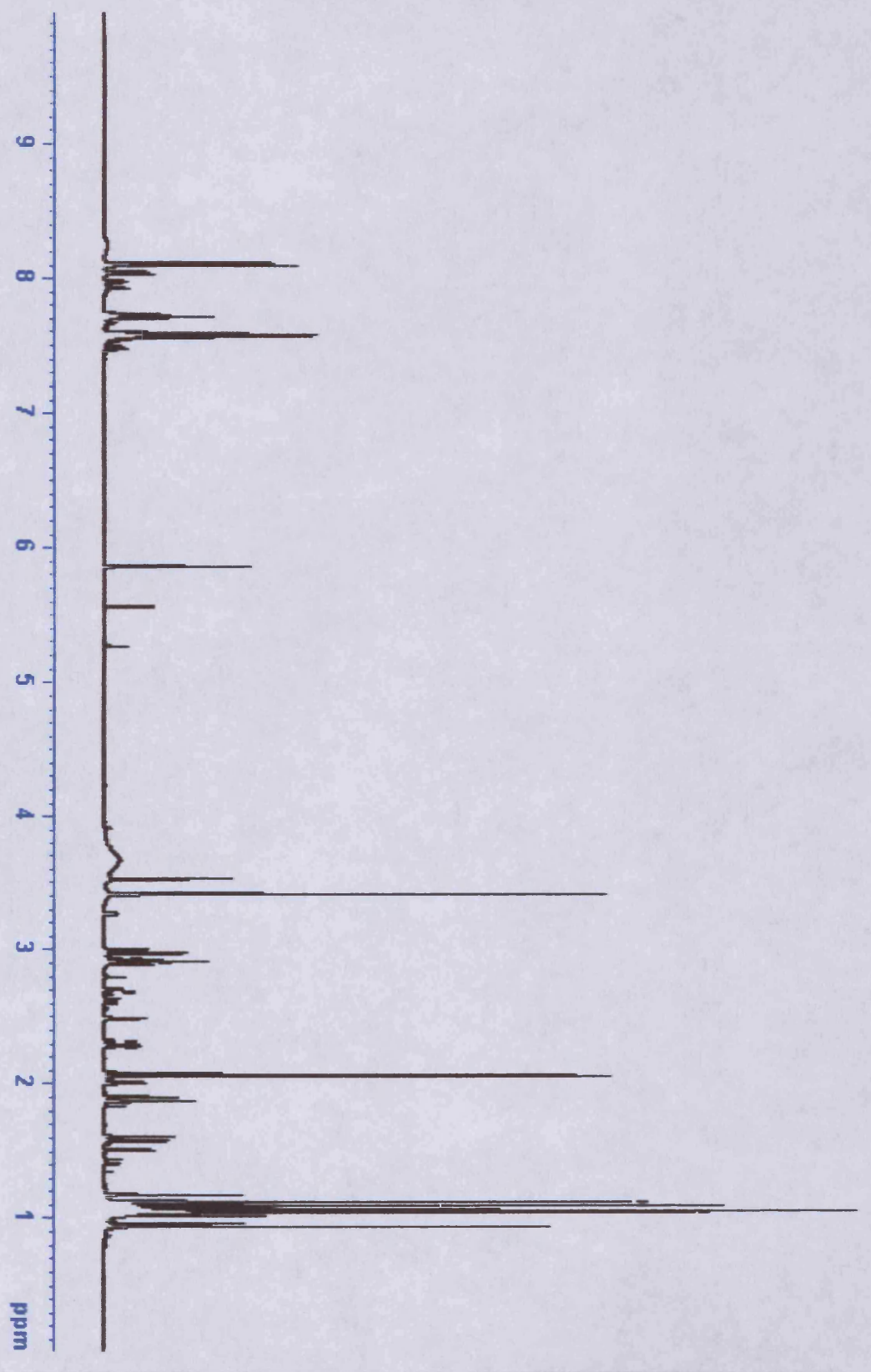
9.5.2 General Procedure 11: ^1H NMR reaction monitoring (refined protocol, Chapter 7)

Anhydrous d_6 -DMSO was kept moisture free by standing over 3Å molecular sieves prior to use. Moisture levels were measured using a Mitsubishi CA100 Single Channel Coulometric Karl Fischer Titrator. A solution of *N*-methyl-*O*-benzoyl hydroxylamine hydrochloride **100-HCl** (388 mg, 2.5 mmol), 1,4-dimethoxybenzene (69.5 mg, 0.50 mmol) in d_6 -DMSO (9.0 ml) was prepared in a 25 ml round bottomed flask. 3,3,5,5-Tetramethylcyclohexanone **188** (440 μL , 2.5 mmol) was then added, and a 1 ml aliquot withdrawn and transferred to an NMR tube. The NMR tube was loaded into a Bruker 500 MHz NMR spectrometer with the probe preset at the required temperature and allowed to equilibrate for 20 minutes, during which time the tube was allowed to shim and value for receiver gain noted. ^1H NMR spectra were then acquired at 5 minute intervals. At the end of the experiment, the raw data was processed by the TopSpin-NMR software package (multiple integration across pre-defined chemical shift ranges).

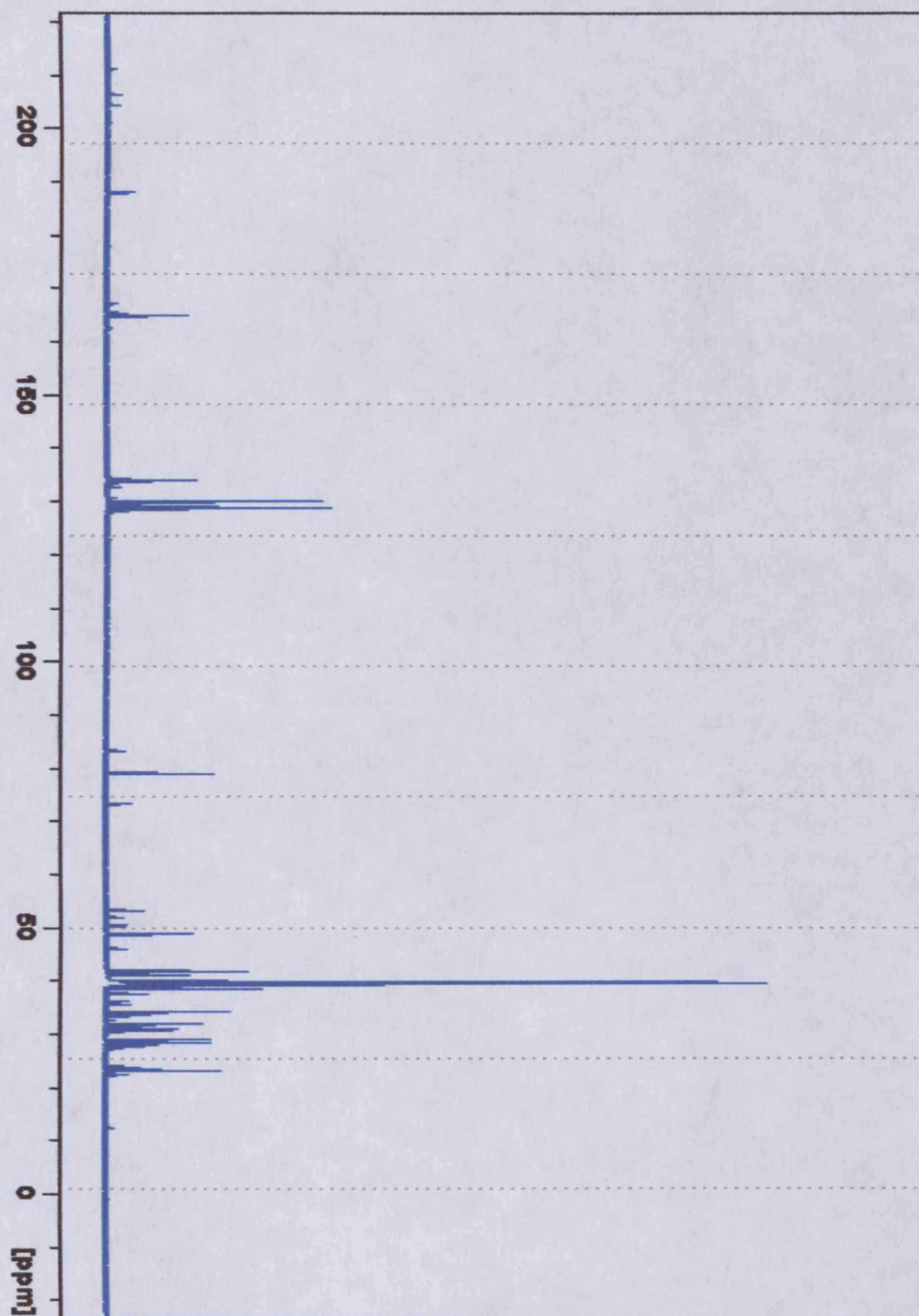
9.5.3 Reaction monitoring by ReactIR™

The experiment was carried out using a Mettler-Toledo ReactIR 1000 with a DiCOMP probe (an in-situ IR using Attenuated Total Reflectance technology). An air IR background was taken from an 80 ml multi-necked jacketed vessel equipped with high P DiCOMP probe, a thermocouple and a rugby ball shaped magnetic stirrer. Anhydrous DMSO- d_6 (18.0 ml) was added and warmed to 21 °C. Acquisition for IR reaction spectra was then started using rapid collection (1 reaction spectrum collected every 3 seconds, resolution = 16, 12 scans per reaction spectrum). After 2 minutes, *N*-methyl-*O*-benzoyl hydroxylamine hydrochloride 100-HCl (0.887 g, 0.005 mol, 1.01 eq.) was added (reaction concentration 0.28 M). After a further 5 minutes, 3,3,5,5-tetramethylcyclohexanone 188 (0.8 ml, 0.005 mol, 1.0 eq.) was added in one portion over 3 seconds. After 30 minutes, acquisition for IR was stopped and a sample was withdrawn for ^1H NMR analysis (1 drop of TMS was added as a reference). The presence of two intermediates in the reaction mixture was confirmed. The solution was then warmed to 33 °C over 10 minutes, then acquisition of IR reaction spectra was resumed (1 spectrum was collected every 2 minutes for the next 4 hours, then every 5 minutes for a further 15 hours). From the real-time quick profile, peaks were unchanged after heating the reaction mixture at 33 °C for 1 hour; therefore water (0.81 ml, 0.045 mol, 9.0 eq.) was added to the reaction mixture. At the end of the reaction time, a sample was withdrawn for analysis by ^1H NMR; this confirmed the presence of product with no traces of starting materials or major intermediates. ReactIR data was processed using the ConclRT software package (1848–648 cm^{-1}).

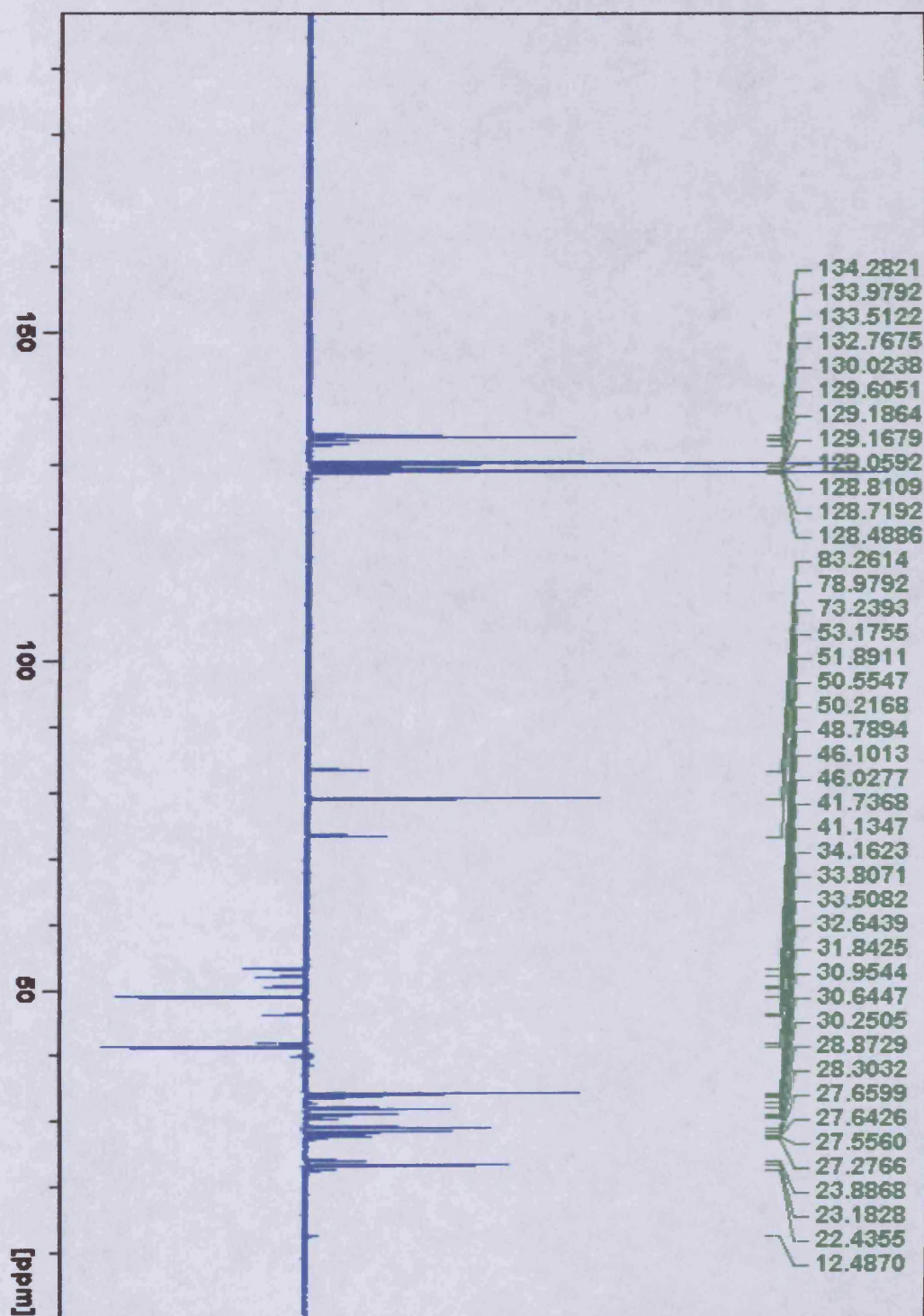
Appendix 1: ^1H NMR spectrum of reaction between 3,3,5,5-tetramethylcyclohexanone 188 and *N*-methyl-*O*-benzoyl hydroxylamine hydrochloride 100-HCl, at 30 °C, 2 hours after start



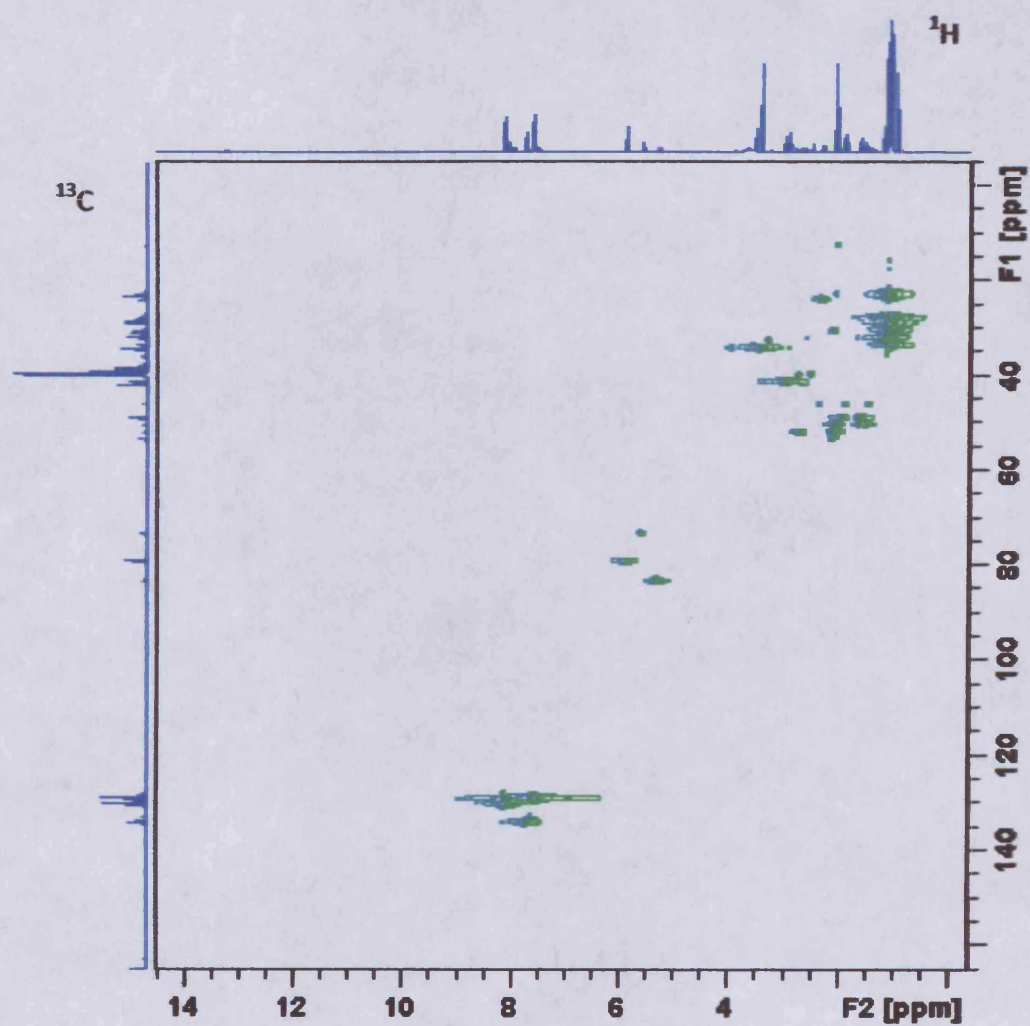
Appendix 2: ^{13}C NMR spectrum of reaction between 3,3,5,5-tetramethylcyclohexanone 188 and *N*-methyl-*O*-benzoyl hydroxylamine hydrochloride 100-HCl, at 30 °C, t = 2 h



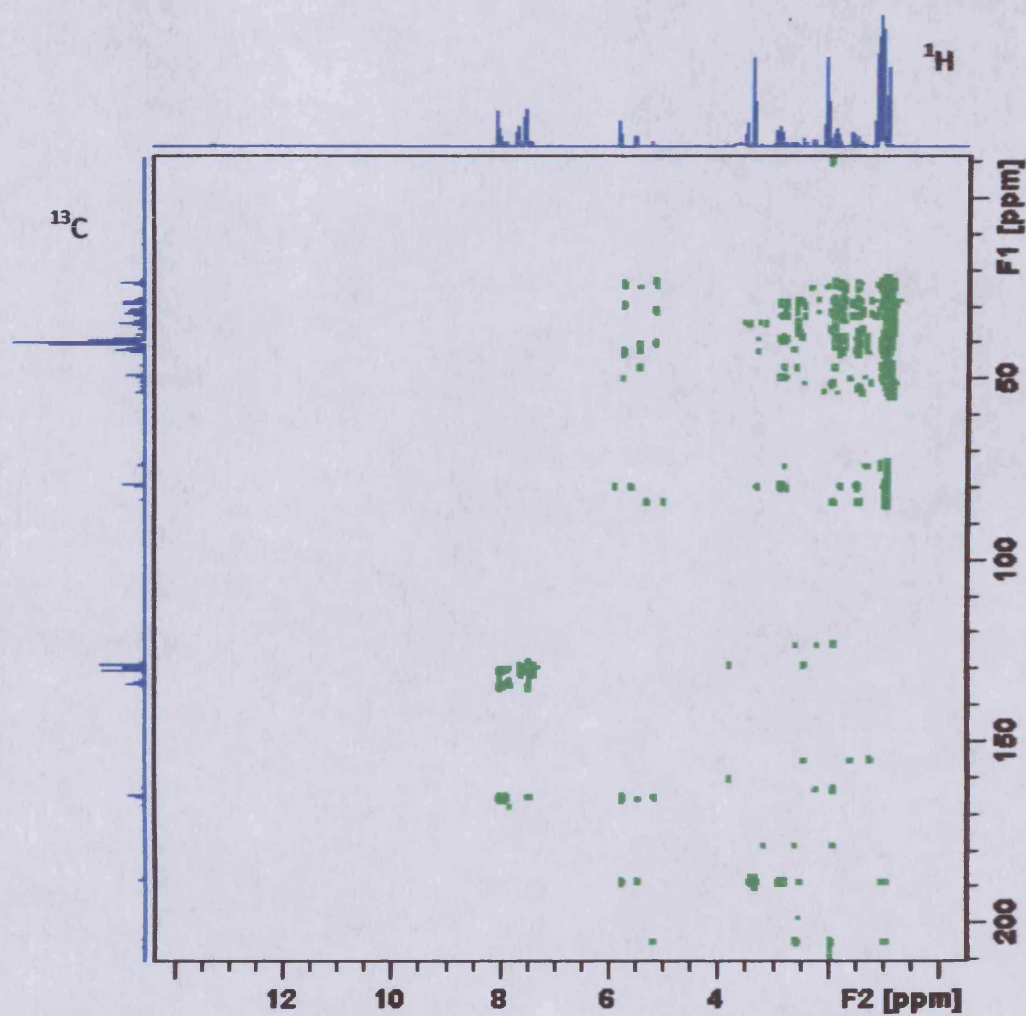
Appendix 3: ^{13}C DEPT spectrum of reaction between 3,3,5,5-tetramethylcyclohexanone 188 and *N*-methyl-*O*-benzoyl hydroxylamine hydrochloride 100-HCl, at 30 °C, t = 2 h



Appendix 4: HSQC spectrum of reaction between 3,3,5,5-tetramethylcyclohexanone 188 and *N*-methyl-*O*-benzoyl hydroxylamine hydrochloride 100-HCl, at 30 °C, t = 2 h



Appendix 5: HSQC spectrum of reaction between 3,3,5,5-tetramethylcyclohexanone 188 and *N*-methyl-*O*-benzoyl hydroxylamine hydrochloride 100·HCl, at 30 °C, t = 2 h



References

1. (a) List, B.; Pojarliev, P.; Martin, H. J. *Org. Lett.* **2001**, *3*, 2423; (b) Paras, N. A.; MacMillan, D. W. C. *J. Am. Chem. Soc.* **2002**, *124*, 7894; (c) Betancort, J. M.; Sakthivel, K.; Thayumanavan, R.; Barbas III, C. F. *Tetrahedron Lett.* **2001**, *42*, 4441.
2. (a) Ahrendt, K. A.; Borths, C. J.; MacMillan, D. W. C. *J. Am. Chem. Soc.* **2000**, *122*, 4243; (b) Northrup, A. B.; MacMillan, D. W. C. *J. Am. Chem. Soc.* **2002**, *124*, 2458.
3. (a) Paras, N. A.; MacMillan, D. W. C. *J. Am. Chem. Soc.* **2002**, *124*, 7894; (b) Betancort, J. M.; Sakthivel, K.; Thayumanavan, R.; Barbas III, C. F. *Tetrahedron Lett.* **2001**, *42*, 4441; (c) List, B.; Pojarliev, P.; Martin, H. J. *Org. Lett.* **2001**, *3*, 2423.
4. Jen, W. S.; Wiener, J. J. M.; MacMillan, D. W. C. *J. Am. Chem. Soc.* **2000**, *122*, 9874.
5. (a) List, B.; Pojarliev, P.; Biller, W. T.; Martin, H. J. *J. Am. Chem. Soc.* **2002**, *124*, 827; (b) List, B. *J. Am. Chem. Soc.* **2000**, *122*, 9336; (c) Pojarliev, P.; Biller, W. T.; Martin, H. J.; List, B. *Synlett* **2003**, 1903.
6. (a) List, B.; Pojarliev, P.; Castello, C. *Org. Lett.* **2001**, *3*, 573; (b) List, B.; Lerner, R. A.; Barbas III, C. F. *J. Am. Chem. Soc.* **2000**, *122*, 2395; (c) Northrup, A. B.; MacMillan, D. W. C. *J. Am. Chem. Soc.* **2002**, *124*, 6798.
7. (a) Brown, S. P.; Brochu, M. P.; Sinz, C. J.; MacMillan, D. W. C. *J. Am. Chem. Soc.* **2003**, *125*, 10808; (b) Zhong, G. *Angew. Chem. Int. Ed.* **2003**, *42*, 4247.
8. (a) List, B. *J. Am. Chem. Soc.* **2002**, *124*, 5656; (b) Bøgevig, A.; Juhl, K.; Kumaragurubaran, N.; Zhuang, W.; Jørgensen, K. A. *Angew. Chem. Int. Ed.* **2002**, *41*, 1790; (c) Kumaragurubaran, N.; Juhl, K.; Zhuang, W.; Bøgevig, A.; Jørgensen, K. A. *J. Am. Chem. Soc.* **2002**, *124*, 6254.
9. Wilson, R. M.; Jen, W. S.; MacMillan, D. W. C. *J. Am. Chem. Soc.* **2005**, *127*, 11616.
10. Mangion, I. K.; MacMillan, D. W. C. *J. Am. Chem. Soc.* **2005**, *127*, 3696.
11. (a) March, J. *Advanced Organic Chemistry, Reactions, Mechanisms and Structure*, 3rd ed. John Wiley & Sons: New York, 1985; (b) Prileschajew, N. *Ber. Dtsch. Chem. Ges.* **1909**, 4811.
12. (a) Baeyer, A.; Villiger, V. *Ber. Dtsch. Chem. Ges.* **1899**, 3625; (b) Baeyer, A.; Villiger, V. *Ber. Dtsch. Chem. Ges.* **1900**, 858.

13. (a) Wall, M. E.; Wani, M. C. *J. Ethnopharmacol.* **1996**, *51*, 239; (b) Oberlies, N. H.; Kroll, D. J. *J. Nat. Prod.* **2004**, *67*, 129; (c) Wall, M. E. *Med. Res. Rev.* **1998**, *18*, 299; (d) Torck, M.; Pinkas, M. *J. Pharm. Belg.* **1996**, *51*, 200.
14. For a discussion on these and related processes see: Smith, M. B.; March, J. *March's Advanced Organic Chemistry*, Fifth Edition, Smith, M. B.; March, J. Wiley-Interscience: New York, **2001**, 915.
15. (a) Vedejs, E. *J. Am. Chem. Soc.* **1974**, *96*, 5944; (b) Vedejs, E.; Engler, D. A.; Telschow, J. E. *J. Org. Chem.* **1978**, *43*, 188.
16. Anderson, J. C.; Smith, S. C. *Synlett* **1990**, 107.
17. (a) Davis, F. A., Haque, M. S. *Advances in Oxygenated Processes*; Baumstark, A. L. Ed. JAI Press Inc: Greenwich, CT, 1990; Vol 2, Chapter 2, 61; (b) Davis, F. A., Jenkins, R. H., Jr. *Asymmetric Synthesis*, Morrison, J. D., Ed.; Academic Press: New York, 1984, Vol. 4, Chapter 4, 313.
18. Davis, F. A.; Sheppard, A. C. *Tetrahedron* **1989**, *45*, 5703-5742.
19. (a) Bach, R. D.; Wolber, G. J. *J. Am. Chem. Soc.* **1984**, *106*, 1410; (b) Bach, R. D.; Coddens, B. A.; McDouall, J. J. W.; Schlegel, H. B.; Davis, F. A. *J. Org. Chem.* **1990**, *55*, 3325; (c) Davis, F. A.; Billmers, J. M.; Gosciniak, D. J.; Towson, J. C.; Bach, R. D. *J. Org. Chem.* **1986**, *51*, 4240.
20. Davis, F. A.; Sheppard, A. C.; Chen, B. C.; Haque, M. S. *J. Am. Chem. Soc.* **1990**, *112*, 6679.
21. Davis, F. A.; Chen, B.-C. *Chem. Rev.* **1992**, *92*, 919.
22. Hayashi, Y.; Yamaguchi, J.; Hibino, K.; Shoji, M. *Tetrahedron Lett.* **2003**, *44*, 8293.
23. (a) Bøgevig, A.; Sunden, H.; Cordova, A. *Angew. Chem. Int. Ed.* **2004**, *43*, 1109; (b) Hayashi, Y.; Yamaguchi, J.; Sumiya, T.; Shoji, M. *Angew. Chem. Int. Ed.* **2004**, *43*, 1112.
24. House, O., Richey, F. A. *J. Org. Chem.* **1969**, *34*, 1430.
25. (a) Sheradsky, T. *Tetrahedron Lett.* **1966**, *7*, 5225; (b) Mooradian, A. *Tetrahedron Lett.* **1967**, *8*, 407; (c) Kaminsky, D., Shavel, J., Jr., Meltzer, R. I. *Tetrahedron Lett.* **1967**, *8*, 859; (d) Mooradian, A., Dupont, P. E. *Tetrahedron Lett.* **1967**, *8*, 2867.
26. (a) Katritzky, A. R.; Chapman, A. V.; Cook, M. J.; Millet, G. H. *J. Chem. Soc., Perkin Trans. 1* **1980**, 2743; (b) Traynelis, V. J., Pacini, P. L. *J. Am. Chem. Soc.* **1964**, *86*, 4917; (c) Traynelis, V. J., Martello, R. F. *J. Am. Chem. Soc.* **1958**, *80*, 6590.

27. Cummins, C. H.; Coates, R. M. *J. Org. Chem.* **1983**, *48*, 2070.
28. (a) Claisen, L. *Ber. Dtsch. Chem. Ges.* **1912**, *45*, 3157; (b) Claisen, L., Tietze, E. *Ber. Dtsch. Chem. Ges.* **1925**, *58*, 275; (c) Claisen, L., Tietze, E. *Ber. Dtsch. Chem. Ges.* **1926**, *59*, 2344.
29. For a review see: Bennett, G. B. *Synthesis* **1977**, 589.
30. (a) Wick, A. E.; Felix, D.; Steen, K.; Eschenmoser, A. *Helv. Chim. Acta* **1964**, *47*, 2425; (b) Wick, A. E.; Felix, D.; Gschwend-Steen, K.; Eschenmoser, A. *Helv. Chim. Acta* **1969**, *52*, 1030.
31. Johnson, W. S.; Werthemann, L.; Bartlett, W. R.; Brocksom, T. J.; Tsung-Tee, L.; Faulkner, D. J.; Petersen, M. R. *J. Am. Chem. Soc.* **1970**, *92*, 741.
32. (a) Ireland, R. E.; Mueller, R. H. *J. Am. Chem. Soc.* **1972**, *94*, 5897; (b) Ireland, R. E.; Willard, A. K.; Tetrahedron Lett. **1975**, *16*, 3975; (c) Ireland, R. E.; Mueller, R. H.; Willard, A. K.; *J. Am. Chem. Soc.* **1976**, *98*, 2868.
33. Kurth, M. J.; Decker, O. H. W.; *J. Org. Chem.* **1985**, *50*, 5769.
34. (a) Overman, L. E. *J. Am. Chem. Soc.* **1974**, *96*, 597; (b) Overman, L. E. *J. Am. Chem. Soc.* **1976**, *98*, 2901.
35. Overman, L. E.; Carpenter, N. E. *Org. React.* **2005**, *66*, 1.
36. Chen, Y. K.; Lurain, A. E.; Walsh, P. J. *J. Am. Chem. Soc.* **2002**, *124*, 12225.
37. Anderson, C. E.; Overman, L. E. *J. Am. Chem. Soc.* **2003**, *125*, 12412.
38. Chen, B.; Mapp, A. K. *J. Am. Chem. Soc.* **2005**, *127*, 6712.
39. (a) Cope, A. C.; Hardy, E. M. *J. Am. Chem. Soc.* **1940**, *62*, 441; (b) Rhoads, S. J.; Rollins, N. R. *Org. React.* **1975**, *22*, 1.
40. (a) Berson, J. A.; Jones Jr., M. *J. Am. Chem. Soc.* **1964**, *86*, 5017; (b) Berson, J. A.; Jones Jr., M. *J. Am. Chem. Soc.* **1964**, *86*, 5019.
41. Evans, D. A.; Golob, A. M. *J. Am. Chem. Soc.* **1975**, *97*, 4765.
42. Horowitz, R. M.; Geissman, T. A. *J. Am. Chem. Soc.* **1950**, *72*, 1518.
43. Kürti, L.; Czakó, B. *Strategic Applications of Named Reactions in Organic Synthesis*, Elsevier Academic Press: London, 2005, 22.
44. (a) Fischer, E.; Jourdan, F. *Ber. Dtsch. Chem. Ges.* **1883**, *16*, 2241; (b) Fischer, E., Hess, O. *Ber. Dtsch. Chem. Ges.* **1884**, *17*, 559.
45. Bratelescu, G. *Tetrahedron Lett.* **2008**, *49*, 984.

46. Enders, D.; Knopp, M. *Tetrahedron* **1996**, *52*, 5805.
47. Nissen, A.; Rebafka, W.; Aquila, W. U.S. Patent 4,288,636, **1981**.
48. Boland, W.; Pohnert, G; Maier, I. *Angew. Chem. Int. Ed.* **1995**, *34*, 1602.
49. Beshara, C. S.; Hall, A.; Jenkins, R. L.; Jones, T. C.; Parry, R. T.; Thomas, S. P.; Tomkinson, N. C. O. *Chem. Commun.* **2005**, 1478.
50. (a) Beshara, C. S.; Hall, A.; Jenkins, R. L.; Jones, K. L.; Jones, T. C.; Killeen, N. M.; Taylor, P. H.; Thomas, S. P.; Tomkinson, N. C. O. *Org. Lett.* **2005**, *7*, 5729; (b) Jones, T. C.; Tomkinson, N. C. O. *Org. Synth.* **2007**, *84*, 233.
51. Hall, A.; Jones, K. L.; Jones, T. C.; Killeen, N. M.; Pörzig, R.; Taylor, P. H.; Yau, S.-C.; Tomkinson, N. C. O. *Synlett* **2006**, 3435.
52. Hall, A.; Huguet, E. P.; Jones, K. L.; Jones, T. C.; Killeen, N. M.; Yau, S.-C.; Tomkinson, N. C. O. *Synlett* **2007**, 293.
53. John, O. R. S.; Killeen, N. M.; Knowles, D. A.; Yau, S.-C.; Bagley, M. C.; Tomkinson, N. C. O. *Org. Lett.* **2007**, *9*, 4009.
54. Biloski, A. J.; Ganem, B. *Synthesis* **1983**, 537.
55. Milewska, M. J.; Chimiak, A. *Synthesis* **1990**, 233.
56. Wang, Q. X.; King, J.; Phanstiel IV, O. J. *Org. Chem.* **1997**, *62*, 8104.
57. Zhuang, W.; Saaby, S.; Jørgensen, K. A. *Angew. Chem. Int. Ed.* **2004**, *43*, 4476.
58. Zhong, G. F.; Fan, J. H.; Barbas III, C. F. *Tetrahedron Lett.* **2004**, *45*, 5681
59. (a) Betancort, J. M.; Sakthivel, K.; Thayumanavan, R.; Tanaka, F.; Barbas III, C. F. *Synthesis* **2004**, 1509; (b) Betancort, J. M.; Barbas III, C. F. *Org. Lett.* **2001**, *3*, 3737.
60. Cavill, J. L.; Elliott, R. L.; Evans, G.; Jones, I. L.; Platts, J. A.; Ruda, A. M.; Tomkinson, N. C. O. *Tetrahedron* **2006**, *62*, 410.
61. (a) Carey, F. A.; Sundberg, R. J. *Advanced Organic Chemistry: Structures and Mechanisms*, 5th Ed., Springer Science, 2007, 345; (b) Tsukamoto, T.; Kitazume, T. *Chem. Lett.* **1992**, 1377; (c) Roos, E. C.; Mooiweer, H. H.; Hiemstra, H.; Speckamp, W. N.; Kaptein, B.; Boesten, W. H. J.; Kamphuis, J. J. *Org. Chem.* **1992**, *57*, 6769; (d) Saito, S.; Uedo, E.; Kato, Y.; Murakami, Y.; Ishikawa, T. *Synlett* **1996**, 1103; (e) Sugiura, M.; Hagio, H.; Hirabayashi, R.; Kobayashi, S. *J. Am. Chem. Soc.* **2001**, *123*, 12510; (f) Frank, K. E.; Aubé, J. *Tetrahedron Lett.* **1998**, *39*, 7239; (g) Padwa, A.; Rashatasakhon, P.; Rose, M. J. *Org. Chem.* **2003**, *68*, 5139.

62. (a) Schreiner, P. R. *Chem. Soc. Rev.* **2003**, 32, 289; (b) Pikho, P. M. *Angew. Chem. Int. Ed.* **2003**, 43, 2062; (c) Takemoto, Y. *Org. Biomol. Chem.* **2005**, 3, 4299; (d) Taylor, M. S.; Jacobsen, E. N. *Angew. Chem. Int. Ed.* **2005**, 45, 1520.
63. (a) Etter, M. C.; Panunto, J. J. *Am. Chem. Soc.* **1988**, 110, 5896; (b) Etter, M. C. *Acc. Chem. Res.* **1990**, 23, 120.
64. Curran, D. P.; Kuo, L. H. *J. Org. Chem.* **1994**, 59, 3259.
65. Curran, D. P.; Kuo, L. H. *Tetrahedron Lett.* **1995**, 36, 6647.
66. Tsogoeva, S. B.; Wei, S. *Chem. Commun.* **2006**, 42, 1451.
67. Schreiner, P. R.; Wittkopp, A. *Chem. Eur. J.* **2003**, 9, 407.
68. (a) Jacobsen, E. N.; Sigman, M. S. *J. Am. Chem. Soc.* **1998**, 120, 4901; (b) Jacobsen, E. N.; Vachal, P. J. *Am. Chem. Soc.* **2002**, 124, 10012.
69. Jacobsen, E. N.; Wenzel, A. G. *J. Am. Chem. Soc.* **2002**, 124, 12964.
70. Taylor, M. S.; Jacobsen, E. N. *J. Am. Chem. Soc.* **2004**, 126, 10558.
71. Fields, J. D.; Kropp, P. J. *J. Org. Chem.* **2000**, 65, 5937.
72. Aslanzadeh, S.; Heydari, A. *Adv. Synth. Catal.* **2005**, 347, 1223.
73. Pellicciari, R.; Natalini, B.; Sadeghpour, B. M.; Marinozzi, M.; Snyder, J. P.; Williamson, B. L.; Kuethe, J. T.; Padwa, A. *J. Am. Chem. Soc.* **1996**, 118, 1.
74. González-García, E. M.; Grognum, J.; Wahler, D.; Reymond, J.-L. *Helv. Chim. Acta* **2003**, 86, 2458.
75. Magnus, P.; Mansely, T. E. *Tetrahedron Lett.* **1999**, 40, 6909.
76. Muccio, D. D.; Copan, W. G.; Abrahamson, W. W.; Mateescu, G. D. *Org. Magn. Resonance*, **1984**, 22, 121.
77. Image reproduced courtesy <http://www.cosa-instrument.com>.
78. Scholz, E. *Karl Fischer Titration*, Springer Verlag: Berlin-Heidelberg-New York **1984**.
79. Amonoo-Neizer, E. H.; Ray, S. K.; Shaw, R. A.; Smith, B. C. *J. Chem. Soc.* **1965**, 6250.
80. We wish to thank Dr. Lai Chun Chan of Process R and D, AstraZeneca, Macclesfield for performing the reaction monitoring experiment with ReactIR™.
81. We wish to thank Dr. Ian Ashworth of Process R and D, AstraZeneca, Macclesfield for carrying out the kinetic modelling with Micromath Scientist®.
82. Perrin, D. D.; Armarego, W. L. F.; Perrin, D. R. *Purification of Laboratory Chemicals*, 2nd Ed; Pergamon Press: Oxford, 1980.

83. Still, W. C.; Kahn, Mitra, M. A. *J. Org. Chem.*, **1978**, *43*, 2923.
84. Carrasco, M. R.; Brown, R. T.; Serafimova, I. M.; Silva, O. *J. Org. Chem.* **2003**, *68*, 195.
85. White, E. H.; Reefer, J.; Erickson, R. H.; Dzadzic, P. M. *J. Org. Chem.* **1984**, *49*, 4872.
86. Wathen, S. P.; Czarnik, A. W. *J. Org. Chem.* **1992**, *57*, 6129.
87. D. Geffken, *Chem. Ber.*, **1986**, *119*, 744.
88. M. Psiorz, G. Zinner, *Synthesis*, **1984**, *3*, 217.
89. G. M. Rubottom, R. C. Mott, H. D. Juve, *J. Org. Chem.*, **1981**, *46*, 2717.

